The University Of Sheffield.

Cements of the Future and Future Nuclear Cements

Shaun Daniel Nelson

Thesis submitted in partial fulfilment of the requirements for the degree of

Doctor of Philosophy

The University of Sheffield

Faculty of Engineering

Department of Materials Science and Engineering

March 2023

Contents

Abstract 5

Acknowledgements 6

Thesis Introduction 7

Key Acronyms and Nomenclature 9

List of Figures 12

List of Tables 22

1. Literature Review 24

1.1. Cement – A Brief Summary 24

1.2. The UK Nuclear Industry 28

1.3. Cement in Nuclear 32

1.4. Cement Classification Overview 36

1.4.1. Portland Cement 37

1.4.2. Calcium Sulfoaluminate Cements 39

1.4.3. Alkali Activated Materials 44

2. Materials and Methods 49

2.1. Calcium Sulfoaluminate 49

2.2. Metakaolin Geopolymer 51

2.3. Methodology 53

2.3.1. Scanning Electron Microscopy (SEM) and Energy Dispersive X-Ray Spectroscopy (EDS) 54

2.3.2. Thermogravimetric Analysis (TGA) with Mass Spectrometry (TG-MS) 55

2.3.3. X-ray diffraction (XRD) and Rietveld Analysis 55

2.3.4. Thermodynamic Modelling 57

2.3.5. Fourier Transform Infrared Spectroscopy (FTIR) 57

2.3.6. Mercury Intrusion Porosimetry (MIP) 57

3. Calcium Sulfoaluminate Cements as a Future Encapsulant 59
3.1. Introduction 59
3.2. A Brief History of Calcium Sulfoaluminate Cements 59
3.3. Calcium Sulfoaluminate Cement and the UK Nuclear Industry 63
3.4. Published Paper – "Hydrate Assemblage Stability of Calcium Sulfoaluminate-belite Cements with Varying Calcium Sulfate Content" 64
3.4.1. Abstract 65
3.4.2. Introduction 65
3.4.3. Results and discussion 69
3.4.5. Ettringite formation 77
3.4.6. Phase assemblage 79
3.4.7. Belite Hydration Products 81
3.4.8. Thermodynamic Modelling Phase assemblage 83
3.4.9. Conclusions 89
3.5. Further Results and Discussion 91
3.5.1. Thermogravimetric Analysis (TGA) with Mass Spectroscopy (TG-MS) 91
3.5.2. X-ray diffraction 95
3.5.3. Rietveld Analysis 96
3.5.4. Mercury Intrusion Porosimetry 100
3.5.5. Conclusions and Future Investigations 103
3.6. Acknowledgements 105
4. Alkali-Activated Material as a Future Encapsulant 107
4.1. Introduction 107
4.2. A Brief History of Alkali Activated Material 107
4.3. Alkali Activated Material and the UK Nuclear Industry 109

4.4. Results and Discussion 110
4.4.1. XRD Results 110
4.4.2. TG-MS Results 114
4.4.3. FTIR Results 118
4.4.4. SEM, EDS, and Optical Observations 122
4.5. Conclusions and Future Investigations 132
4.6. Acknowledgements 133
5. Heavy Industry 134
5.1. Introduction 134
5.2. The Rise of Portland Cement 134
5.3. High Alumina Cement (HAC) 139
5.4. Understanding Heavy Industries 142
5.5. Disrupting Heavy Industry 153
5.6. Climate Change 160
5.7. Innovation, the Chasm of Adoption, and the Technology Readiness Level assessment 166
6. Future Directions 174
6.1. Introduction 174
6.2. Calcium Sulfoaluminate 174
6.3. Metakaolin Geopolymer 180
7. Conclusion 185
References 186

Abstract

There has been dramatic change in the operation of UK heavy industry over the past few decades, putting the availability of materials crucial to currently established Portland cement compositions for the application of radioactive waste encapsulation under question. The uncertainty surrounding the availability of these materials means that it is now viable for the nuclear industry to explore options with regards to successor cements, many of which are now in reliable and continuous supply, with demonstrable records of performance in experimentation and construction. This is an opportunity for investigation into cements that may not only be more sustainable, and therefore more likely to be easily obtainable for decades to come, but also those that may offer enhanced performance characteristics.

This thesis aims to build upon the knowledge base of two potential cements for nuclear applications: calcium sulfoaluminate and metakaolin geopolymers. In collaboration with the UK nuclear industry, two large scale series of commercially available grout trials were conducted, followed by an extensive review of the phase assemblage in the context of the unique requirements for the encapsulation and/or immobilisation of radioactive waste. This represents a significant step in the maturity of both of these systems and their potential adoption by the industry, bridging the gap between small scale laboratory experiments and full-scale mix trials. The robustness of both systems was proved on a 90-day timescale and beyond, with a range of mixing variables appropriate for nuclear applications.

Following this, the technology readiness level of each cement is considered, as well as the likelihood of these cements being adopted by the wider cement market so much as to ensure the security of their supply. Not only is this assessed in terms of the maturity of the technology, but also a discussion is held about the adoption of Portland cement almost two centuries prior, and the behaviour of heavy industry, particularly towards emerging technologies. Any similarities may then be drawn to better understand how the cements market might react in the future to these alternative binder systems. Both of these cement systems are actively being researched and have been used successfully. Calcium sulfoaluminate is of particular interest to the construction industry, with an increasing case portfolio of rapid set and strength gain applications, and a more familiar production and application method.

Acknowledgements

For John Arthur Nelson

Inspiration, mentor, grandfather.

This thesis would not have been possible without the help and support of almost 100 individuals. Firstly, I need to express how grateful I am for the support of my loving family and my partner Mollie, all of whom gave me my foundations during this rather tumultuous couple of years. My gratitude also extends to the staff of the National Nuclear Laboratory of Workington, whose hard work and guidance allowed me to produce this thesis, and who made me feel so welcome during my work placement in Cumbria.

The encouragement from my supervisors, John, Mike, Martin, and Gavin, was always unwavering and their input always invaluable. I would also like to thank my friends at the University of Sheffield, for although a thesis is written in solitary, being a part of the cements group made me feel like part of a team. Particularly I would like to thank Dan Geddes and Sarah Kearney for their considerable efforts in helping to make this thesis a reality.

Finally, I would like to show my appreciation to Nuclear Decommissioning Authority and the Engineering and Physical Sciences Research Council for funding this project, as well as Sellafield Ltd and Nuclear Waste Services for their thoughtful cooperation.

"I think cement is… more interesting… than people think!" – John Cleese, as Mr. Gumby.

Monty Pythons Flying Circus, S.1 Ep.11, The battle of Trafalgar sketch, 1969.

Thesis Introduction

The 2022 UK Radioactive Waste Inventory details 5.1 million tons of material, ranging from spent nuclear fuel to contaminated material [1]. This inventory is uniquely diverse, as anything can be classified as a contaminated material if exposed to a source of radiation. Laboratory consumables, scientific equipment, tools, clothing, appliances, lubricants, windows, doors, plant machinery, concrete, and soil, are just some examples of material that is required to be isolated from the environment and disposed of. Accounting for estimated future arisings, the current total reported volume of radioactive waste equates to 4.58 million m^3 of material [1]. Of this, <0.1% is classified as high-level waste (HLW) (see section 1.2) which incorporates the spent nuclear fuel and the majority of fission products [2]. 60% is classified as very low-level waste (VLLW, section 1.2) and is due for disposal via conventional means such as landfill with along with ordinary household waste. The leaves approximately 40% of the inventory which requires some form of encapsulation as part of an engineered barrier system, removing it from the wider ecosystems for sufficient time so allow for its radioactivity to decay to a level that poses no ecological threat to the environment [1]. Final disposal is due to be achieved using a near surface and deep geological disposal facilities where appropriate [3, 4].

The following results chapters focus upon cementitious alternative binder systems for the encapsulation of intermediate level waste (ILW, section 1.2). This work was done in collaboration between the National Nuclear Laboratory, the University of Sheffield, and Sellafield Ltd of whom operate the encapsulation plants that incorporate much of the UK's ILW into wasteforms, ready for later GDF disposal. In these chapters the phase assemblage of calcium sulfoaluminate (CSA) (chapter 3) and metakaolin geopolymers (chapter 4) are examined when produced within a formulation envelope that has been developed to best suit the process requirements of ILW encapsulation. These studies were conducted to assess robustness of the alternative binder systems, through large scale trials with multiple mixing variables. This work was done in tandem of a more mechanical focused study done by NNL themselves, which together with the work presented here has allowed for the nuclear industry to evaluate the characteristics and performance of each cement grout system.

Furthermore, a key focus of this thesis is an attempt to understand why, despite both of these alternative cement systems having existed from at least the mid-20th century, they are still considered as alternative, or novel binder systems. First, a consideration is made as to how, and the timescale of how, Portland cement (PC) came to be the market dominator amidst the competition of the 19th century. This is followed by a brief look into the high alumina cement system which was adopted significantly in the 20th century before being excluded from structural applications. Then, an examination through case studies is made towards the general behaviour of heavy industries like that of the cements and construction industries, as well as to how these conservative entities respond to disruption, due to innovative technologies or otherwise.

Finally, a discussion is held upon the technology readiness level of these alternative cement systems. In order to be a viable alternative against PC for radioactive waste encapsulation, the materials must be commercially available for the long term to ensure a security of supply for long term operations. Their position to be adopted by industry and taken forward as a practicable and available product in the UK is evaluated.

Key Acronyms and Nomenclature

AAM – Alkali Activated Material

BFS – Blast Furnace Slag (see also GGBFS)

CCS – Carbon Capture and Storage

CSA – Calcium Sulfoaluminate

EDS – Energy Dispersive X-Ray Spectroscopy (also EDX)

ETA – European Technical Assessment

FA – Fly Ash (see also PFA)

FTIR – Fourier Transform Infrared Spectroscopy

GDF – Geological Disposal Facility

GDP – Gross Domestic Product

GGBFS – Ground Granulated Blast Furnace Slag (see also BFS)

HAC – High Alumina Cement

HLW – High Level Waste

ILW – Intermediate Level Waste

LLW – Low Level Waste

MIP – Mercury Intrusion Porosimetry

NDA – Nuclear Decommissioning Authority (UK)

NNL – National Nuclear Laboratory (UK)

PC – Portland Cement (also OPC)

PFA – Pulverised Fuel Ash (see also FA)

SCM – Supplementary Cementitious Materials

SEM – Scanning Electron Microscopy

TGA – Thermogravimetric Analysis

TG-MS – Thermogravimetric Analysis with Mass Spectroscopy

TRL – Technology Readiness Level

UK – United Kingdom

XRD – X-Ray Diffraction

Cement chemistry abbreviated notation is used throughout, where C represents CaO, A is Al_2O_3, S is SiO_2, H is H_2O, and \$ or $\bar{S}$ is SO_3.

A note from the author:

This publication features both the traditional English spelling of the element ‘sulphur’, as well as the internationally recognised spelling ‘sulfur’. This spelling of ‘sulfur’ has been used where possible and in publications with potential international reach, as it is the convention in a large proportion of the English-speaking world. This publication also uses the term Geopolymer to describe a low or negligible calcium containing alkali activated material. Otherwise, the term alkali activated material is used.

List of Figures

Figure 1. Depiction of the nuclear fuel cycle, showing both the open and closed cycle routes [49]. ... 29

Figure 2: Simplified diagram illustrating the dry Portland cement clinkerization process, based upon the description of Taylor et al. [95]. ... 38

Figure 3: The crystal structure of ettringite as given in Cody et al. [108]. Image A shows the ettringite column structured crystals in a hexagonal prismatic structure extending along the c-axis. Image B then shows the arrangement of these columns from a top down view, surrounding sulfate molecules [108]. ... 41

Figure 4: Data from Zhou et al.[111] showing the hysteresis loop of stable and reformation area for ettringite (far left zone), the area of the potential conversion to meta-ettringite (central zone), and the area of ettringite decomposition (far right zone), with a temperature uncertainty value given in parenthesis for each datapoint [111]. ... 42

Figure 5: From Baquerizo et al. [106] showing the hysteresis loop with the reformation area for ettringite (far left zone), the area of ettringite stability (central zone), and the area of ettringite decomposition (far right zone) similar to that presented in Zhou et al. [111]. The “theoretical zero” curve is a boundary between expected zones of ettringite stability and decomposition [106]. ... 43

Figure 6: Si tetrahedra (SiO_4) and Al tetrahedra (AlO_4) respectively, showing individual and overall charges (within brackets). Al tetrahedra display a higher negative charge, which is balanced in AAM by nearby alkali metal species. ... 46

Figure 7: A representation of the C-A-S-H type gel based upon the work of Myers et al. [132]. Ca^{2+} and H^+ species are represented by blue circles, balancing the charge of the blue Si tetrahedra. Orange circles represent the Na^+ and K^+ species that balance the charge of the Al substituted tetrahedra [133]. All of these species, as well as water, form the interlayer between the aluminosilicate chains, which are made up of dreierketten units. ... 46

Figure 8: A flow chart detailing the key distinctions between the high and low calcium AAM systems, by Provis and Bernal. [131]. ... 47

Figure 9: A flow chart representing the proposed main stages of geopolymer formation by Duxson et al. [136]. 48
Figure 10: Raw material component XRD, showing key phases present for anhydrite and gypsum calcium sulfate sources, as well as Alipre and Alpenat CSA clinker. 50
Figure 11: TOPAS working file showing the calculated fit in red overlaying the experimental data in blue, which is almost completely overlaid. The raw experimental data is also show above in blue. The thicker dark blue line at the bottom illustrates the peaks for ettringite and how they intercept the peaks identified in the working model. 56
Figure 12: A diagram representing the phase formation with temperature during the clinkerization process for PC. Image from Hanein et al. [192] and adapted from Taylor [5]. This image highlights the region in which alite is formed, which can be compared to CSA phases, including ye'elimite that forms at approximately 1250 ℃ [103]. 61
Figure 13: A phase depicting the formation of belite ye'elimite ferrite (BYF) CSA clinker, reconstructed from Ben Haha et al. [196] to show the units in Celsius for easier direct comparison [196]. 62
Figure 14: The Shenyang Long Distance Telecommunication Hub, which involved CSA concrete laid in as low as -20 ℃, as detailed in Zhang et al. [177]. 63
Figure 15: XRD pattern for Alipre clinker, with anhydrite at either 15% or 35% and a w/s ratio of 0.5 or 0.7. Increased ye'elimite hydration can be observed by the decrease of the main peak at 23.7 °2θ with increasing calcium sulfate and water content. Background levels have been reduced, most notably preceding 8 °2θ, in order to generate this figure. 72
Figure 16: XRD pattern for Alpenat clinker, with gypsum at either 15% or 35% and a w/s ratio of 0.5 or 0.7. The signature for strätlingite is visible at 7.2 °2θ, (red dot) in the low gypsum and high-water mix at 28 days and beyond. Background levels have been reduced, most notably preceding 8 °2θ, in order to generate this figure. 73
Figure 17: This concentric Rietveld analysis plot, for an Alipre mix containing 35% anhydrite and a w/s ratio of 0.7, displays the weight percentage (%) of main phases detected over the 90-day period.

Most notably, the increased production of ettringite between 7 and 28 days, as opposed to between 28 and 90 days, is clearly shown in this mix. 74
Figure 18: TGA for Alipre clinker, with anhydrite at either 15% or 35% and a w/s ratio of 0.5 or 0.7. An increase in ettringite content is evident with an increase in anhydrite, and to a lesser extent, water content. 75
Figure 19: TGA for Alpenat clinker, with gypsum at either 15% or 35% and a w/s ratio of 0.5 or 0.7. The signature for strätlingite is visible at approximately 220 °C in the low gypsum and high-water mix at 28 days and beyond. 76
Figure 20: An ettringite 'nest', where the lath shaped crystals have grown into a pore; a clear indication of ettringite growth after the initial setting of the Alpenat mix with low gypsum (15%) and a w/s ratio of 0.7. This sample was taken at 90 days. 78
Figure 21: SEM imagery showing very similar structures of ettringite lath crystals within an aluminium hydroxide matrix, between differing clinkers, types of calcium sulfate, and w/s ratios. Un-hydrated calcium sulfate and clinker particles can also be observed. 79
Figure 22: SEM-EDS mapping of Alipre with high gypsum (35%) and a w/s ratio of 0.7. Ettringite, belite and aluminium hydroxide can clearly be identified their characteristic elemental signatures. 80
Figure 23: CemGEMS simulation for Alipre clinker at an anhydrite addition of 15% and a w/s ratio of 0.5. The level of hydration, so as to be comparative to experimental results, was set to 66%. Anhydrite levels are predicted to become depleted, leading to the generation of monosulfoaluminate. 85
Figure 24: CemGEMS simulation for Alipre clinker at an anhydrite addition of 35% and a w/s ratio of 0.7. The level of hydration, so as to be comparative to experimental results, was set to 76%. The potential for late stage belite hydration is shown as a small quantity of strätlingite formation. 86
Figure 25: CemGEMS simulation for Alpenat clinker at a gypsum addition of 15% and a w/s ratio of 0.5. The level of hydration, so as to be comparative to experimental results, was set to 63%. The increased quantity of belite when compared to Alipre clinker, has allowed for Alpenat to form more strätlingite, though a significant proportion remains unreacted. >1% C-S-H has been simulated up until 20 hours, where it is proceeded by the appearance of monosulfate and the increasing quantity of strätlingite. 87

Figure 26: CemGEMS simulation for Alpenat clinker at a gypsum addition of 35% and a w/s ratio of 0.7. The level of hydration, so as to be comparative to experimental results, was set to 75%. Increase ettringite formation has likely hindered belite hydration, however; some belite hydration has occurred without the presence of gibbsite, forming C-S-H (Eq.3.4). 88
Figure 27: CemGEMS simulation for Alpenat clinker at an anhydrite addition of 35% and a w/s ratio of 0.7. The level of hydration, so as to be comparative to experimental results, was set to 65%. The formation of strätlingite appears to prefer the presence of gypsum over anhydrite, as development of strätlingite is negligible, with only a small quantity of C-S-H. The simulation does not identify any calcium hydroxide..... 89
Figure 28: TGA with accompanying MS for an Alpenat mix with a gypsum addition of 25%, a water to solid ratio of 0.6, conducted at a high shear, highlighting the correspondence between TGA and MS signals. Ettringite and gibbsite (aluminium hydroxide) peaks are highlighted. Trace amounts of carbonation and the decarbonation of the small quantity of calcium carbonate present at 650 °C..... 93
Figure 29: TGA for midpoint formulation samples (as marked in each panel) at 7, 28, 90 and >900 days. Differences in age for the later-age samples are representative of the time between when mixes were conducted, due to the extensive series of samples produced, with the arresting of hydration then commencing at the same time. All were conducted under high shear mixing..... 94
Figure 30: TGA scans for high calcium sulfate and water samples (as marked in each panel) at 7, 28, 90 and >800 days. Differences in age for the later-age samples are representative of the time between when mixes were conducted, due to the extensive series of samples produced, with the arresting of hydration then commencing at the same time. All were conducted under high shear mixing..... 95
Figure 31: XRD diffractograms produced from midrange mix samples at 7, 28, 90, and >900 days of curing before hydration was arrested. The potential, very minor indication of strätlingite is highlighted with the red dot beneath and shown close up in the red box..... 96
Figure 32: Rietveld analysis percentage quantities shown in a concentric circle diagram. Diagram highlights the difference between 90 days and prior, to 913 days for an Alipre midpoint formulation containing anhydrite..... 97

Figure 33: Rietveld analysis percentage quantities shown in a concentric circle diagram. Diagram highlights the difference between 90 days and prior, to 920 days for an Alipre midpoint formulation containing gypsum. 98
Figure 34: Rietveld analysis percentage quantities shown in a concentric circle diagram. Diagram highlights the difference between 90 days and prior, to 932 days for an Alpenat midpoint formulation containing anhydrite. 98
Figure 35: Rietveld analysis percentage quantities shown in a concentric circle diagram. Diagram highlights the difference between 90 days and prior, to 926 days for an Alpenat midpoint formulation containing gypsum. 99
Figure 36: CemGEMS simulation for Alipre clinker at an anhydrite addition of 25% and a w/s ratio of 0.6. The level of hydration, so as to be comparative to experimental results, was set to 65%. This simulation demonstrates a greater quantity of strätlingite formation than is suggested in the Rietveld analysis and observed in the XRD. 100
Figure 37: MIP results highlighting any relationship between the porosity percentage and the addition of anhydrite, for both types of CSA clinker (L/M/H indicate Low – 15%, Medium – 25%, High – 35%). The water to solid ratio is given for each sample on the x-axis, along with the mix shear component (High / Low). Figure prepared by S. Kearney. 101
Figure 38: MIP results highlighting any relationship between the porosity percentage and the addition of gypsum, for both types of CSA clinker (L/M/H indicate Low – 15%, Medium – 25%, High – 35%). The water to solid ratio is given for each sample on the X-axis, along with the mix shear component (High / Low). Figure prepared by S. Kearney. 102
Figure 39: MIP results highlighting any relationship between the porosity percentage and the availability of water, for both types of CSA clinker. The type of calcium sulfate (Anhydrite / Gypsum) is given alongside the amount (Low – 15%, Medium – 25%, High – 35%) upon the x-axis, alongside with the mix shear component (High / Low). Figure prepared by S. Kearney. 103
Figure 40: XRD patterns for Metamax metakaolin geopolymers between 7 and 90 days. SiO_2/K_2O 1.4, H_2O/K_2O 11, K_2O/Al_2O_3 1.0, low shear. Clearly displays the characteristic amorphous region between

20-40 °2θ that is indicative of the metakaolin geopolymer structure. Main anatase (TiO_2) peak is shown. 112
Figure 41: XRD patterns for Argicem metakaolin geopolymers between 7 and 90 days. SiO_2/K_2O 1.4, H_2O/K_2O 11, K_2O/Al_2O_3 1.0, low shear. Displays the characteristic amorphous region between 20-40 °2θ that is indicative of the metakaolin geopolymer structure. Main anatase (TiO_2) and quartz (SiO_2) peaks are shown. 112
Figure 42: XRD patterns for Metamax metakaolin geopolymers between 7 and 90 days. SiO_2/K_2O 1.0, H_2O/K_2O 15, K_2O/Al_2O_3 1.5, low shear. Clearly displays the characteristic amorphous region between 20-40 °2θ that is indicative of the metakaolin geopolymer structure, as well as the efflorescence encountered at approximately 30 °2θ. Main anatase (TiO_2) peak is also shown. 113
Figure 43: XRD patterns for Argicem metakaolin geopolymers between 7 and 90 days. SiO_2/K_2O 1.0, H_2O/K_2O 15, K_2O/Al_2O_3 1.5, low shear. Clearly displays the characteristic amorphous region between 20-40 °2θ that is indicative of the metakaolin geopolymer structure, as well as the efflorescence encountered at approximately 30 °2θ. Main anatase (TiO_2) and quartz (SiO_2) peaks are also shown. 113
Figure 44: TGA of four mixes metakaolin geopolymer mixes at between 7 and 90-days. A – MetaMax, SiO_2/K_2O 1.4, H_2O/K_2O 11, K_2O/Al_2O_3 1.0, low shear. B – MetaMax, SiO_2/K_2O 1.0, H_2O/K_2O 15, K_2O/Al_2O_3 1.5, low shear. C – Argicem, SiO_2/K_2O 1.2, H_2O/K_2O 13, K_2O/Al_2O_3 1.2, high shear. D – Argicem, SiO_2/K_2O 1.0, H_2O/K_2O 15, K_2O/Al_2O_3 1.0, low shear. Structural water signature can be clearly seen at approximately 120 °C, as well as a minor calcium carbonate signature at 650 °C only found in Argicem mixes. Derivative weight loss is significantly reduced in Argicem mixes due to the high quantity of unreactive quartz present. Curves are very similar over all mixing variables, demonstrating the formation of a consistent structure. 116
Figure 45: TG-MS for Argicem, SiO_2/K_2O 1.4, H_2O/K_2O 11, K_2O/Al_2O_3 1.0, high shear. MS demonstrates a temperature relationship that helps identify the decomposition of phases; however, the amplitude is not representative of the derivative weight loss shown. 117
Figure 46: TG-MS for Argicem, SiO_2/K_2O 1.4, H_2O/K_2O 15, K_2O/Al_2O_3 1.5, high shear. This mix experienced segregation, which at 90 days is compared against the rest of the solid product. A

signature for potassium hydrogen carbonate is clearly visible in the segregated layer (peak of 150 ℃)[255]. 117
Figure 47: FTIR analysis performed on an Argicem mix at 7, 28 and 90 days. SiO_2/K_2O 1.2, H_2O/K_2O 13, K_2O/Al_2O_3 1.2, low shear..... 120
Figure 48: FTIR analysis performed on an Argicem mix at 7, 28 and 90 days. SiO_2/K_2O 1.2, H_2O/K_2O 13, K_2O/Al_2O_3 1.2, high shear. 120
Figure 49: FTIR analysis performed on a MetaMax mix at 7, 28 and 90 days. SiO_2/K_2O 1.2, H_2O/K_2O 13, K_2O/Al_2O_3 1.2, low shear. The amplitude of the scan at 90 days is slightly less than that of the other two time periods, however; it affects all features equally, this is due to the equipment and not the sample itself. 121
Figure 50: FTIR analysis performed on a MetaMax mix at 7, 28 and 90 days. SiO_2/K_2O 1.2, H_2O/K_2O 13, K_2O/Al_2O_3 1.2, high shear. 121
Figure 51: An example of the white potassium carbonate efflorescence that has formed upon SEM prepared samples of both Argicem (left) and MetaMax (right) geopolymers. Approximately 5 mm by 10 mm surface area. 122
Figure 52: SEM images of geopolymers at ×40 magnification, clearly showing the formation of efflorescence upon the surface of samples prepared for SEM after 7 days of curing, but more prominently within cracks shown upon the surface. Top left: Argicem, SiO_2/K_2O 1.0, H_2O/K_2O 15, K_2O/Al_2O_3 1.5, low shear. Top right: MetaMax, SiO_2/K_2O 1.0, H_2O/K_2O 15, K_2O/Al_2O_3 1.5, high shear. Bottom left: Argicem, SiO_2/K_2O 1.0, H_2O/K_2O 11, K_2O/Al_2O_3 1.5, high shear. MetaMax, SiO_2/K_2O 1.4, H_2O/K_2O 15, K_2O/Al_2O_3 1.5, high shear. 124
Figure 53: SEM imagery of surface efflorescence at 90 days and ×250, ×500, ×1000 and ×2500 magnification for Argicem geopolymers, SiO_2/K_2O 1.0, H_2O/K_2O 15, K_2O/Al_2O_3 1.5, high shear. . 125
Figure 54: SEM images of MetaMax geopolymers, SiO_2/K_2O 1.4, H_2O/K_2O 11, K_2O/Al_2O_3 1.0, low shear after 7 days of curing. Magnification at ×250, ×500, ×1000, and ×2500. 126
Figure 55: SEM images of MetaMax geopolymers, SiO_2/K_2O 1.0, H_2O/K_2O 15, K_2O/Al_2O_3 1.5, low shear after 7 days of curing. Magnification at ×250, ×500, ×1000, and ×2500. 126

Figure 56: SEM images of MetaMax geopolymers, SiO_2/K_2O 1.4, H_2O/K_2O 11, K_2O/Al_2O_3 1.0, low shear after 90 days of curing. Magnification at ×250, ×500, ×1000, and ×2500. 127
Figure 57: SEM images of MetaMax geopolymers, SiO_2/K_2O 1.0, H_2O/K_2O 15, K_2O/Al_2O_3 1.5, low shear after 90 days of curing. Magnification at ×250, ×500, ×1000, and ×2500. 127
Figure 58: SEM images of Argicem geopolymers, SiO_2/K_2O 1.2, H_2O/K_2O 13, K_2O/Al_2O_3 1.2, high shear after 7 days of curing. Magnification at ×250, ×500, ×1000, and ×2500. 128
Figure 59: SEM images of Argicem geopolymers, SiO_2/K_2O 1.0, H_2O/K_2O 15, K_2O/Al_2O_3 1.0, low shear after 7 days of curing. Magnification at ×250, ×500, ×1000, and ×2500. 128
Figure 60: SEM images of Argicem geopolymers, SiO_2/K_2O 1.2, H_2O/K_2O 13, K_2O/Al_2O_3 1.2, high shear after 90 days of curing. Magnification at ×250, ×500, ×1000, and ×2500. 129
Figure 61: SEM images of Argicem geopolymers, SiO_2/K_2O 1.0, H_2O/K_2O 15, K_2O/Al_2O_3 1.0, low shear after 90 days of curing. Magnification at ×250, ×500, ×1000, and ×2500. 129
Figure 62: EDS maps at ×1000 magnification of Argicem geopolymer, SiO_2/K_2O 1.4, H_2O/K_2O 11, K_2O/Al_2O_3 1.5, high shear after 7 days of curing. Scan highlights the inclusion of unreacted quartz within the solid. 130
Figure 63: EDS maps at ×1000 magnification of Argicem geopolymer , SiO_2/K_2O 1.2, H_2O/K_2O 13, K_2O/Al_2O_3 1.2, low shear after 90 days of curing. Scan highlights the potassium carbonate that has formed. 131
Figure 64: EDS maps at ×1000 magnification of MetaMax geopolymer, SiO_2/K_2O 1.2, H_2O/K_2O 13, K_2O/Al_2O_3 1.2, low shear after 7 days of curing. 131
Figure 65: The patent filed by Joseph Aspdin in 1824 for Portland cement [274]. 135
Figure 66: An epitaph written within one of the controversial gullwing style stainless steel doors by members of the Dunmurry workforce during the final days of DeLorean DMC-12 production [311]. 149
Figure 67: A diagram illustrating the movement of hunting oscillation and its detriment to railed transport, as depicted in Mazilu [319]. 151
Figure 68:The ROHR Inc tracked air cushion vehicle (TACV) in Pueblo, Colorado. Driven by a linear induction motor to 145 mph, with a seating capacity of 60 in airline style comfort [323]. 152

Figure 69: The remains of the abandoned Paris to Orléans Aérotrain link as can be seen currently [323]. 153
Figure 70: Diagram from the phase 1 Grenfell Tower fire report showing the insulation and cladding structure attached to the original concrete tower exterior (image top). This shows the composite cassettes hung upon the exterior of the building, with the void which accelerated the fire's spread [325]. 155
Figure 71: Aerial view of Ffos-y-fran open cast coal mine, the largest left in the UK [337]. 157
Figure 72: Oilseed meal briquettes [342]. 158
Figure 73: A comparison between the percentages of those employed in service, manufacturing, agricultural, and construction industries in the UK, separated by 65 years. Study and image by the Office of National Statistics [346]. 159
Figure 74: Figure from the 2018 Chatham House report compiled by Lehne & Preston [6], showing the required trajectory, split into individual technologies, required to achieve the 2DS scenario by 2050. Also shown are the beyond 2DS and reference technology scenarios [6]. 163
Figure 75: Lignite Energy Council advertising their award as part of their sizable funding towards local high schools in the North Dakota area [382, 385]. 164
Figure 76: Billboard erected by the Lignite Energy Council to promote their 'Thank a Coal Worker' campaign, where individuals can submit praise online via their website in regards to the coal industry [387]. 164
Figure 77: Propaganda from the lobbyist group 'Count on Coal', published in March 2023, in reference to Germany being forced to turn back to thermal coal power due to gas shortages as a result of the war in Ukraine [353, 380, 384]. 165
Figure 78: Climate activists sabotaging the Lafarge-Holcim Marseille Cement Plant in December of 2022 [388]. 165
Figure 79: Representation of the first half of the technology adoption profile, showing the theoretical chasm between the early adopters and the pragmatic. 167
Figure 80: The original drawing of the technology adoption profile, shown in 1989 [395]. 167
Figure 81: TRL assessment as adopted and used by NASA [412]. 170

Figure 82: TRL scale adopted for use by the IEA, adapted to feature 11 different levels so as to account for greater levels of maturity demanded by conservative heavy industries [415]. 172
Figure 83: Conclusions drawn by the IEA in 2020 for the progress and TRL of CCS technologies, utilising the 11 tier system defined in Figure 79 [415]. 173
Figure 84: Illustration depicting the manufacturing processes for sodium hydroxide and sodium silicate, commonly used for the production of geopolymer alkali activator solutions, as depicted by Turner & Collins [434]. 181

List of Tables

Table 1: Ready-mix concrete pricing approximations for the UK calculated in both 2019 and 2022. Pricing is exclusive of delivery, value added tax, and other potential pricing variables [24, 25]. 26

Table 2: The UK radioactive waste four subcategories, accounting for radioactivity and heat generation [2, 4, 60, 61]. 30

Table 3: Rietveld analysis composition for Italcementi Alipre and Vicat Alpenat CK clinkers, showing phases of significance. 49

Table 4: Identified clinker compound percentages when theoretically adjusted for the calcium sulfate addition. 50

Table 5: Composition of Argicem and Metamax metakaolin as identified using XRF, as well as loss on ignition (LOI) at 950 °C, identified by NNL 51

Table 6: Argicem and MetaMax powder characteristics as identified by NNL using laser diffraction and Blaine fineness 52

Table 7: Metakaolin geopolymer mix matrix, with each mix being produced using each of the two different metakaolin powders used. The SiO_2/K_2O and H_2O/K_2O ratios refer specifically to the composition of the activating solution, and the K_2O/Al_2O_3 ratio defines the relationship between the activator and metakaolin contents. 53

Table 8: Sources of the CIF files used from literature in order to conduct the Rietveld analysis. 56

Table 9: A modified and updated version of the table first presented by Aranda et al. [178]. Consider also the different spellings of ‘sulfur/sulphur’, and how that may reduce the visibility of some publications when searched for online [179]. 60

Table 10: Rietveld analysis results displaying the weight percentage (wt. %) of each phase detected, for all 120 mixes that contain either Alipre clinker (Ali - blue) and Alpenat CK clinker (Alp -green) clinkers. Inert phases detected, or those that could be classed as minor, were omitted. The full list of phases identified is given in Table 8. 71

Table 11: Rietveld analysis of the XRD data displayed in Figure 31. Difference in age is representative of the time between when mixes were conducted due to the extensive series, with the arresting of hydration then commencing at the same time. 97
Table 12: FTIR signals that are commonly associated with metakaolin geopolymers. Adapted from the work of Geddes [141]. 118
Table 13: TRL defined scale, based upon the descriptions by Hills et al. [371] which itself is based upon the NASA adopted scale [371, 412]..... 171
Table 14: TRL evaluation conducted by Hills et al. [371] for a number of innovative carbon capture technologies [371]..... 171
Table 15: TRL assessment for the CSA family of cements, as based upon the NASA criteria [412] 178
Table 16: TRL assessment for geopolymers, based upon the NASA criteria [412]. 183

1. Literature Review

1.1. Cement – A Brief Summary

The international cements industry is overwhelmingly based on Portland cement (PC); a hydraulic clinker material produced from limestone and clay, or a material of similar composition, and interground with calcium sulfate [5]. An estimated 4 billion tonnes of cement are produced worldwide every year [6]. It has been claimed that concrete, the material produced upon the hydration of cement mixed with aggregate, is second only to water as the most used material on earth [7-9]. Assuming that concrete on average contains 250 kg of cement per m^3, this equates to 2 m^3 of concrete for every person on earth per year [6, 9, 10]. Now fundamental to the needs of the construction industry, concrete has been used as a building material for millennia. One of the earliest known examples is that of the fishing hut floor of Lepenski Vir, Serbia, which hosts a lime concrete floor dating back to as far as 5600 BC [11].

PC was not the first commercially available cementitious material. What became to be known as 'Roman' cement was patented in 1796 by James Parker, which consisted of septarian nodules found in London clay, broken and calcined at approximately 1000 ˚C before being ground to form a clinker [12, 13]. Prior to this, the Roman empire developed its own concrete, using naturally occurring pozzolanic material, such as volcanic ash which is readily available in the Mediterranean, as the basis of what is now referred to as a lime-pozzolan cement [14]. Many of these impressive structures, like the Pantheon in Rome, are still standing after two millennia [15]. Comparable alkali-activated cement systems are now being investigated due to their lower carbon footprint compared to that of a Portland cement system [16]. Both of these alternative 'Roman' cement systems were side-lined once PC became the market dominator.

Whilst PC was originally patented in 1824, it was not until approximately 30 years later that what can now be recognised to be a PC was first put into production – though the exact date and person responsible for this are still open to some interpretation [9, 11, 17, 18]. PC has evolved into the material we know today, often with small incremental changes and improvements made over its lifetime

encouraged through technological advancement and more demanding requirements [18]. This has resulted in a material that is cheap, practical, largely predictable, and that can be produced to numerous different specifications and classifications to fulfil a wide range of purposes [17].

The global cements industry has risen significantly within the past decade, with production rising from 3.3 to 4.3 billion tonnes from between 2010 and 2020 [19]. In 2018, the Royal Institute of International Affairs [6] forecast an increase in global cement production from 4 billion to 5 billion tonnes in the next 30 years, fuelled by the rapid rate of urbanisation in areas such as south east Asia, India, and China [6]. The 2018 United Nations World Urbanisation report [20] finds that 55% of the world's population is now living in urban areas, up from 30% in 1950 and expected to climb to 68% by 2050, with India and China projected to contribute 416 million and 255 million more urban dwellers respectively [20]. A more recent 2021 report by the International Energy Agency [19] forecasts that in a net zero emissions scenario, cement production will plateau at approximately 4.3 billion tonnes as production in China reduces, offsetting the increased production in other markets [19]. China will still be the nation that produces the most cement, however, currently producing 55% of cement globally, followed by India contributing 8% [19].

The construction industry, as the dominant consumer of cement, has great influence over cement specifications, chief among which, due to the vast quantities of cement required to produce the 10 billion tonnes of concrete consumed annually, is that the unit price of cement has to be kept low. May 2019 prices for a 50 kg bag of ordinary PC in Mumbai were in the region of £3.20 each when purchased in bulk, or £3.50 in 2022 [21]. In 2022, the price of one metric ton of PC was approximately $130 per ton [22]. In the UK, a single 25kg bag of general-purpose PC typically retails at approximately £5; however, the UK is primarily a user of ready-mix concrete that is mixed off-site and delivered [23]. The cost of concrete delivered to a construction site will be heavily dependent upon the specification, bulk quantity, delivery distance and ease of application. For example, if concrete is needed for floor laying within a structure or any site without vehicular access, the concrete may need to be pumped with additional equipment and adhere to flow characteristics that make it possible to do so. An approximate pricing structure is given in in Table 1.

Table 1: Ready-mix concrete pricing approximations for the UK calculated in both 2019 and 2022. Pricing is exclusive of delivery, value added tax, and other potential pricing variables [24, 25].

Strength (MPa at 28 days)	Price per m^3 (£)		£/MPa.m^3	
	2019	2022	2019	2022
8	80	100	10.00	12.50
10	80	100	8.00	10.00
15	85	105	6.00	7.00
20	90	105	4.25	5.30
25	90	110	3.60	4.40
30	95	110	3.20	3.70
35	100	115	2.90	3.30
40	100	115	2.50	2.90
45	105	120	2.30	2.70

Due to PC being relatively inexpensive as a material, localised production is conducted where possible as it is often more cost effective than importation [9, 26]. Only a comparatively small 200 million tonnes of cement are exported each year globally, since keeping transport costs low is vital for maintaining the profitability of production [9, 27, 28]. The cements market is dominated globally by a small number of extremely large producers, with Swiss based company Holcim (formerly LafargeHolcim) having the greatest capacity [28, 29]. Although these large companies operate over multiple continents, there are some noticeable differences in how cement is produced and is carried out in different regions. The way in which cement is sold depends upon the gross domestic product (GDP) of a nation; the higher the GDP, the more likely that cement is sold in bulk as opposed to being sold in standardised bags of 25kg or 50kg [9]. For example, Sri Lanka in 2000 had 98% of all its cement sold in bags [9]. The same trend is then seen in the concrete market, in that the higher a nations GDP the larger its concrete market, meaning a higher proportion of cement is bought in bulk and sold as concrete to a consumer, as opposed to the consumer mixing and producing their own concrete from cement bags on site [9].

The production of cement is highly established in Europe, with some manufacturing plants operating on the same site they have for several decades. Much of the development that led to modern grades of cement was carried out in Europe during the first and second industrial revolutions [11, 17, 30, 31]. This has led to many cement manufacturing plants having evolved and being upgraded over time, implementing new and upgraded systems into pre-existing infrastructure. Whilst this is a more economically viable way of keeping facilities competitive and keeping to efficiency requirements, compared to tearing down and rebuilding large portions of a cement plant, which would incur large investment and considerable down time, it does mean that the facility will be hindered by its older foundational infrastructure, restricting its output and efficiency capabilities [9]. Europe has some of the oldest cement plants in the world, and whilst they may still be profitable, they are outclassed by many of the more modern cement plants. A European cement plant capable of a one-million-tonne output capacity will likely require an investment in the region of approximately £150 million to start up, making cement production very capital intensive [9, 27].

In contrast to Europe, India and other large emerging economies have some of the most advanced facilities in the world, achieving unprecedented output and efficiency targets by taking advantage of the latest technologies and developments. These included the latest developments in dry kiln technology, more efficient pre-heaters, grinders, and separators, as well as modern instrumentation and control systems that allow for enhanced emission management [9, 32, 33]. With the recent requirement for enormous quantities of cement in order to fuel its rapid urbanisation and the expenses associated with importing cement, India has constructed brand new facilities where they are needed and in the vicinity of the raw materials required [33, 34].

In the context of cement for nuclear, the behaviour of the supply chain is an important element for decision making. The maturity of the European cements market is advantageous for its security of supply, however, as a relatively small volume user with very specific product requirements, the UK nuclear industry is greatly affected by its evolution.

1.2. The UK Nuclear Industry

With its development following the end of the second world war, the UK brought online the world's first commercial scale civil nuclear reactor, Calder Hall, in 1956 [35]. Preceded only by the small 5 MWe Russian Obninsk Nuclear Power Plant of 1954, Calder Hall's four 60 MWe reactors provided electricity to the national grid until the site was shut down in 2003 [36, 37]. Calder Hall 1, the first reactor to come online in 1956, operated for 47 years; a significant achievement given that the intended lifespan of a Magnox reactor was just 25 years, and which was achieved by every unit in the UK [38, 39]. The UK civil nuclear program was an offspring of its nuclear defence program, with the Calder Hall program being given the code name 'PIPPA' – standing for Pressurised Pile Producing Power and Plutonium [40].

For a time, the UK pushed for innovation in a number of fields, chief amongst which were its nuclear fuel reprocessing and fast reactor programs [40]. Both of these programs aimed to further a more efficient use of nuclear fuel, as global reserves of viable fissile material are finite [41, 42]. Nuclear fuel reprocessing allows for the removal, reconditioning, and re-use of nuclear fuel from a quantity of spent fuel that has served in a reactor core, of which 97% can typically be reprocessed for further use [43]. Fast reactor technologies allow for a more efficient use of nuclear fuel and can also break down some of the more problematic long-lived radionuclides, thereby reducing the long-term activity of a waste stream. Fast breeder reactors, such as the Prototype Fast Reactor at Dounreay, are capable of producing more fissile material than is consumed in the operation, by converting reprocessed fertile waste material into fissile material [44, 45].

The nuclear fuel cycle (Figure 1) illustrates the production of fissile fuel material, as well as the possible outcomes once that material has been used in a nuclear reactor. In an open nuclear fuel cycle, spent fuel is conditioned and then disposed of, whilst in a closed nuclear fuel cycle, fuel is reprocessed to conserve material reserves and reduce the volume of waste produced (Figure 1) [46-49]. The unfortunate drawback of much of this pioneering work, much of which stems from the early days of nuclear engineering, is that the UK now has a large quantity and huge variety of often complicated nuclear wastes [50].

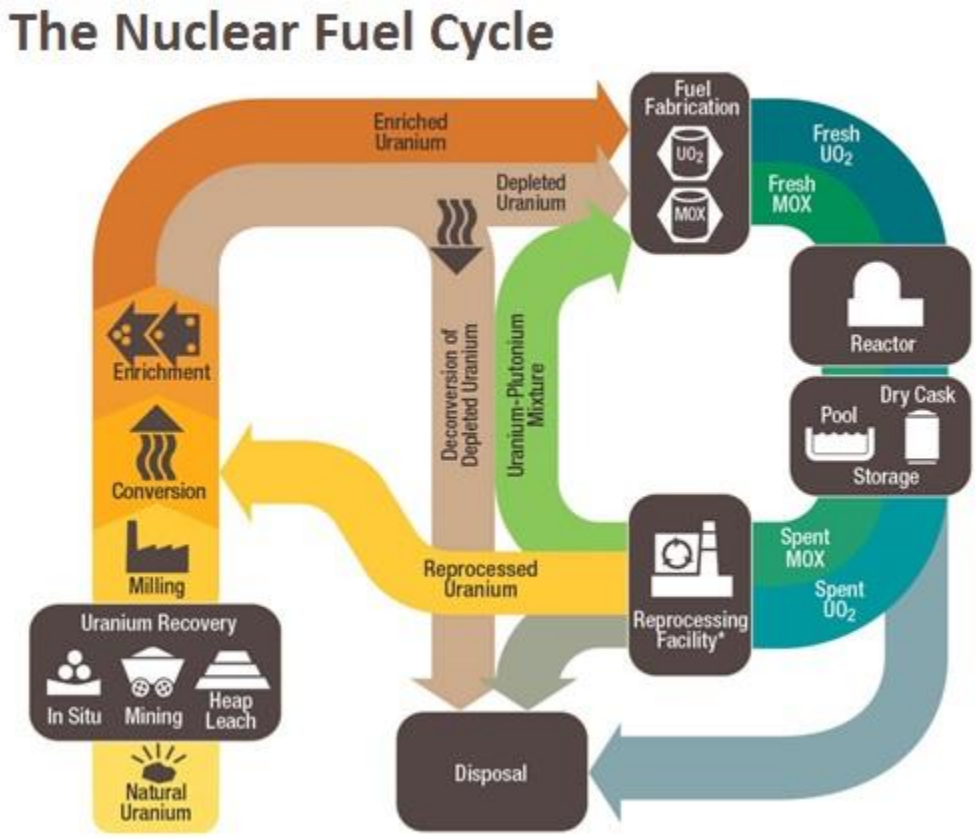

Figure 1. Depiction of the nuclear fuel cycle, showing both the open and closed cycle routes [49].

Towards the end of the 20th century the civil nuclear industry suffered a global decline. High profile incidents such as those at the Three Mile Island and Chernobyl nuclear power stations severely damaged the reputation of nuclear power generation, with many losing faith in the safety of the industry. Denmark and Ireland have gone so far as to outlaw the production of electricity through nuclear means within their borders, and Italy held a referendum in 1987 to phase out its nuclear power production following the 1986 Chernobyl disaster, which was reaffirmed in 2011 with a 94% majority [51-54]. The rising cost of building and running nuclear power facilities also became a limiting factor; whilst fossil fuel fired power stations at the time offered cheap, reliable, and easily adaptable electricity [55].

The start of the 21st century has, however, seen nuclear power return to the political agenda. A new generation of reactors are being put forward, and for the first time in decades, new nuclear power stations are currently under construction in the UK [56]. The requirement for high energy production with low associated carbon emissions has potentially made new-build nuclear a viable option again

[55]. Whilst more conventionally sized facilities, like Hinckley Point C in Somerset are being pursued, new small modular reactor designs offer an interesting alternative. Their modular nature reduces the cost of construction and decommissioning significantly, potentially greatly increasing the financial viability of such reactors [57].

Key to the viability of nuclear power, and what is likely to be the main contentious issue, is how the nuclear waste produced is managed. Historically, in the UK much of the nuclear fuel has indeed been reprocessed to produce new fuel elements, however since 2022 the UK's reprocessing efforts at Sellafield have now ceased. This is due to both a downturn in the demand for processed fuel resulting in the closure of thermal oxide reprocessing plant (THORP) in 2018, and the completion of the reprocessing of the Magnox fuel stockpile in 2022 [58, 59]. The tailings from the reprocessing operations, as well as materials that have come into contact with radioactive substances, such as fuel rod cladding, laboratory equipment, and handling equipment, must also be disposed of. Of particular importance, due to the large amount of diverse nuclear legacy facilities, is the waste produced from decommissioning [1, 50]. The UK radioactive waste inventory is divided into four subcategories (Table 2) [4, 60, 61]:

Table 2: The UK radioactive waste four subcategories, accounting for radioactivity and heat generation [2, 4, 60, 61].

Category	Definition	Further Details
High Level Waste (HLW)	Exceeding 4 GBq per tonne of alpha activity, or 12 GBq per tonne of beta/gamma activity, with a risk of a significant heat output.	HLW, consisting of material from spent nuclear fuel, a significant proportion of which has been reprocessed in the UK to remove uranium and plutonium. The majority of materials therefore are transuranic elements as well as fission products such as caesium-137, strontium-90 and iodine-129. These are vitrified into 150 litre stainless steel canisters and kept in an air-cooled intermediate storage facility for approximately 50 years. This allows for the material to cool and the activity to decrease, improving the ease of transport for disposal in a geological disposal facility or similar engineered facility.

Intermediate Level Waste (ILW)	Exceeding 4 GBq per tonne of alpha activity, or 12 GBq per tonne of beta/gamma activity, without significant heat output.	ILW contains material such prepared metal fuel cladding swarf, graphite moderator, and other contaminated materials such as by plutonium, caesium-137 and strontium-90. This is encapsulated in grout within 500 litre stainless steel drums and stored in an intermediate storage facility. Final disposal will take place within a geological disposal facility or similar engineered facility.
Low Level Waste (LLW)	Not exceeding 4 GBq per tonne of alpha activity, or 12 GBq per tonne of beta/gamma activity, without significant heat output.	LLW, lower activity contaminated materials or disposables, such as soils and spent infrastructure, is grouted in large steel ISO shipping style containers, and stored in a low-level waste repository site near Drigg, Cumbria. Once enough containers are in place within a vault, a concrete lined open plan pit, the vault is capped with a series of layers such as impermeable clays and soil.
Very Low-Level Waste (VLLW)	Below 4 GBq per tonne of alpha activity, or 12 GBq per tonne of beta/gamma activity, by a significant margin, with no heat output.	VLLW, such as concrete rubble, soil and building materials from decommissioned sites, is often appropriate for disposal in common landfill sites. Otherwise, the waste is disposed of as if it were LLW.

The UK as yet has no long-term storage for its stockpiles of conditioned and prepared HLW and ILW [60]. The proposed solution is a deep Geological Disposal Facility (GDF); a network of concrete vaults between 200 m and 1000 m underground so as to be positioned beneath the water table, in which the wasteform containers will be entombed in a cementitious or clay backfill and contained within the vault housed in the host bedrock [3, 62, 63].

A GDF is internationally recognised as the safest storage solution for intermediate and higher-level radioactive waste materials [3, 50]. Having been first officially recommended to the UK government in 2006, following the investigations of the Committee on Radioactive Waste Management (CoRWM), a policy of deep geological disposal has since been adopted by UK and Welsh governments. The Scottish government recommends a closer-to-surface facility instead, located in proximity to where the waste

was generated [64]. There are no plans for a GDF in Northern Ireland, with its policy regarding a GDF as of yet unannounced [64, 65].

The UK government is committed to a policy of community engagement, not wishing to force a GDF upon a population without the general consent of nearby residents, local councils, and relevant governing bodies [64, 66]. The latest renewed effort began in 2018, following a failed 2013 vote by the Cumbria County Council, resulting in their withdrawal from that iteration of the process [67]. Areas with potentially suitable host geology have had preliminary investigations, with working groups and latterly community partnerships currently established in two areas along the Cumbrian coast, mid and south-Copeland, as well as Theddlethorpe on the Lincolnshire east coast.

Suitability investigations and community outreach projects are currently ongoing in all three potential areas. Seismic testing has been conducted in the Irish sea off of the Cumbrian coast, allowing for a better understanding of the geological suitability undersea as sites may extend up to 12 nautical miles from the coastline [64, 68]. Preparations have also been made for bore hole trials, with work conducted into how these holes will be sealed afterwards, before applications for drilling are made [69]. Crucially, however, no GDF sites have yet been formally identified; only potential areas [69].

The lack of a GDF is holding back the development of the nuclear industry in the UK. Without a means of disposing of all categories of radioactive waste, the UK cannot deal with its stockpile of legacy waste and does not have a completed nuclear fuel cycle. This can be interpreted as a reason for not investing in the next generation of nuclear reactors.

1.3. Cement in Nuclear

Cement is used by the UK nuclear industry for the encapsulation and immobilisation of radioactive material of intermediate and low-level classification (Table 2). The high fluidity achievable when using a cementitious grout allows for the encapsulation of large volumes of often very fine and complex waste items, resulting in a dense barrier that acts as a radiation shield and works to contain more mobile radioisotopes and materials effectively. A waste material may be encapsulated or immobilised in the

cement matrix; immobilisation requires the waste to react in some way with the cement matrix in order to be retained within its structure, and encapsulation is the isolation of a waste by completely surrounding it. A waste material with highly mobile radioactive constituents, such as an actinide-containing floc, requires immobilisation to keep it retained within the wasteform [70]. In currently employed cement formulations, C-S-H with its intrinsic nano porosity provides a large surface area and potential sorption sites able to accommodate radionuclides such as the fission product ^{137}Cs, wherein they are retained by weak electrostatic interactions between the species and the cement phase offering high retention over prolonged periods [71-74]. Other phases, such as the AFm phase calcium monosulfoaluminate, may also host anions via sulfate site substitution, or solid solution, such as Cr(IV) [75].

Concrete is an effective shield against radiation and has been used extensively in nuclear construction since its inception. Properties such as its compressive strength will, however, be negatively affected with a sufficient dose [75-77]. The radiolysis of water within the system, resulting in the release of hydrogen, is also a factor that must be considered [17, 78-80].

The UK operates three means of encapsulating and immobilising waste in cement at its Sellafield site: grout infilling, in drum mixing, and supercompaction annulus grouting [81]. Grout infilling relies upon the fluidity of the cement grout to adequately surround the individual pieces of material within a containing drum. The drum can be vibrated in order to help the grout fill voids, displacing any pockets of air that may exist in between the pieces of waste. Fuel rod cladding, ILW from Magnox and Advanced Gas-cooled Reactors (AGR), is encapsulated using this method. The cladding is cut into small sections to form hulls, for increased packing efficiency of the wasteform [82]. Once the grout has set, the wasteform may be capped with a Pulverised Fuel Ash (PFA) blended PC grout. The system feed lines are also pigged, which involves bungs being sent through the feed lines to clear out any remaining residue from the system. These are then left within the grouted wasteform. For LLW, this same method is carried out on a much larger scale without vibration, using a superplasticised PFA-blended PC grout [83, 84].

In drum mixing is a method of waste immobilisation within a cement matrix and is similar in many respects to the grout infilling method. Waste slurries, such as barium carbonate and iron hydroxide flocculate, are mixed into a grout within the container with a paddle. The paddle is left in situ, and after which the wasteform may be capped with a grout. Supercompactation involves contaminated wastes, such as used lab equipment and personal protective equipment (PPE) that has come into contact with radioactive material, being placed into a 200 L mild steel drum which is then subsequently compacted into a cylindrical puck. Several of these pucks are then placed in a 500 L waste container that is subjected to grout infilling performed using an annulus, wherein the grout in poured in a ring around the pucks .

UK nuclear encapsulation procedures currently exclusively use PC blended with either Ground Granulated Blast Furnace Slag (GGBFS) or PFA [81]. Blast furnace slag (BFS) is a by-product generated from the smelting process of iron ore and is a glassy source of calcium oxide, alumina and silica [85]. PFA is the ash produced from fossil fuel fired furnaces, which in cement comes from coal fired power stations and contains significant quantities of aluminates and silicates (BS EN 197-1) [5, 9, 86]. BFS is latently hydraulic and hydrates much slower than PC, facilitated by the alkalinity of the pore solution generated upon the hydration of PC, [81, 85]. Siliceous PFA is pozzolanic, reacting with the presence of calcium hydroxide [87].

In construction, BFS and PFA are used to increase the resistance of a cementitious material against aggressive chemicals such as chlorides, reducing their mobility and therefore their corrosive potential, improving the durability of the system [81, 88, 89]. Substituting PC for some BFS and PFA is also a means of reducing the temperature of the hydration reaction which is very important in large volume applications. High temperatures can result in a loss of water, allowing the grout to dry out, crack and ultimately fail in encapsulating the wasteform. High temperatures may also result in thermal stress cracking. Cement encapsulation is not used for the direct treatment of HLW, but as part of an engineered barrier system, since the significant heat output the HLW generates may disrupt the hydration of the cement [88].

PC, BFS, and PFA particle size distribution (PSD) are important for the usability of a cement blend [90]. Too small a particle and it may react too fast and reduce the time in which the grout has an adequate flow property; too large and it may not react, acting only as a filler. PSD also has a significant impact upon the water demand and particle packing of a system, affecting the grout fluidity and its potential to bleed water from its pore network.

Modern PC (BS EN 197-1 CEM I 52,5N) and GGBFS (BS EN 15167-1 GGBS) typically has a much finer PSD than those available 30 years ago, with a more reactive product and a faster setting time being generally more desirable for the construction industry, whilst also making up for the increasing content of lower reactivity supplementary cementitious materials (SCM) [81, 91]. Alternative fuels with a higher chloride content are also more commonly used in PC manufacturing, increasing the chloride content within materials which may increase the corrosion potential within wasteforms over their centuries-long lifespan [81].

The nuclear industry historically required a minimum of 150 minutes of high grout fluidity in order to be able to produce and test the grout in an inactive area, before pumping it to the active working area for it to be used for grouting the wasteform . Current encapsulation efforts in the UK are set to standards of material that are no longer as widely available as they once were, and getting material to the current standards has become more difficult due to economic changes, industrial change, and changes in standards [81, 91]. Encapsulation procedures also use far more BFS and PFA blended with PC than would typically be employed in other applications, with a BFS/PC ratio of between 2.3 – 9 (Magnox encapsulation plant grout), and a PFA/PC ratio of 2.3 – 4 (capping grout) [81].

There are numerous other requirements for cement to give acceptable encapsulation of waste, including the heat generated during hydration. The strength of the grout must also be adequate to cope with the wasteform being handled. The hardened grout will have a degree of porosity, allowing any gases produced to escape such as through radiolysis or decay, but either too much porosity or pores that are too large will increase the mobility of radioactive species. Water retained in the pores will be the main mechanism for the transportation and potential escape of radioactive species, with any cracks or large

pores aiding this transportation through an increase in permeability. Therefore, free water must be kept to a minimum to reduce any bleed water from the mortar. Free water is also capable of radiolysis in a radioactive environment, producing hydrogen. However, sufficient water must be present for proper hydration and also to obtain the desired flow properties. The flow must be adequate enough to envelop all of the individual pieces of waste without leaving voids, but a flow with too little viscosity may cause the grout to splash within the active work zone and will likely exhibit a bleed [74, 91].

The set of the grout must take place within an adequate timeframe, retaining its flow properties for a minimum of approximately 150 minutes and setting within 48 hours. Whilst a set that occurs too quickly would be problematic and could severely damage equipment in an active zone, a set that is too slow is a waste of time and will slow down the rate at which waste can be processed. The setting process must also be dimensionally stable; expansion could pressurise the container and may cause the set grout to fail, increasing the mobility of the waste, with shrinkage also increasing the mobility of the waste within the container [74, 91].

The pH level of the waste encapsulant is a key factor in its long-term effectiveness, as there is the potential for different metallic wastes to react within a certain pH environment, generating gas and other corrosion products that will cause the wasteform to expand. Significant expansion is likely to cause cracking and failure within the waste form and potentially the containment vessel itself, greatly increasing the mobility of contained waste [74].

One important issue with the encapsulation method is that encapsulating a wasteform increases the volume of that waste, which in turn increases the requirement for the size of storage. This is an issue given that the UK has no current long-term storage facilities for ILW [88, 92, 93].

1.4. Cement Classification Overview

The following is an introduction into the cement systems that will be covered or referred to throughout this thesis. Further details are given within respective chapters.

1.4.1. Portland Cement

Portland cement (PC) is the clinkered product of calcium carbonate and aluminosilicates, which are typically supplied in the form of limestone and clay (hydrous aluminium phyllosilicates). Manufacturing takes place in regions where both of these materials are in close proximity, for example; between the counties of Kent and Essex in the UK, chalk and alluvial mud are readily available, whilst in Derbyshire, blue Liassic limestone and shale are most prevalent [94]. Other minor ingredients such as iron ore, blast furnace slag, or bauxite can also be included if these components can make up for a deficiency of one necessary constituent, for example iron, within the raw materials presented.

The more modern and energy efficient method of clinkering is to process the material dry (Figure 2). First, the raw materials are crushed and blended together, before entering a preheater. The preheater, which utilises hot gases from the later rotary kiln wherein the powders are introduced to a series of gravity fed cyclone chambers, heats the material to approximately 800 °C before ejection, resulting in around 40% of the calcium carbonate being decarbonated to produce lime (CaO) and CO_2. Many rotary kilns are also preceded by a precalciner, heating the material to 900 °C and increasing the lime component to upwards of 90% and reducing the processing time required in the rotary kiln [95].

The rotary kiln is typically a 100 m long cylinder, angled slightly downwards at approximately 3°, that rotates at a maximum of 4 rev/min. Material flows slowly against the flow of hot air, towards the flame of the kiln located at the bottom end. Towards the cooler end of the kiln, the calcination of any remaining calcium carbonate occurs, as well as the decomposition of aluminosilicates, followed by the reaction of the produced components to give belite, aluminate and ferrite phases. Upon exceeding 1350 °C, clinkering occurs, where a melt is formed, from which a majority of the belite and lime react to produce alite. Upon exiting the kiln, the clinker undergoes a controlled cooling, allowing for the crystallisation of the aluminate and ferrite phases and the production of the desired polymorphs of alite and belite [9, 95, 96]. The clinker nodules are then ground and blended with additives such as calcium sulfate.

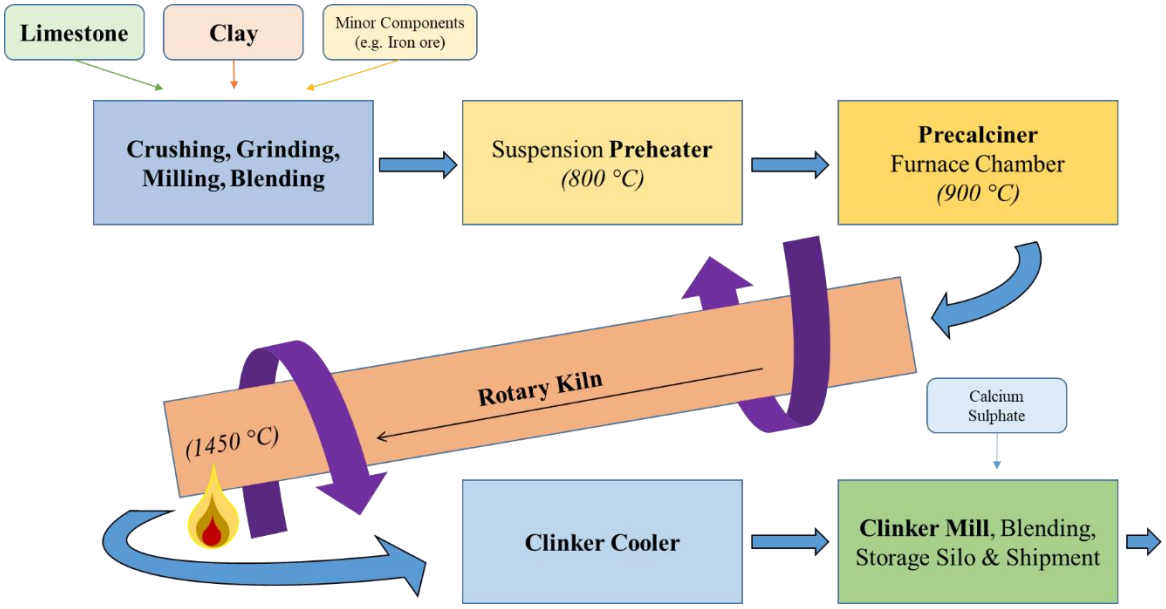

Figure 2: Simplified diagram illustrating the dry Portland cement clinkerization process, based upon the description of Taylor et al. [95].

The hydration of PC occurs through the dissolution of clinker phases. Ions then rearrange within the solution phases, eventually forming solid hydrate phases. At the first instance of the wetting of the clinker phases, the dissolution of alite (C_3S) begins, alongside that of tricalcium aluminate (C_3A), which reacts rapidly to form ettringite in the presence of calcium sulfate supplied, for example, by gypsum (Eq. 1.1.) [97, 98].

$$C_3A + 3C\$ + 32H \rightarrow C_6A\$_3H_{32}$$

(Eq. 1.1.)

The rapid formation of ettringite provides the initial set of PC, however; the formation of calcium aluminate hydrate metastable phases in the presence of insufficient calcium sulfate can cause a flash set, wherein a rapid set occurs with poor ultimate strength [99]. The optimum amount of calcium sulfate acts as a retarder, slowing the hydration of C_3A by the adsorption of sulfate ions upon its surface, allowing for the precipitation and growth of ettringite crystals, whilst ensuring the desired workability and strength characteristics are retained [98, 99]. More information on ettringite is found in section 1.4.2. If the alumina/sulfate ratio is too high, ettringite is consumed to form monosulfoaluminate (Eq. 1.2.) [5].

$$2C_3A + C_6A\$_3H_{32} + 4H_2O \rightarrow 3C_4A\$H_{12}$$

(Eq. 1.2.)

The hydration of alite occurs not long thereafter, with the formation of calcium silicate hydrate (C-S-H) and calcium hydroxide (CH) also known as portlandite (Eq. 1.3.) [100].

$$C_3S + 5.3\,H \rightarrow C_{1.7}SH_4 + 1.3CH$$

(Eq. 1.3.)

Alite contributes the majority of the overall strength through the production of C-S-H, and its products make up the majority of the PC phases formed. CH contributes little to the overall strength, but is responsible for the approximate pH 13 of the pore solution which allows for the passivation of steel reinforcement and the pozzolanic reaction of SCM such as fly ash [100, 101]. The understanding of the exact mechanism behind the hydration of alite is still under development [102]. Belite hydrates over a much longer timescale than alite, contributing to long term strength development, forming a much greater proportion of C-S-H than CH in comparison to alite (Eq. 1.4.) [100].

$$C_2S + 4.3\,H \rightarrow C_{1.7}SH_4 + 0.3CH$$

(Eq. 1.4.)

1.4.2. Calcium Sulfoaluminate Cements

Calcium sulfoaluminate cements (CSA) are a group of hydraulic clinkers that contain a significant quantity of ye'elimite (also known as Klein's compound or in itself as calcium sulfoaluminate). CSA cements also commonly contain a significant quantity of belite, but can also contain ferrite, ternesite, and in some cases alite. CSA production typically includes limestone, an alumina rich material such as bauxite, alumino silicate clay, calcium sulfate, and iron ore [103].

The clinkering temperature for CSA is lower than for PC, at approximately 1250 °C depending upon the composition [104]. Like PC, hydration occurs through the dissolution and reformation of phases through a series of exothermic reactions. The main hydration products of ye'elimite are ettringite ($C_3A{\cdot}3C\${\cdot}32H$) and aluminium hydroxide (AH_3). Hydration requires an addition source of calcium sulfate in order to form ettringite, such as anhydrite (Eq. 1.5.) or gypsum (Eq. 1.6.).

$C_4A_3\$ + 2C\$ + 38H \rightarrow C_3A{\cdot}3C\${\cdot}32H + 2AH_3$

(Eq. 1.5.)

$C_4A_3\$ + 2C\$H_2 + 34H \rightarrow C_3A{\cdot}3C\${\cdot}32H + 2AH_3$

(Eq. 1.6.)

If insufficient calcium sulfate is available but there is still available free water, the calcium monosulfoaluminate AFm – *mono* – phase is formed in its stead (Eq. 1.7.) [105]

$C_4A_3\$ + 18H \rightarrow C_3A{\cdot}C\${\cdot}12H + 2AH_3$

(Eq. 1.7.)

Ettringite is an AFt – *tri* – phase, forming crystals in long hexagonal prismatic columns with a water content of 30 – 32 H_2O moles per mole of Al_2O_3 [106, 107]. AFt, or alumina-ferric oxide-tri phases, are characterised by the form of these columns and associated channels in the intercolumnar space. These columns then arrange around sulfate molecules, with additional water also inhabiting the channels in-between columns (Figure 3) [108, 109]. Hydration of ye'elimite occurs quickly, leading to high early strength characteristics achieved with ettringite [110]. Alternatively, AFm, or alumina-ferric oxide-mono phases are formed in a layered structure [109].

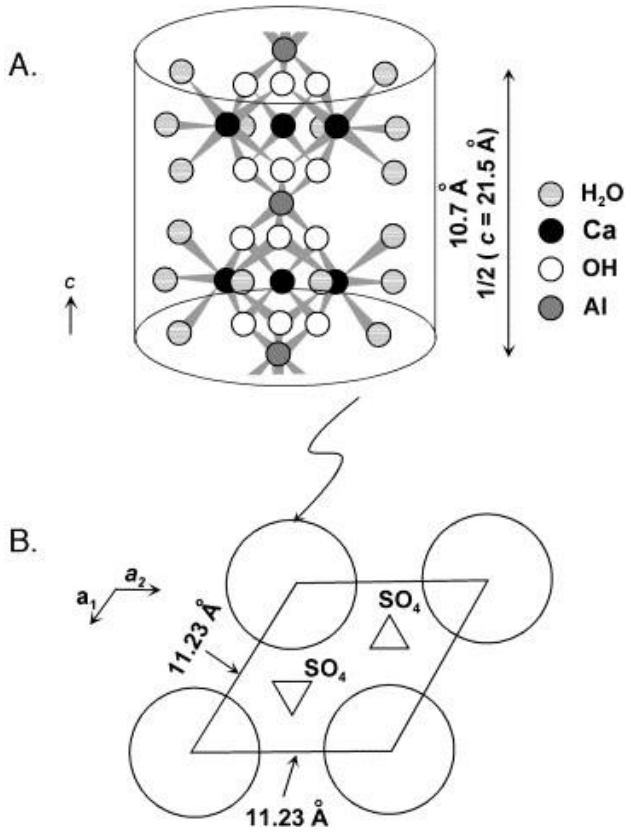

Figure 3: The crystal structure of ettringite as given in Cody et al. [108]. Image A shows the ettringite column structured crystals in a hexagonal prismatic structure extending along the c-axis. Image B then shows the arrangement of these columns from a top down view, surrounding sulfate molecules [108].

As the main strength giving phase, the stability of ettringite is an important topic when discussing CSA and is in part a function of temperature and water vapour pressure. Zhou *et al.* [111] explain the hysteresis loop shown in Figure 4, as the dehydration of ettringite into meta-ettringite. Meta-ettringite has a water content of 9 – 13 H_2O per mol of Al_2O_3. In that study, each synthetic ettringite sample was contained at a fixed temperature, with a controlled flow of water vapour in nitrogen over the sample to maintain a fixed water vapour pressure over a period of up to 2 weeks. Dehydration is shown to occur when the water vapour pressure is 75 mmHg (10 kPa) and the temperature is above 75 °C, and at 400 mmHg (53 kPa) when the temperature exceeds 85 °C [106, 111]. The conversion to meta-ettringite occurs though dehydroxylation, where water molecules are removed. The distance between ettringite cation columns is reduced, forming an amorphous phase due to the loss of crystallinity, whilst still retaining the ettringite needle structure and the same Ca/Al/S ratios [112, 113].

Zhou *et al.* [112] describe the formation of meta-ettringite from ettringite as topotactic, as the crystal structure is retained in all 3 dimensions when the water molecules are removed [112]. This process is reversible and is highly temperature dependent. Ettringite will reform from meta-ettringite and remain stable if environmental conditions re-enter the zone of reformation, and ettringite will decompose into meta-ettringite if conditions are within the zone of decomposition. The area between these two zones represents when both ettringite and meta-ettringite will remain stable if they are present [111].

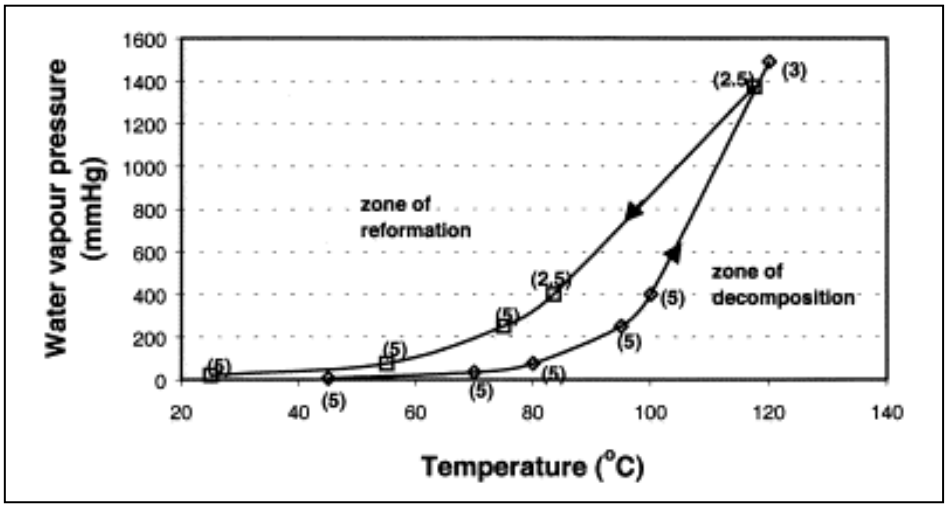

Figure 4: Data from Zhou et al.[111] showing the hysteresis loop of stable and reformation area for ettringite (far left zone), the area of the potential conversion to meta-ettringite (central zone), and the area of ettringite decomposition (far right zone), with a temperature uncertainty value given in parenthesis for each datapoint [111].

Baquerizo *et al.* [106], Figure 5, demonstrates a slight change to the model presented in Figure 4, with a larger area of reformation below 60 °C but the same exponential relationship between temperature and the availability of free water [106]. This relationship is being studied further, as the thermodynamic properties of meta-ettringite has been cited as being in need of future study, which will allow for more accurate prediction of this behaviour [114]. Temperatures in excess of 100 °C can also cause the decomposition of ettringite to calcium monosulfoaluminate (monosulfate), an AFm –*mono*– phase, with the precipitation of calcium sulfate [111, 115]. In solution, ettringite and monosulfate have also shown to be stable up to 100 °C [116, 117]. Although observed as a product of ettringite decomposition, monosulfate can also be converted to ettringite in the presence of excess calcium sulfate; this mechanism is sometimes known in PC chemistry as delayed ettringite formation, and can also result

from sulfate attack [118]. The process of ettringite being formed, as an expansive product, after the system has set and hardened has the potential to cause internal stress [119]. This can lead to cracking and a reduction in the mechanical properties of the paste, as larger ettringite crystals form in space previously occupied by monosulfate [115].

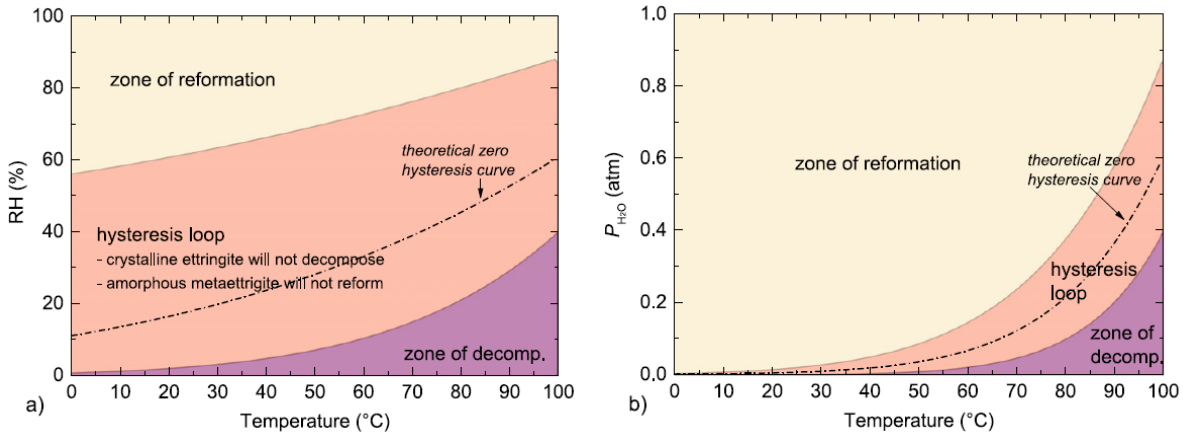

Figure 5: From Baquerizo et al. [106] showing the hysteresis loop with the reformation area for ettringite (far left zone), the area of ettringite stability (central zone), and the area of ettringite decomposition (far right zone) similar to that presented in Zhou et al. [111]. The "theoretical zero" curve is a boundary between expected zones of ettringite stability and decomposition [106].

As opposed to using a pure synthesised ettringite, Ndiaye et al. [113] used a commercially available CSA powder with composition similar to that of the Alipre used in chapter 3, with a 20% anhydrite addition. Under dry conditions (3 – 8% relative humidity) ettringite only began to form meta-ettringite at 50 °C and would reform if hydrated through many cycles [113]. Jiménez et al. [120] also conducted experiments using synthetic and naturally occurring ettringite. Synthetic ettringite began to decompose below 50 °C, whilst naturally occurring ettringite remained stable up until 75 °C, under uncontrolled atmospheric conditions [120]. Similarly, Yuke et al. [121] found that ettringite synthesised through hydration, as opposed to through solution synthesis, both had a lower mass loss and lower rate of mass loss under thermal decomposition. It is as yet unclear if the presence of meta-ettringite is detrimental to CSA in terms of strength, dimensional stability, or the retention of radionuclides. Brown *et al.* [122] report that ettringite formation and stability appear to be less favourable in increasingly alkaline

solutions, with further studies reporting that ettringite is however stable between a pH of 9 and 13.4 [116, 122, 123].

Belite, or dicalcium silicate (C_2S), hydrates slowly to form either calcium silicate hydrate (C-S-H) (Eq. 1.8.) or the silica-substituted AFm phase strätlingite (Eq. 1.9.) [5, 107]. Belite hydration in the absence of aluminium hydroxide forms C-S-H and portlandite (calcium hydroxide), which could increase the pH of the pore solution (Eq. 1.8.) and the corrosive potential of some encapsulated metals. However, the hydration of belite in the presence of a high concentration of aluminium rich amorphous hydrates, such as aluminium hydroxide, encourages the formation of strätlingite over C-S-H (Eq. 1.9.) [103, 124]

$$C_2S + 2H \rightarrow C\text{-}S\text{-}H + CH \qquad \textit{(Eq. 1.8.)}$$

$$C_2S + AH_3 + 5H \rightarrow C_2ASH_8 \qquad \textit{(Eq. 1.9.)}$$

Belite has been shown to take in excess of three months to begin to react to a significant extent in a belitic-CSA cement system, but appears to improve compressive strength once the slow process of hydration has begun [125]. Kaufmann [115] also suggested that belite content in CSA may hinder the formation of monosulfoaluminate.

1.4.3. Alkali Activated Materials

Alkali activated materials (AAM) is a term used to describe the product of a silicate powder precursor, which when combined with an alkali solution forms a gel structure. This general term encompasses a huge variety of precursors and alkali activators, of which many may be in the form of industrial wastes, chemical by-products, or naturally occurring resources.

A precursor can be in the form of a calcium silicate, though many are aluminosilicates; with blast furnace slag, fly ash, or calcined clay being some well-known examples. In order for the precursor to be activated, it must receive the alkali metal cations from, and begin dissolution with, the activating solution. The alkali activator must also therefore be sufficiently soluble so as to generate the solution, as well as raising the solution pH enough to begin the reaction of the mixture [14]. A typical activating

solution is sodium silicate with sodium hydroxide, the later component increasing the system pH and allowing for the enhanced dissolution of the precursor [126]. Alkali activation is not just confined to AAM, however; within PC, pozzolanic (silicate) material is activated by the calcium hydroxide (portlandite) within the PC pore solution to form calcium silicate hydrate (C-S-H) and calcium aluminate hydrate [14, 127, 128]. A gel structure, such as that formed by an AAM, can be described non-crystalline or amorphous, with only short to medium range order on the nanocrystalline level. This can consist of molecular chains or layers, linked to form 3D networks.

There is an important distinction to be made between AAM with significant quantities of calcium, and those without. An AAM containing a high quantity of calcium forms phases not far removed from the C-S-H structures found in the hydration of alite and belite in PC – although with some key structural differences. An example of a high calcium precursor might be blast furnace slag, shown to contain as much as 37 wt.% CaO [129]. Upon the dissolution and nucleation of the dissolved species into a gel structure, the calcium content drives the formation of a C-A-S-H type structure. This structure features noticeable similarities to the natural mineral tobermorite (defined in 1880 after its discovery in Tobermory, Scotland), a comparable and often used natural representation of C-S-H [130, 131].

As proposed by Myers et al. [132], the C-A-S-H type gel forms aluminosilicate chains representative of a disordered tobermorite structure with Al^{3+} substituting some Si^{4+}, hence C-A-S-H as opposed to C-S-H. These chains consist of three silicate tetrahedra in a ‘dreierketten unit’, between Ca-O and interlayer sheets. Interlayer sheets consist of water and the positively charged species that balance the negative charge of the Al substituted silicate tetrahedra (Figure 6). This system can be described as C-(N-)A-S-H so as to include alkali species bound (in this case Na). These Al substituted tetrahedra, when placed at bridging sites, can link to opposing tetrahedra across the interlayer regions. This is known as crosslinking [132-135] (Figure 7).

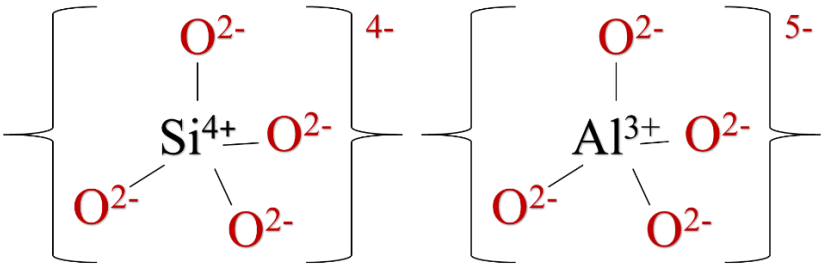

Figure 6: Si tetrahedra (SiO_4) and Al tetrahedra (AlO_4) respectively, showing individual and overall charges (within brackets). Al tetrahedra display a higher negative charge, which is balanced in AAM by nearby alkali metal species.

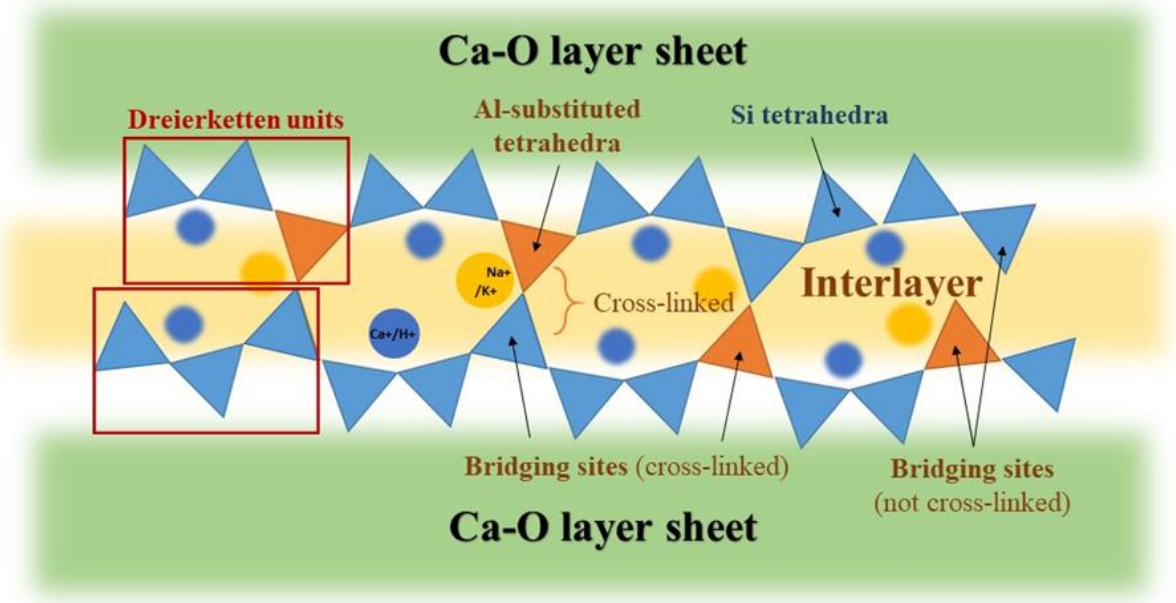

Figure 7: A representation of the C-A-S-H type gel based upon the work of Myers et al. [132]. Ca^{2+} and H^+ species are represented by blue circles, balancing the charge of the blue Si tetrahedra. Orange circles represent the Na^+ and K^+ species that balance the charge of the Al substituted tetrahedra [133]. All of these species, as well as water, form the interlayer between the aluminosilicate chains, which are made up of dreierketten units.

An AAM with low or negligible Ca content will form a (N)-A-S-H type gel (in the case of using a Na activator), otherwise known as alkali aluminosilicate hydrate gel [135]. These gel types form the basis of what are known as geopolymers, named so as to differentiate them from the C-A-S-H disordered tobermorite type systems outlined previously, and to better represent the mechanism from which they are formed (Figure 8) [131].

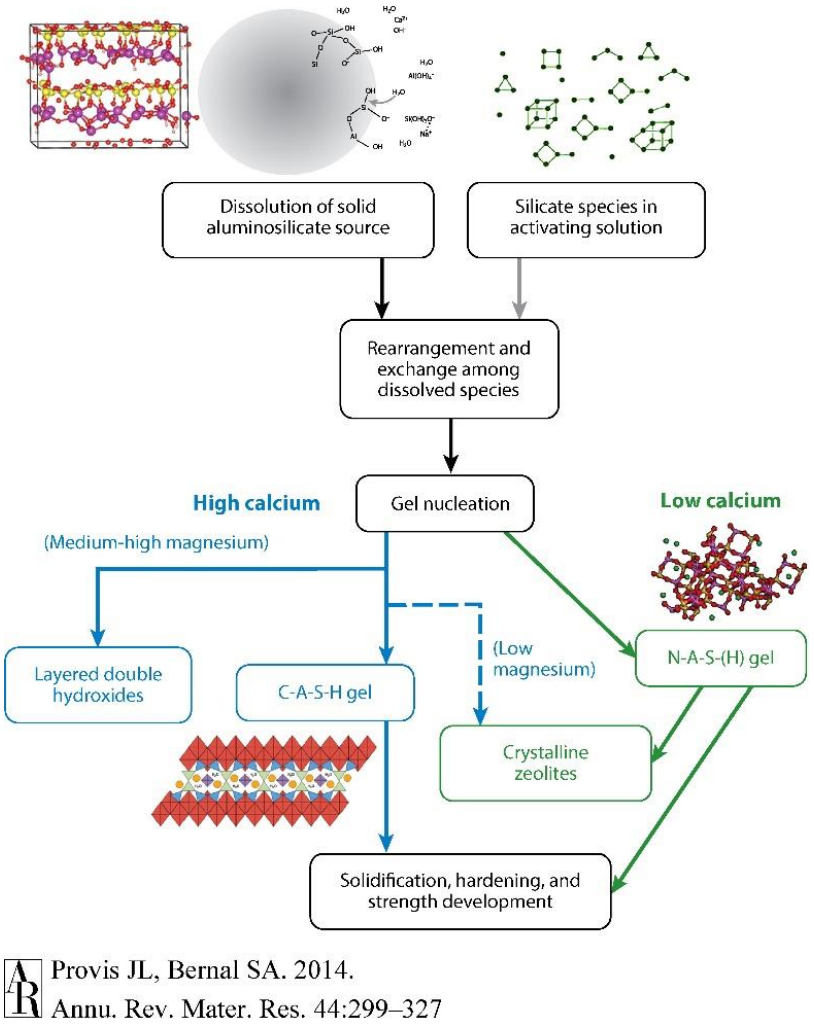

Figure 8: A flow chart detailing the key distinctions between the high and low calcium AAM systems, by Provis and Bernal. [131].

Geopolymer formation begins with the dissolution of the solid aluminosilicate precursor within the alkali activating solution, producing aluminate and silicate species. The high pH solution quickly becomes supersaturated, then the rearrangement and gel nucleation proceeds [136]. In the absence of Ca, the formation of a highly disordered amorphous 3D network (Figure 8) reportedly occurs through a number of intermediate steps (Figure 9). The gel network consists of Si and Al tetrahedra (Figure 6) corner linked by sharing oxygen. The increased negative charge of the Al tetrahedra is balanced by nearby alkali cations.

The gel initially formed is Al rich, as proposed by Fernández-Jiménez et al. [137], due to the weaker Al-O bonds allowing for an increased concentration of Al^{3+} to precipitate earlier on, with Si^{4+}

concentration increasing soon thereafter, resulting in a greater amount of Si substitution and a second gel structure [131, 137]. Gelation is followed by polymerization, wherein the connectivity of the gel increases, producing the amorphous 3D gel network (Figure 9) [136].

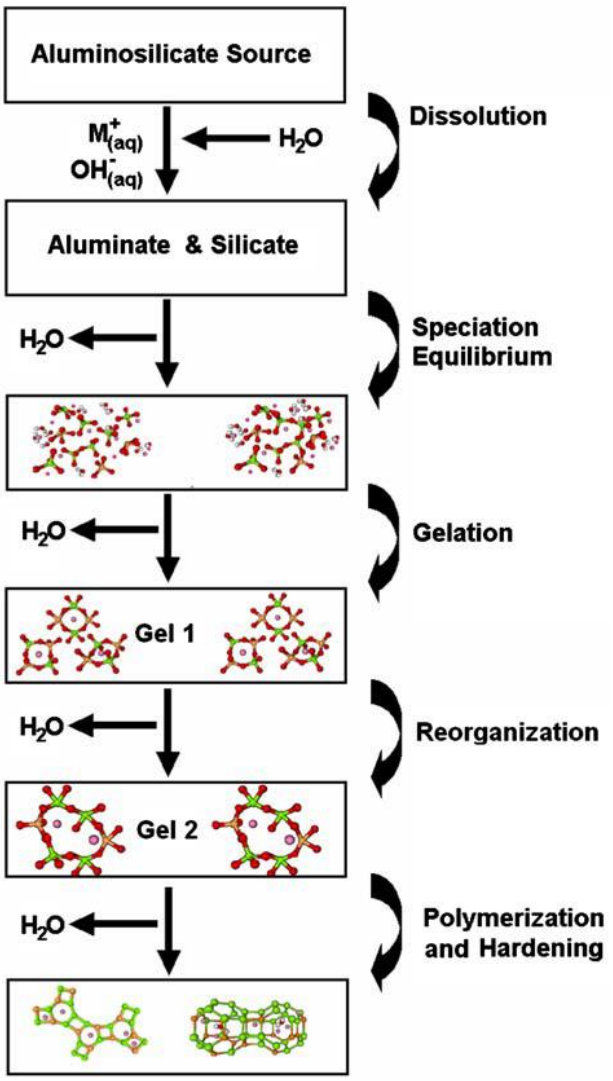

Figure 9: A flow chart representing the proposed main stages of geopolymer formation by Duxson et al. [136].

The amorphous N-A-S-H gel network formed has been compared by Provis et al. [138] to a disordered zeolite structure, much in the same way that the C-A-S-H gel bears distinct similarities to the tobermorite structure [138]. Geopolymers are covered in further detail in chapter 4.

2. Materials and Methods

2.1. Calcium Sulfoaluminate

Two commercial CSA-belite clinkers were selected; Alipre supplied by the Italcementi Group, and Alpenat CK supplied by Vicat Cement. The clinker composition was provided by the manufacturers, and a Rietveld analysis of a raw clinker sample XRD pattern was conducted to confirm this (Table 3 and Table 8). The Alipre clinker contains a relatively high ye'elimite content and low belite, while the Alpenat clinker is not quite so rich in ye'elimite and with a much higher belite content. Air permeability (Rigden) tests established that the powder finenesses of Alipre and Alpenat clinkers were 528 and 530 m^2/kg, respectively, with loss on ignition values of 0.87% and 0.50% respectively at 950 ℃ . The calcium sulfate was used in the form of either anhydrite or gypsum, both supplied by Saint-Gobain Construction Products. The anhydrite and gypsum exhibited Blaine finenesses of 452 and 385 m^2/kg, respectively. No additional additives were used. In this study, results are generated from a total of 40 mixes, each of 3-litres. The clinkers were blended with additional anhydrite or gypsum at levels of 15, 25, or 35 wt.% of the total pre-blended solids in the mix design. The water to solids mass ratio (w/s), calculated on the basis of total solids (clinker + calcium sulfate), was set to either 0.5, 0.6 or 0.7, and mixed to either a low or high shear mixing method.

Table 3: Rietveld analysis composition for Italcementi Alipre and Vicat Alpenat CK clinkers, showing phases of significance.

Clinker compositions – Rietveld analysis				
Compound	**Chemical formula**	**Cement nomenclature**	**Percentage identified in Alipre**	**Percentage identified in Alpenat**
Ye'elimite	$Ca_4Al_6(SO_4)O_{12}$	$C_4A_3\$$	65.0	50.9
Belite (beta)	β-Ca_2SiO_4	C_2S	8.8	19.9
Belite (alpha)	α-Ca_2SiO_4	C_2S	8.9	8.1
Perovskite	$CaTiO_3$	CT	4.4	11.7
Merwinite	$Ca_3Mg(SiO_4)_2$	C_3MS_2	4.0	6.3
Anhydrite	$CaSO_4$	C$	2.7	2.9
Fluorellestadite	$3(2CaO{\cdot}SiO_2){\cdot}3CaSO_4{\cdot}CaF_2$	$C_{10}S_3\$_3\underline{F}_2$	1.7	-
Periclase	MgO	M	0.7	-
Bredigite	$Ca_7Mg(SiO_4)_4$	C_7MS_4	3.2	-
Quartz	SiO_2	S	0.5	0.2

Table 4: Identified clinker compound percentages when theoretically adjusted for the calcium sulfate addition.

Compound	Alipre	Alpenat	15%		25%		35%	
Ye'elimite	65.0	50.9	55.3	43.3	48.8	38.2	42.3	33.1
Belite (beta)	8.8	19.9	7.5	16.9	6.6	14.9	5.7	12.9
Belite (alpha)	8.9	8.1	7.6	6.9	6.7	6.1	5.8	5.3
Perovskite	4.4	11.7	3.7	9.9	3.3	8.8	2.9	7.6
Merwinite	4.0	6.3	3.4	5.4	3.0	4.7	2.6	4.1
Anhydrite	2.7	2.9	2.3	2.5	2.0	2.2	1.8	1.9
Fluorellestadite	1.7	-	1.4	-	1.3	-	1.1	-
Periclase	0.7	-	0.6	-	0.5	-	0.5	-
Bredigite	3.2	-	2.7	-	2.4	-	2.1	-
Quartz	0.5	0.2	0.4	0.2	0.4	0.2	0.3	0.1

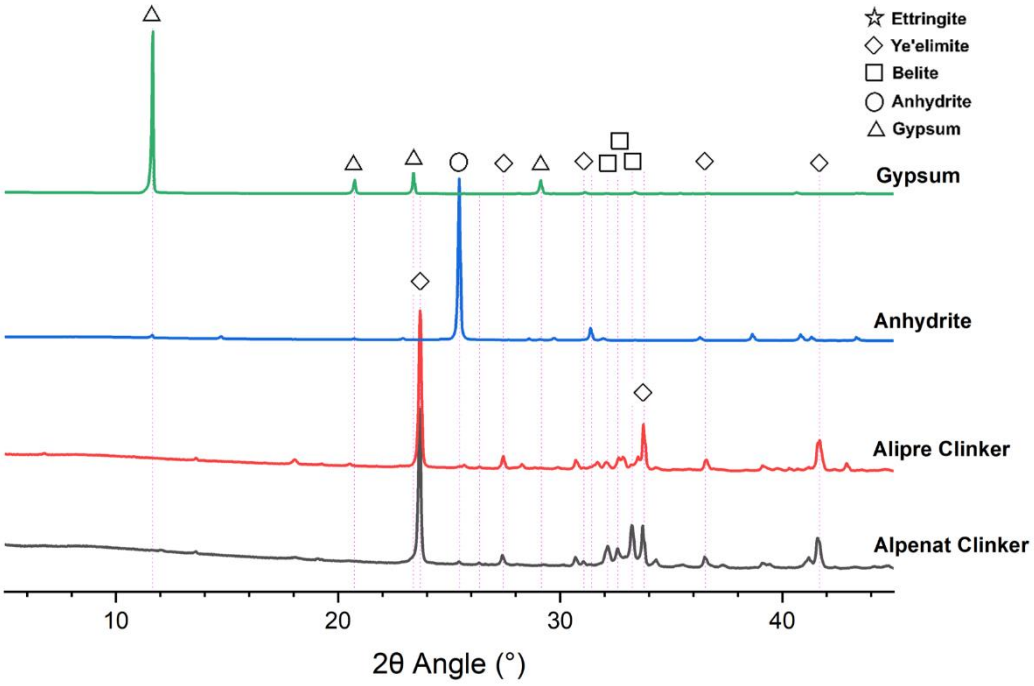

Figure 10: Raw material component XRD, showing key phases present for anhydrite and gypsum calcium sulfate sources, as well as Alipre and Alpenat CSA clinker.

2.2. Metakaolin Geopolymer

Metakaolin ($Al_2O_3 \cdot 2SiO_2$) is the calcined product of the naturally occurring clay mineral kaolinite ($Al_2O_3 \cdot 2SiO_2 \cdot 2H_2O$) and is used primarily in the production of porcelain. High reactivity metakaolin is produced from high purity kaolinite, calcined in a kiln at between 650 to 850 °C, and can be used as a pozzolanic supplementary cementitious material for Portland cement and lime mortars [139]. This study employed two high reactivity metakaolin materials from European manufacturers, considered by the UK nuclear industry as potential suppliers. Both comply with the pozzolan description given in BS EN 197-1:2011 [86, 140].

Powder composition testing, particle size distribution, and loss on ignition testing on the powders used in this chapter was conducted by the National Nuclear Laboratory (NNL), Workington UK, using X-ray fluorescence (XRF) and laser diffraction . The compositions identified are very similar and directly comparable to both the manufacturers' data, and other studies that have employed the same sources of metakaolin [140-147].

Argicem (Table 5) is flash calcined [147]. Notably, Argicem reportedly also contains an approximate 48.0 wt.% of quartz, alongside 3.9 wt.% iron oxide which gives the metakaolin a characteristic red colour [140]. MetaMax (Table 5) is calcined in a rotary kiln at <900 °C. This metakaolin is of high purity and is off-white in colour.

Table 5: Composition of Argicem and Metamax metakaolin as identified using XRF, as well as loss on ignition (LOI) at 950 °C, identified by NNL.

Argicem	SiO_2	Al_2O_3	TiO_2	Fe_2O_3	CaO	K_2O	MgO	LOI (wt.%)
Wt. % Identified	67.0	23.1	1.2	3.9	1.7	<0.5	<0.5	2.4
MetaMax								
Wt.% Identified	44.5	52.6	1.7	<0.5	<0.5	<0.5	<0.5	1.0

Table 6: Argicem and MetaMax powder characteristics as identified by NNL using laser diffraction and Blaine fineness .

Argicem	D_{10} (µm)	D_{50} (µm)	D_{90} (µm)	Fineness (m^2/kg)
Particle Size Distribution	5.2	38.5	127.7	3614
MetaMax				
Particle Size Distribution	1.2	3.5	11.1	706

A potassium silicate activating solution was chosen for this experimental series, as experimentation by Geddes [140] found that metakaolin geopolymer mixes exhibited lower viscosity when employing potassium silicate solutions as opposed to sodium silicate [140]. In an encapsulation process, this would aid in the envelopment of wasteforms within a container, lowering the potential for air entrapment and voids. Lower viscosity grouts also allow for the encapsulation of thicker sludges and slurries, increasing waste loading and waste package efficiency, which in turn reduces the total number of required wasteforms. The potassium silicate used contained (wt.%): 21.8 K_2O, 31.4 SiO_2, 46.8 H_2O, with a SiO_2:K_2O molar ratio of 2.25. The activating solution was made by blending this to the appropriate K_2O/SiO_2 ratio, using potassium hydroxide flakes of <15% H_2O . Any additional water used was deionised and was not chilled.

In total, 36 metakaolin geopolymer mixes were performed in 3-litre batches. This included the aforementioned two different metakaolin powders; Argicem and MetaMax, each being used to produce every mix in the matrix outlined below (Table 7).

Table 7: Metakaolin geopolymer mix matrix, with each mix being produced using each of the two different metakaolin powders used. The SiO_2/K_2O and H_2O/K_2O ratios refer specifically to the composition of the activating solution, and the K_2O/Al_2O_3 ratio defines the relationship between the activator and metakaolin contents.

SiO_2/K_2O	H_2O/K_2O	K_2O/Al_2O_3	Shear
1.0	11	1.0	Low
1.0	11	1.0	High
1.0	11	1.5	Low
1.0	11	1.5	High
1.0	15	1.0	Low
1.0	15	1.0	High
1.0	15	1.5	Low
1.0	15	1.5	High
1.2	13	1.2	Low
1.2	13	1.2	High
1.4	11	1.0	Low
1.4	11	1.0	High
1.4	11	1.5	Low
1.4	11	1.5	High
1.4	15	1.0	Low
1.4	15	1.0	High
1.4	15	1.5	Low
1.4	15	1.5	High

2.3. Methodology

Mixing was conducted using a Hobart N50 mixer, with the water or potassium silicate activating solution pre-prepared at120 20 +/-1 °C. Pre-blended solids would be added to the mixer bowl already containing the water or activator, at a consistent rate over a period of 5 minutes with the mixer running at 62 rpm. Once all powder was added to the mix, a further 5 minutes of mixing at 62 rpm would proceed, bringing the total mixing time thus far to 10 minutes. At this point, designated 'high shear' mixes would be moved onto the Silverson high shear mixer for a period of 10 minutes at 4500 rpm, whilst designated 'low shear' mixes would remain on the Hobart mixer at 62 rpm for the duration. Once this total 20 minutes of mixing had been met, the fluidity of each mix was assessed using the NNL Colflow grout fluidity measurement technique. If 1 quart (1.14 litres) of grout flows ≤ 500 mm down

the grout flow trough once released from its container, then it is deemed that the fluidity is too low and thus the viscosity is too high, and further mixing is deemed unsuitable with samples being cast immediately. If the flow of the mix remains favourable under no given time limit, it remains at 62 rpm for a maximum duration of 150 minutes, with the flow being assessed at 30-minute intervals. The maximum mixing time is therefore 170 minutes in total. The low and high shear mix methods, as well as the total mixing duration, were developed so as to best represent the parameters achievable and necessary using the full 500 litre scale equipment and infrastructure currently employed in UK radioactive waste encapsulation [148].

Samples analysed in this study were cast in 15 mL plastic centrifuge tubes and then cured at 20 +/-1 ℃ in a high humidity (>90% RH) walk-in chamber. These samples had their curing and hydration arrested at either 7, 28 or 90 days using a solvent exchange method, as proposed by Winnefeld et al. [149] for Portland cement-based materials. Free water was removed by submerging samples in isopropanol, which was routinely changed over a period of several hours, with samples then being dried to constant weight in a desiccator [149]. For analysis by powder X-ray diffraction (XRD), thermogravimetric analysis (TGA), and Fourier transform infrared spectroscopy (FTIR), samples were ground to a powder and sieved to <63 μm and kept under vacuum in a laboratory desiccator afterwards, isolated in sealed bags within the desiccator. All procedures were conducted at a room temperature of approximately 20 °C.

2.3.1. Scanning Electron Microscopy (SEM) and Energy Dispersive X-Ray Spectroscopy (EDS)

Samples for SEM and EDS were sectioned into approximate 5 mm^3 slices before being cold mounted in epoxy resin. These samples were then ground and polished, using isopropanol as a lubricant, up to a 0.25 μm diamond grade. Samples were then carbon coated in a vacuum and given conductive liquid silver dag paint tracks for improved conductivity in order to prevent overcharging. SEM and EDS analysis were carried out by using a Hitachi TM3030 instrument, with EDS conducted using a Quantax 70 detector. Images were taken at magnifications of 40×, 250×, 500×, 1000× and 2500×, using an electron accelerating voltage of 15 kV and a working distance of 8 mm. EDS was conducted for all samples at either 1000× or 2500× magnification, and was set up to identify Al, C, Ca, K, Mg, and Si.

2.3.2. Thermogravimetric Analysis (TGA) with Mass Spectrometry (TG-MS)

TGA or TG-MS was conducted on <63 μm powdered samples, using a Perkin Elmer TGA 4000 coupled with the option of a Hiden Analytical Mass Spectrometer. Testing involved 40 ± 2 mg samples in alumina crucibles, under an inert nitrogen atmosphere, at a heating rate of 10 °C/min from room temperature to 950 °C. Analysis was conducted using the Pyris Manager software. The mass spectrometer identified ions according to mass/charge ratios assigned to carbon dioxide, sulfur dioxide carbon monoxide, and water.

2.3.3. X-ray diffraction (XRD) and Rietveld Analysis

XRD was conducted on <63 μm powdered samples, using a PANalytical X'pert^3 Powder instrument with Cu-Kα radiation. Sample holders were backloaded to reduce the degree of preferred crystal orientation. These samples were analysed over the º2θ range of 5 – 70 º2θ, at a step size of 0.026 °2θ and a time per step of 4 s.

Quantification via Rietveld analysis was conducted upon CSA samples in the TOPAS software, for both unreacted clinkers and hydrated products, using the fundamental parameter approach for all phases and without the use of an internal standard. Ettringite values for comparable mixes, differing only in the shear history of the mix, were found to vary by an average of 2%, indicating good stability and reproducibility of the refinement methodology. An average Rwp value of 1.83 was generated from all refinements, indicative of a successful final structure model and refinement [150].

The calculation of error within the values generated by Rietveld analysis is difficult, especially in systems with a large number of phases, and may result in an error ranging from one to several percent or more [151]. A margin of error is best theorised using Table 4, where the percentage adjusted for the calcium sulfate addition is very occasionally a couple of percent under what was identified in the hydrated sample. Quantification of accuracy must take into account instances of preferred crystal orientation, X-ray micro absorption, the amorphous phase content, the quality of the reference patterns, and any other potential factors [151, 152]. Whilst these factors were mitigated where possible, the focus

will be a comparison between the extensive range of samples, produced in a controlled manner, covering several different key variables.

Table 8: Sources of the CIF files used from literature in order to conduct the Rietveld analysis.

Phase	Identification	Authors
Ettringite	155395-ICSD	F. Goetz-Neunhoeffer and J. Neubauer [153]
Gibbsite	6162-ICSD	H. Saalfeld and M. Wedde [154]
Monosulfate (Kuzelite)	0014757-AMCSD	R. Allmann [155]
C-S-H (Hillebrandite)	0001745-AMCSD	Y. Dai and J. Post [156]
Ye'elimite	80361-ICSD	N. Calos et al. [157]
Anhydrite	16382-ICSD	A. Kirfel and G. Will [158]
Gypsum	230283-ICSD	T. Fukami et al. [159]
Belite α (Orthorhombic)	81097-ICSD	W. Mumme et al. [160]
Belite β (Monoclinic)	81096-ICSD	W. Mumme et al. [160]
Portlandite	15471-ICSD	H. Petch [161]
Quartz	41414-ICSD	G. Will et al. [162]
Lime	52783-ICSD	D. Smith and H. Leider [163]
Hemihydrate	79528-ICSD	C. Bezou et al. [164]
Perovskite	62149-ICSD	S. Sasaki et al. [165]
Merwinite	431125-ICSD	X. Bao et al. [166]
Fluorellestadite	97203-ICSD	I. Pajares et al. [167]
Periclase	9863-ICSD	S. Sasaki et al. [168]
Bredigite	0000494-AMCSD	P. Moore and T. Araki [169]
Strätlingite	69413-ICSD	R. Rinaldi et al. [170]

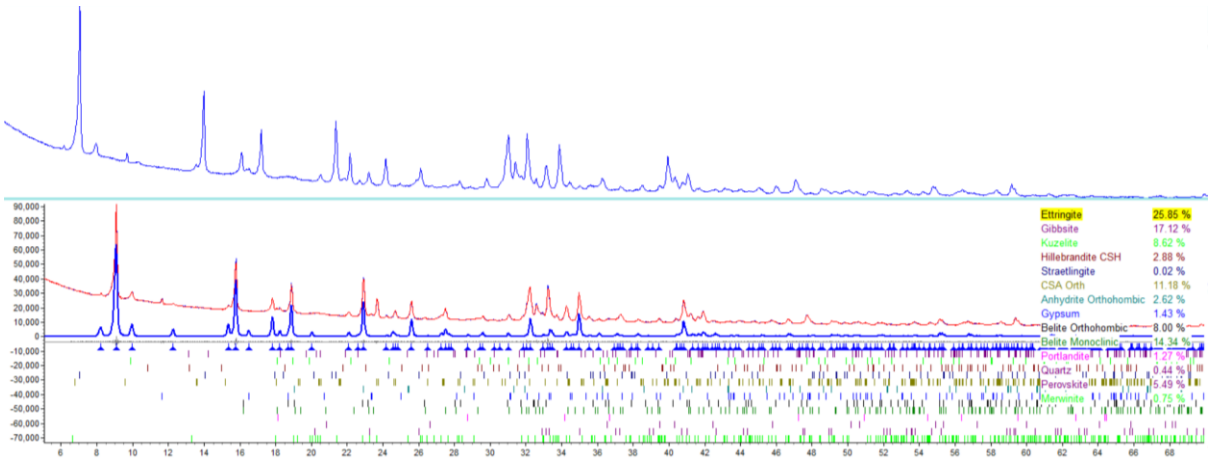

Figure 11: TOPAS working file showing the calculated fit in red overlaying the experimental data in blue, which is almost completely overlaid. The raw experimental data is also show above in blue. The thicker dark blue line at the bottom illustrates the peaks for ettringite and how they intercept the peaks identified in the working model.

2.3.4. Thermodynamic Modelling

Gibbs Energy Minimization Software (GEMS) was used in the form of CemGEMS, a browser-based application based upon the GEMS3K code, that allows the user to load and modify cement recipe templates and conduct computations using the Cemdata18 and PSI/Nagra databases [171]. The template available for CSA-belite cement is based upon the work of Jeong et al. [151], which was modified in order to reproduce the compositions of the Alipre and Alpenat clinkers, accompanied by the addition of appropriate calcium sulfate and water to match the experimental mixes. Component enthalpy values and their degree of hydration were retained as given in Jeong et al. [151].

Simulations were run to account for every change in mix parameters, except shear rate, at a pressure of 100kPa and temperature of 20 °C. The duration was allowed to exceed 10,000 years, representative of the extremely long timescales that radioactive waste repositories will function [3]. Cement hydration as a function of time was plotted using the 5 parameter logistic (5PL) function, and was based around 100g of clinker with the additional calcium sulfate then added [171]. The extent of reaction for each mix was calculated using the percentage of remaining ye'elimite identified by Rietveld analysis at 90 days, with an extent of reaction between 63% and 76% exhibiting the same quantity of ye'elimite remaining at 90 days, allowing for a model more representative of its experimental equivalent.

2.3.5. Fourier Transform Infrared Spectroscopy (FTIR)

FTIR was performed using a Perkin Elmer Frontier FTIR spectrometer, with a triglycine sulfate detector, and potassium bromide beam splitter optics. 2 mg of <63 μm powdered sample was mixed with 200 mg of anhydrous potassium bromide and then pressed into a pellet using 10 tonnes of force. 16 scan iterations were taken at between 4000 – 500 cm^{-1} at a resolution of 2 cm^{-1}.This was done in accordance to work previously conducted by Geddes upon metakaolin geopolymers [140].

2.3.6. Mercury Intrusion Porosimetry (MIP)

90-day samples were subjected to MIP testing to assess the impact of formulation parameters upon sample porosity, which was carried out using a Micrometrics Autopore V instrument. Samples were removed from their centrifuge tubes, sectioned into pieces approximately 20 mm^3 in size, and subjected

to the hydration arresting process described above. Once this was completed, sample sections were again sectioned into quarters for MIP, producing a total sample mass of 2.20 ± 0.2 g. MIP was conducted using a contact angle of 130°, a mercury temperature of between 19 – 22 ℃, and with a surface tension of 0.485 Nm^{-1} used for calculations [140, 172]. MIP was carried out a minimum of twice for each sample, from which an average porosity was then calculated, along with a sample standard distribution as a measure of the difference between the replicate tests.

3. Calcium Sulfoaluminate Cements as a Future Encapsulant

3.1. Introduction

In this chapter, a brief history of CSA and its use within industry is presented, including information on why it is of interest to the UK nuclear industry. The following section is comprised of material that was published as the academic paper 'hydrate assemblage stability of calcium sulfoaluminate-belite cements with varying sulfate content', which was accepted for publication by Construction and Building Materials on the 6th of April 2023 [148]. The materials and methods section has been removed, and the information provided in chapter 2. Further results and discussions are given then provided, beyond the scope of what could be presented in the journal article. Furthermore, testing was conducted on a number of samples far in excess of the maximum 90-day hydration period initially presented.

3.2. A Brief History of Calcium Sulfoaluminate Cements

CSA, in comparison to PC, is a relatively new technology. Pioneered in the 1950's, CSA has been employed as both an additive and an alternative binder system in its own right. CSA can be used as an umbrella term for cements containing a significant quantity of ye'elimite, typically between 20 – 80 %, whilst differentiating itself from the more mature high alumina cement family of binders (see section 5.3.) [103].

CSA began with the work of Alexander Klein at the University of California, and the patent for Klein's compound (or salt), otherwise known as ye'elimite, in 1963 [173]. Klein's original objective was the development of an expansive additive for PC, in order to combat the effects of shrinkage, however CSA would soon be developed as a system in its own right [174]. During the 1970's, the China Building Materials Academy developed CSA for use in low temperature environments, before standardising the new system in 1981, around the same time as CSA was beginning to be adopted in the United States [72, 173, 175].

Since then, the term CSA has come to represent a multitude of different types of clinker. Aranda et al. [176] summarised many of the different types in 2013, which highlights a degree of overlap and potential confusion in regard to names and what they represent [176]. The table resulting from that work has been modified and updated to produce Table 9, which is presented below.

Table 9: A modified and updated version of the table first presented by Aranda et al. [176]. Consider also the different spellings of 'sulfur/sulphur', and how that may reduce the visibility of some publications when searched for online [177].

Acronym	Definition	Reference
CSA	Calcium sulfoaluminate cement	[176]
CSAB	Calcium sulfoaluminate belite	[178]
BCSA	Belite calcium sulfoaluminate	[173]
BCSAF	Iron-rich belite calcium sulfoaluminate cement	[176]
BCSAA	Aluminium-rich calcium sulfoaluminate cement	[176]
ACSA	Alite calcium sulfoaluminate cement	[176]
CSAF	Calcium sulfoferroaluminate	[179]
SAC	Sulfoaluminate cement	[175]
BSA	Belite sulfoaluminate	[180]
CSAC	Calcium sulfoaluminate cement	[72]
SCC	Sulfoaluminate cement clinker	[181]
FAC	Ferroaluminate cement	[175]
SFAB	Sulfoferroaluminate belite	[182]
SAB	Sulfoaluminate belite	[183]
BSAF	Belite sulfoaluminate ferrite	[182]
BYF	Belite ye'elimite ferrite	[184]
BCT	Belite calciumsulfoaluminate ternesite	[185]
TSC	Third Series Cement	[175]
TCS	Third Cement Series	[186]

CSA cements have drawn interest from various different industries and organisations for a number of reasons. Their most eye-catching quality might be the potential reduction in CO_2 emissions when compared to a generic PC. Analysis by García-Maté [103] concluded that up to a 40% reduction in CO_2 is achievable when manufacturing CSA, with Hanein et al. [187] suggesting a reduction of between 25 – 35% [103, 187].

Firstly, this is due to the lower calcium, higher alumina content of the required raw materials, reducing the CO_2 emissions associated with decarbonisation of limestone. Secondly, a significantly lower processing temperature of between 1250 and 1350 °C is typical of CSA, with PC requiring a clinkering temperature of 1450 °C. Unlike in PC, CSA clinker is typically absent of alite (C_3S), which requires

higher clinkering temperatures (Figure 12) [103, 104, 188-191]. CSA also carries other desirable characteristics, such as the aforementioned shrinkage compensation or dimensional stability, rapid curing, high early strength, a lower system pH, and increased chemical resistance compared to PC [88, 103, 125, 188, 192, 193].

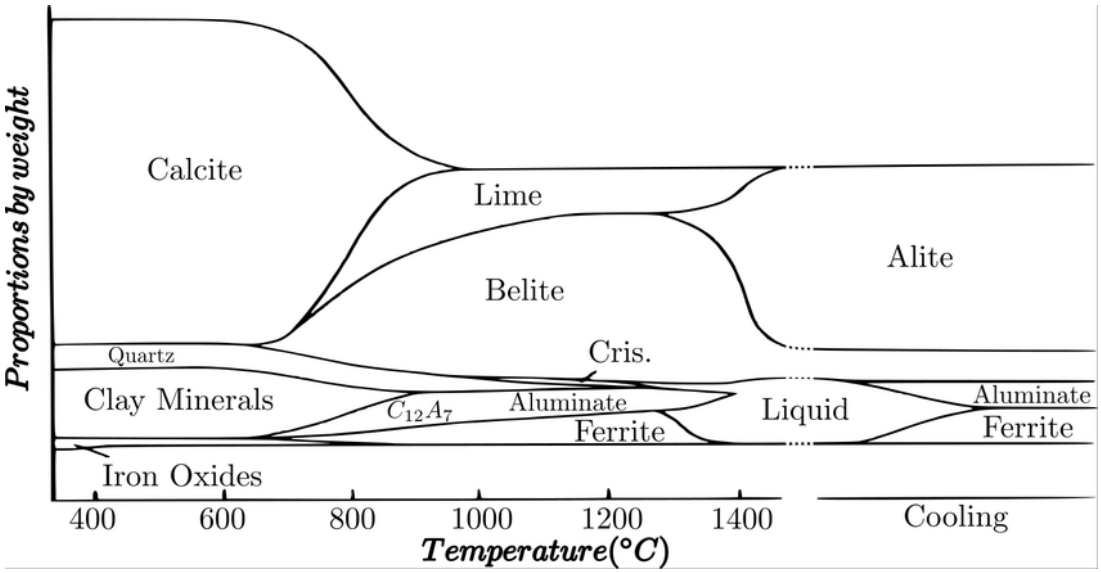

Figure 12: A diagram representing the phase formation with temperature during the clinkerization process for PC. Image from Hanein et al. [190] and adapted from Taylor [5]. This image highlights the region in which alite is formed, which can be compared to CSA phases, including ye'elimite that forms at approximately 1250 ℃ [103].

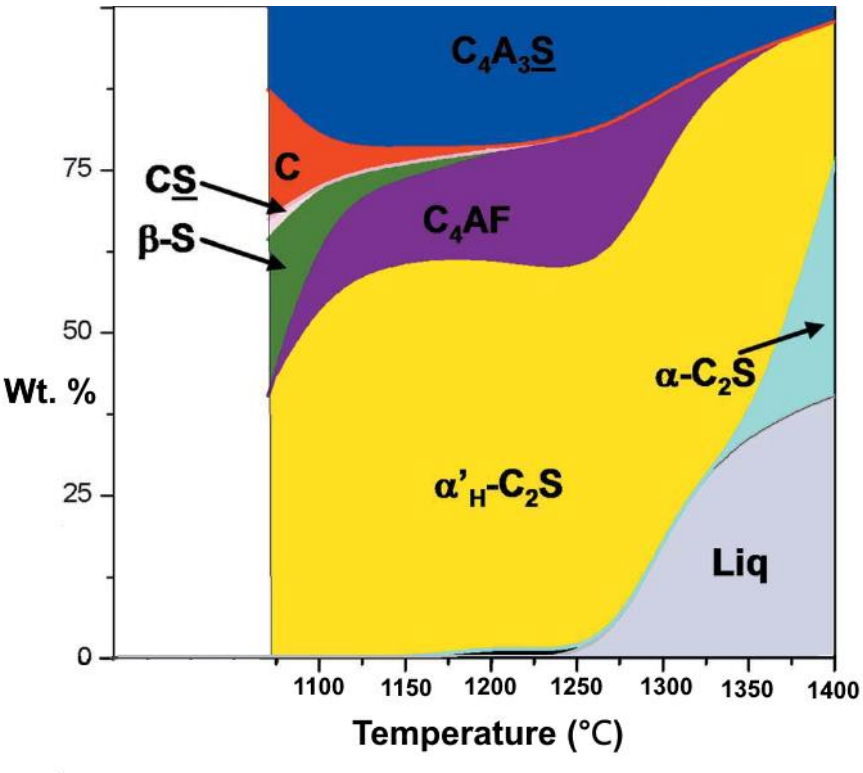

Figure 13: A phase depicting the formation of belite ye'elimite ferrite (BYF) CSA clinker, reconstructed from Ben Haha et al. [194] to show the units in Celsius for easier direct comparison [194].

In order to simplify the extensive and overlapping range of cements (Table 9), it is useful to separate CSA into those that contain predominately ye'elimite, and those with a majority of another component such as belite. Many CSA-belite cements, such as those employed in this study, have been designed primarily as an additive for PC to produce a shrinkage compensating cement, also known as type K or expansive cements [104]. For example, Caltra recommend a 1:2 ratio addition of their Calumex CSA binder to PC for shrinkage compensation [195]. This does not mean that predominantly ye'elimite cements cannot be employed as a primary binder however, although the price and availability in comparison to PC has limited its use to more specialist applications. Zhang et al. [175] detailed examples of the use of SAC and FAC (Table 9) in China, where the distinctive properties of these predominantly ye'elimite binders are advantageous [175]. For example, these systems can be used for smaller pre-cast concrete shapes, which can dispense with the steam curing required for PC and speed up production, and in larger construction projects, these CSA binders have been used in winter construction conducted in temperatures as low as -20 °C when aided with admixtures (Figure 14) [175].

Figure 14: The Shenyang Long Distance Telecommunication Hub, which involved CSA concrete laid in as low as -20 °C, as detailed in Zhang et al. [175].

Of CSA cements with a minority ye'elimite content, the most common majority component is belite (Table 9). Belite-CSA cements, or belitic cements, are targeted more towards a direct replacement for PC in more generic scenarios. Since 1975 when it was first patented in the United States by Borje Ost, the high dimensional stability, rapid curing, and high early strength have proven advantageous for applications such as highway road and airport runway paving [125, 174, 193]. Key to its adoption as a viable competitor and alternative to PC is enhancement of the reactivity of the belite component, which can otherwise typically take in excess of 3 months to hydrate significantly in a belitic CSA [173]. This can be achieved by either increasing the belite reactivity through means such as boron doping, or introducing another reactive phase that provides the development between the early stage of ye'elimite and the later stage of belite, such as ternesite which reacts with aluminium hydroxide [184, 194, 196]. Both CSAB and BCSA have now been awarded European Technical Assessment approval, in 2016 and 2020 respectively [197-199].

3.3. Calcium Sulfoaluminate Cement and the UK Nuclear Industry

The UK nuclear industry is considering CSA as an alternative binder system primarily because of its need to replace the supplementary cementitious materials currently employed with PC, that are becoming increasingly difficult to obtain reliably and to a consistent quality [88]. The powder

specification for PC itself has also deviated away from the set standard defined in the 1980's by the then authority, British Nuclear Fuels Limited (BNFL), and is now finer and faster reacting, though this has been offset by lower reactivity BFS [81, 84].

The differences in the hydration chemistry, as well as the defining characteristics of CSA, offer a number of key advantages for the encapsulation of low and intermediate level radioactive wastes. CSA is able to tolerate species that can hinder the hydration reaction and setting of PC, such as boron and phosphates, which is achieved through the substitution of ions into calcium, aluminium, hydroxide, and sulfate sites in ettringite [107, 200-202]. Ettringite also holds a large quantity of chemically bound water, which both allows for high water and thus low viscosity mixes which can better envelop complex waste, and the significant incorporation of the water into the structure of ettringite may remove it from the pore network [88, 203]. This therefore may reduce the transmission of ions throughout the network and reduce the rate of metal corrosion reactions [201]. CSA mixes can also exhibit a pore solution pH of 10-11.5, which reduces the corrosion and hydrogen generation rate of aluminium waste products [88]. The reduction in free water may also have the potential to reduce radiolytic hydrogen generation.

The binders chosen for investigation by the UK nuclear sector are high ye'elimite clinkers without a pre-blended quantity of calcium sulfate. This is to maximise the benefit of the low system pH with the production of ettringite and aluminium hydroxide, the immobilisation of target species, the high water retention, and chemical resistance, but also because high ye'elimite CSA binders are readily available from a number of European and international manufacturers for shrinkage compensating and rapid set applications [195, 199]. The absence of pre-blended calcium sulfate allows for a greater level of control of the hydration process in order to best serve the purpose of waste encapsulation.

3.4. Published Paper – "Hydrate Assemblage Stability of Calcium Sulfoaluminate-belite Cements with Varying Calcium Sulfate Content".

This section consists of work from the academic paper 'hydrate assemblage stability of calcium sulfoaluminate-belite cements with varying sulfate content', which has been reorganised so that the

materials and methods content is included as part of chapter 2 and is included in its as published state as Appendix 1. It was accepted for publication by Construction and Building Materials on the 6th of April 2023 [148]. The contributions of co-authors and sources of funding are described in Section 3.6.

3.4.1. Abstract

To assess the feasibility of employing calcium sulfoaluminate (CSA)-belite cements for radioactive waste encapsulation purposes, a series of 40 mixes were conducted on a 3-litre scale. This series of tests incorporated two commercially available CSA-belite clinkers, a gypsum or anhydrite addition at 15, 25 or 35 wt.%, a water to solid ratio of 0.5, 0.6 or 0.7, and a high or low mixing shear regime. CSA clinkers chosen contain predominantly ye'elimite, with some belite, and a small quantity of calcium sulfate as anhydrite. This paper outlines the effect of these parameters upon the phase composition and structure of these CSA samples tested at 7, 28, and 90 days. The development of the hydrate assemblage was monitored in order to assess the suitability of these grouts for use in encapsulation processes. The trends in phase development and evolution are consistent across both clinkers tested. The levels of ettringite formed as a hydration product are dependent upon the levels of calcium sulfate addition and the availability of water, with ettringite production evident, though at a decreasing rate, from between 7 and 90 days. Throughout the entire catalogue of mixes, no ettringite decomposition was detected. The majority of belite within both clinkers appears to remain unreacted, with a small increase in mixes producing less ettringite. Simulations also show similar phase assemblages to those encountered experimentally, with little phase development after 90 days.

3.4.2. Introduction

Calcium sulfoaluminate cement (CSA) is being considered by the UK nuclear industry as a potential future encapsulant for radioactive waste [88]. CSA has the potential to improve encapsulation performance and help secure a supply of cementitious material for long term future use, offering several potential key advantages such as: enhanced chemical resistance, an early age pore solution pH below 12, high water retention, and lower associated CO_2 emissions [88, 103, 188, 192]. CSA is being developed as a low CO_2 alternative cement for applications requiring rapid strength development and high dimensional stability with shrinkage compensation, and has seen successful deployment in

highway repair and runway paving [125, 193]. It has also been used extensively in China since the 1970's, where it is referred to as TCS or 'third cement series', with high alumina cement and Portland cement (PC) accounting for the second and first series' respectively [192, 204, 205]. Whilst having shown promise in both large-scale projects and laboratory testing, CSA is a relatively new cement in comparison to PC and does not have nearly the same wealth of past experience associated with it. The UK nuclear industry has long relied upon PC based systems, combined with supplementary cementitious materials (SCMs), to encapsulate and immobilise its low and intermediate level waste streams within steel vessels of 500 litres or larger [60, 88]. Ground granulated blast furnace slag (GGBFS) and pulverised fuel ash (PFA) are SCMs that are employed both to enhance the performance of the wasteform, and to reduce the exotherm and the maximum temperature experienced by the mix, due to their slower rate of reaction in comparison to PC clinker [81, 88]. Obtaining a consistent and standardised supply of these materials has become increasingly difficult throughout the past two decades, due to GGBFS being a by-product of iron production and PFA a waste generated from coal fired electricity generation; these are two industries that have undergone significant changes and that will continue to do so in the immediate future [81, 206, 207].

When combined with the ongoing development of alternative cements and the performance opportunities that these may afford, this has led the UK nuclear industry to begin exploring alternative cementitious binder systems. CSA-belite cements are produced from a clinker that consists predominantly of ye'elimite, with a smaller proportion of belite. Ye'elimite is also commonly referred to as Klein's compound, and is the naturally occurring form of calcium sulfoaluminate, with the abbreviated cement chemical formula ($C_4A_3\$$) [1]. It is formed when an alumina bearing material such as bauxite is heated with calcium sulfate and calcium carbonate. CSA is typically clinkered at between 1250 and 1350 °C, significantly lower than the PC clinkering temperature of 1450 °C [104, 188]. This reduction in temperature is achievable in part due to the absence of alite (C_3S), responsible for the early strength development in PC. In CSA, this role is fulfilled by the hydration of ye'elimite [184]. The main product of hydration is expected to be ettringite (the archetype of the AFt – *tri* – phase family of hydrous calcium sulfoaluminates), with aluminium hydroxide (gibbsite or amorphous), formed through the

consumption of both ye'elimite and an interground calcium sulfate source. In this study, the sulfate source is either anhydrite (Eq. 3.1) or gypsum (Eq. 3.2)[1]. If a sufficient quantity of calcium sulfate is not available, then ye'elimite will hydrate to form calcium monosulfoaluminate, commonly referred to as monosulfate, and a representative of the AFm (*mono*) phase family (Eq. 3.3).

$$C_4A_3\$ + 2C\$ + 38H \rightarrow C_3A{\cdot}3C\${\cdot}32H + 2AH_3 \quad \textit{(Eq. 3.1.)}$$

$$C_4A_3\$ + 2C\$H_2 + 34H \rightarrow C_3A{\cdot}3C\${\cdot}32H + 2AH_3 \quad \textit{(Eq. 3.2.)}$$

$$C_4A_3\$ + 18H \rightarrow C_3A{\cdot}C\${\cdot}12H + 2AH_3 \quad \textit{(Eq. 3.3.)}$$

Ettringite has gathered interest for radioactive waste immobilisation, as it has been shown to act as a host for a number of radioactive and heavy metal waste ions [107]. This is achieved through hosting ions within the columnar and channel sections of the AFt crystal structure, as well as through substitution of the calcium (e.g. by Ba^{2+}), aluminium (e.g. by Cr^{3+}), hydroxide, and sulfate sites (e.g. by IO_3^- and AsO_4^{3-}) [107, 120, 202, 208]. Ettringite crystals form in hexagonal prismatic columnar morphology, and have a water content of 30 – 32 H_2O per Al_2O_3 ($C_6A\bar{S}_3H_{32}$) [106, 107]. In PC, ettringite is formed early in the hydration reaction sequence, and provides much of the mechanism for the initial setting of the cement. The rate at which ettringite forms, and the greater quantity produced by CSA hydration, enables these cements to exhibit a much higher early strength when compared to PC [209, 210]. The ettringite component is key to the overall stability of CSA. Studies upon ettringite have shown a sensitivity to both the availability of water and temperature, which may cause dehydration and a reversible transition to meta-ettringite or decomposition into calcium monosulfate [106, 111-113, 120, 121]. Jiménez *et al.* [120] shows that the stability of naturally occurring ettringite outperforming that of synthetic ettringite, and so it is important that stability of ettringite can be established in a large scale series of commercially applicable formulations [120, 121].

[1] Chemical reaction equations in this paper are presented using cement chemistry abbreviated notation, where C represents CaO, A is Al_2O_3, S is SiO_2, H is H_2O, and \$ is SO_3.

Belite, (C_2S), is responsible for the later-stage strength development of PC. Similarly, in CSA-belite cements, belite also hydrates relatively slowly. Hydration of belite forms either calcium silicate hydrate (C-S-H) (Eq. 3.4), which has also been shown to be able to host a number of waste ions, or the silica-substituted AFm phase strätlingite (Eq. 3.5) [5, 107]. Belite hydration in the absence of aluminium hydroxide forms C-S-H and portlandite (calcium hydroxide), which could increase the pH of the pore solution (Eq. 3.4) and the corrosive potential of some encapsulated metals such as aluminium. Belite has been shown to take in excess of three months to begin to react to a significant extent in a belitic-CSA cement system, but appears to improve compressive strength once the slow process of hydration has begun [125].

$$C_2S + 2H \rightarrow C\text{-}S\text{-}H + CH \quad \textit{(Eq. 3.4.)}$$

$$C_2S + AH_3 + 5H \rightarrow C_2ASH_8 \quad \textit{(Eq. 3.5.)}$$

This paper reports upon the development of the hydrate assemblage of CSA-belite type cements, based on two commercial clinkers and different sources and levels of sulfate addition, at between 7 and 90 days and on the scale of a 3-litre mix. The impact of different concentrations of anhydrite or gypsum, different water to cement ratios, and different mixing shear regimes are all examined. The 40 mixes in this experimental series have been conducted in order to identify robust formulations of commercially available CSA-belite cements that can be utilised by the UK nuclear industry. A wide scope of successful mixes will demonstrate just how robust CSA can be, as well as allow for future studies to be conducted upon a much larger scale, approaching the 500 litre mixes conducted by the UK nuclear industry for waste encapsulation [60].

The key aims of this study therefore to; establish the behaviour of the CSA-belite system within a large mix formulation envelope and timeframe, identify if the key ettringite phase has remained stable, and assess whether CSA is robust enough for consideration within UK nuclear as well as add to the knowledge and experience of using a CSA cement.

3.4.3. Results and discussion

3.4.3.1. Ye'elimite hydration

Ye'elimite is the hydraulic phase primarily responsible for the production of ettringite when hydrated in the presence of sufficient calcium sulfate (Eq. 3.1, 3.2), and it is relatively rapidly consumed in the hydration of CSA-belite cements. The remaining weight percentage ye'elimite content, as identified by the Rietveld analysis of the solid product and compared against the quantity of ye'elimite present within each mix, at 90 days was between 7% and a maximum of 17% (Table 10). Quantifying the degree of reaction in Alipre clinker whilst accounting for the calcium sulfate addition, it is calculated that between 73% and 83% of the ye'elimite present has reacted with anhydrite during the first 90 days, or between 69% and 81% when the calcium sulfate source is gypsum. Correspondingly for the Alpenat clinker, between 65% and 79% of ye'elimite has reacted with anhydrite, and between 68% and 79% has reacted with gypsum. Gypsum dissolves faster than anhydrite, and has reportedly increased the rate of ye'elimite dissolution and hydration within the first few hours [203, 211]. At 7 days, the earliest point of measurement within this study, there is no clear indication that there is greater ye'elimite hydration in the presence of gypsum at this time period or beyond.

Within all mixes conducted, the majority of ye'elimite has been consumed through hydration. The proportion of ye'elimite consumption between Alipre and Alpenat clinkers is very similar, with Alipre only showing a small increase in the degree of ye'elimite consumption over Alpenat in most comparable mixes. The degree of ye'elimite hydration is linked strongly to the clinker being blended with an increasing quantity of calcium sulfate. This is clearly shown in Figure 15 and

Figure 16, with a sharp decrease in the main ye'elimite peak at 23.7 °2θ with increasing calcium sulfate content. The availability of sulfate is reported to accelerate the hydration of ye'elimite within the first 24 hours, as well as densifying the cement matrix with the rapid generation of hydration products [203, 211, 212]. Berger et al.[212] reports that this densification of the matrix with fine ettringite crystals, which inhibits the passage of water to clinker particles, results in only minor hydration between 7 days and 1 year in systems with a w/s of 0.55. Ye'elimite hydration beyond 7 days is observed as slight (Figure 15 and

Figure *16*), however in these systems there is an indication of consistent ettringite generation after 7 days and up until 90 days at a decreasing rate (Figure 17). The slower reacting anhydrite could result in higher levels of hydration before densification takes place, however within this study there is little to distinguish between anhydrite and gypsum hydration over all mixing variables [203]. To a lesser extent than the calcium sulfate, the quantity of water available is also a contributing factor to the degree of ye'elimite hydration in most mixes, as most clearly shown in Figure 15, between the w/s ratios of 0.5 and 0.7. No correlation is evident that the shear method used has had any effect upon the consumption of ye'elimite within the reported timeframe (Table 10).

Table 10: Rietveld analysis results displaying the weight percentage (wt. %) of each phase detected, for all 120 mixes that contain either Alipre clinker (Ali - blue) and Alpenat CK clinker (Alp -green) clinkers. Inert phases detected, or those that could be classed as minor, were omitted. The full list of phases identified is given in Table 8.

Calcium Sulfate Type	Sulfate Content	w/s Ratio	Shear	Days	Ye'elimite		Belite		Anhydrite		Gypsum		Ettringite		Gibbsite		Mono-sulfate	
					Ali	Alp	Ali	Alp	Ali	Alp	Ali	Alp	Ali	Alp	Ali	Alp	Ali	Alp
Anhydrite	Low (15%)	0.5	Low	7	19	9	16	23	7	6	1	1	30	22	14	17	6	9
				28	15	12	13	18	8	8	1	1	36	25	13	16	7	8
				90	14	11	13	19	9	8	1	1	36	27	14	15	7	8
Anhydrite	Low (15%)	0.5	High	7	17	12	12	21	10	6	1	1	33	22	14	16	7	9
				28	15	11	13	22	13	7	1	1	37	27	9	14	5	8
				90	15	13	13	17	10	4	1	2	35	27	12	16	6	9
Anhydrite	Low (15%)	0.7	Low	7	13	10	16	20	6	6	1	1	34	28	16	15	7	10
				28	12	14	13	20	5	4	1	1	39	29	15	15	7	7
				90	13	15	13	16	5	4	1	1	37	27	16	16	7	8
Anhydrite	Low (15%)	0.7	High	7	13	11	16	20	5	5	1	1	34	28	16	16	9	9
				28	12	14	14	21	4	5	1	1	37	27	14	15	7	7
				90	11	14	13	21	4	3	1	1	37	27	15	16	8	8
Anhydrite	Med (25%)	0.6	Low	7	12	10	12	19	12	9	1	1	39	29	12	13	6	8
				28	12	10	13	19	9	8	1	1	43	31	11	13	6	8
				90	11	12	12	17	11	13	1	1	42	28	11	13	6	6
Anhydrite	Med (25%)	0.6	High	7	12	10	13	20	12	11	1	1	39	25	11	14	6	8
				28	12	10	14	21	12	7	1	1	37	28	11	13	6	8
				90	12	10	12	19	13	8	1	1	41	27	9	15	4	9
Anhydrite	High (35%)	0.5	Low	7	9	7	12	14	22	24	1	1	30	25	11	12	7	6
				28	9	7	11	14	22	25	1	1	33	26	11	11	7	6
				90	7	8	10	15	26	16	1	1	34	30	11	10	5	7
Anhydrite	High (35%)	0.5	High	7	9	11	11	16	24	20	1	1	28	25	12	10	7	6
				28	7	7	11	15	24	21	1	1	32	25	11	13	7	7
				90	8	8	10	16	21	16	1	1	35	33	15	9	5	6
Anhydrite	High (35%)	0.7	Low	7	9	7	10	15	24	18	1	1	36	29	8	11	4	7
				28	9	7	11	14	18	18	1	1	42	34	8	8	5	5
				90	8	7	8	14	19	17	1	1	46	34	7	9	4	7
Anhydrite	High (35%)	0.7	High	7	9	10	11	17	21	16	1	1	39	28	9	11	5	7
				28	10	7	9	14	21	18	0	1	43	32	6	11	3	6
				90	10	7	8	12	26	15	0	1	48	34	3	10	1	7
Gypsum	Low (15%)	0.5	Low	7	17	9	17	21	3	2	3	3	30	23	16	19	7	10
				28	18	11	13	23	3	3	3	2	32	23	15	17	7	10
				90	17	11	12	22	3	3	4	1	34	26	16	17	6	9
Gypsum	Low (15%)	0.5	High	7	17	12	15	21	2	2	3	4	30	26	16	16	9	9
				28	14	14	14	17	3	3	4	2	34	27	16	17	7	9
				90	16	14	12	21	3	5	3	2	35	28	16	16	7	7
Gypsum	Low (15%)	0.7	Low	7	11	11	17	23	3	3	1	1	36	25	17	17	7	10
				28	11	9	14	21	3	2	1	1	40	29	14	18	7	9
				90	11	12	12	20	3	3	1	2	41	28	15	16	8	9
Gypsum	Low (15%)	0.7	High	7	11	11	14	24	3	3	2	1	39	24	15	18	8	9
				28	10	11	13	21	3	3	2	1	41	32	16	14	7	9
				90	11	12	13	16	3	3	1	1	39	38	16	13	8	8
Gypsum	Med (25%)	0.6	Low	7	11	13	15	20	3	3	6	3	35	30	15	14	8	7
				28	10	10	15	20	3	3	6	3	35	31	15	14	8	9
				90	10	9	13	20	3	3	4	3	41	36	15	13	7	7
Gypsum	Med (25%)	0.6	High	7	13	10	14	19	3	3	6	4	39	31	13	14	6	8
				28	13	10	15	20	3	3	4	2	40	32	12	14	6	8
				90	13	13	13	19	3	3	6	2	42	30	11	15	5	8
Gypsum	High (35%)	0.5	Low	7	11	9	11	19	3	2	17	10	36	23	11	15	6	10
				28	10	10	10	18	2	2	17	10	39	32	10	11	6	5
				90	10	10	9	14	2	3	15	7	43	32	10	14	4	9
Gypsum	High (35%)	0.5	High	7	11	10	12	20	3	3	12	10	38	23	12	16	7	7
				28	9	8	10	18	2	2	15	9	42	27	10	17	6	8
				90	11	7	10	16	3	2	13	9	44	29	10	16	5	8
Gypsum	High (35%)	0.7	Low	7	9	11	15	18	3	3	7	7	37	30	13	14	8	8
				28	8	12	13	16	3	3	7	9	41	32	14	12	6	6
				90	9	10	11	16	2	3	8	4	42	42	15	10	7	5
Gypsum	High (35%)	0.7	High	7	8	10	15	16	3	2	9	8	38	33	12	11	8	8
				28	8	13	13	17	3	3	7	5	42	33	14	13	7	7
				90	8	12	12	16	3	3	5	3	43	36	14	12	7	7

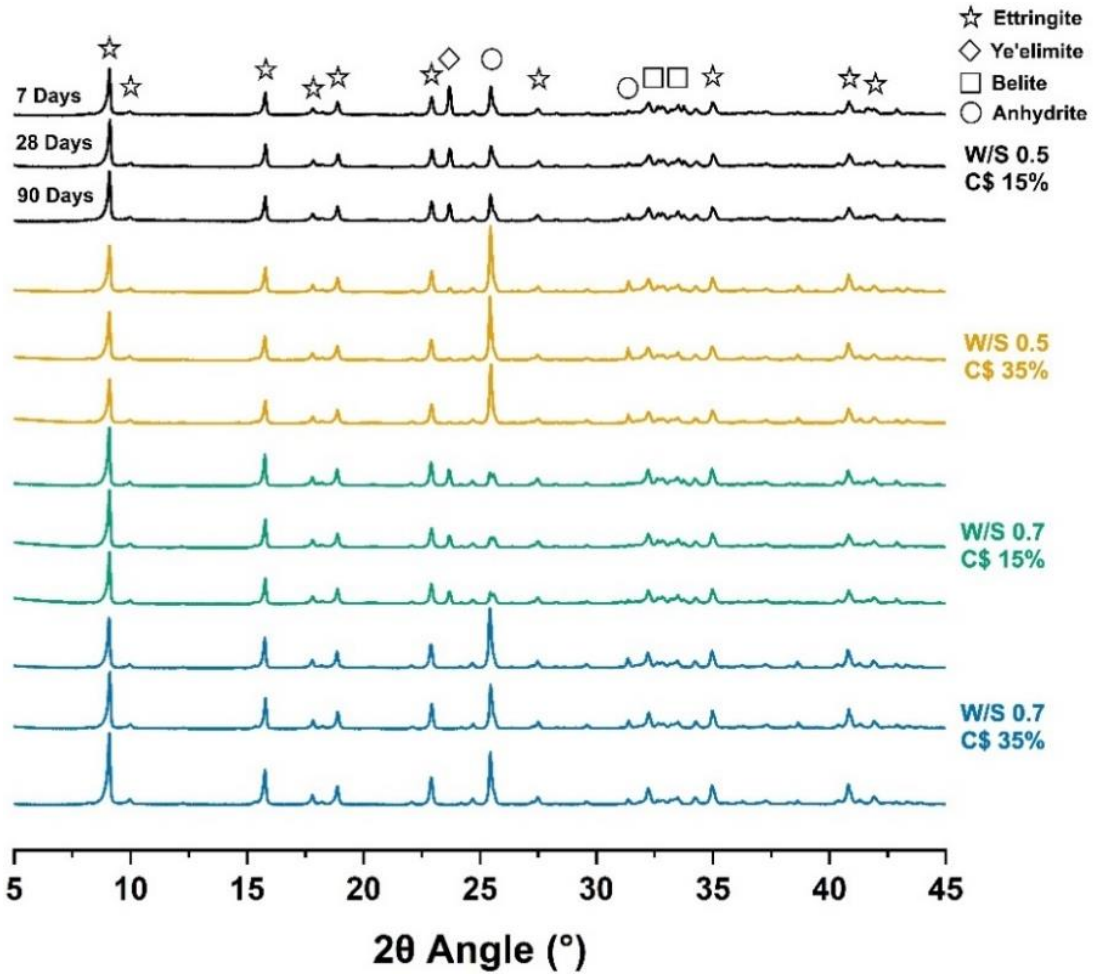

Figure 15: XRD pattern for Alipre clinker, with anhydrite at either 15% or 35% and a w/s ratio of 0.5 or 0.7. Increased ye'elimite hydration can be observed by the decrease of the main peak at 23.7 °2θ with increasing calcium sulfate and water content. Background levels have been reduced, most notably preceding 8 °2θ, in order to generate this figure.

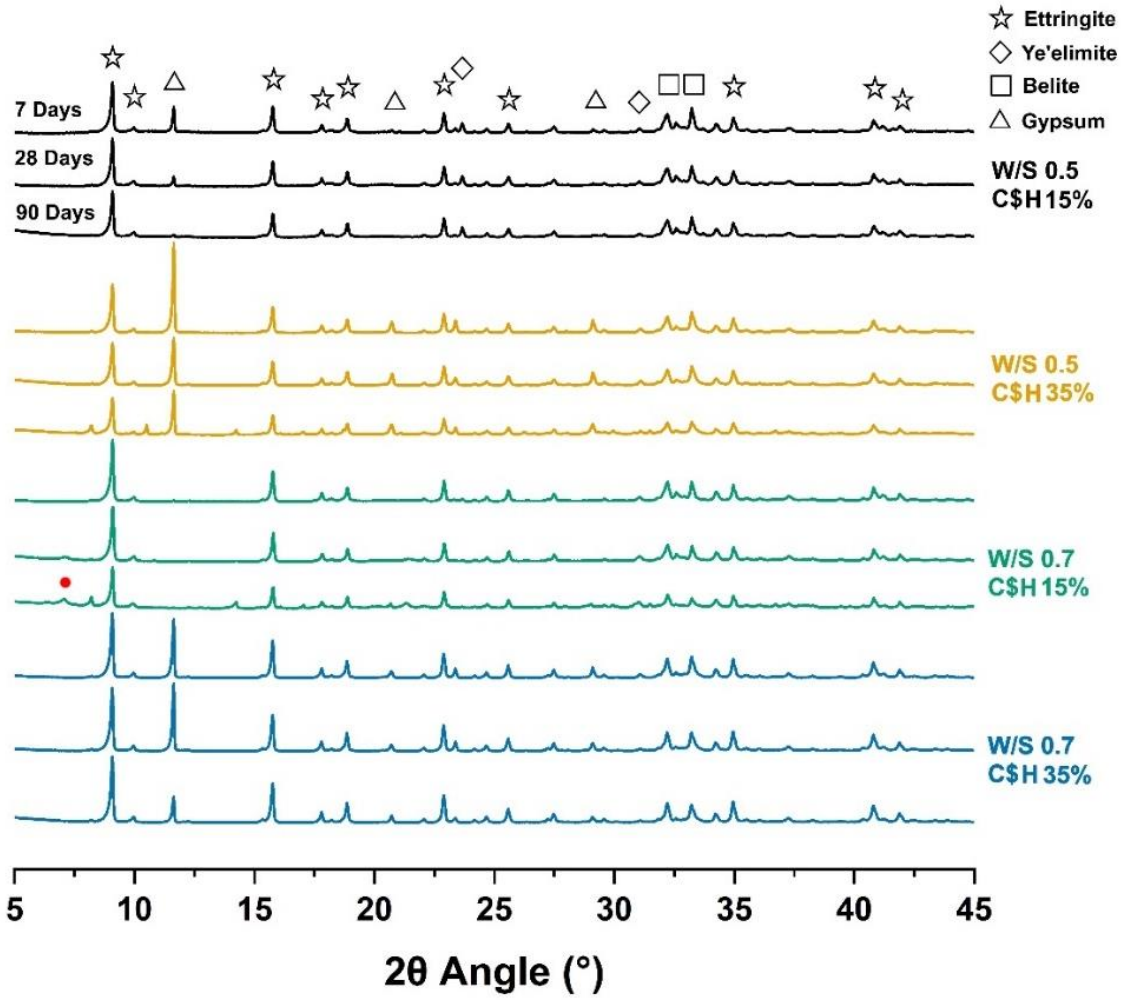

Figure 16: XRD pattern for Alpenat clinker, with gypsum at either 15% or 35% and a w/s ratio of 0.5 or 0.7. The signature for strätlingite is visible at 7.2 °2θ, (red dot) in the low gypsum and high-water mix at 28 days and beyond. Background levels have been reduced, most notably preceding 8 °2θ, in order to generate this figure.

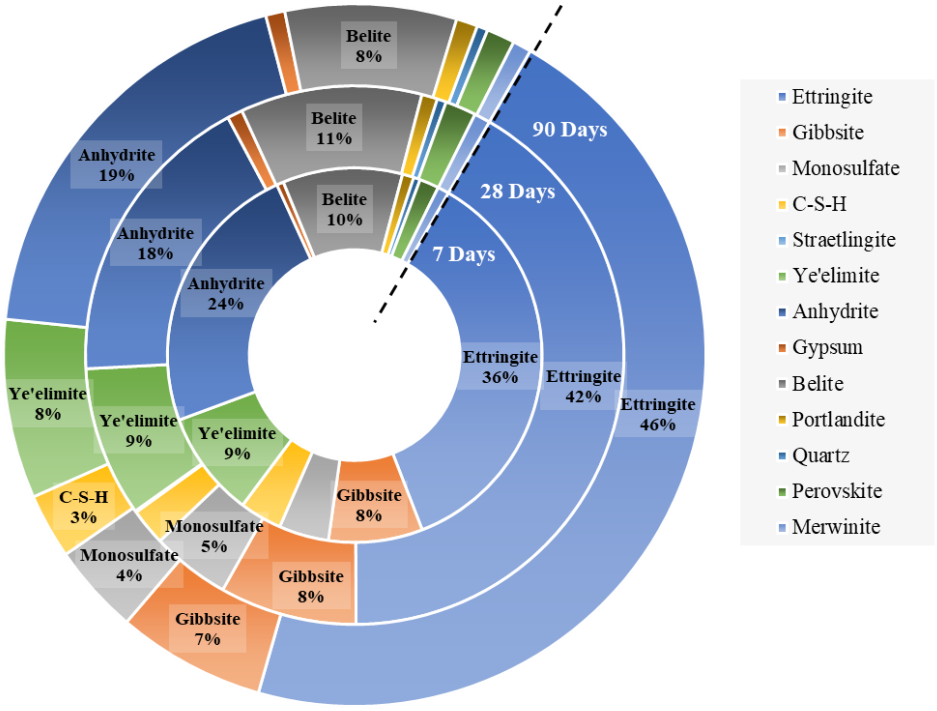

Figure 17: This concentric Rietveld analysis plot, for an Alipre mix containing 35% anhydrite and a w/s ratio of 0.7, displays the weight percentage (%) of main phases detected over the 90-day period. Most notably, the increased production of ettringite between 7 and 28 days, as opposed to between 28 and 90 days, is clearly shown in this mix.

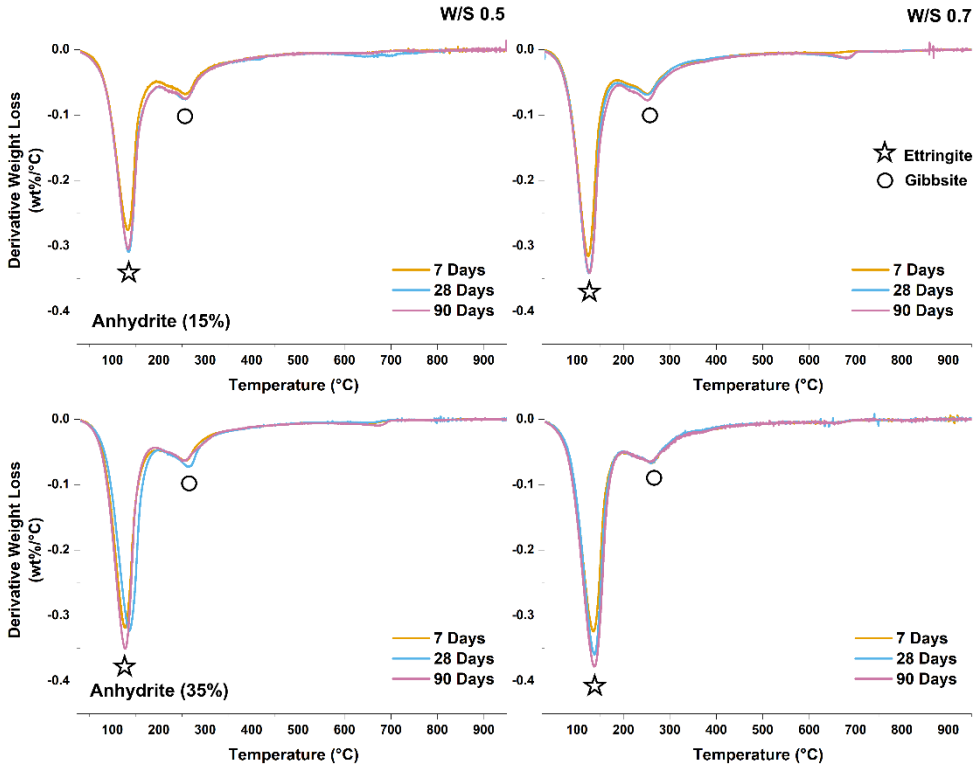

Figure 18: TGA for Alipre clinker, with anhydrite at either 15% or 35% and a w/s ratio of 0.5 or 0.7. An increase in ettringite content is evident with an increase in anhydrite, and to a lesser extent, water content.

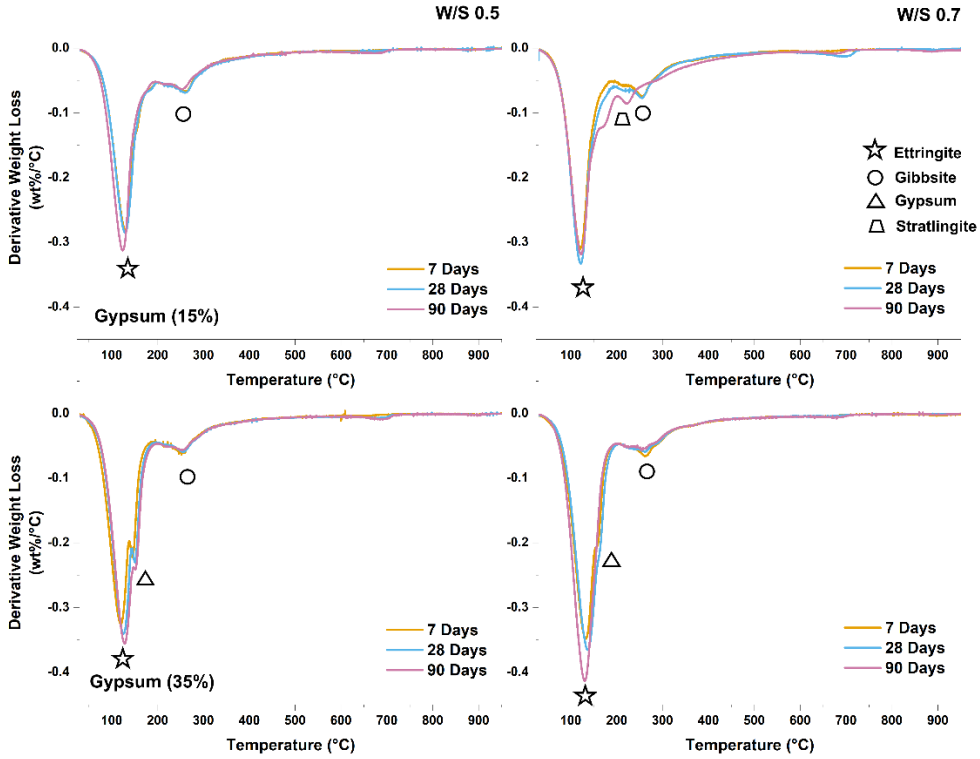

Figure 19: TGA for Alpenat clinker, with gypsum at either 15% or 35% and a w/s ratio of 0.5 or 0.7. The signature for strätlingite is visible at approximately 220 °C in the low gypsum and high-water mix at 28 days and beyond.

3.4.3.2. Belite Hydration

The belite content within hydrated samples produced with both clinkers remains nearly constant, with only a small decrease over the 90-day period in all hydrated samples. Belite levels detected by Rietveld analysis in solid Alipre products are close to that of the initial belite content found in the clinker. Alpenat products have shown some consumption of belite, however the average quantity consumed is only 17% of the total amount within the mix at 90 days (Table 10).

The majority of the belite present in Alpenat is monoclinic (β-C_2S), with a minority of faster hydrating orthorhombic α-C_2S, and each being present in almost equal amounts in Alipre clinker (Table 3) [213]. β-C_2S could be contributing to the low reactivity within the 90-day hydration period [125]. Jeong et al. [151] has also proposed that the rapid formation of ettringite could densify the matrix of the cement, whilst chemically binding (and thus consuming) water and limiting the diffusion of ions, which would explain the very low degree of belite hydration observed in the higher-ye'elimite Alipre system [214]. No relationship is evident between the type of calcium sulfate, the quantity of the calcium sulfate

addition, or the water content of these mixes and the degree of belite hydration from the Rietveld analysis, however; in Alpenat there is an indication of strätlingite in XRD and TGA within 15% gypsum and 0.7 w/s ratio mixes (

Figure *16* and Figure 19). This could be due to the greater overall availability of water for belite hydration, given that levels of ettringite production are lower at these formulations.

3.4.3.3. Ettringite formation

The production of ettringite is dependent upon the availability of ye'elimite, calcium sulfate and water. The absence or depletion of calcium sulfate will result in the production of monosulfate (in crystalline or disordered forms), and this reaction also has approximately half the water requirement of ettringite formation (Eq. 3.3). The ettringite content of the hydrate assemblages resulting from both Alipre and Alpenat clinkers increases significantly with the addition of more calcium sulfate, consistent with expectations based on the reaction stoichiometry with respect to calcium sulfate. An increase in water availability, with a higher water to solids ratio, also increases the quantity of ettringite found. This is consistent with findings that similar CSA-belite systems have self-desiccated at a w/s ratio of approximately 0.5, with additional water allowing for additional production of ettringite [151, 203]. In this experimental procedure however, there was no indication that self-desiccation occurred within any sample.

For both clinkers, there is also no real indication that anhydrite or gypsum produces consistently more ettringite than the other (Table 10). There is the potential for anhydrite to increase the quantity of ettringite present against the faster dissolving and thus faster reacting gypsum, due to gypsum quickly densifying the cement matrix with ettringite and hindering later hydration, but this has not been observed [212]. The quantity of ettringite formed by each clinker, when accounting for the quantity of ye'elimite present in each, is also similar. On average across all mixes, Alpenat mixes contained 24% less ye'elimite than Alipre mixes, and as a result there is a 22% less yield of ettringite after 90 days. The majority of ettringite formation in all mixes occurs at 7 days or before, with a maximum increase in the content of ettringite of only 12% between 7 and 90 days (Alpenat, w/s 0.7, 35% gypsum). More

ettringite formation occurs earlier (7 days or before) in mixes with higher water/cement ratio. This could be due to the higher water availability being able to overcome the densification of the system which may hinder later hydration [203, 212]. The later formation of ettringite, occurring after the initial setting, can be demonstrated in Figure 20. This SEM image shows numerous ettringite crystals that have formed after the initial setting. The porosity shown has formed during the initial set, with the characteristically lath shaped ettringite crystals growing and spanning the width of this pore after it has formed.

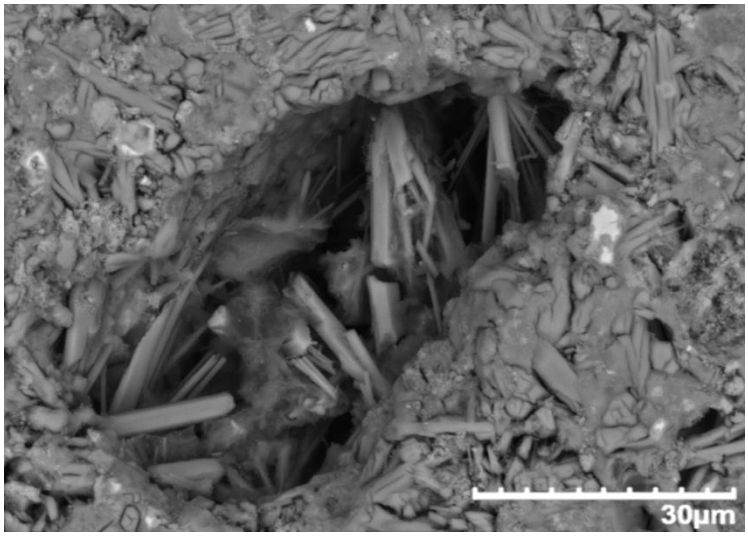

Figure 20: An ettringite 'nest', where the lath shaped crystals have grown into a pore; a clear indication of ettringite growth after the initial setting of the Alpenat mix with low gypsum (15%) and a w/s ratio of 0.7. This sample was taken at 90 days.

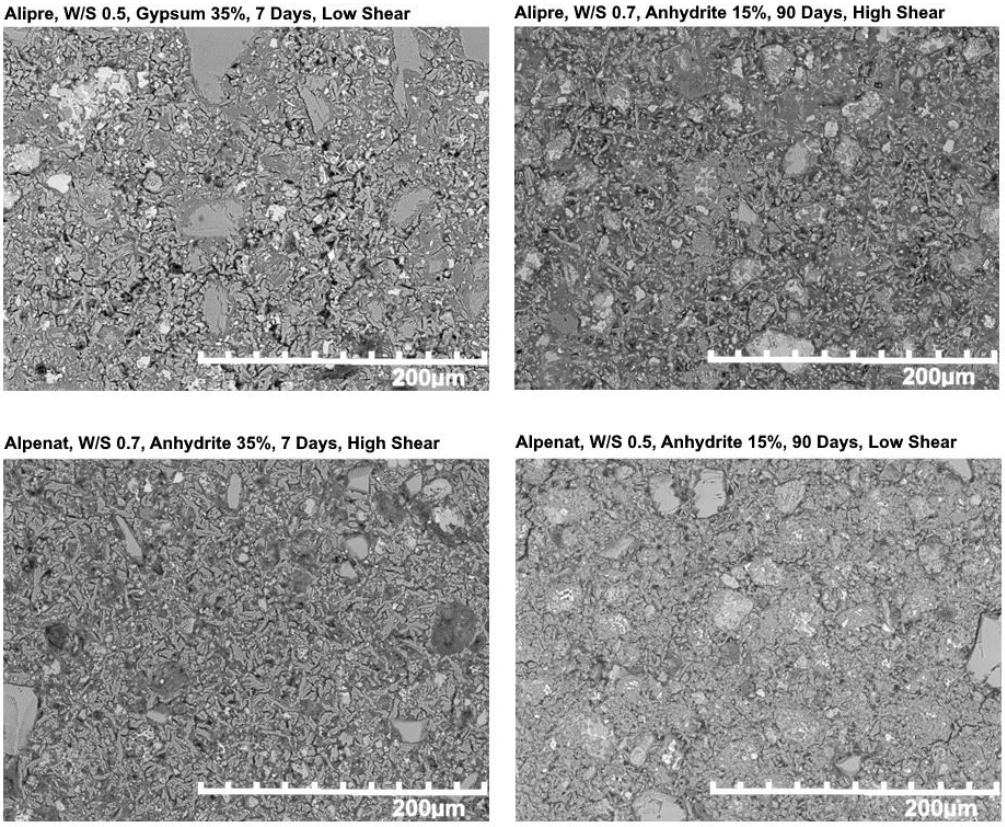

Figure 21: SEM imagery showing very similar structures of ettringite lath crystals within an aluminium hydroxide matrix, between differing clinkers, types of calcium sulfate, and w/s ratios. Un-hydrated calcium sulfate and clinker particles can also be observed.

3.4.3.4. Phase assemblage

SEM and EDS images, as exemplified in Figure 20, Figure 21, and Figure 22, show large networks of ettringite crystals within a matrix of aluminium hydroxide. Ettringite is clearly identifiable by its lath-shaped crystals, and by the high concentration of Ca and S with an absence of Al or Si. The aluminium hydroxide matrix is identifiable by the strong concentration of Al distinct from other phases within the system. Unreacted belite and other minor clinker constituents can also be observed. Ca and Si EDS maps show high concentrations confined to very specific areas, with a minor distribution of silicon elsewhere in the sample, suggesting that the silicon is largely limited to the unreacted belite particles identified. For both clinkers, the significant majority of Si is within the belite phases (Table 3).

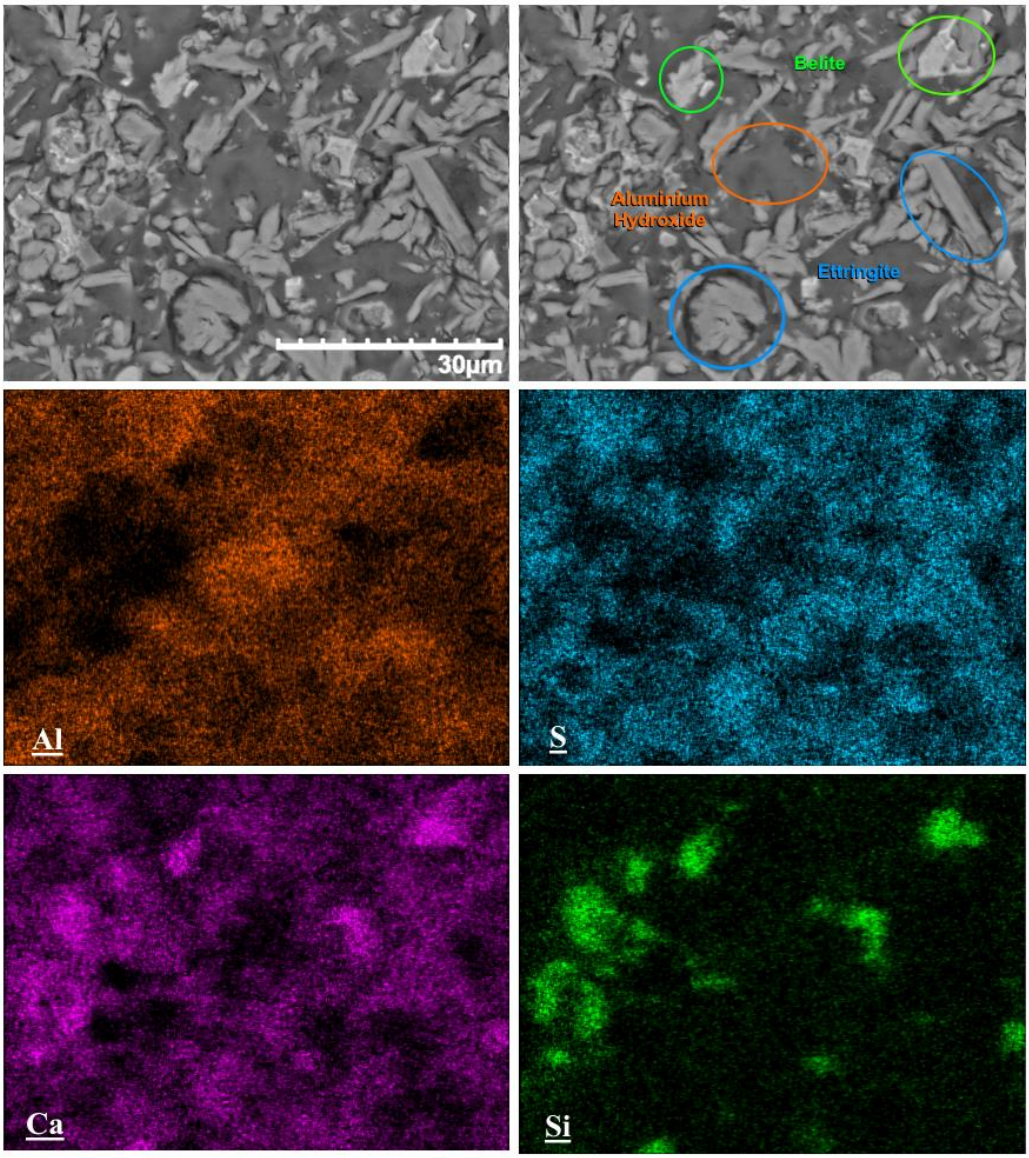

Figure 22: SEM-EDS mapping of Alipre with high gypsum (35%) and a w/s ratio of 0.7. Ettringite, belite and aluminium hydroxide can clearly be identified their characteristic elemental signatures.

Furthermore, there is evidence to suggest that ettringite stability during the hydration period for all samples has been high under the curing and storage conditions used. Rietveld analysis shows an increase in ettringite content over time, with no strong indication of ettringite decreasing; ettringite having shown to be forming within the pore structure after the initial set (Figure 20). The TGA results also give evidence to support that the levels of ettringite have not decreased over time [215]. The derivative weight loss, that occurs at approximately 120 – 130 °C for ettringite, shows that the level of ettringite increases with increased water and sulfate content. As also shown in the Rietveld analysis above, there

is little to separate between the type of calcium sulfate or clinker used. In all instances, there is a small increase in the peak rate of weight loss at 90 days when compared to 7 days, indicating an increase in the quantity of ettringite over time (Figure 18 and Figure 19) as discussed above.

Levels of monosulfate remain at a near constant throughout the hydration periods of each mix as identified in the Rietveld analysis (Table 10) [111, 115]. A significant increase in monosulfate formation could be taken as an indication of the decomposition of ettringite [115]. TGA does not display any significant indication of monosulfate at 150 °C, which would be displayed as a shoulder on the peak attributed to ettringite (Figure 18 and Figure 19). The decomposition of ettringite to monosulfate would also result in the precipitation of calcium sulfate [111, 115]. The levels of anhydrite and gypsum identified in the Rietveld analysis remains largely constant over time. Rietveld, XRD, and TGA all show large quantities of calcium sulfate remaining after 90 days in the higher (35%) calcium sulfate samples, with some residual quantities detected even at the lowest (15%) sulfate addition. Remaining quantities of calcium sulfate shown in the Rietveld analysis more than doubling in the 35% sulfate mixes, when compared to the 25% sulfate mixes (Table 10). Similar levels of residual calcium sulfate were also observed in Berger et al., where gypsum levels remaining at 7 days were approximately 4% for a 20% addition to the clinker, and 15% for a 35% addition at a w/s ratio of 0.55 [212].

Levels of aluminium hydroxide detected by Rietveld analysis do not increase in line with that of ettringite and remain at a consistent level. This could in part be due to the sometimes-amorphous structure of aluminium hydroxide being difficult to detect using XRD, and any change in quantity being difficult to differentiate by its small TGA signature. It is also consumed in the hydration of belite to form strätlingite (Eq 3.5).

3.4.3.5. Belite Hydration Products

The high quantity of remaining belite observed within both clinkers suggests that a large proportion has not yet hydrated. This is also evident given the lack of belite hydration products detected in the majority of samples. The C-S-H content identified in the Rietveld analysis was consistently low at an average of 3%, and negligible strätlingite was detected; however, the amorphous structure of C-S-H can make

identification using XRD difficult, whilst the main strätlingite peak occurs at 7.2 °2θ in a range susceptible to high background noise. The distribution of calcium and silicon in EDS shows high concentrations confined to very specific areas, with a minor distribution of silicon elsewhere in the sample (Figure 22). This would suggest that the silicon concentration is limited to the unreacted belite particles identified.

The hydration of belite without the presence of aluminium hydroxide generates C-S-H along with calcium hydroxide, which could be responsible for a later-age increase in pH in some CSA-belite cements (Eq. 3.4). The quantities of C-S-H and portlandite identified by Rietveld are consistently low, with an average across all mixes of 3% and 1% at 90 days, respectively. The consistency of this generation could potentially be due to the similar quantities of faster reacting α-C_2S being present across all mixes. C-S-H is also not clearly identifiable in the TGA, and whilst it would dehydrate at a similar temperature to the main ettringite peak and AFm of approximately 150 °C, there is no significant shoulder to this peak that would suggest a strong secondary phase within this TGA curve. Gypsum also strongly occupies this region (Figure 19). The significance of a presence of calcium hydroxide brought about by the generation of C-S-H needs to be fully understood if these cements are to be used in encapsulation of some classes of wastes which are not compatible with highly alkaline conditions. Jeong et al. [151] however, does suggest that strätlingite is the primary long term hydration product of belite when there is a presence of aluminium hydroxide (Eq. 3.5), the example clinker having a ye'elimite and belite composition similar to that of Alipre (Table 3) [151, 216].

Similar to C-S-H, the Rietveld, as well as the XRD and TGA cannot identify any significant strätlingite, with two noticeable exceptions. Alpenat mixes which feature the higher belite content, when combined with the highest water content (0.7 w/s) and the lowest gypsum content only (15%), exhibit a small but characteristic main strätlingite peak in the XRD at 7.2 °2θ (

Figure *16*) and the indicative derivative weight loss in the TGA after 28 days (Figure 19) [125, 216]. Smaller XRD indications of strätlingite are also noticeable in some minimal calcium sulfate Alpenat mixes at 90 days. This supports the observations of Jeong et al. [151] wherein the production of

ettringite hinders the hydration of belite [151]. There is a potential therefore, that Rietveld has been unable to identify the formation of strätlingite in these cases due to high background noise preceding the 8 °2θ range.

3.4.3.6. Thermodynamic Modelling Phase assemblage

Thermodynamic modelling conducted using CemGEMS [171] predicts a phase assemblage largely similar to that identified by the Rietveld analysis and complemented by the other analytical methods, as well as past studies that applied thermodynamic modelling to CSA-belite cements [105, 151]. Ettringite and aluminium hydroxide (in the form of gibbsite) are majority phases, as has been determined practically. Two phases differ significantly between the simulations and the experimental mixes: the quantities of monosulfate, and that of strätlingite, most notably in 15% calcium sulfate mixes (Figure 23 and Figure 25). The quantities of these phases within these simulations are much larger than that observed within the Rietveld analysis, with negligible strätlingite detected in all experimental mixes, although other indications of strätlingite having been identified.

Monosulfate, formed when ye'elimite reacts in the absence of sufficient calcium sulfate (Eq. 3.3), decreases sharply in simulations when levels of calcium sulfate addition are raised above 15%, to the extent that it is entirely absent in 35% simulated mixes (Figure 24 and Figure 26). Whilst this deviates from what is seen in the Rietveld analysis, monosulfate levels do remain stable, with no more than a 1% increase within the mix between 7 days and the full duration of the simulation. There is, therefore, no significant amount of monosulfate generation, or consumption to form further ettringite within both simulated and experimental mixes. The increased levels of strätlingite are a function of the increased belite hydration, however residual belite levels are very similar to those identified in the experimental mixes. Strätlingite levels also significantly decrease with increasing ettringite formation, which corresponds to the findings of Jeong et al. [151], strätlingite preferring lower calcium sulfate mixes [217]. Also of note, a small quantity of C-S-H is formed in high calcium sulfate regardless of the water content, potentially driven by this preference, the increased generation of C-S-H having not been identified experimentally (Figure 24 and Figure 26).

Simulations have shown the levels of ettringite greater than that identified by Rietveld, however they do remain at a near constant level past 90 days with a smaller corresponding quantity of aluminium hydroxide. Ettringite levels only increase, with no indication of any decomposition. Levels of residual calcium sulfate and ye'elimite also appear to remain at a near constant after 90 days. The quantity of ettringite also appears to increase strongly with increasing levels of calcium sulfate within that 90-day timeframe, as has been observed in the Rietveld analysis. There were no cases of self-desiccation shown within any of the simulations, with a small increase in water consumption for anhydrite mixes as also identified in the findings of Coumes et al. [203].

As mentioned previously, high levels of unreacted belite remain beyond the 90-day period. The belite phase, however, is the only phase to show significant signs of further reactivity beyond 90 days, albeit on a small scale. In Figure 24, a small quantity of strätlingite begins to form at approximately 250,000 hours (29 years), indicating a potential for belite hydration well in excess of the 90-day experimental duration. Simulations containing gypsum appear to be more inclined to the formation of strätlingite, as shown when comparing Figure 26 and Figure 27. This is also highlighted in

Figure *16*, which displays the strätlingite signature at 7.2 °2θ, which is not shown in XRD diffractograms in mixes identical other than the calcium sulfate type being anhydrite. There is, however, little difference between the consumption of ye'elimite and the generation of ettringite. Little difference is displayed between the behaviours of either clinker composition, other than the increased quantity of ye'elimite in Alipre leading to increased quantities of ettringite. The increased availability of water also appears to lead to a minor increase in the production of ettringite, as has been experienced experimentally.

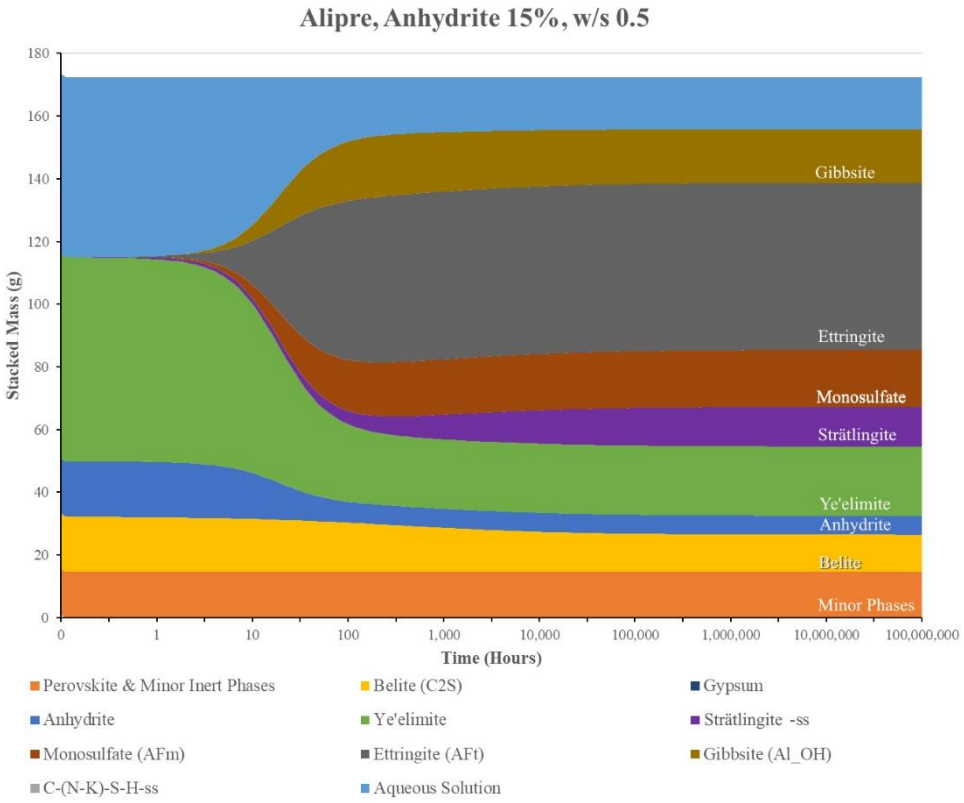

Figure 23: CemGEMS simulation for Alipre clinker at an anhydrite addition of 15% and a w/s ratio of 0.5. The level of hydration, so as to be comparative to experimental results, was set to 66%. Anhydrite levels are predicted to become depleted, leading to the generation of monosulfoaluminate.

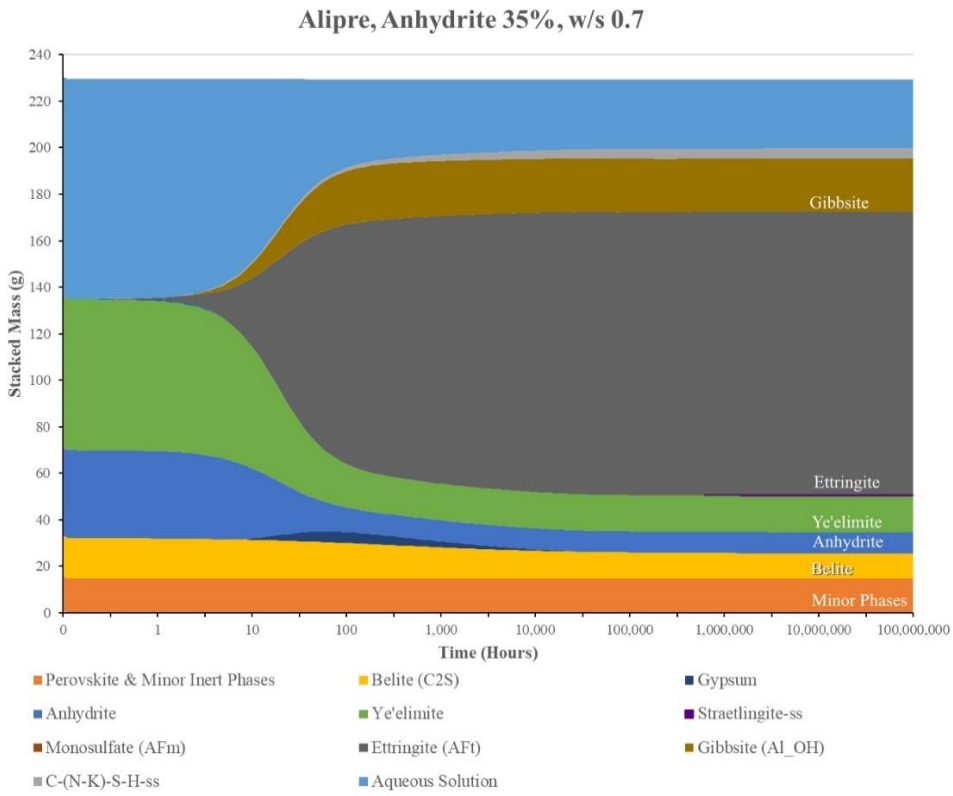

Figure 24: CemGEMS simulation for Alipre clinker at an anhydrite addition of 35% and a w/s ratio of 0.7. The level of hydration, so as to be comparative to experimental results, was set to 76%. The potential for late stage belite hydration is shown as a small quantity of strätlingite formation.

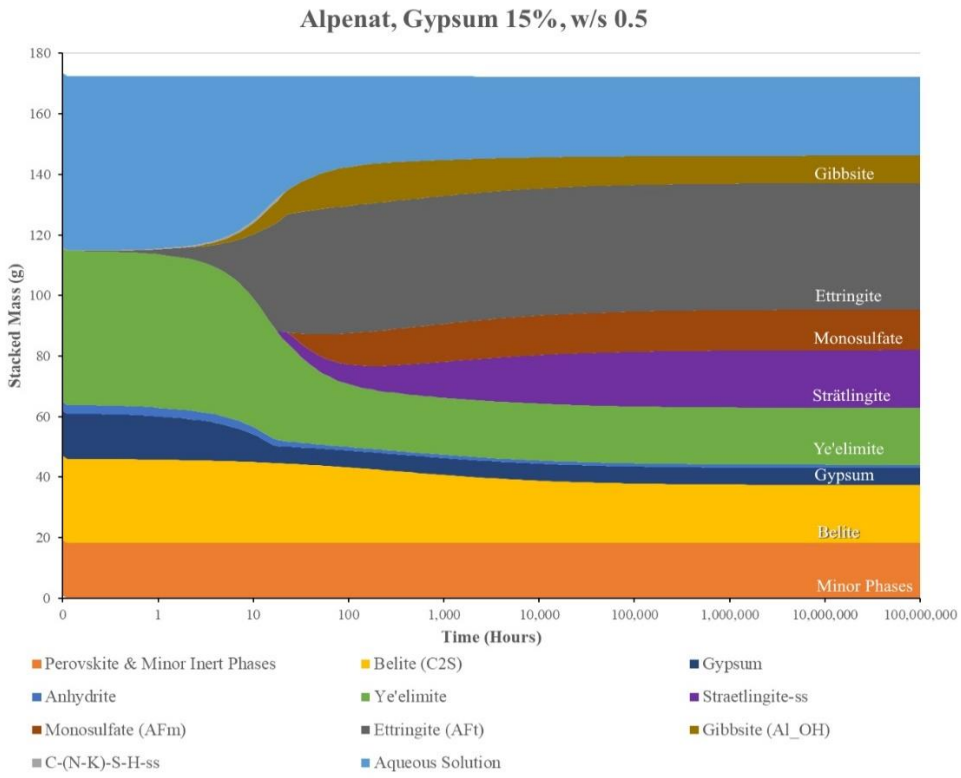

Figure 25: CemGEMS simulation for Alpenat clinker at a gypsum addition of 15% and a w/s ratio of 0.5. The level of hydration, so as to be comparative to experimental results, was set to 63%. The increased quantity of belite when compared to Alipre clinker, has allowed for Alpenat to form more strätlingite, though a significant proportion remains unreacted. >1% C-S-H has been simulated up until 20 hours, where it is proceeded by the appearance of monosulfate and the increasing quantity of strätlingite.

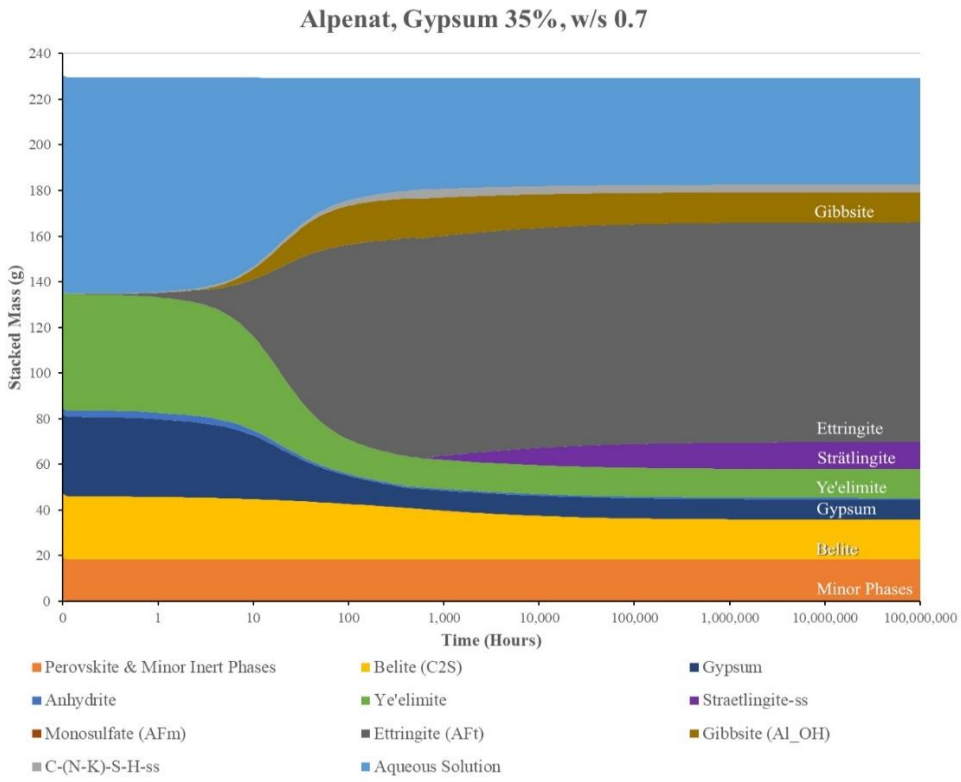

Figure 26: CemGEMS simulation for Alpenat clinker at a gypsum addition of 35% and a w/s ratio of 0.7. The level of hydration, so as to be comparative to experimental results, was set to 75%. Increase ettringite formation has likely hindered belite hydration, however; some belite hydration has occurred without the presence of gibbsite, forming C-S-H (Eq.3.4).

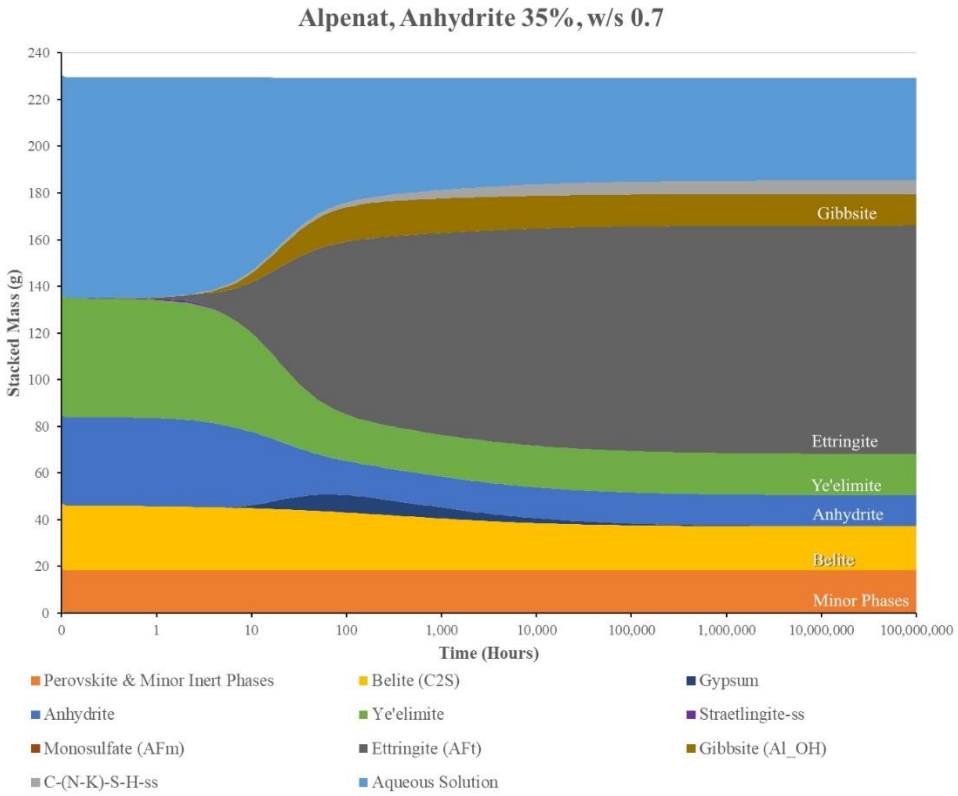

Figure 27: CemGEMS simulation for Alpenat clinker at an anhydrite addition of 35% and a w/s ratio of 0.7. The level of hydration, so as to be comparative to experimental results, was set to 65%. The formation of strätlingite appears to prefer the presence of gypsum over anhydrite, as development of strätlingite is negligible, with only a small quantity of C-S-H. The simulation does not identify any calcium hydroxide.

3.4.4. Conclusions

The 90-day development of the hydrate assemblage for two different commercial CSA clinkers, with variable quantities of anhydrite, gypsum, and water present, has been monitored and supported by thermodynamic modelling. The shear of the mix does not seem to have had any noticeable impact upon the 7 to 90-day hydrate assemblage, indicating that the low shear method has ensured effective mixing at this scale. Between the 7 and 90-day time period, all mixes experience some degree of further ettringite growth, after ettringite having predominantly formed prior to the 7-day measurement point. The formation of ettringite is strongly dependent upon the availability of calcium sulfate, as well as water. The difference between anhydrite and gypsum appears to have had no significant difference upon the amount of ettringite formed. More ettringite was formed within Alipre mixes, simply due to the greater quantity of ye'elimite within the clinker.

The majority of ye'elimite hydrated within all mixes, with a range of between 35% and 17% of the original ye'elimite remaining after 90 days. With the hydration of ye'elimite and the formation of ettringite, the quantity of aluminium hydroxide detected by Rietveld analysis did not increase linearly with ettringite and accounted often for less than half the weight percentage of ettringite. Such quantities are not dissimilar to those seen in the simulations. This could in part be due to the occasionally amorphous structure of aluminium hydroxide being difficult to detect, or its consumption in the hydration of belite to form strätlingite.

The hydration of belite within all mixes appears to be low, as also predicted in the simulations conducted. Some instances of strätlingite or C-S-H formation are displayed, but in the practical experimentation, only some noticeable strätlingite is observed in gypsum mixes and aided by the increased belite quantity within Alpenat clinker. Belite hydration also increases with a decreasing presence of ettringite. Some minor belite hydration is shown to be possible in the distant future by means of simulation, however this only indicates a potential for further hydration past 90 days. Further hydration of belite over time should lead to further strength development, but longer-term practical studies should be carried out to verify this.

Other than gypsum appearing to increase the potential for strätlingite formation, little differences have been shown between the choice of calcium sulfates. A significant quantity of both remain at 90 days in solid products containing a 35% addition, with as much as 20% of the product being identified as unreacted anhydrite as a maximum.

In all mixes, there is no evidence to suggest ettringite instability within the 90-day time frame. Within these samples cured at 20°C and >90% RH, ettringite has only increased over time, with levels of calcium monosulfate remaining stable, and no other mechanisms for decomposition established. Ettringite crystal size and distribution are consistent throughout this aging period and between mixes. The structure can be clearly defined using EDS mapping, with large ettringite crystals clearly distinguishable amongst the aluminium hydroxide matrix.

The predominant ettringite and aluminium hydroxide structure remains consistent throughout the varying system parameters and age under the curing conditions studied and has not broken convention at the extremities of this extensive mix formulation envelope, nor has it behaved uncharacteristically from what is expected given the variables. Both clinkers, and sources of calcium sulfate, have formed very similar phase assemblages. The calcium sulfoaluminate system therefore looks to be a robust and promising avenue for future research into the encapsulation and immobilisation of radioactive wasteforms. A scaling up of experiments towards the 500 litre mixes practised within the nuclear industry, as well as a more complete understanding of the long-term reactivity of belite within this system and its effect upon the pore solution pH if C-S-H were to be generated, would allow for even greater confidence in CSA-belite as a potential encapsulant for radioactive waste.

3.5. Further Results and Discussion

Corresponding with the analysis conducted at the University of Sheffield outlined in section 3.4, the Encapsulants Integrated Research Team (EIRT) of the National Nuclear Laboratory (NNL) Workington conducted a series of mechanical and dimensional stability tests upon samples generated from the CSA mixes carried out. Dimensional stability testing involved the monitoring of solid grout product prisms in a single dimension, and observations generally showed a plateau in microstrain after approximately 7-days . These samples were retained after the 90-day trial period and were monitored in order to confirm that that plateau observed was indeed a constant, given that long term dimensional stability is a key requirement for a cementitious encapsulant. Samples were kept in the same high humidity (>90% RH) walk in chamber at 20 +/-1 °C that all samples were cured in and were allowed to remain curing for in excess of 800 days. Once testing had concluded, the opportunity was taken to send a small selection of these dimensional stability samples to the University of Sheffield for further analysis. Samples were subjected to the same TGA and XRD powder preparation as described in section 2.3, including arresting hydration by use of isopropanol to the same standard described.

3.5.1. Thermogravimetric Analysis (TGA) with Mass Spectroscopy (TG-MS)

TG-MS was conducted on <63 μm powdered samples, using a Perkin Elmer TGA 4000 coupled with a Hiden Analytical mass spectrometer. The mass spectrometer identified ions according to mass/charge

ratios assigned to carbon dioxide and water. This was carried out for all 7, 28, and 90-day samples, as well as samples cured in excess of 800 days.

The mass spectroscopy element of initial TGA investigation was omitted due to a large degree of variability in results generated over time. The considerably large sample set and the prolonged time it took to run all 120 analyses likely allowed for the detector to degrade, which whilst maintained accordingly, still significantly affected the amplitude of the mass responses generated following both degradation and repair. All samples were run without a specific order to avoid potential unconscious bias, which whilst possible, made the use a normalisation method difficult. Therefore, it was decided that the valuable quantifiable data was better represented by the TGA results [218].

The TG-MS conducted can, however, be used to better identify key features shown in the TGA. The mass response for CO_2 is first shown during the dehydration of the ettringite component at approximately 120 ℃, which corresponds with a much more significant response for water. Levels of carbonation are consistently very low throughout the entire experimental series, which indicates that the sealing during storage of these samples was indeed effective. The most notable signal occurs at approximately 650 ℃, which corresponds to the decarbonisation of any trace amounts of calcium carbonate present [219]. After the dehydration of ettringite, the other main signal for H_2O corresponds to the dehydration of aluminium hydroxide at approximately 250 ℃ [219].

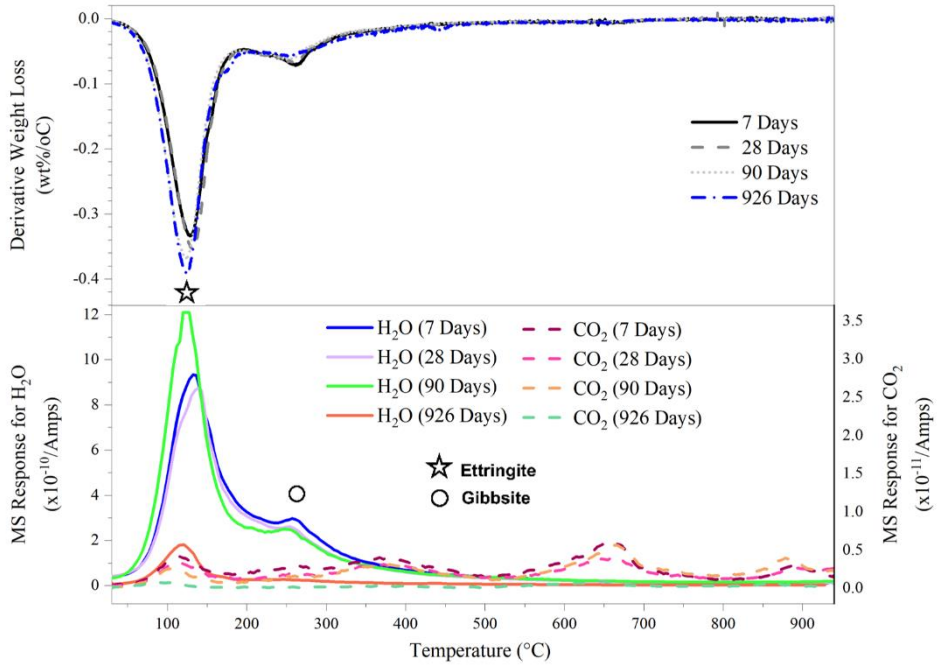

Figure 28: TGA with accompanying MS for an Alpenat mix with a gypsum addition of 25%, a water to solid ratio of 0.6, conducted at a high shear, highlighting the correspondence between TGA and MS signals. Ettringite and gibbsite (aluminium hydroxide) peaks are highlighted. Trace amounts of carbonation and the decarbonation of the small quantity of calcium carbonate present at 650 ℃.

Additional TGA was conducted upon midpoint formulation samples and high water and calcium sulfate samples, after allowing for them to cure for in excess of 800 days. This test was carried out to give any indication as to whether ettringite production had reached a plateau at 90 days, or whether there was a potential for further generation of this phase.

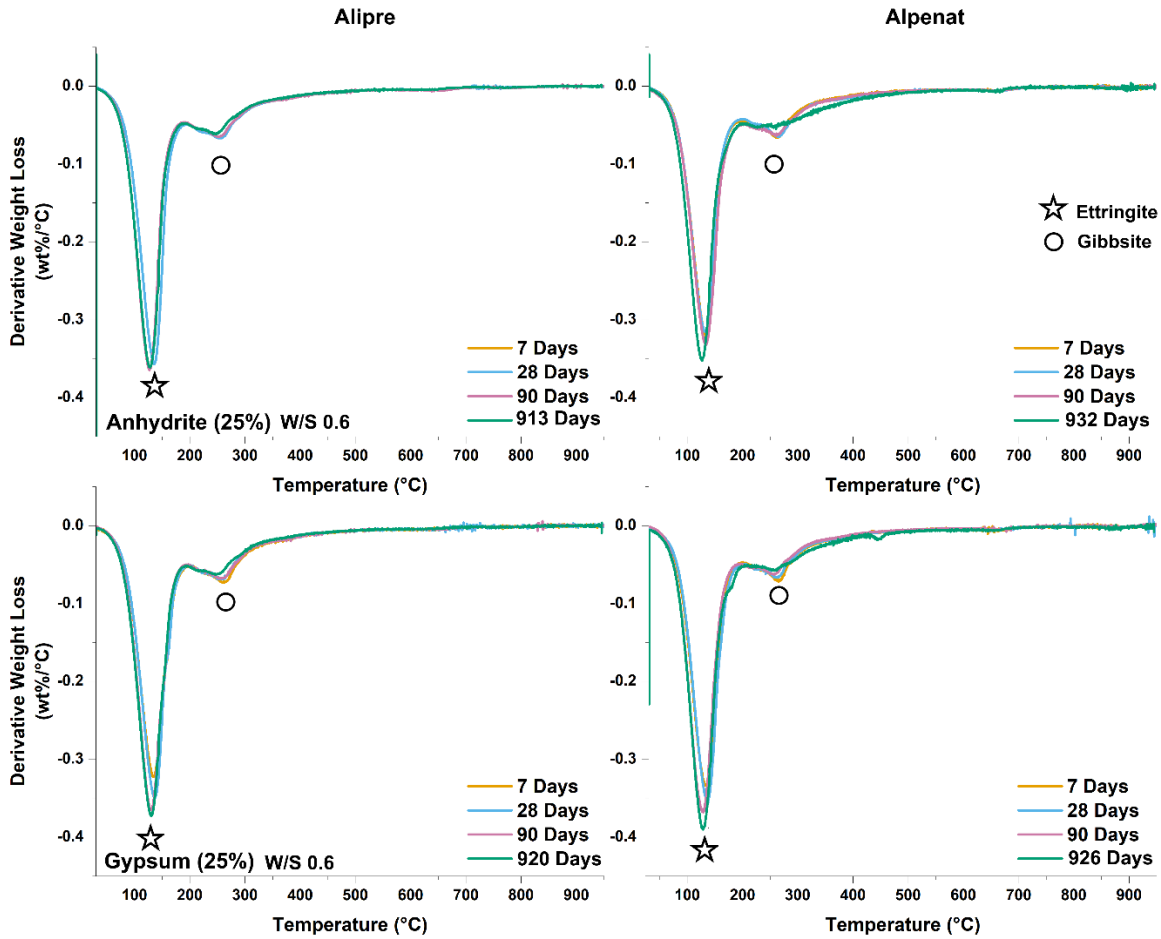

Figure 29: TGA for midpoint formulation samples (as marked in each panel) at 7, 28, 90 and >900 days. Differences in age for the later-age samples are representative of the time between when mixes were conducted, due to the extensive series of samples produced, with the arresting of hydration then commencing at the same time. All were conducted under high shear mixing.

As shown in Figure 29, the midpoint formulation samples involving Alipre clinker do not show a noticeable amount of additional ettringite generated after 90 days, and neither is there an increase in the quantity of aluminium hydroxide. The Alpenat clinkers with high levels of calcium sulfate, however, do appear to suggest a small increase in ettringite over this prolonged time period. In the two high water and calcium sulfate mixes selected (Figure 30) an increase in the quantity of ettringite over this time period is much more noticeable and occurs for both clinker types. This increase is comparable to that which was experienced in the time period between 7-90 days, suggesting that although the production of ettringite has occurred after 90 days, its generation has slowed significantly over the prolonged time

period to more constant rate, similar to the long term rate of hydration reaching a near constant in PC [220].

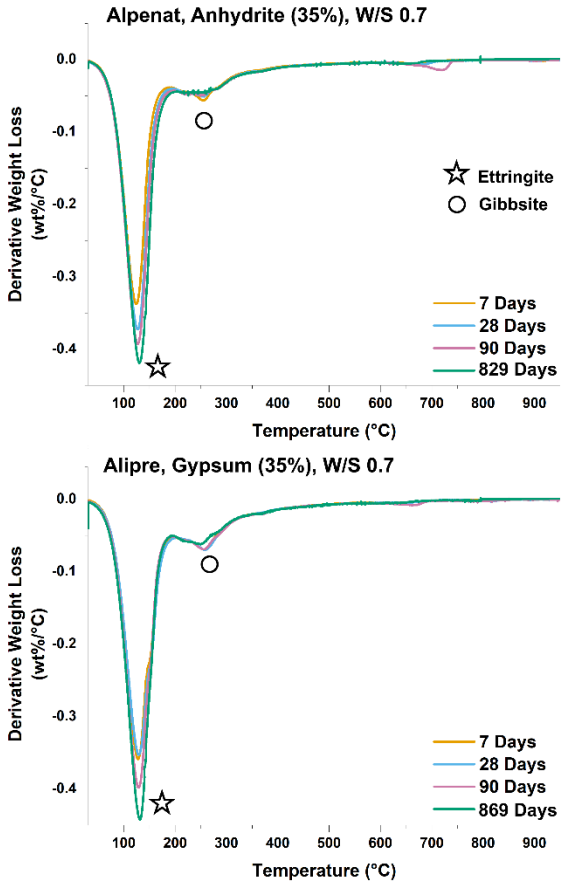

Figure 30: TGA scans for high calcium sulfate and water samples (as marked in each panel) at 7, 28, 90 and >800 days. Differences in age for the later-age samples are representative of the time between when mixes were conducted, due to the extensive series of samples produced, with the arresting of hydration then commencing at the same time. All were conducted under high shear mixing.

3.5.2. X-ray diffraction

XRD was conducted upon midpoint samples that were allowed to cure for in excess of 900 days, as described in section 2.3. From comparing the heights of specific peaks across scans at different times, whilst taking into account variations in the total counts recorded across mixes, there appears to be little discernible difference between the major hydrous or anhydrous phases in the 90 day and >900-day scans in any mix. Alpenat with anhydrite (Figure 31) may show a minor decrease in anhydrite, even once factoring in the typically lower amplitudes of the >900-day scans that were collected here.

More notably, however, there is some slight indication that the belite has begun to hydrate and form strätlingite with a very small peak beginning to form at 7.2 °2θ [124]. This is not shown in any other of the mixes shown. The levels of ettringite visible also do not appear to be significantly increasing from the comparative peak amplitudes alone, although this is better represented in the following Rietveld analysis of this data.

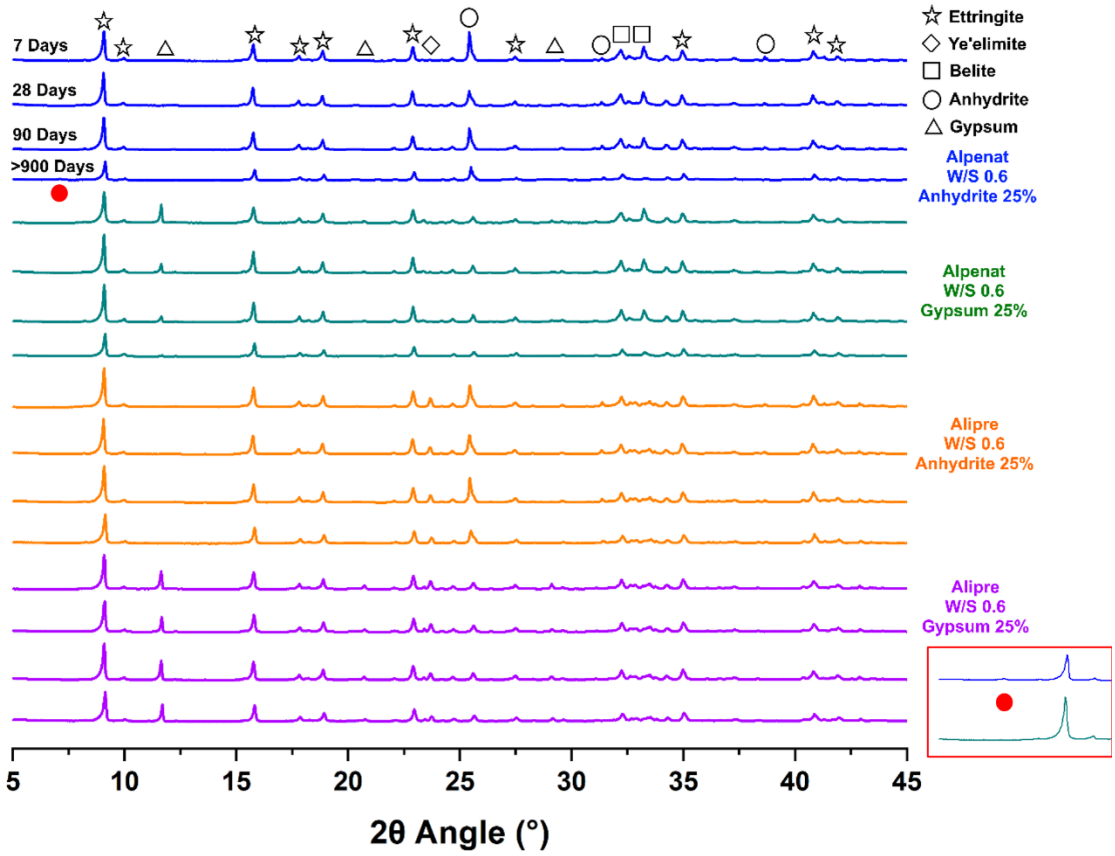

Figure 31: XRD diffractograms produced from midrange mix samples at 7, 28, 90, and >900 days of curing before hydration was arrested. The potential, very minor indication of strätlingite is highlighted with the red dot beneath and shown close up in the red box.

3.5.3. Rietveld Analysis

The Rietveld analysis (Table 11) was conducted as described in section 2.3, using the same parameters and data files in order to quantify the percentage phase composition for the >900-day curing formulation midpoint samples. This has allowed for direct comparison against the data produced from the analysis conducted on earlier samples, with the comparison presented visually in the concentric Rietveld plots.

Table 11: Rietveld analysis of the XRD data displayed in Figure 31. Difference in age is representative of the time between when mixes were conducted due to the extensive series, with the arresting of hydration then commencing at the same time.

Clinker Type	Calcium Sulfate Type	Sulfate Content	w/s Ratio	Shear	Days	Ye'elimite	Belite	Anhydrite	Gypsum	Ettringite	Gibbsite	Mono-sulfate
Alipre	Anhydrite	Med (25%)	0.6	High	7	12	20	11	1	39	11	8
					28	12	21	7	1	37	11	8
					90	12	19	8	1	41	9	9
					913	12	16	9	1	41	11	8
Alipre	Gypsum	Med (25%)	0.6	High	7	13	19	3	4	39	13	8
					28	13	20	3	2	40	12	8
					90	13	19	3	2	42	11	7
					920	12	17	3	1	43	12	9
Alpenat	Anhydrite	Med (25%)	0.6	High	7	10	13	12	1	25	14	6
					28	10	14	12	1	28	13	6
					90	10	12	13	1	27	15	4
					932	11	12	9	1	31	15	6
Alpenat	Gypsum	Med (25%)	0.6	High	7	10	14	3	6	31	14	6
					28	10	15	3	4	32	14	6
					90	13	13	3	6	30	15	5
					926	11	12	3	6	34	15	6

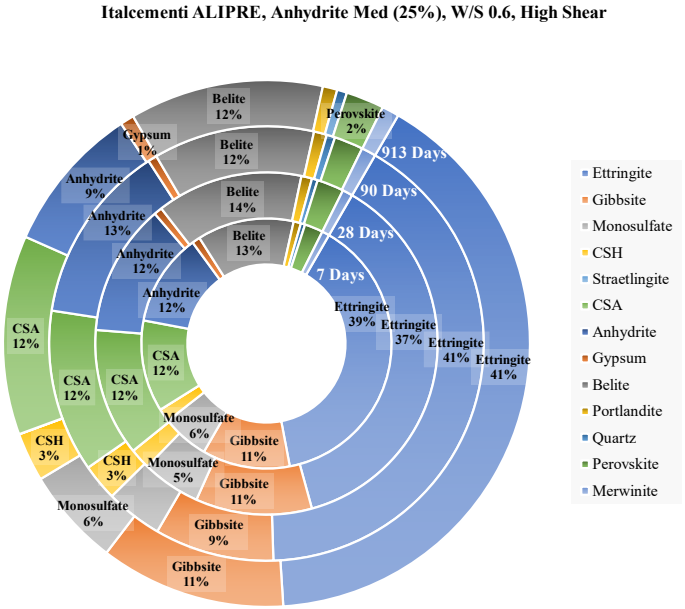

Figure 32: Rietveld analysis percentage quantities shown in a concentric circle diagram. Diagram highlights the difference between 90 days and prior, to 913 days for an Alipre midpoint formulation containing anhydrite.

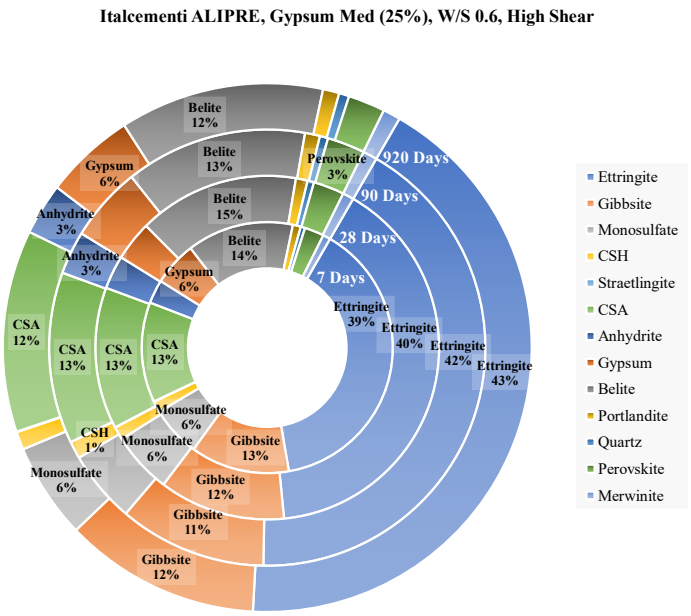

Figure 33: Rietveld analysis percentage quantities shown in a concentric circle diagram. Diagram highlights the difference between 90 days and prior, to 920 days for an Alipre midpoint formulation containing gypsum.

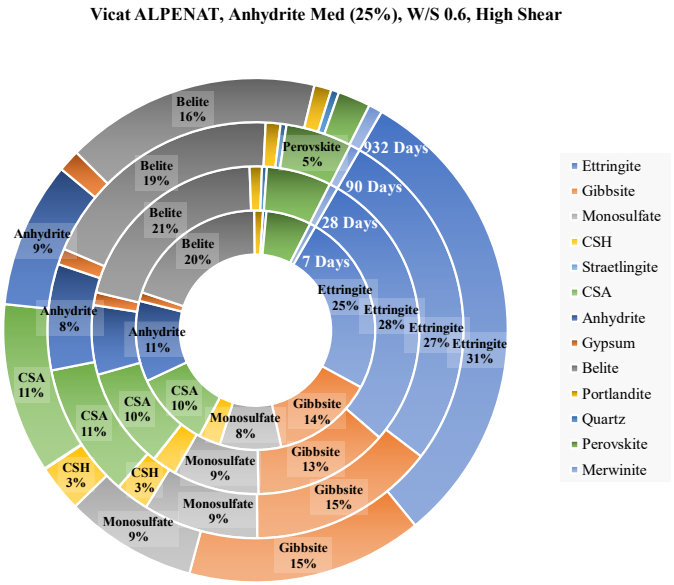

Figure 34: Rietveld analysis percentage quantities shown in a concentric circle diagram. Diagram highlights the difference between 90 days and prior, to 932 days for an Alpenat midpoint formulation containing anhydrite.

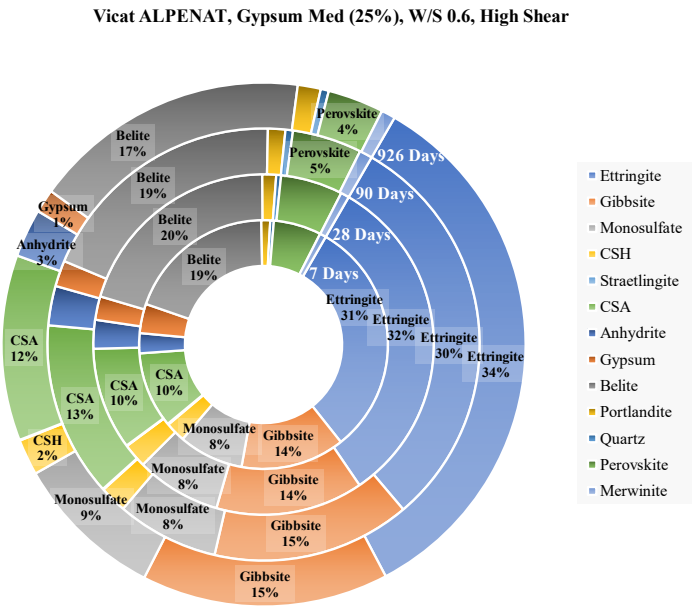

Figure 35: Rietveld analysis percentage quantities shown in a concentric circle diagram. Diagram highlights the difference between 90 days and prior, to 926 days for an Alpenat midpoint formulation containing gypsum.

Results generated from these samples correspond to a number of observations made using other analytical techniques. Firstly, there is no indication of the decomposition of ettringite over this prolonged time period. Ettringite levels have only increased from the Rietveld analysis conducted at 90 days. Whilst in the case of Alipre this increase is marginal, in Alpenat it suggests a small increase in the ettringite content after 90 days, as was also suggested in the TGA (Figure 29). This also adds evidence to the conclusion in section 3.4.4, that the phase assemblage has remained stable with no signs of decomposition, and that there was nothing to suggest that it would begin to decompose after 90 days. This was also backed up by the thermodynamic models generated, as described below.

The thermodynamic models do, however, suggest a higher proportion of strätlingite formation in both clinkers (Figure 36), which does not appear to be the case given the consistency of the belite content. The small indication of some strätlingite formation, shown in Figure 31 is not therefore represented here. As also found in the previous set of Rietveld analysis, no indication of strätlingite was able to be detected by the Rietveld analysis.

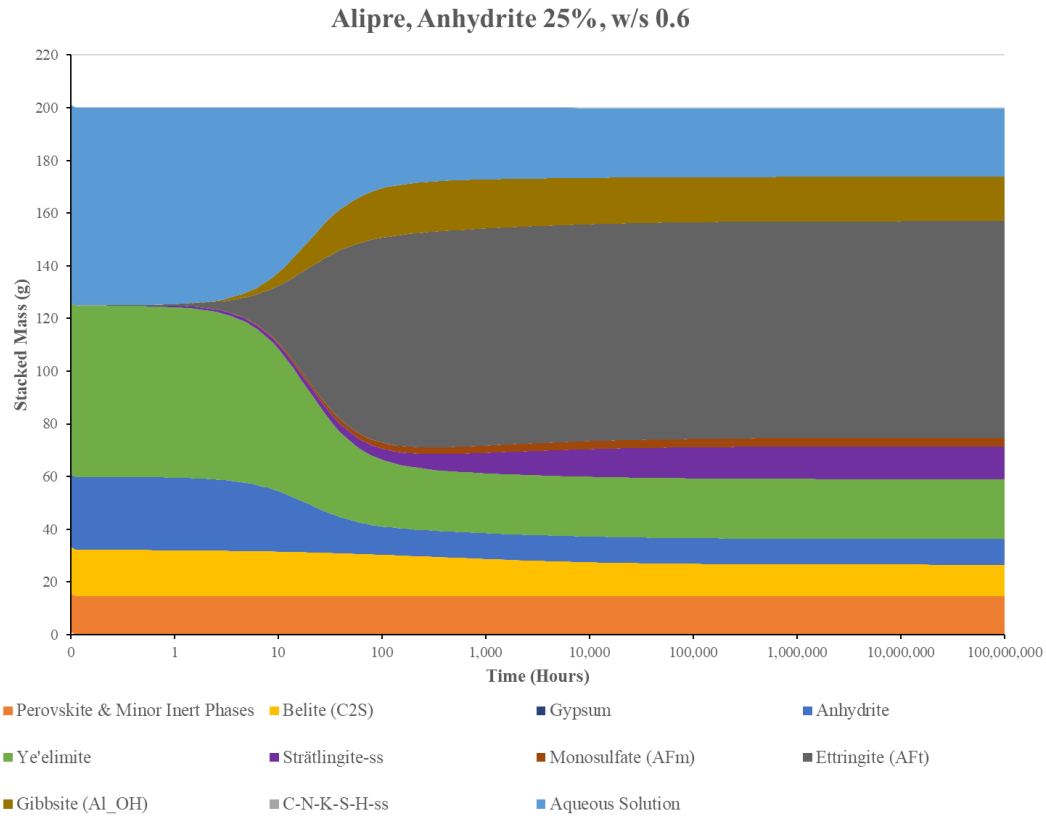

Figure 36: CemGEMS simulation for Alipre clinker at an anhydrite addition of 25% and a w/s ratio of 0.6. The level of hydration, so as to be comparative to experimental results, was set to 65%. This simulation demonstrates a greater quantity of strätlingite formation than is suggested in the Rietveld analysis and observed in the XRD.

3.5.4. Mercury Intrusion Porosimetry

Average total porosity across all formulations ranged between 24 – 45%, which is within the expected range for CSA-belite cements [123, 221, 222]. No significant trends are observed between the Alipre and Alpenat clinkers; the range in average total porosity falls between 27 – 43 % for Alipre, and 24 – 45 % for Alpenat. There is no clear indication of a relationship between an increase in the availability of calcium sulfate and the development of porosity. Neither does the increase of anhydrite (Figure 37) or gypsum (Figure 38) appear to have any effect upon the porosity of the system, and no trend is observed that exceeds the uncertainty established by the standard deviation of the analysis results.

Similarly, there is no evident relationship between the shear applied to the mix and porosity. A potential relationship may be observed between increasing the water content and an increasing percentage porosity (Figure 39), which is to be as expected within CSA as well as PC systems [222, 223]. However,

this perceivable trend does not sufficiently exceed the sample standard deviation, and therefore the recorded error, in a way that would enable it to be considered a conclusive result.

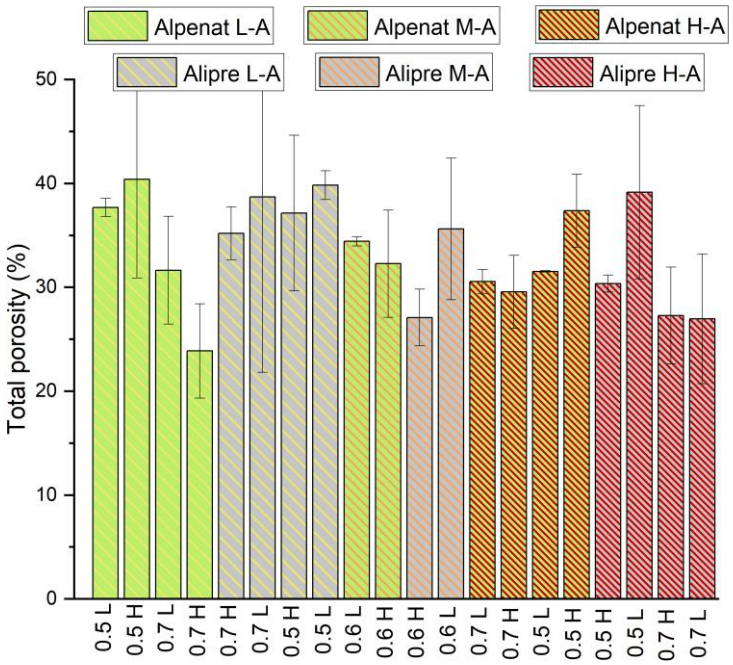

Figure 37: MIP results highlighting any relationship between the porosity percentage and the addition of anhydrite, for both types of CSA clinker (L/M/H indicate Low – 15%, Medium – 25%, High – 35%). The water to solid ratio is given for each sample on the x-axis, along with the mix shear component (High / Low). Figure prepared by S. Kearney.

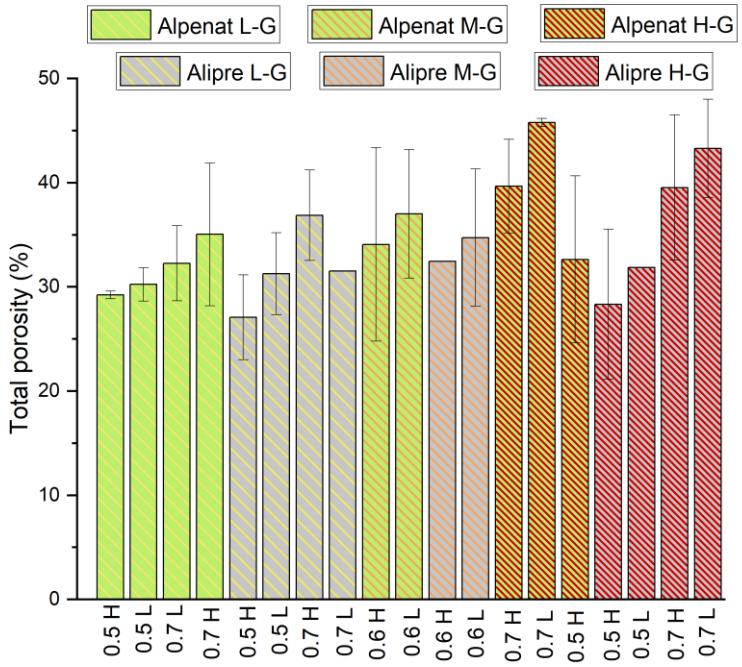

Figure 38: MIP results highlighting any relationship between the porosity percentage and the addition of gypsum, for both types of CSA clinker (L/M/H indicate Low – 15%, Medium – 25%, High – 35%). The water to solid ratio is given for each sample on the X-axis, along with the mix shear component (High / Low). Figure prepared by S. Kearney.

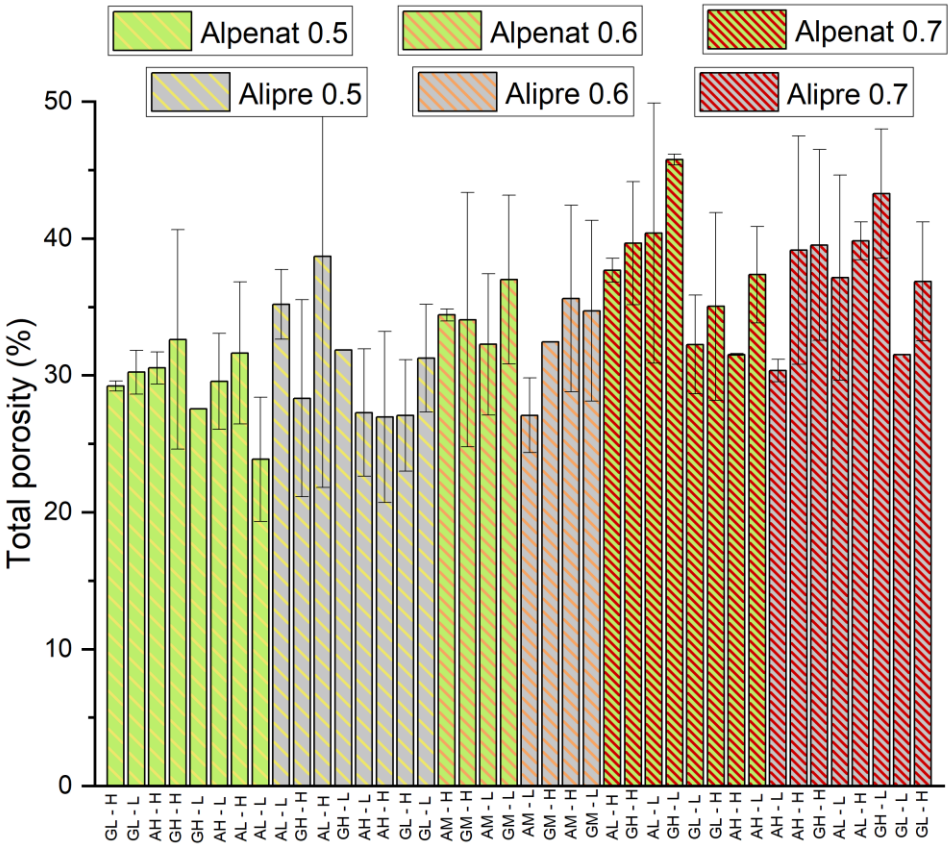

Figure 39: MIP results highlighting any relationship between the porosity percentage and the availability of water, for both types of CSA clinker. The type of calcium sulfate (Anhydrite / Gypsum) is given alongside the amount (Low – 15%, Medium – 25%, High – 35%) upon the x-axis, alongside with the mix shear component (High / Low). Figure prepared by S. Kearney.

3.5.5. Conclusions and Future Investigations

The aim of this shorter experimental series was to assess whether the conclusions drawn in section 3.4.4 did indeed extend over a more prolonged time period. Whilst still relatively short in the grand scheme of the operational timescale of a geological disposal facility, with estimates of approximately 150 years before closure followed by thousands of years of containment, this study has aided in establishing the trajectory of the CSA-belite systems beyond a service life of 3 years [63]. Most importantly, the mixes tested have indicated that the phase assemblage has not decomposed within this timeframe under these storage conditions, and as an extension from the previous 90-day testing, it would seem unlikely to do so without an external factor. This is also in line with the thermodynamic simulations carried out. The trends established between mixing variables in the previous study have not changed within this time period either.

Ettringite levels have been observed to either remain stable or increase. Potential increases at a calcium sulfate addition of 25% are marginal in Alipre mixes, and more likely a factor but still minor in Alpenat mixes. The TGA data for higher calcium sulfate mixes showed a more noticeable increase in ettringite production, which whilst not subjected to XRD and Rietveld, can be estimated as the signature for water increases between 90 and >900 days by the same amount as between 7 and 28 days. In section 3.4, this equated to an increase of approximately 4%. This investigation was also supplemented by MIP, which only showed a potential link between an increase of porosity and the availability of water, which is to be expected.

CSA-belite has therefore, once again shown promise as a potential future encapsulant from a phase assemblage point of view. The mechanical and dimensional stability testing results are being evaluated by the UK nuclear industry, in conjunction with the results presented. If considerations from these studies are met, the next stage is to select formulations to use in full scale 500 litre trails. This is a necessary step, as it includes many elements that cannot be accurately replicated or simulated in a small-scale scenario, such as the interaction of the mixing equipment upon a large quantity of grout, the behaviour of a bulk supply of powder, the rheology of such a large mix, but also crucially the heat of the hydration reaction exotherm and its impact on such a large scale. A successful 500 litre trial will leave a large safety tolerance when operations include waste loading, which will dilute the mix and significantly reduce the peak hydration temperature.

The storage conditions must then also be considered. Geological disposal facilities (GDF) have been proposed with a maximum depth of 1000 m [3]. Busby et al. [224] took ground temperature readings across the UK at a depth of 1000 m, recording an approximate ground temperature for the Cumbria coast of 34 °C [224]. Prentice et al. [63] have estimated that the first 100 years of GDF operation will remain close to this figure, at between 30-40 °C, after which the GDF will be closed and backfilled [63]. Considering the heat generated from the hydration of the backfill, and given that the GDF is by this time sealed, it is estimated that the temperatures within the GDF could reach a maximum of 80 °C within 5 years, before cooling to 50 °C and then to ambient temperatures over the next 25 years [63].

The stability of ettringite is crucial if CSA is to be introduced successfully as a future encapsulant of radioactive waste, and these experimental investigations do not consider the effects of this storage environment, since all samples were cured at 25°C and >90% relative humidity. It is therefore worth investigating how CSA and the ettringite phase behave under a range of conditions relevant to the interim storage and disposal of potential waste products, including alkalinity, humidity, and temperature.

3.6. Acknowledgements

The author would like to acknowledge the contribution of Dr Daniel Geddes, Dr Sarah Kearney, and Dr Cassandre Le Galliard for their considerable time and effort in helping to manage and process this huge quantity of samples.

The author would also like to express their gratitude to the co-authors and contributors to the publication 'hydrate assemblage stability of calcium sulfoaluminate-belite cements with varying sulfate content', which was accepted for publication by Construction and Building Materials on the 6th of April 2023 [148].

These contributions are as follows: Shaun Nelson: Methodology, Investigation, Formal analysis, Data curation, Writing – original draft, Visualization. Daniel A. Geddes: Methodology, Investigation, Resources, Writing – review & editing. Sarah A. Kearney: Methodology, Investigation, Formal analysis, Writing – visualization, review & editing. Sally Cockburn: Investigation, Resources, Data curation, Writing – review & editing. Martin Hayes: Conceptualization, Methodology, Validation, Writing – review & editing, Supervision, Project administration. Michael J. Angus: Conceptualization, Methodology, Validation, Writing – review & editing, Supervision. Gavin Cann: Conceptualization, Methodology, Writing – review & editing. John L. Provis: Conceptualization, Methodology, Writing – review & editing, Supervision, Project administration.

Funding for this work was provided by Sellafield Ltd and supported by the Nuclear Decommissioning Authority iCASE scheme, including partial studentship funding through this scheme from the Engineering and Physical Sciences Research Council (UK).

4. Alkali-Activated Material as a Future Encapsulant

4.1. Introduction

Alkali activated materials (AAM) are under consideration by the UK nuclear industry as a potential radioactive waste encapsulant. AAM is a broad term used to describe materials produced from a number of precursors that may be activated by a range of alkali solutions. Both BFS and PFA are popular and advantageous precursors; however, as discussed previously, the UK nuclear industry wishes to move away from materials that cannot be sourced with a consistent specification, ideally available from a national supplier that is not reliant upon declining industries. A geopolymer (low-calcium AAM) is therefore the system of choice, within which a metakaolin precursor has been selected. The following chapter contains a brief history of AAM and their use within industry, as well as why AAM are of interest to the UK nuclear industry. A study comparable to that presented in chapter 3 is then conducted, wherein an extensive range of geopolymer mixes are conducted, in order to assess the robustness and suitability of the geopolymer system for consideration by UK nuclear and potential up scaled testing.

4.2. A Brief History of Alkali Activated Material

The process of using alkali activation to produce or aid in the development of solid cementitious products is not a recent innovation. There are a number of theories which suggest that AAM was utilised by ancient civilisations, most notably that of Davidovits [225], who argues that the ancient Egyptians knowingly used AAM to produce stone blocks in situ for the great pyramids of Giza [9, 14, 225, 226]. AAM technology was, however, first patented in 1895 by Jasper Whiting [227] of Chicago, followed by German chemist Hans Kühl [228] in 1908 with his slag-based cement product [14, 140, 227, 228]. AAM technology was further developed by the pioneering work of Purdon in 1940 [229] and his studies of using different alkali activators on blast furnace slag (BFS), noting a significant improvement in strength when a using sodium hydroxide activating solution [229, 230].

Beginning in the second half of the 20th century, development was led by the Soviet Union and the People's Republic of China [14]. During this period, both nations employed centrally controlled

economies, with great emphasis placed upon rapid industrialisation and the development of heavy industry through 'five-year plans' now synonymous with the Stalin era [231]. Both this and China's 'great leap forward' leant heavily on the production of steel in vast quantities [231]. This also coincided with a lack of PC availability in both regions, which when combined with the increasing availability of BFS, greatly incentivised the development of AAM [14]. This was epitomised by the work of Glukhovsky [232], and his 1959 publication of 'Gruntosilikaty' (or soil silicates), exploring alkali-carbonate activation of these metallurgical slag waste by-products [14, 232, 233]. Much of the infrastructure created around this time which utilised AAM is still in service [234].

The term geopolymer came into use during the end of the 1970's, first used and popularised by Davidovits [235], in describing alkali activation in the absence of calcium (see section 1.4.3.) [235]. In more recent literature, Davidovits has claimed that geopolymers are not in fact AAM, but a distinct classification of material in themselves [236]. This is not the only instance of confusing terminology, as AAM technology carries with it, as stated by Provis & van Deventer [14], *"a plethora of names applied to the description of very similar materials, including 'mineral polymers,' 'inorganic polymers,' 'inorganic polymer glasses,' 'alkali-bonded ceramics,' 'alkali ash material,' 'soil cements,' 'soil silicates', 'SKJ binder', 'F-concrete', 'hydroceramics,' 'zeocements', 'zeoceramics', and a variety of other names"* [14].

Since the 1980's the development and understanding of AAM has accelerated rapidly, with pioneering work conducted at the Eduardo Torroja Institute for Construction Science in Madrid, the University of Melbourne, and the University of Sheffield, with significant and ongoing research into the gel chemistry and developing an understanding of how AAM react to their environment [14, 134, 136, 237, 238]. AAM technology is an active area of research, which has been implemented successfully in both the 20th and 21st centuries. Both Palomo [234] and Roy [226] give a comprehensive list of examples of past, present and potential future applications of AAM, from residential and highway construction, to pre-cast structure elements and oil well grouts [226, 234].

AAM can give a diverse array of benefits according to their design, though it is it important to clarify that some properties may be mutually exclusive. For example, AAM can reduce water demand for areas that suffer from droughts, lower heat of hydration, resistance against chemical and particularly acid attack, as well as tailorable porosity and strength characteristics that can rival or exceed the standards of PC [14, 70, 140, 239, 240]. Particularly of note, is the potential for significant reductions in carbon emissions compared to conventional cement systems, as well as the potential to make use of varied waste materials much in the same way that using BFS or PFA was a mutually beneficial arrangement, combining both the reduction of landfill waste with a reduction of associated emissions by diluting the cement binder requirement [7, 226, 241, 242].

4.3. Alkali Activated Material and the UK Nuclear Industry

The versatility of AAM has drawn the interest of the international nuclear community for the encapsulation of its diverse portfolio of waste materials [70]. The UK nuclear industry is particularly interested in metakaolin geopolymer technology for similar reasons as to why it is considering CSA, most notably the removal of the reliance upon increasingly difficult to source cementitious materials [81, 84, 88]. Metakaolin geopolymers are an alternative binder system with a chemistry that differs significantly from PC, offering a number of key advantages for the encapsulation of low and intermediate level radioactive waste streams.

In recent years, geopolymers have been identified as a potential avenue for the immobilisation of radioactive ^{137}Cs and ^{90}Sr species, through both incorporation into the gel structure and precipitation as low solubility hydroxide and carbonate phases [93, 243, 244]. In 2006, Vitreous State Laboratory, Washington D.C, patented a geopolymer formulation known as DuraLith, for the purpose of the immobilisation of ^{99}Tc and ^{129}I [245, 246]. These would allow for the incorporation of ion exchange material, such as that used in the PUREX process (plutonium uranium reduction extraction), with the immobilisation of associated radionuclides [247, 248]. Control of the alkali activating solution can also modify the system pH of the geopolymer in relation to the material that is to be encapsulated. Kuenzel

et al. [143] chose metakaolin and sodium silicate activating solutions that lowered the solution pH to make it more appropriate for aluminium fuel cladding, reducing its corrosive potential [143].

One of the more novel potential applications is the encapsulation of organics and viscous liquids, such as oils. Radioactive waste is uniquely diverse, in that anything can become contaminated and required isolation from both the general population and the environment. Equipment used in both running and decommissioning activities in a radiological environment will require disposal once they have been relieved of their duties, and oil is a key component of any mechanical system. The porosity of a geopolymer system form in a way that produces an enclosed and non-connected network of pores, which theoretically would allow for the incorporation and encapsulation of these oils in this network. The work Geddes [140] demonstrates the successful incorporation of both thin and viscous silicon based oils into a potassium silicate activated metakaolin geopolymer system [140]. Geopolymer systems have also demonstrated high thermal stability, which exceeds the estimated requirements for a deep geological disposal facility [63, 70]. A system using an alkali activating solution based upon potassium silicate and potassium hydroxide has been selected for investigation by the UK Nuclear Industry, as studies by Geddes [140] indicate that this produces a lower viscosity mix, allowing for a grout to better penetrate the components of a wasteform than a metakaolin systems utilising sodium silicate [140].

4.4. Results and Discussion

4.4.1. XRD Results

X-ray diffractograms generated from both Argicem and Metamax metakaolin geopolymers exhibit the characteristic humped region between 20 – 40 °2θ, indicative of the amorphous structure of a metakaolin geopolymer [138, 140]. This is shown most prominently in Metamax mixes, as Argicem contains a 48 wt.% quantity of crystalline quartz (SiO_2) which produces strong characteristic peaks that dominate this non-crystalline region [140]. The occasional quartz peak is identifiable in Metamax mixes; however, this is likely to be merely a sand impurity which could be attributed to contamination during sample grinding and preparation. The main peak identifiable in Metamax mixes occurs at 25.3

°2θ and is attributed to anatase (TiO_2) (Figure 40). Anatase is also identifiable in Argicem mixes (Figure 41) [140, 145].

Diffraction patterns remain largely consistent between mixes at different points of time, with no discernible trends of any phase change between 7, 28, or 90-day time periods (Figure 40 and Figure 41). There is also no discernible change between different high or low shear mixing mechanisms within this timeframe.

The most noticeable of changes occurs at the higher K_2O/Al_2O_3 ratio of 1.5. In both mixes, though most prominent in Metamax likely due to them being unobscured by the intense quartz peaks within Argicem, there are a series of inconsistent peaks at around 30 °2θ (Figure 42). Samples from mixes of both metakaolin type experienced visible efflorescence if the K_2O/Al_2O_3 ratio was 1.5, and this coincides with the appearance of these peaks. The intensity of these peaks can also be increased if the SiO_2/K_2O ratio is low, keeping the K content overwhelmingly high, as well as when the H_2O/K_2O ratio is high.

These aforementioned peaks can be attributed to a potassium carbonate (K_2CO_3) efflorescence, which exhibits characteristic peaks at 29.4, 31.1, 31.5, and 32.8 °2θ (Figure 42 and Figure 43) [249]. This alkali salt forms upon the reaction of potassium hydroxide with carbonic acid, which is present due to the dissolution of atmospheric carbon dioxide into the water [145, 250, 251]. Zeolite crystals can be seen in metakaolin geopolymers that utilise a sodium-based alkali activating solution, however, potassium zeolites are more difficult to synthesize [233].

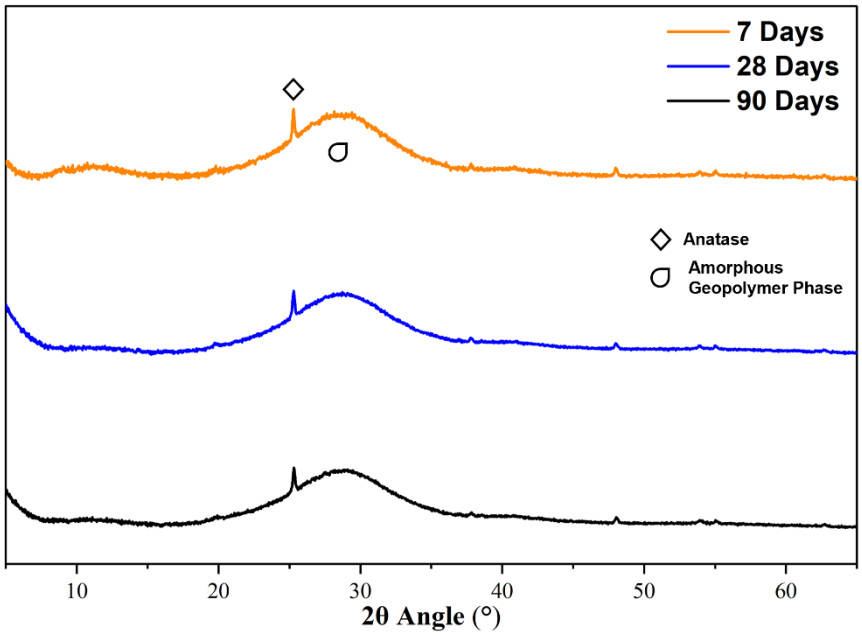

Figure 40: XRD patterns for Metamax metakaolin geopolymers between 7 and 90 days. SiO_2/K_2O 1.4, H_2O/K_2O 11, K_2O/Al_2O_3 1.0, low shear. Clearly displays the characteristic amorphous region between 20-40 °2θ that is indicative of the metakaolin geopolymer structure. Main anatase (TiO_2) peak is shown.

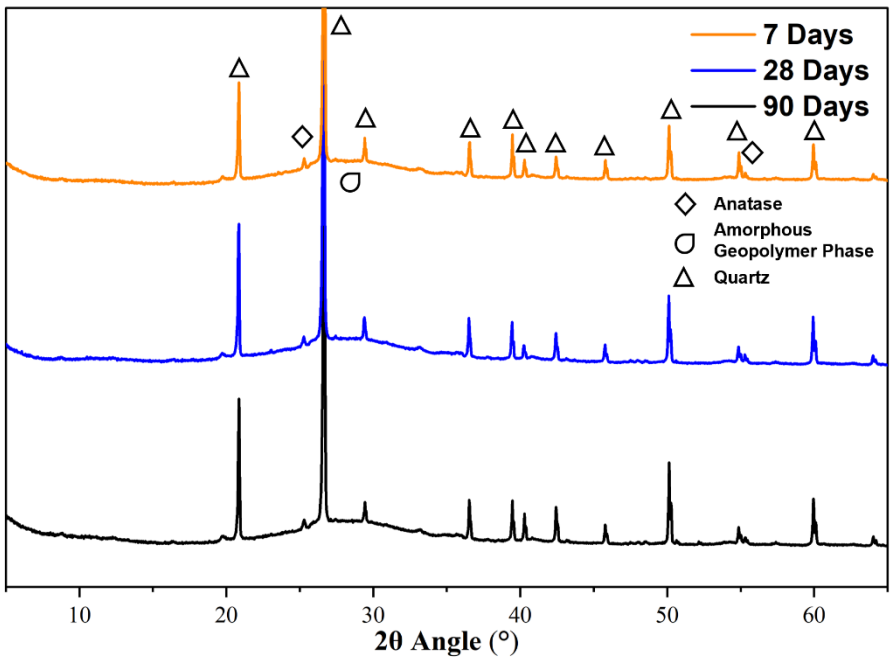

Figure 41: XRD patterns for Argicem metakaolin geopolymers between 7 and 90 days. SiO_2/K_2O 1.4, H_2O/K_2O 11, K_2O/Al_2O_3 1.0, low shear. Displays the characteristic amorphous region between 20-40 °2θ that is indicative of the metakaolin geopolymer structure. Main anatase (TiO_2) and quartz (SiO_2) peaks are shown.

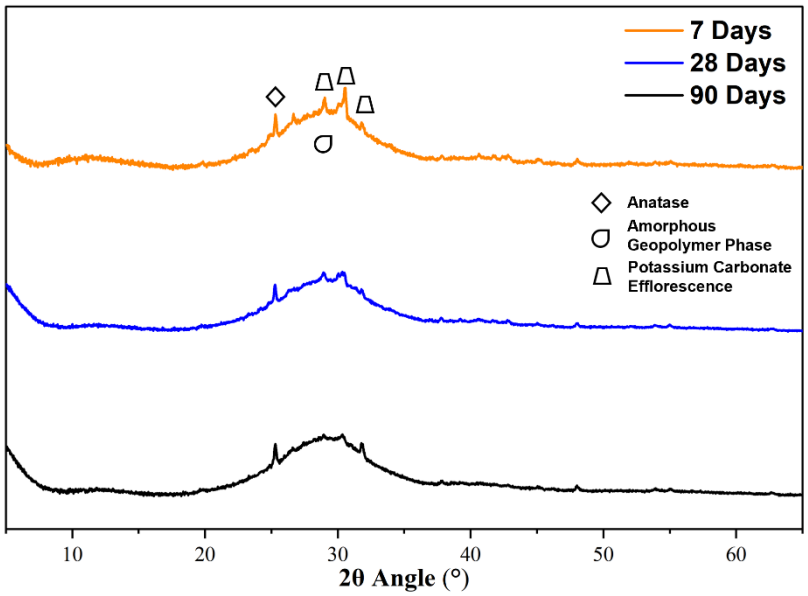

Figure 42: XRD patterns for Metamax metakaolin geopolymers between 7 and 90 days. SiO_2/K_2O 1.0, H_2O/K_2O 15, K_2O/Al_2O_3 1.5, low shear. Clearly displays the characteristic amorphous region between 20-40 °2θ that is indicative of the metakaolin geopolymer structure, as well as the efflorescence encountered at approximately 30 °2θ. Main anatase (TiO_2) peak is also shown.

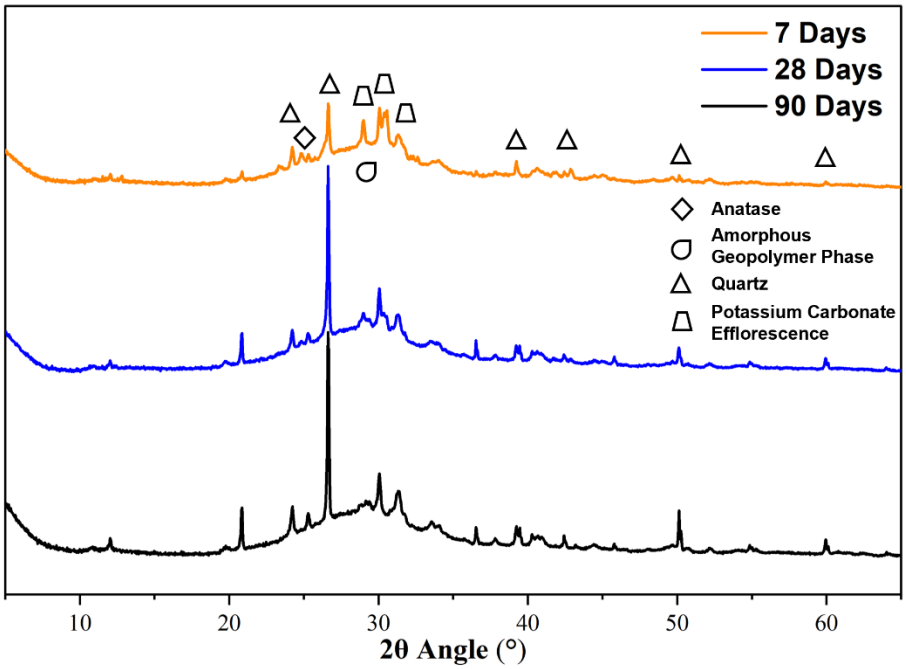

Figure 43: XRD patterns for Argicem metakaolin geopolymers between 7 and 90 days. SiO_2/K_2O 1.0, H_2O/K_2O 15, K_2O/Al_2O_3 1.5, low shear. Clearly displays the characteristic amorphous region between 20-40 °2θ that is indicative of the metakaolin geopolymer structure, as well as the efflorescence encountered at approximately 30 °2θ. Main anatase (TiO_2) and quartz (SiO_2) peaks are also shown.

4.4.2. TG-MS Results

TGA curves show negligible change over the 90-day aging period for any mix conducted. Similarly, the water content present within Argicem or MetaMax mixes is largely consistent regardless of the mixing variables, demonstrating the successful formation of hydrated gel structures throughout, as well as the successful and reliable removal of free water using the arresting hydration process. When comparing Argicem to MetaMax, the derivative weight loss associated with water at approximately 120 °C is slightly more than half the size of that for MetaMax. The reduced quantity of water bound into the gel structure is a result of the significant quantity of unreactive quartz present (Figure 44).

The MS data for both H_2O and CO_2 has unfortunately proven to be unreliable. The amplitude of the MS response can vary and does not follow any particular trend. This can be seen particularly when comparing the H_2O MS between mixes over the curing period and is more than likely caused by an external factor (Figure 46). Whilst no conclusions can be drawn from the MS response amplitudes, the positioning of the responses are indicative of structural changes within the materials. The response for H_2O clearly coincides with the release of the bound structural water at approximately 120 °C (Figure 45).

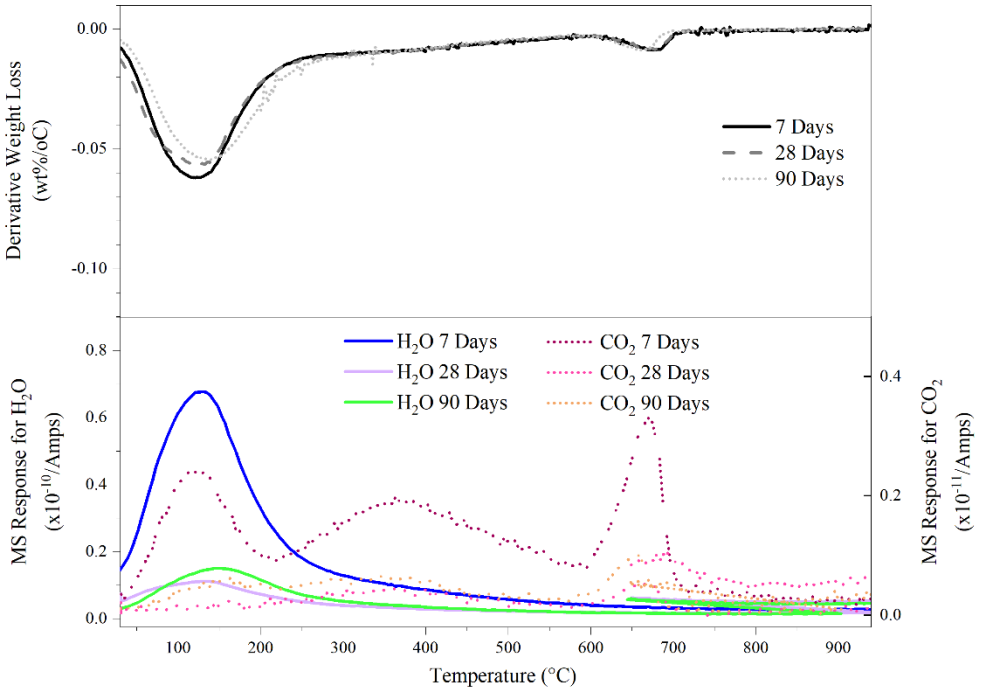

There is also a noticeable release of CO_2 only in Argicem products at around 650 °C, which coincides with a similarly noticeable loss of weight. As this is a unique observation to Argicem mixes, with

seemingly no relation to the mixing variables applied, this must be a factor of the additional SiO_2, Fe_2O_3, or CaO content. Potentially, it could be the decomposition of calcium carbonate. CO_2 encountered at approximately 150 °C is from the decomposition of potassium hydrogen carbonate to potassium carbonate [252]. Other instances of noticeable carbonation could be due to the aforementioned K_2CO_3 (Figure 45). The total amount of carbonation observed through TG-MS is minimal, especially when compared to the MS response of H_2O, owing to the samples being stored under vacuum.

Segregation was also encountered atop Argicem mixes combining both a high-water content and a K_2O/Al_2O_3 ratio of 1.5. This occurs when activating solution forms a bleed layer on the top of a mix with a lower quantity of metakaolin. In Argicem, the amount of reactive metakaolin is already reduced significantly in comparison to MetaMax, allowing for a bleed to form. A comparison between the sample and its segregated layer show that geopolymerisation has occurred in the segregated layer despite the reduced metakaolin available, however, there is a significant increase in carbonation in the region that can be assigned to a potassium carbonate, such as potassium hydrogen carbonate (Figure 46) [252].

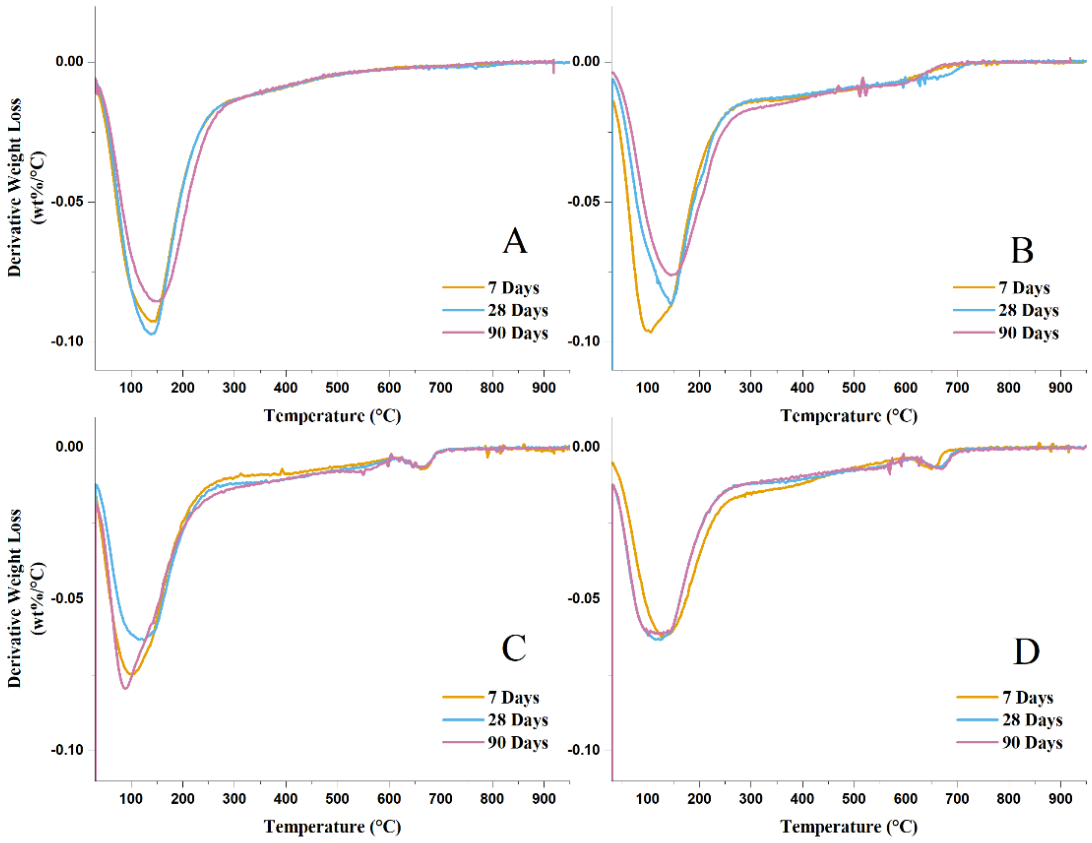

Figure 44: TGA of four mixes metakaolin geopolymer mixes at between 7 and 90-days. A – MetaMax, SiO_2/K_2O 1.4, H_2O/K_2O 11, K_2O/Al_2O_3 1.0, low shear. B – MetaMax, SiO_2/K_2O 1.0, H_2O/K_2O 15, K_2O/Al_2O_3 1.5, low shear. C – Argicem, SiO_2/K_2O 1.2, H_2O/K_2O 13, K_2O/Al_2O_3 1.2, high shear. D – Argicem, SiO_2/K_2O 1.0, H_2O/K_2O 15, K_2O/Al_2O_3 1.0, low shear. Structural water signature can be clearly seen at approximately 120 °C, as well as a minor calcium carbonate signature at 650 °C only found in Argicem mixes. Derivative weight loss is significantly reduced in Argicem mixes due to the high quantity of unreactive quartz present. Curves are very similar over all mixing variables, demonstrating the formation of a consistent structure.

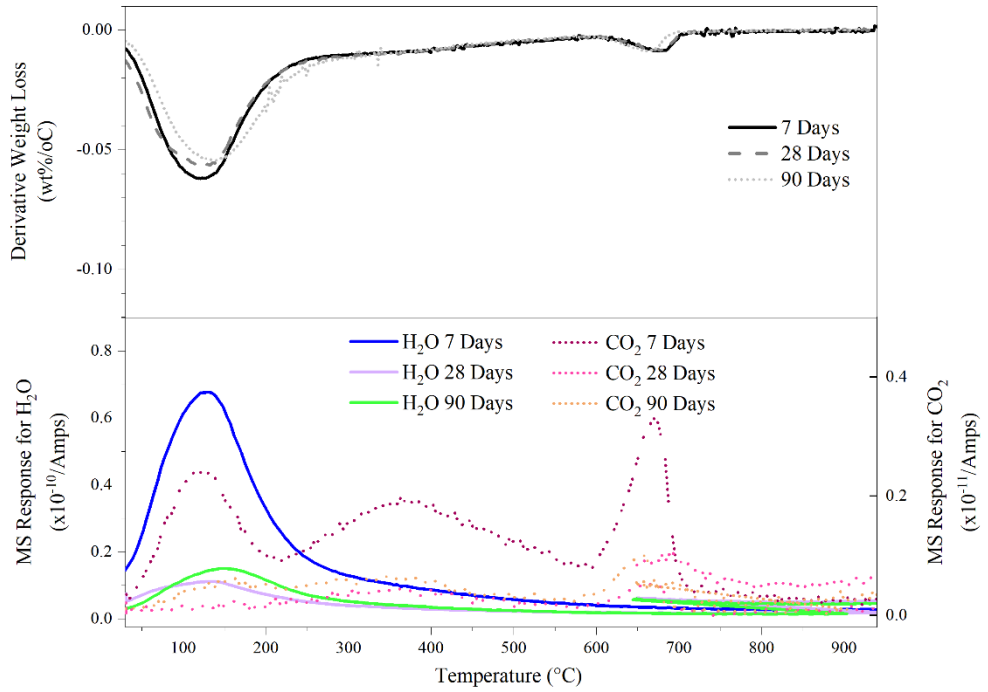

Figure 45: TG-MS for Argicem, SiO_2/K_2O 1.4, H_2O/K_2O 11, K_2O/Al_2O_3 1.0, high shear. MS demonstrates a temperature relationship that helps identify the decomposition of phases; however, the amplitude is not representative of the derivative weight loss shown.

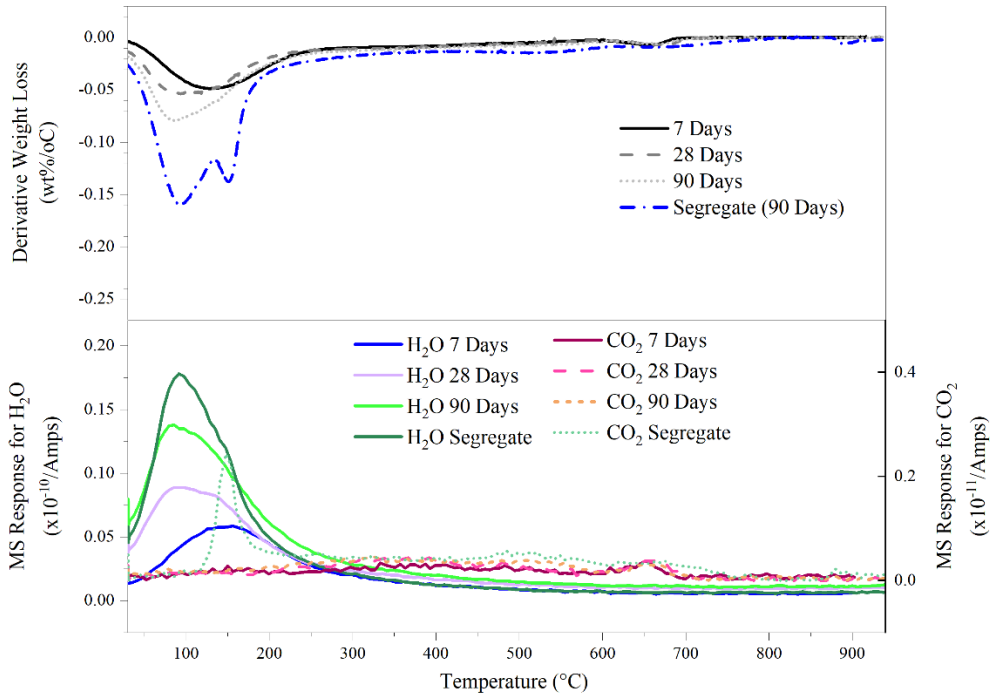

Figure 46: TG-MS for Argicem, SiO_2/K_2O 1.4, H_2O/K_2O 15, K_2O/Al_2O_3 1.5, high shear. This mix experienced segregation, which at 90 days is compared against the rest of the solid product. A signature for potassium hydrogen carbonate is clearly visible in the segregated layer (peak of 150 °C)[252].

4.4.3. FTIR Results

Table 12, adapted from the work of Geddes [140], identifies key features commonly associated with FTIR of metakaolin geopolymers by the wavenumber range. Firstly, at approximately 3450 cm^{-1}, there is a strong signal for OH^- bond stretching vibrations. Following the solvent exchange that these samples were subjected to, this signal can be attributed to the bound water content (Figure 47, Figure 48, Figure 49, and Figure 50). There is no significant difference, within the age range of any mix, in the signature of the water content. As also noted in the TG-MS results, this not only shows consistency throughout curing, but also suggests that the arresting hydration technique used was consistent and successful in removing the free water from the samples. Similarly, H – OH bond stretching shown at approximately 1650 cm^{-1} displays the same consistency.

Table 12: FTIR signals that are commonly associated with metakaolin geopolymers. Adapted from the work of Geddes [140].

Wavenumber (cm^{-1})	**Associated Bonds**	**Description of Signal**
3466 – 3432	OH^-	Stretching vibrations [253, 254]
1648 – 1644	H – OH	Bond stretching [253, 254]
1385 – 1378	Potentially associated with CH_3 as a result of residual isopropanol from the solvent exchange procedure, as well as C – O stretching within an alkali carbonate species [255, 256].	
1150 – 980	Si – O – (Si or Al)	Asymmetric stretching in geopolymers [257, 258].
900 – 840	Si – O – (Si or Al)	Occurring with Al beginning to substitute into the Si site, correlating to the K-A-S-H gel [254, 257].
700 - 690	Al – O – Si	Bending within a ring structure [253].
450 – 436	O – Si – O	Amorphous stretching from the unreacted metakaolin [254, 259].

As described in the work of Geddes [140], the signal shown at approximately 1380 cm^{-1} is potentially associated with residual isopropanol, or any C – O bond stretching as a result of an alkali carbonate species, such as $KHCO_3$ or potentially K_2CO_3 [140].

The most characteristic features associated with metakaolin geopolymers occur at around 1000 cm^{-1}. This signal represents the asymmetric stretching of the Si – O – (Si,Al) bonds [140, 260, 261]. The shoulder upon this signal, around 900 cm^{-1}, may be a product of the Al substitution into Si sites as a function of K-A-S-H gel formation. As with the water content, these signatures show no discernible change in the structure over the 90-day curing duration (Figure 47, Figure 48, Figure 49, and Figure 50). Up until this point, the many similarities have been discussed between all sets of FTIR data shown. FTIR was conducted upon samples at the formulation midpoint only with the metakaolin source and the mixing shear variables applied, with the latter appearing to have no consequence upon the 7 - 90 day curing of these samples.

When comparing between the two sources of metakaolin used, Argicem (Figure 47 and Figure 48) and MetaMax (Figure 49 and Figure 50), the most noticeable difference is a broader signature for the Si – O – (Si/Al) bond stretch in Argicem samples, which differentiate them from the MetaMax. This broader signal is likely a result of the high quartz content in Argicem. Whilst the reduction in the amount of reactive metakaolin product will reduce this feature, as gel formation decreases, a strong characteristic quartz signal occurs at approximately 1060 cm^{-1} which would cause a shoulder and broaden the characteristic Si – O – (Si/Al) bond stretch signal [262]. The strongest quartz signal occurs at approximately 450 cm^{-1}, which is outside of the range of these FTIR scans, but the beginning of this signal could be interpreted from a substantial drop away at the very end of the Argicem scans.

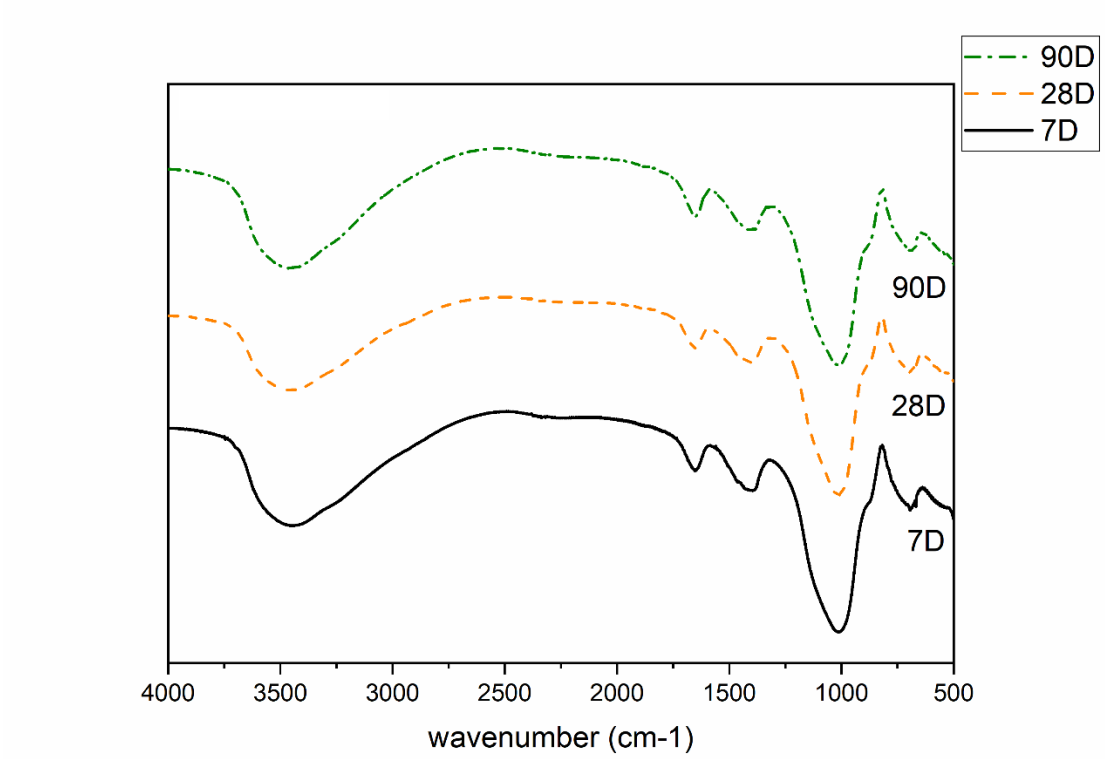

Figure 47: FTIR analysis performed on an Argicem mix at 7, 28 and 90 days. SiO_2/K_2O 1.2, H_2O/K_2O 13, K_2O/Al_2O_3 1.2, low shear.

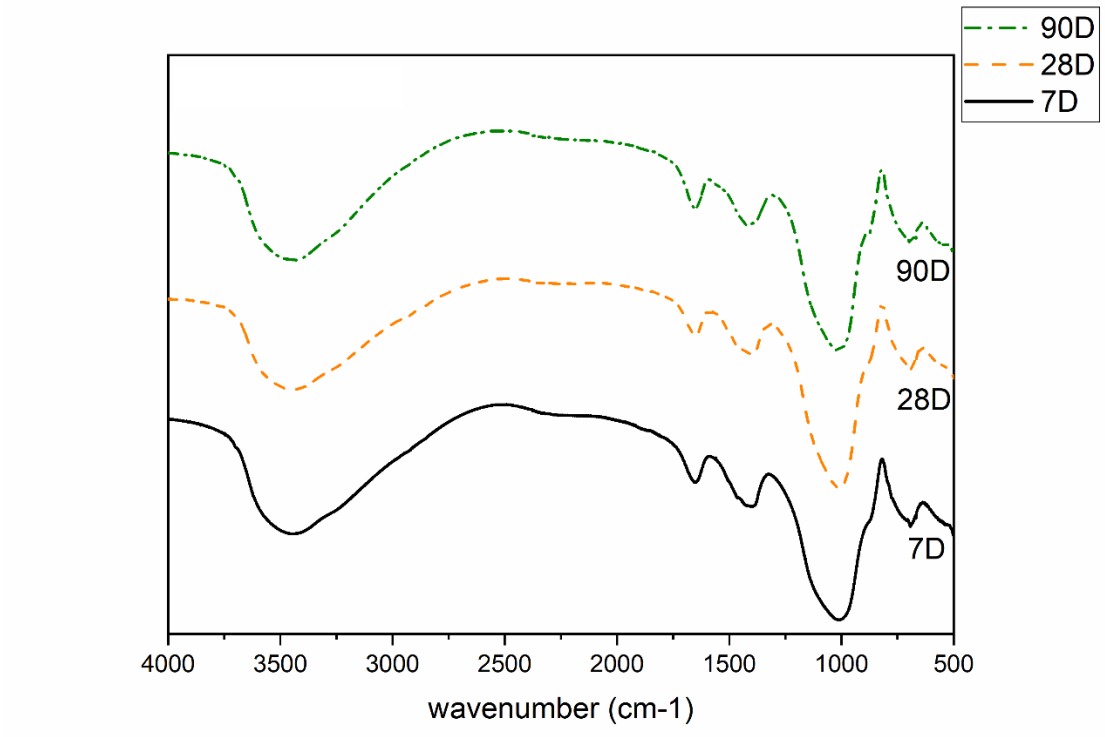

Figure 48: FTIR analysis performed on an Argicem mix at 7, 28 and 90 days. SiO_2/K_2O 1.2, H_2O/K_2O 13, K_2O/Al_2O_3 1.2, high shear.

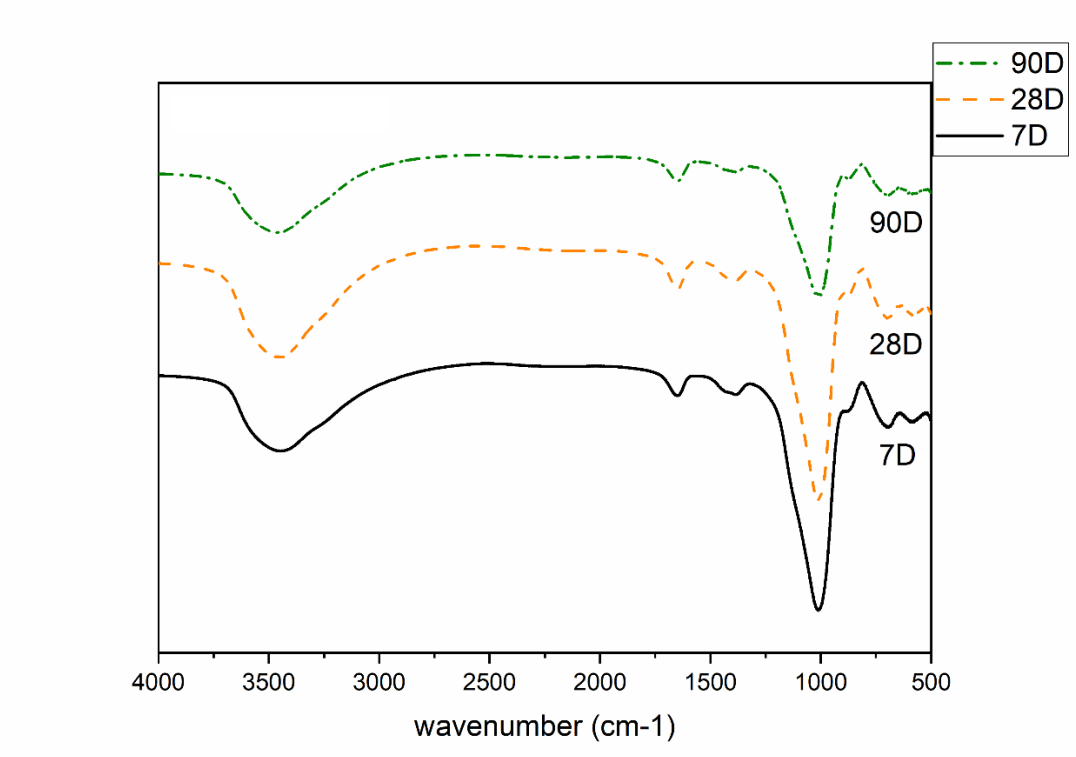

Figure 49: FTIR analysis performed on a MetaMax mix at 7, 28 and 90 days. SiO_2/K_2O 1.2, H_2O/K_2O 13, K_2O/Al_2O_3 1.2, low shear. The amplitude of the scan at 90 days is slightly less than that of the other two time periods, however; it affects all features equally, this is due to the equipment and not the sample itself.

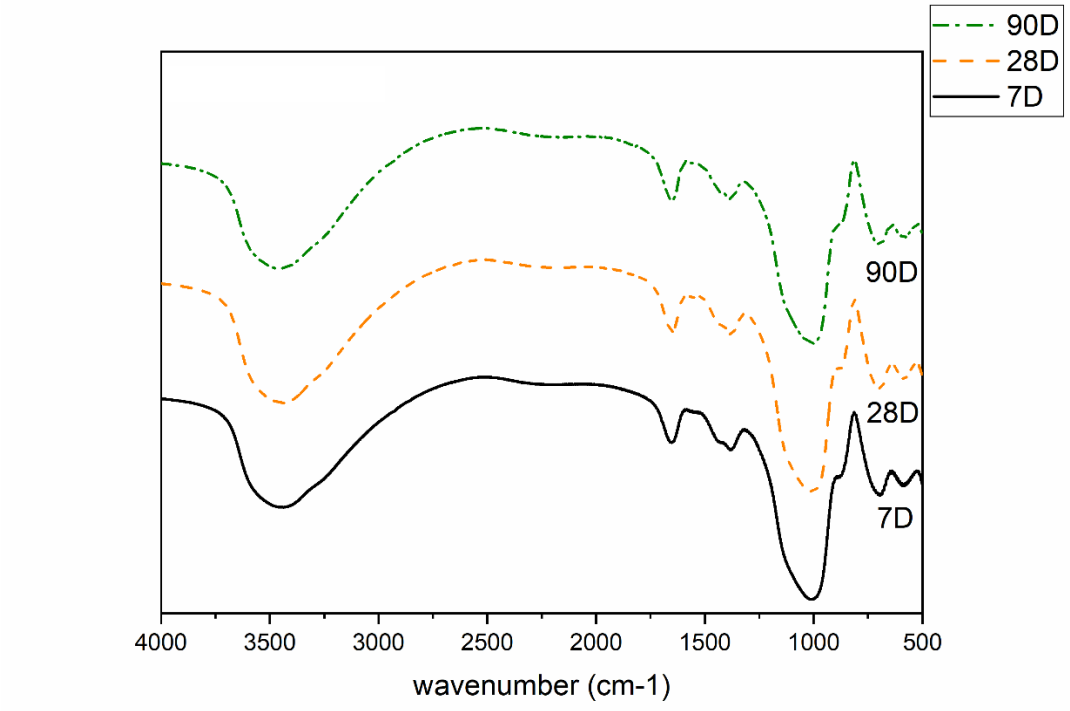

Figure 50: FTIR analysis performed on a MetaMax mix at 7, 28 and 90 days. SiO_2/K_2O 1.2, H_2O/K_2O 13, K_2O/Al_2O_3 1.2, high shear.

4.4.4. SEM, EDS, and Optical Observations

Visually, samples can be clearly distinguished by the red colour of Argicem and the off-white colour of MetaMax, owing to the iron oxide content and high purity of the metakaolins, respectively. In the mixes conducted, the most obvious and impactful observation is the of the efflorescence encountered, which occurs visually, by eye, in mixes with a K/Al ratio of 1.5. Figure 51 demonstrates clearly the effloresces observed upon samples made using both types of metakaolin.

Figure 51: An example of the white potassium carbonate efflorescence that has formed upon SEM prepared samples of both Argicem (left) and MetaMax (right) geopolymers. Approximately 5 mm by 10 mm surface area.

As mentioned previously, the efflorescence encountered is likely a potassium carbonate ($KHCO_3/K_2CO_3$), which has been allowed to form due to an excess of potassium alkali activating solution present within the system. Assuming that this mechanism operates similarly to the efflorescence encountered in the more researched sodium activated geopolymers, unreacted potassium cations are present near-to the surface of the sample, allowing them to react with carbon dioxide and form the white carbonate surface deposit [263]. A K/Al ratio of 1.5 would result in a significant excess

of K^+ ions available during the K-A-S-H gel structure, and thus available for the formation of this efflorescence [144, 264-266].

Figure 51 is taken after the preparation of solid arrested hydration samples for SEM. The preparation for this technique, which involves grinding and polishing, will increase the exposure of the samples to atmospheric CO_2, as performing these actions in a vacuum or inert environment would be extremely impractical. Whilst this cannot be quantitatively determined, it can be noted that the amount of efflorescence observed upon the solid samples which were subjected to the arresting hydration procedure, was much more noticeable on samples that were polished for SEM analysis than on those that remained unpolished.

As mentioned previously, these polished samples would have been exposed to atmospheric CO_2 for much longer than samples that remained under controlled storage conditions. During grinding and polishing, surface material is removed in order to achieve a level surface suitable for SEM. The removal and exposure of new material to atmospheric CO_2 may also factor in the increased efflorescence, as internally there may be a higher concentration of potassium cations. These cations may be present within the internal geopolymer pore network and were not removed from the system during the solvent exchange process, which likely removed cations contained within the removed free water. During the grinding process, isopropanol is used to aid the removal of geopolymer and epoxy particles by washing them away from in between the sample and the grinding paper. The face of the sample that is being prepared for SEM faces downwards. Being exposed to this isopropanol wash, may allow for the transportation of potassium cations towards the surface of the sample, in essence taking the place of the pore solution medium. This would again allow for a raise in the alkali cation concentration at or close to the surface which would increase the efflorescence observed.

SEM images taken show that the efflorescence can nucleate upon the surface, but more commonly will bloom from cracks within the geopolymer structure, potentially due to a greater availability of alkali cations. The cracks observed are likely due to the stresses caused during handling, preparation, and the vacuum drawn during storage and by the SEM. All samples handled were fragile and would break

easily, particularly MetaMax, as the unreacted quartz contained within Argicem acted as a fine aggregate. Radioactive waste encapsulation does not require an excessively strong grout as it is always supported by a robust container [83].

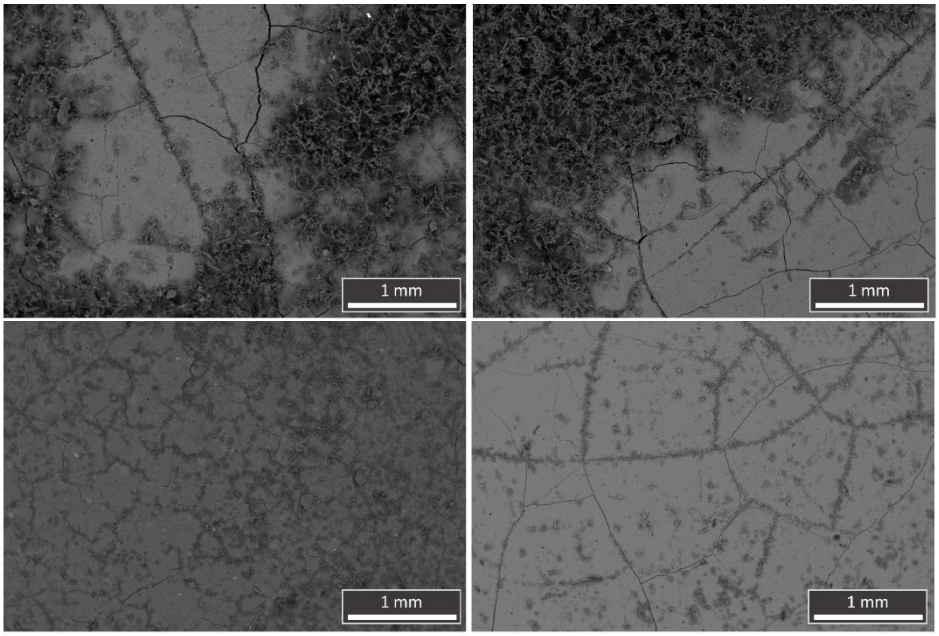

Figure 52: SEM images of geopolymers at ×40 magnification, clearly showing the formation of efflorescence upon the surface of samples prepared for SEM after 7 days of curing, but more prominently within cracks shown upon the surface. Top left: Argicem, SiO_2/K_2O 1.0, H_2O/K_2O 15, K_2O/Al_2O_3 1.5, low shear. Top right: MetaMax, SiO_2/K_2O 1.0, H_2O/K_2O 15, K_2O/Al_2O_3 1.5, high shear. Bottom left: Argicem, SiO_2/K_2O 1.0, H_2O/K_2O 11, K_2O/Al_2O_3 1.5, high shear. MetaMax, SiO_2/K_2O 1.4, H_2O/K_2O 15, K_2O/Al_2O_3 1.5, high shear.

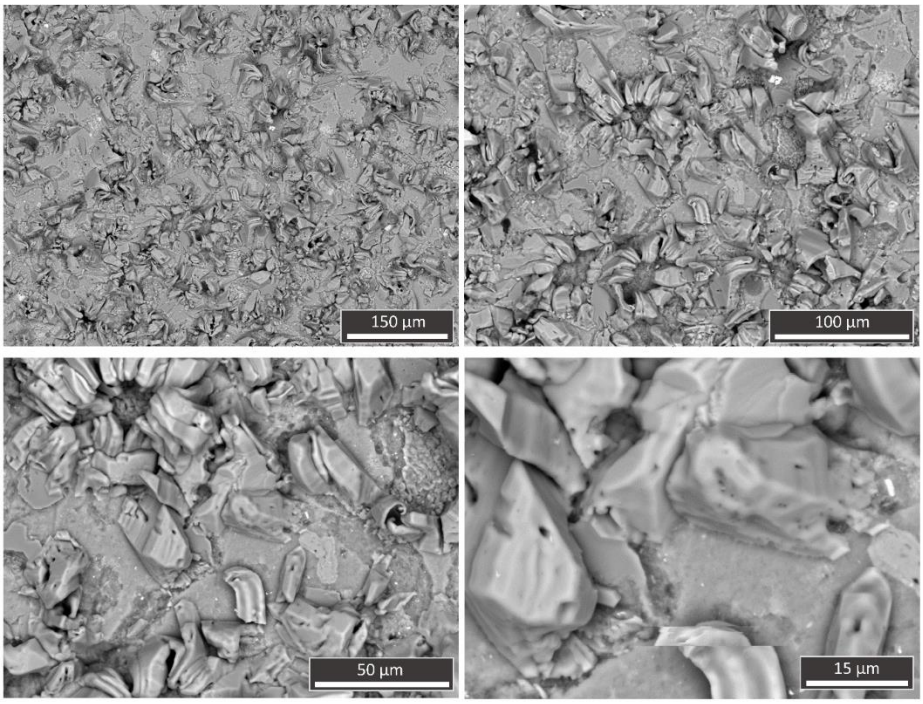

Figure 53: SEM imagery of surface efflorescence at 90 days and ×250, ×500, ×1000 and ×2500 magnification for Argicem geopolymers, SiO_2/K_2O 1.0, H_2O/K_2O 15, K_2O/Al_2O_3 1.5, high shear.

Efflorescence was also observed in samples of 7, 28, or 90 days, with no discernible trend between the extent of curing and the propensity to experience efflorescence, further highlighting that an external variable was aiding the format of efflorescence, most likely the SEM sample preparation. Following on from the trends established by the other analytical techniques, mix variables aside from the K_2O/Al_2O_3 ratio discussed above appear to have no visible impact upon either geopolymer. An increased quantity of water in the mix could potentially increase the porosity, as would be expected [223, 267, 268]. Similarly, there is no obvious difference between SEM images between 7 and 90 days of curing for any mix.

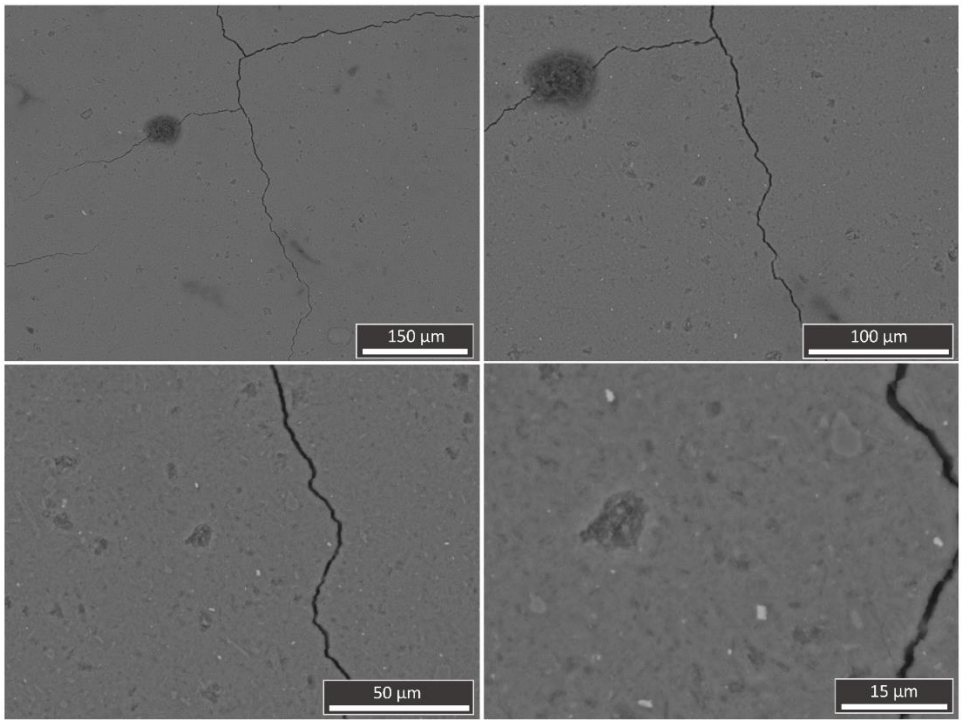

Figure 54: SEM images of MetaMax geopolymers, SiO_2/K_2O 1.4, H_2O/K_2O 11, K_2O/Al_2O_3 1.0, low shear after 7 days of curing. Magnification at ×250, ×500, ×1000, and ×2500.

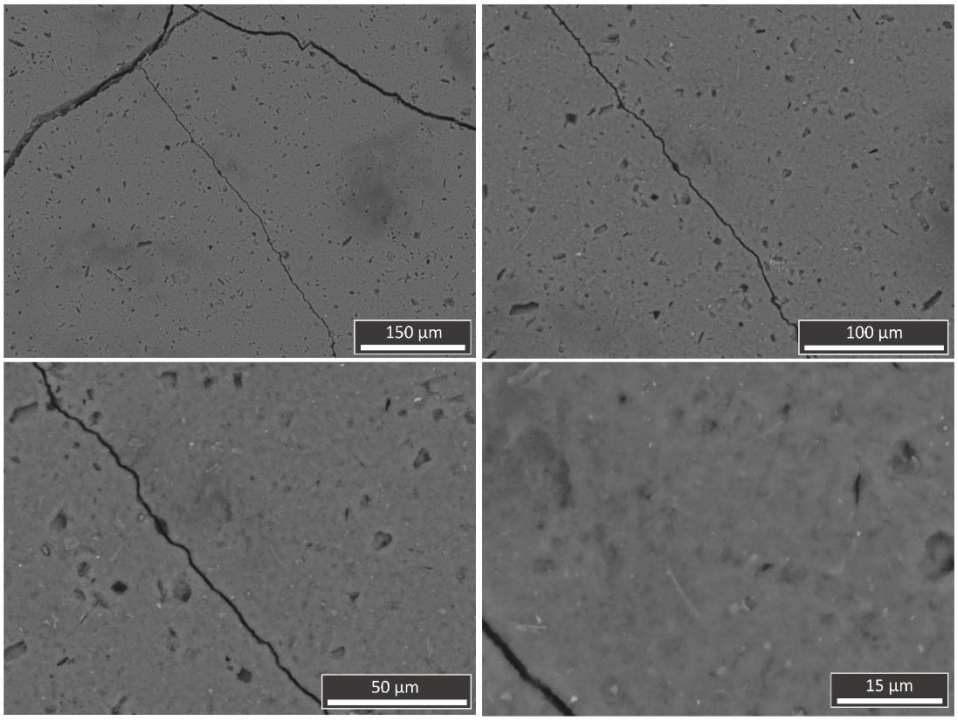

Figure 55: SEM images of MetaMax geopolymers, SiO_2/K_2O 1.0, H_2O/K_2O 15, K_2O/Al_2O_3 1.5, low shear after 7 days of curing. Magnification at ×250, ×500, ×1000, and ×2500.

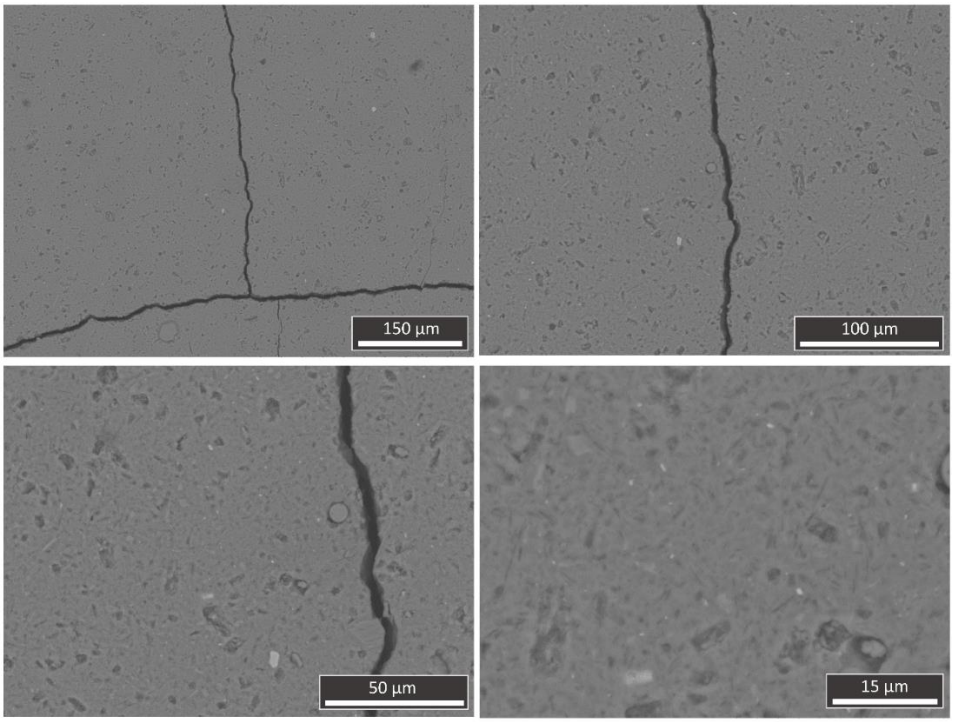

Figure 56: SEM images of MetaMax geopolymers, SiO_2/K_2O 1.4, H_2O/K_2O 11, K_2O/Al_2O_3 1.0, low shear after 90 days of curing. Magnification at ×250, ×500, ×1000, and ×2500.

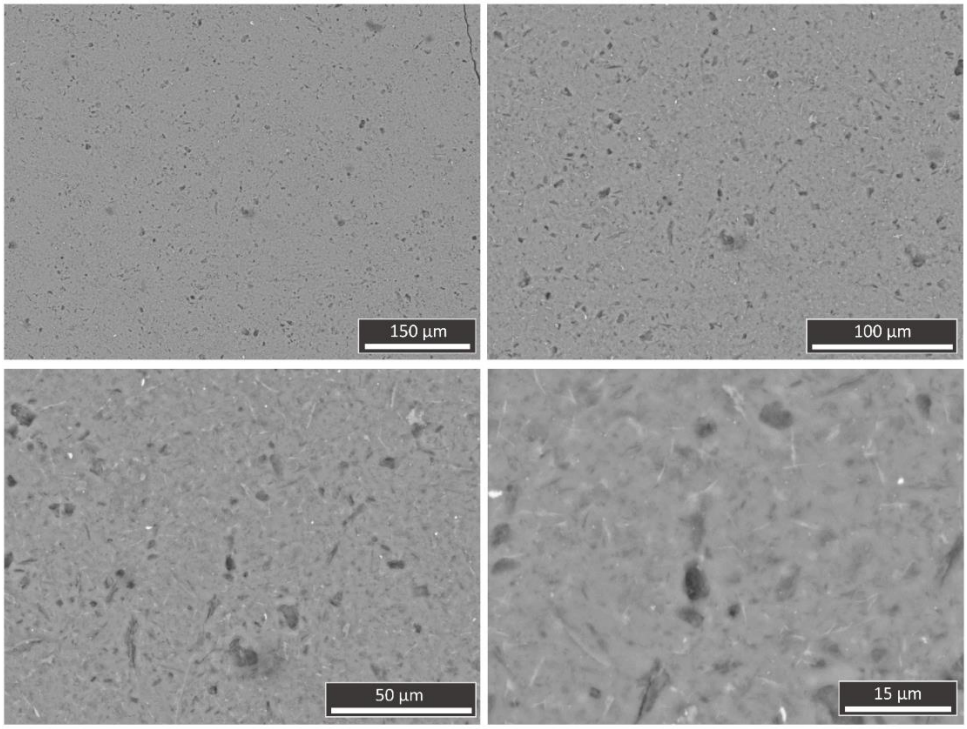

Figure 57: SEM images of MetaMax geopolymers, SiO_2/K_2O 1.0, H_2O/K_2O 15, K_2O/Al_2O_3 1.5, low shear after 90 days of curing. Magnification at ×250, ×500, ×1000, and ×2500.

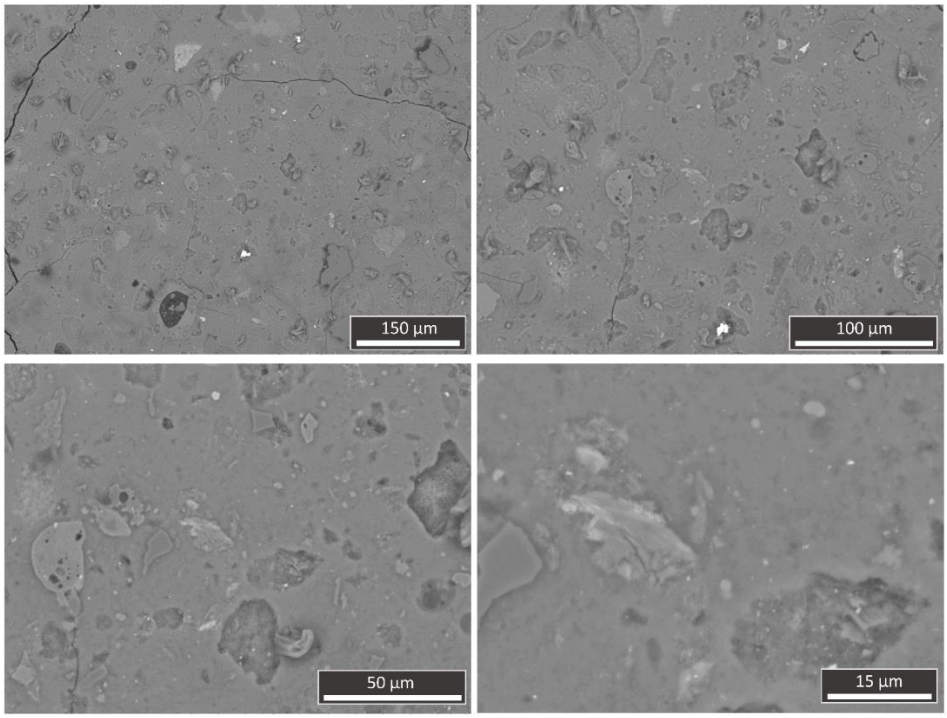

Figure 58: SEM images of Argicem geopolymers, SiO_2/K_2O 1.2, H_2O/K_2O 13, K_2O/Al_2O_3 1.2, high shear after 7 days of curing. Magnification at ×250, ×500, ×1000, and ×2500.

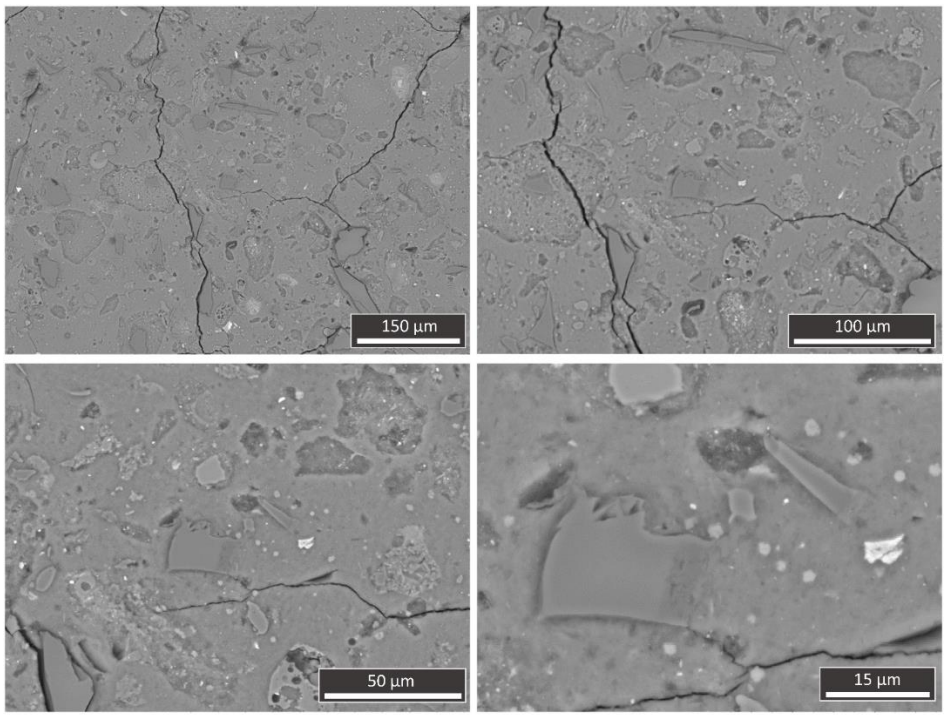

Figure 59: SEM images of Argicem geopolymers, SiO_2/K_2O 1.0, H_2O/K_2O 15, K_2O/Al_2O_3 1.0, low shear after 7 days of curing. Magnification at ×250, ×500, ×1000, and ×2500.

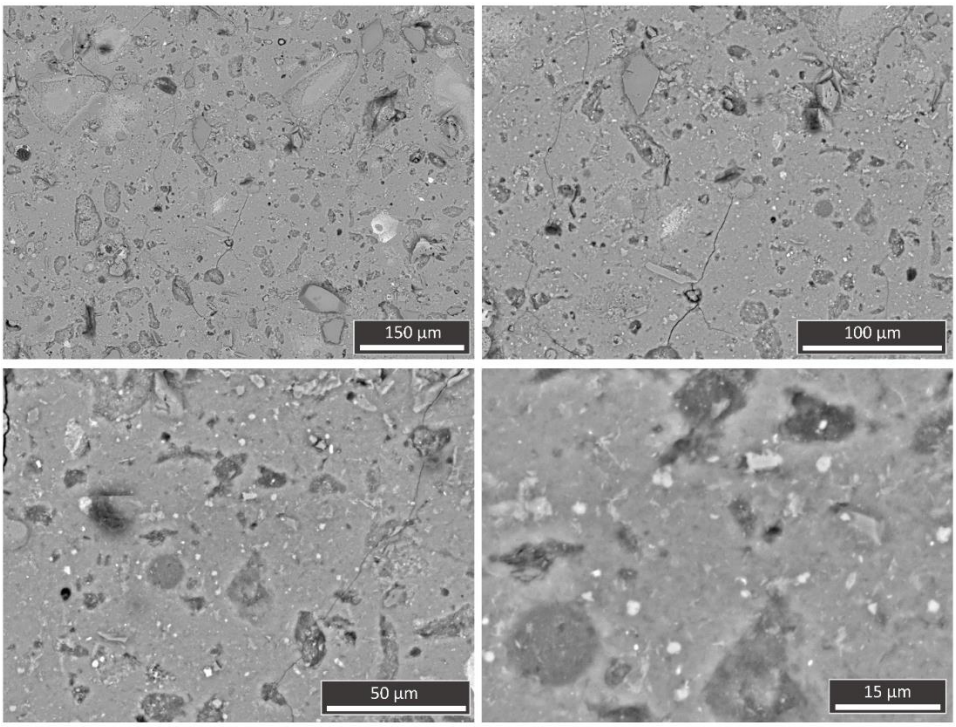

Figure 60: SEM images of Argicem geopolymers, SiO_2/K_2O 1.2, H_2O/K_2O 13, K_2O/Al_2O_3 1.2, high shear after 90 days of curing. Magnification at ×250, ×500, ×1000, and ×2500.

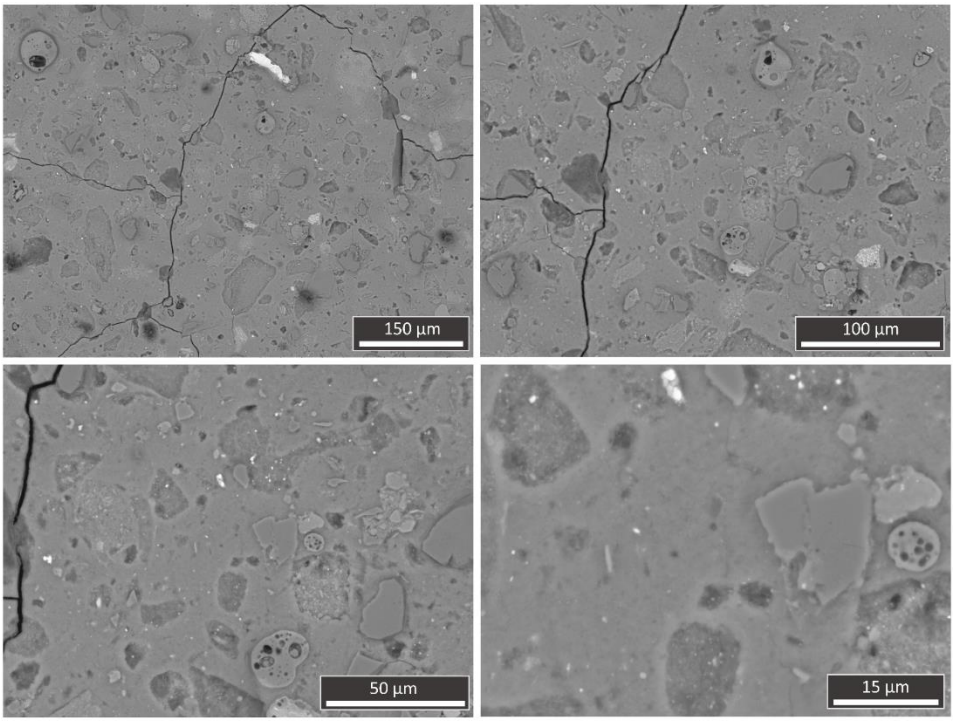

Figure 61: SEM images of Argicem geopolymers, SiO_2/K_2O 1.0, H_2O/K_2O 15, K_2O/Al_2O_3 1.0, low shear after 90 days of curing. Magnification at ×250, ×500, ×1000, and ×2500.

The main difference between Argicem and MetaMax based metakaolin geopolymers is most clearly seen when employing EDS. Argicem products display Si rich, sharp edged particles which can be strongly identified as the unreacted quartz component (Figure 62). Other features include a small level of coarse porosity, as well as larger voids, likely formed by the removal of unreacted metakaolin particles being pulled away from the structure during sample preparations, with smaller porosity not visible at these magnification levels. Levels of carbon should be evenly distributed, due to the carbon coating that each SEM sample was subjected to in order to give the SEM image the correct contrast and stop the surface of the sample overcharging. There are, however, particulates that carry both strong C and K signatures, which is likely potassium carbonate efflorescence (Figure 63). Notably, whilst other analysis and visual inspections have shown efflorescence occurring at K_2O/Al_2O_3 of 1.5, Figure 63 shows what appears to be efflorescence occurring at K_2O/Al_2O_3 of 1.2.

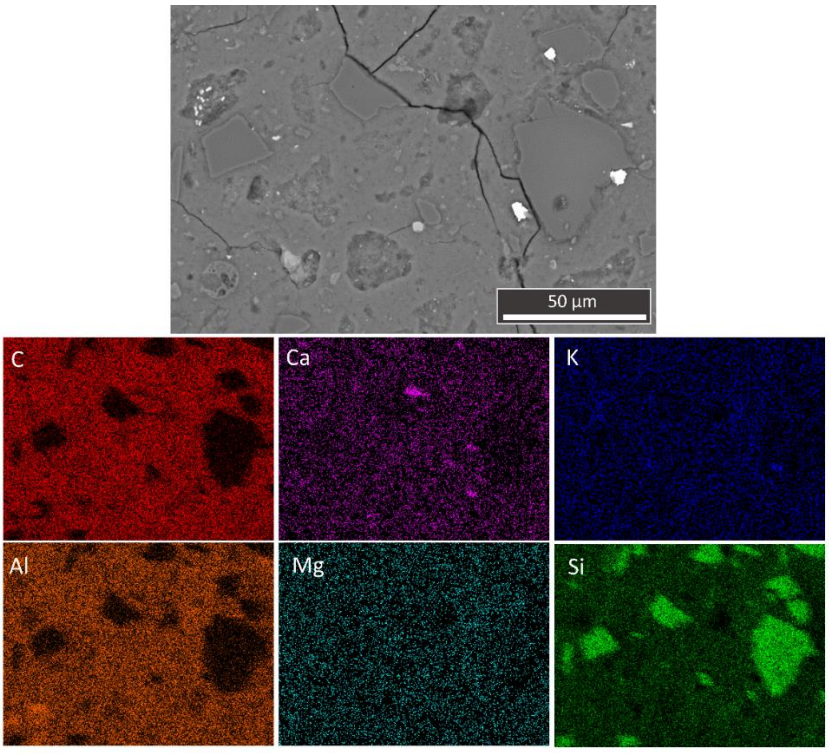

Figure 62: EDS maps at ×1000 magnification of Argicem geopolymer, SiO_2/K_2O 1.4, H_2O/K_2O 11, K_2O/Al_2O_3 1.5, high shear after 7 days of curing. Scan highlights the inclusion of unreacted quartz within the solid.

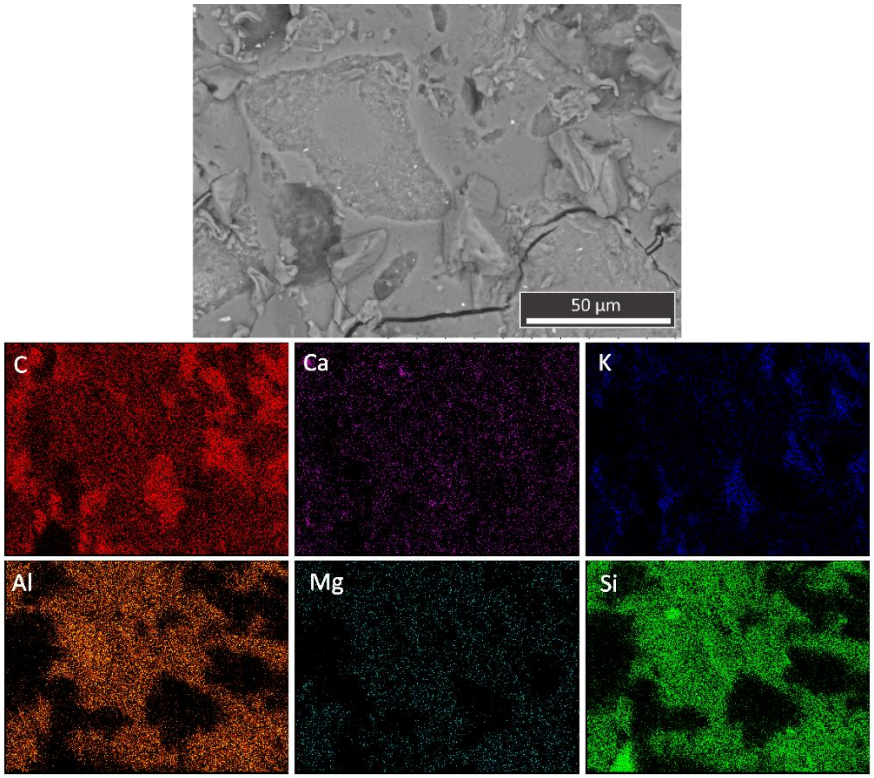

Figure 63: EDS maps at ×1000 magnification of Argicem geopolymer , SiO_2/K_2O 1.2, H_2O/K_2O 13, K_2O/Al_2O_3 1.2, low shear after 90 days of curing. Scan highlights the potassium carbonate that has formed.

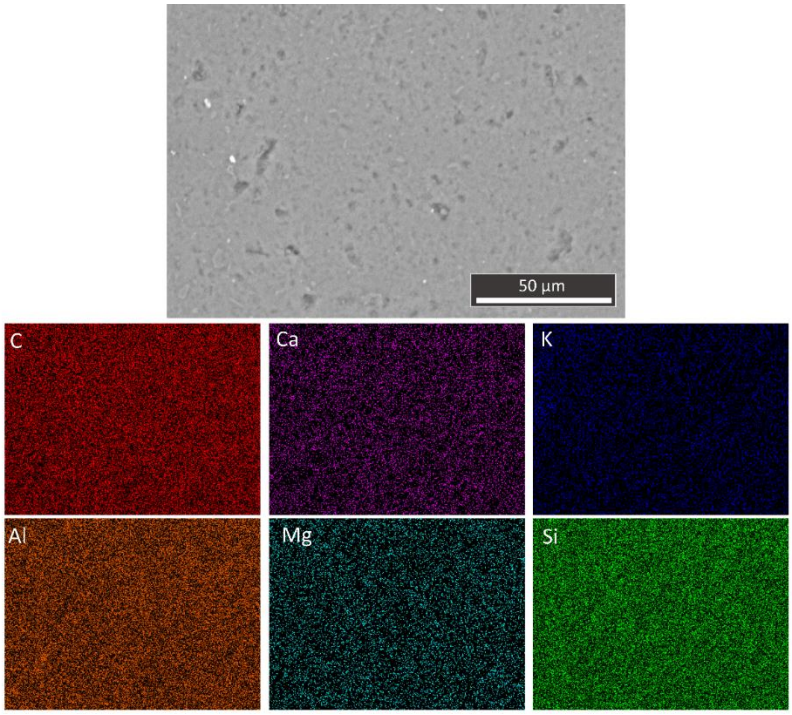

Figure 64: EDS maps at ×1000 magnification of MetaMax geopolymer, SiO_2/K_2O 1.2, H_2O/K_2O 13, K_2O/Al_2O_3 1.2, low shear after 7 days of curing.

4.5. Conclusions and Future Investigations

This series of 36 geopolymer mixes, consisting of two different types of commercially available metakaolin and different formulations of potassium alkali activating solution, have all successfully produced solid products. Two phenomena have been observed at the extremities of the formulation envelope; the production of potassium carbonate efflorescence primarily at a K_2O/Al_2O_3 ratio of 1.5, and segregation occurring prior to hardening as a form of bleed at the top of the Argicem product when the reactive metakaolin product is diluted by both the high quartz content and the greatest content of water from the activator (Argicem, K_2O/Al_2O_3 1.5, H_2O/K_2O 15).

This means therefore, that the majority of mixes conducted have produced products shown to be stable over the 90-day testing period. The formation of the characteristic geopolymer gel network is clear, with no signs of deterioration, delayed development, or any other structural changes over the curing 7-90 day timescale. All samples have shown reproducibility within each mix, with even the occurrence of efflorescence seemingly having little do to with the curing duration. Both the SiO_2/K_2O ratio and the shear rate of the mix procedure have had seemingly no noticeable effect upon the structure of these samples. Reactivity of the metakaolin has been high, with MetaMax mixes showing a particularly well reacted microstructure, with only some evidence of embedded residual metakaolin particulates in some samples.

Recommendations would therefore be to further develop the understanding of mixes below the upper limitations of water content (H_2O/K_2O 15) and potassium content (K_2O/Al_2O_3 1.5) that this study has identified. Particularly, a limit can be identified as to where efflorescence may begin to occur, such as in the case where a small amount was detected by EDS in Figure 63 after SEM preparation, despite this formulation not exhibiting strong potassium carbonate signatures under other analysis techniques. The efflorescence mechanism is worth exploring further, to safeguard this system from efflorescence forming in cracks and features, densifying, and causing internal stresses. A more robust system will be achieved with greater control over the potassium alkali content. This investigation has been successful in refining an acceptable formulation envelope, allowing for future experiments to be more focused, and a set of mix parameters to be honed for maximum performance in encapsulation scenarios. The

impact upon the porosity of the system is another important aspect for the encapsulation of waste, with particular focus upon the ability for closed porosity to incorporate oil-based waste streams. Mercury Intrusion Porosimetry upon the open porosity was unfortunately unable to be completed in the duration of this study due to instrument breakdowns. A study of the open and closed porosity, using a technique such as X-ray tomography, but would benefit future studies within the refined formulation envelope [269].

4.6. Acknowledgements

The author would like to acknowledge the contribution and direction provided by Dr Daniel Geddes and Dr Sarah Kearney, whose considerable help and expertise made this analysis possible.

5. Heavy Industry

5.1. Introduction

In this chapter, the subject of heavy industries is discussed. Their behaviour is fundamental to the introduction of any new engineering product, and its commercial availability thereafter. Whilst it is tempting to believe that a technology is able to succeed based solely on its merits alone, history would have us believe that this is rarely the case. Heavy industries are by their very nature, conservative, and are typically reluctant to any disruptive change, such as what the adoption of an alternative binder system might bring about. It is a justifiable position given the exposure of their business operations and does not rule out change under the right circumstances. Backed up by historical case studies, the following chapter aims to define the conditions that allow, or force, heavy industries to change. This is achieved by looking at both technological breakthroughs that have been adopted, and those that have not. Events or pressures that may accelerate, decelerate, or stop disruptive change are also discussed through past examples. By understanding these behaviours and conditions, the likelihood of whether a novel technology is going to be adopted commercially, and to what extent, can also be better understood.

5.2. The Rise of Portland Cement

Portland cement (PC) (see section 1.4.1) has dominated the cements industry throughout the 20th and 21st centuries. In contrast, the introduction and development of PC as it is recognised today took place during the extreme competition and rapid industrial growth of the 18th and 19th centuries. There are a number of contributing reasons as to why PC is now ubiquitous, and when considering if an alternative cement can be brought successfully to market, it is worth considering these circumstances.

The patent for PC was filed on the 15th of December 1824 by Joseph Aspdin of Leeds (Figure 65). The patent itself is intentionally vague, omitting crucial material component information, quantities, and processing temperatures [270]. From the description given, and what is known about cement manufacturing at the time, it is unlikely that any vitrification of the clinker occurred during this process. The production of lime was conducted at the time so as to in fact avoid the formation of a melt, with

any vitrified products discarded as waste. Like J. Aspdin himself, many early cement manufacturers started out as brick makers, where burnt and therefore undesirable bricks are referred to as ‘clinkers’. [271]. The exact means of how PC was manufactured by J. Aspdin was a closely guarded secret, with strict control upon who entered the factory site and himself reportedly having direct involvement with the loading of every kiln [271]. The cement produced at the time is therefore not what is recognised today as PC, although exactly what was produced by J. Aspdin is difficult to ascertain.

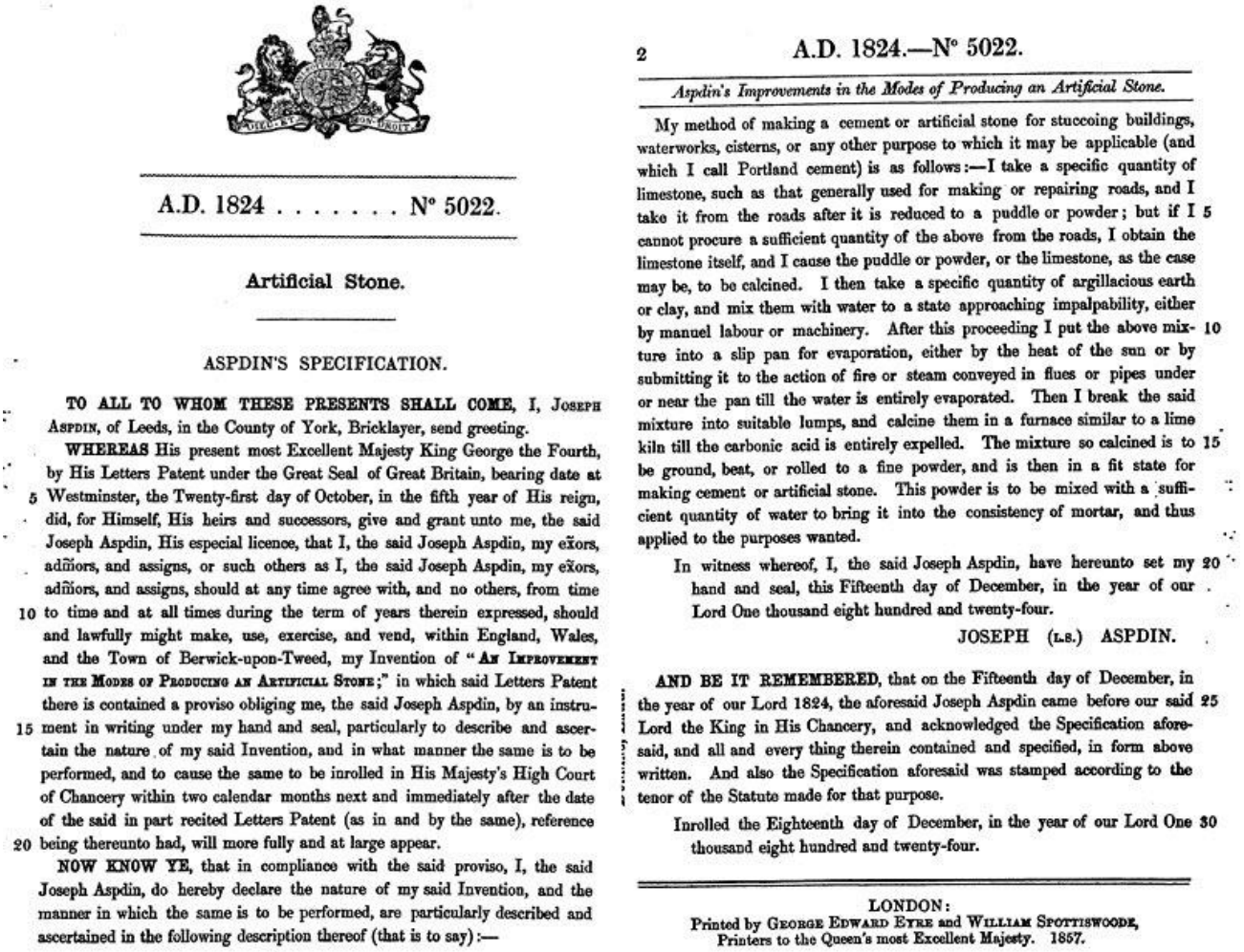

A.D. 1824 . . . . . N° 5022.

Artificial Stone.

ASPDIN'S SPECIFICATION.

TO ALL TO WHOM THESE PRESENTS SHALL COME, I, JOSEPH ASPDIN, of Leeds, in the County of York, Bricklayer, send greeting.

WHEREAS His present most Excellent Majesty King George the Fourth, by His Letters Patent under the Great Seal of Great Britain, bearing date at Westminster, the Twenty-first day of October, in the fifth year of His reign, did, for Himself, His heirs and successors, give and grant unto me, the said Joseph Aspdin, His especial licence, that I, the said Joseph Aspdin, my exors, admors, and assigns, or such others as I, the said Joseph Aspdin, my exors, admors, and assigns, should at any time agree with, and no others, from time to time and at all times during the term of years therein expressed, should and lawfully might make, use, exercise, and vend, within England, Wales, and the Town of Berwick-upon-Tweed, my Invention of "AN IMPROVEMENT IN THE MODES OF PRODUCING AN ARTIFICIAL STONE;" in which said Letters Patent there is contained a proviso obliging me, the said Joseph Aspdin, by an instrument in writing under my hand and seal, particularly to describe and ascertain the nature of my said Invention, and in what manner the same is to be performed, and to cause the same to be inrolled in His Majesty's High Court of Chancery within two calendar months next and immediately after the date of the said in part recited Letters Patent (as in and by the same), reference being thereunto had, will more fully and at large appear.

NOW KNOW YE, that in compliance with the said proviso, I, the said Joseph Aspdin, do hereby declare the nature of my said Invention, and the manner in which the same is to be performed, are particularly described and ascertained in the following description thereof (that is to say):—

2 A.D. 1824.—N° 5022.

Aspdin's Improvements in the Modes of Producing an Artificial Stone.

My method of making a cement or artificial stone for stuccoing buildings, waterworks, cisterns, or any other purpose to which it may be applicable (and which I call Portland cement) is as follows:—I take a specific quantity of limestone, such as that generally used for making or repairing roads, and I take it from the roads after it is reduced to a puddle or powder; but if I cannot procure a sufficient quantity of the above from the roads, I obtain the limestone itself, and I cause the puddle or powder, or the limestone, as the case may be, to be calcined. I then take a specific quantity of argillacious earth or clay, and mix them with water to a state approaching impalpability, either by manuel labour or machinery. After this proceeding I put the above mixture into a slip pan for evaporation, either by the heat of the sun or by submitting it to the action of fire or steam conveyed in flues or pipes under or near the pan till the water is entirely evaporated. Then I break the said mixture into suitable lumps, and calcine them in a furnace similar to a lime kiln till the carbonic acid is entirely expelled. The mixture so calcined is to be ground, beat, or rolled to a fine powder, and is then in a fit state for making cement or artificial stone. This powder is to be mixed with a sufficient quantity of water to bring it into the consistency of mortar, and thus applied to the purposes wanted.

In witness whereof, I, the said Joseph Aspdin, have hereunto set my hand and seal, this Fifteenth day of December, in the year of our Lord One thousand eight hundred and twenty-four.

JOSEPH (L.S.) ASPDIN.

AND BE IT REMEMBERED, that on the Fifteenth day of December, in the year of our Lord 1824, the aforesaid Joseph Aspdin came before our said Lord the King in His Chancery, and acknowledged the Specification aforesaid, and all and every thing therein contained and specified, in form above written. And also the Specification aforesaid was stamped according to the tenor of the Statute made for that purpose.

Inrolled the Eighteenth day of December, in the year of our Lord One thousand eight hundred and twenty-four.

LONDON:
Printed by GEORGE EDWARD EYRE and WILLIAM SPOTTISWOODE,
Printers to the Queen's most Excellent Majesty. 1857.

Figure 65: The patent filed by Joseph Aspdin in 1824 for Portland cement [271].

The Portland name was used to evoke a comparison between concrete and stone quarried from the land-tied isle of Portland, located off of the Dorset coast, UK. The reputation of Portland stone, a limestone world-renowned for high quality and declared one of six Global Heritage Stone Resources in 2017, was used to bolster the reputation of PC despite being of little geographical relevance [272]. Aspdin was not

the first to consider a material consisting of limestone and clay, nor was he the first to compare that material to Portland stone. John Smeaton, designer of the Eddystone lighthouse of 1759, at the time wrote of his hydraulic mortar that it *"would equal the best merchantable Portland stone in solidity and durability"*. William Lockwood is also listed as a trader of 'Roman' and Portland cement for the year of 1823. Both precede Aspdin's patent [270, 271, 273]. Aspdin did undoubtedly, however, secure a valuable and prestigious trademark when being issued with the patent, one that could carry a perceived reputation even by those not familiar with the concept of cement itself.

The patent of British cement was secured by James Frost in 1822, a hydraulic cement consisting of limestone and silica with an absence of alumina, and although not as strong as the preceding 'Roman' cement it was sold as a less expensive alternative [270]. Whilst another name of perceived prestige and value, especially during the height of the British Empire, British cement would fail to impact the market in the same way as PC.

Referring once again to the PC patent (Figure 65), there are indications as to a number of advancements in cement manufacture. Firstly, the necessity to mix the material thoroughly. The use of a kiln twice would also allow for an ease of grinding of what would otherwise be hard mountain limestone, reducing the labour requirement at only the expense of cheap fuel [271]. This was also achieved by the acquisition of already broken up limestone powder from road surfaces, as mentioned in the patent filed (Figure 65) [271]. Slaking the lime after the first calcination step would also achieve fine subdivision, increasing the interaction with the clay admixture [270].

Shrouded in secrecy and aided by the work of Joseph's later disinherited son, William Aspdin, PC reportedly continued to improve. When the secret behind the successful manufacture of PC was finally independently discovered in 1845 by Isaac Johnson, modern analysis of period structures confirms that that W. Aspdin clinkered material at temperatures that allowed for a melt to form and the calcium-silicate reactions to occur, producing what is recognised today as PC [270, 271, 274]. This breakthrough had allowed W. Aspdin to produce a material with strength characteristics almost twice that of 'Roman'

cement, as independently verified by Grissell & Peto in around 1844, and helped justify the much higher cost of PC in comparison to its competitors [273].

A prestigious name and a growing reputation for high performance allowed for PC to establish itself in the cements market dominated by 'Roman' cement. Potentially even more importantly, however, was the aggressive marketing by W. Aspdin (both of PC and of himself), who on occasion employed both lies and deception. Following the disinheritance by his father in 1841, William Aspdin moved to London where he acted independently, before entering into a partnership that led to the formation of J. M. Maude, Son & Co in 1843 [274]. Well aware of the difficulty of bringing a new product to market, W. Aspdin leant upon his association with his father and concocted a marketable story for both his partners and public consumption.

W. Aspdin claimed that the use of his PC was prevalent in the north of England, which it was not, having been invented by his father decades earlier. J. M. Maude, Son & Co, according to this story, were able to make a deal with Aspdin, to secure William's expertise and bring the renowned PC to London at a reduced price [274]. His most infamous deception, advertised several times in the trade periodical known as *Builder*, claimed that his father's PC was used to plug the 1828 Thames Tunnel breach. Both Isambard Kingdom Brunel's and Richard Beamish's journals clearly state that they used sacks of clay to seal the breach, but the truth never got in the way of a good story [273]. So successful was this act of marketing, that it is still repeated to this day [275].

Whilst W. Aspdin's dishonesty would eventually culminate in multiple acts of financial fraud, him fleeing to Germany, financial ruin, and premature demise; the promise of PC outshone its unscrupulous pioneer. In one of his last Germanic enterprises, Aspdin co-founded Edward Fewer & Co. in 1862, before being expelled in as little as 6 months by said named partner. This company would one day become part of the huge Swiss Holcim firm [273].

The uptake of PC, and how quickly its adoption spread, was also aided by how similar its manufacture was to the preceding cements of the time. Whilst the vitrified clinker material is much harder to grind than lime, which contributed to lime manufacturers' willingness to dispose of it as it would greatly

increase the wear upon the mill stones, its production is an adaptation and progression of the original method. All of the materials required were also already readily available and prevalent within the areas where cement was being produced [271].

"Portland cement, as it is very absurdly called, is in fact nothing but an artificial hydraulic lime, but which resists the effects of salt water admirably if we may judge from so short an experience of 8 or 9 years".

– Uncredited engineer, 1874 [271].

PC was initially met with some scepticism, not helped by cement manufacturing and usage being in its infancy and therefore unreliable. For example, calcium sulfate would not be used as a set regulator until 1890, with the ball mill and rotary kiln being invented not long after (kilns before this time were therefore static) [270]. However, the final key to the uptake and market dominance of PC is the state of the market at the time. The UK was in a time of explosive infrastructural development and economic industrial boom. Much of the buildings and infrastructure laid around this time are still in use to this day, especially in urban centres such as London. A particularly ground-breaking example was the use of PC by the London drainage works, the first large scale and ultimately successful trial of PC in 1859 as a material used for more than just the typical aesthetic and plastering works; a trial that *"settled the question of its superiority"* over 'Roman cement' [270]. Ambitious and extensive transport links were also installed around this time, bringing population hubs closer together than ever before. Following the grand opening of the Liverpool to Manchester railway in 1830, 'railway mania' struck Britain, with the length of the rail network expanding from 125 to over 13,000 miles between then and 1871 [276]. With such a demand came an ever-increasing appetite for cement and concrete construction, and with more demand came a drive for continued improvement in the quality control of PC [270, 277, 278].

To summarise the point; PC managed to penetrate the market and proved to be the superior cement product for a number of reasons:

- Substantial improvements in performance over its predecessors, upon which it could justify its higher price.

- A progression of similar preceding systems, utilising the raw materials that were already employed and readily available.
- Exposure and aggressive marketing during a time when civil engineering and infrastructure were in the public consciousness.
- A considerable appetite for construction materials and innovative technology in the marketplace

PC has not been the only cement to reach widespread usage. However, PC has been the only binder to retain its position as the dominant system. As described in Section 4.2. the BFS AAM binder system was employed for numerous construction projects where an abundance of that material was available, but its usage was tied directly to the availability of this material and the lack of PC cement. 'Roman cement' is another example of an alternative binder material to be widely adopted, but potentially the most significant example in recent times is described below.

5.3. High Alumina Cement (HAC)

(Law No. 233) *"If a builder builds a house for someone, even though he has not yet completed it; if then the walls seem toppling, the builder must make the walls solid from his own means".* (Law No. 229*) "If a builder builds a house for someone, and does not construct it properly, and the house which he built falls in and kills its owner, then that builder shall be put to death."* (Law No. 230) *"If it kills the son of the owner, the son of that builder shall be put to death."* – The laws of Babylon as decreed by Hammurabi, king of Babylon from 1792 – 1750 BC. Translated by Leonard W. King (1915) [279, 280].

Brueckner & Lambert [279] list a number of cement systems for the benefit of identification and sympathetic restoration of structures by historians [279]. These include PC with a calcium chloride additive to speed up setting – although at the cost of accelerating the corrosion of embedded steel, PC blended with asbestos fibres for fire resistance, and the early iteration of AAM developed by Hans Kühl [228] which utilised some addition of PC to produce the necessary alkali conditions [228, 279]. These

PC additives have largely fallen out of favour, and AAMs have progressed to make more efficient use of their precursors. High alumina cement (HAC) is another example of a historic cement system which was once commonly employed but has since been banned from structural applications in the UK after a string of unfortunate high-profile failures. These failures were attributed to poor work practises and an insufficient understanding of the HAC system, but even now that industry and the scientific community are better informed, they have not been successful in lifting the ban on its use [281, 282].

HAC, or calcium aluminate cement (CAC), contains primarily monocalcium aluminate, produced using lime and a high alumina bearing material such as bauxite, with hydration producing calcium aluminate hydrates [283]. It was developed by Jules Bied in France, 1908, and mass-adopted in the UK for pre-stressed beams in ambitious redevelopment projects following the extensive infrastructural damage suffered during World War II [279, 284]. HAC is a fast setting, high strength system, developed predominantly to be resistant to sulfate attack [279, 284]. Its higher heat of hydration allows it to be laid in a low temperature environment and HAC is particularly suited to flooring where it exhibits low shrinkage, resistance against acid attack of $pH < 4$, thermal shock, and abrasion [283]. It is still employed as a refractory material, withstanding temperatures up to 2000 ℃ [281].

During the use of HAC in the UK, it was common practice to use a water to solid ratio as high as 0.6, whilst it is now advised that a limit of 0.4 should be used with HAC [279, 281]. The hydration reaction can form metastable phases dependent upon the environmental temperature, which can transition to form stable phases with increased temperature, humidity, as well as merely a prolonged timescale.

$$CA + 10H \rightarrow CAH_{10} \quad \text{(Room temperature)} \qquad \textit{(Eq. 5.1.)}$$

$$2CA + 11H \rightarrow C_2AH_8 + AH_3 \quad (\leq 38\ ℃) \qquad \textit{(Eq. 5.2.)}$$

$$3CA + 12H \rightarrow C_3AH_6 + 2AH_3 \quad (\geq 40\ ℃) \qquad \textit{(Eq. 5.3.)}$$

The formation of these metastable phases could lead to occurrence known as conversion reactions.

$$3CAH_{10} \rightarrow C_3AH_6 + 2AH_3 + 18H$$

(Eq. 5.4.)

$$3C_2AH_8 \rightarrow 2C_3AH_6 + AH_3 + 9H$$

(Eq. 5.5.)

This series of conversion reactions can increase the porosity of the system, as the density of the final stable phases are greater than that of the metastable phases, essentially allowing the porosity to grow [281]. This effect is exacerbated by high levels of water within the system, as the already increased porosity will increase further still potentially resulting in a noticeable loss of strength, and in this scenario it will not benefit from the release of water through further hydration that may offset the loss of strength [279, 281, 284].

Whilst the stable product is a system capable of all of the enhanced properties described, its poor implementation led to the failure and collapse of a number of buildings. Some examples given by Houghton [281] and Neville [282] are:

- The partial collapse of a building roof, University of Leicester, (1973)
- The collapse of the hall roof at Camden School for Girls, London (1973)
- The roof collapse of a swimming pool at a School in Stepney, London (1974)

Shortly following these high-profile failures, an investigation resulted in HAC being withdrawn from the Code of Practice for the use of structural concrete (CP 110, also in BS 8110) [284, 285]. HAC is still produced today, albeit limited to non-structural applications such as refractory structures, and in the UK, it has been unable to recover from the reputation that resulted from the 1970's failures [281, 284, 286].

Such high-profile failures are difficult to resolve and amend, regardless of the advances made to a system, material, or technology. The adoption of a new cement system into structural applications, without fully understanding it, undoubtedly hindered the introduction of other novel cements into structural applications in the UK.

In another example, the introduction and later dominance of PC was helped by the high-profile failure of 'Roman' cement, in the Euston station collapse of 1848, wherein a wall collapsed which led to the death of two workmen [271]. The architect attributed this failure to the use of the cement in prohibitively cold weather and careless work practice, although William Aspdin took the opportunity to blame defective cement no less than a fortnight after the incident [271].

5.4. Understanding Heavy Industries

"Heavy industry: the manufacture of large, heavy articles and materials in bulk." – Oxford Lexico [287].

Heavy industry, much of which was pioneered in the UK during the industrial revolutions of the 18th century and thereafter, includes a great number of industries and processes. These include but are not limited to [288]:

- Construction – Housing, infrastructure.
- Manufacturing – Machining, forging, assembly.
- Material production – Cement, chemical, metallurgical, glasswork.
- Mining and logging – Mineral, wood, oil, and gas.
- Transport – Aerospace, automotive, shipbuilding, locomotive works.

Another defining feature of heavy industry is the prolific use of resources. Heavy industries typically require significant natural resources, infrastructure, land, personnel, and capital. The generation of, or gaining access to, the resources required is no mean feat. The required collaboration between large groups of investors, managers, workers, and governing body officials, makes starting a heavy industry operation an extremely difficult, labouring, and financially risky enterprise. For these reasons, heavy industry can generally be described as risk averse and conservative.

The production of cement is one such industry that can be considered conservative. As mentioned in sections 1.1 and 5.2, the Portland cement industry has existed for nearly two centuries. At its core, it

has revolved around the production of calcium silicates within a kiln to produce a clinker [17]. The process has been refined throughout generations and it will prove difficult for the industry to move away from such a mature technology. There are many industries that make use of cement to produce forms of specialist concrete. As well as for radioactive waste immobilisation and encapsulation, cement is used to produce other specialist grouts, sealants, and ceramics. Two other notable examples of low volume use of cement are in dentistry (zinc phosphate cement for example) and the capping of oil wells using a concrete plug [79]. Most cement, however; goes into civil construction, which has similarly gone through an evolutionary development in balance between new available technologies, the trends of the time, what is practicable, and what is economically viable.

The variables that go into decision making within heavy industry can broadly be simplified into what is available, what is desirable, and what is justifiable. The following section is a selection of examples from history, explaining where these variables have come into play in either the success or failure of a heavy industrial operation.

The invention and improvement of PC was a huge development in the construction sector, as was the use of steel frames and the later evolution of steel rebar reinforced concrete. The advent of new technology allowed for more ambitious, desirable, and practical construction to go ahead. Skyscrapers and tower blocks were a product of rapid urbanisation, wherein people followed the employment available in the worlds growing cities. With this demand for urban accommodation came a rise in the value and desirability of land central to a city, and the appetite for bigger and more ambitious housing complexes.

Dense urban populations have existed for millennia. Insula buildings were the apartment complexes of ancient Rome, rapidly constructed and economic housing blocks with multiple floors that would house several families of low social standing. Space was extremely limited for those financially tied to large urban cities, whether due to their employment in the case of sailors or labourers or merely to increase their likelihood of survival with access to food, with conditions being squalid. The construction height of insula was reportedly regulated and limited by the first Roman emperor Caesar Augustus to

approximately 70 feet, and later even decreased by subsequent rulers in order to decrease the occurrence of these buildings collapsing [289]. This is potentially one of the first example of an enforceable building regulation, and an acknowledgement of the limitations of cheaply built wood and masonry structures. This practicable limitation would largely remain until the development of more affordable, higher tensile strength materials that could surpass masonry construction.

Crucible steel was the highest tensile strength steel available in Europe in its day. Independently discovered by Sheffield horologist Benjamin Huntsman around 1740, it was a resource intensive and very valuable commodity [290]. Sharp tools such as scythes would commonly feature only a crucible steel edge, with the remainder of the blade being wrought iron to reduce costs, such tools being known as edge tools [291]. Large masonry buildings of the time, such as the Ditherington flax mill and Arkwright mills, would employ cast iron pillars and beams to secure their internal structures, but were limited in their dimensions by heavy masonry. In the 1840's, attempts were made in the UK to construct buildings utilising external cast iron structures, but these were met with scathing criticism on fire safety and architectural grounds, with cast iron banned from being used as part of a building's main external structure by the 1844 London building code [292].

Whilst cast iron preforms well under compression, its approximate 3% carbon content with impurities makes it a brittle material [293]. The development of more ductile, very low carbon wrought iron began to improve iron structures as more efficient methods of production were developed, driving down costs. This continual development culminated in the Bessemer process of 1856, which not only gave far more control over the material composition, but also drastically increased the efficiency of the process. The crude molten pig iron from a smelter is subjected to an airstream, wherein oxygen is introduced into the melt and combines with carbon and other impurities, forming either a gas or the oxide slag that is skimmed from the top of the melt [294]. The end product was high quality and economically produced steel, pushing the envelope of what was practicable in terms of high-performance structures and making opportunities available for future construction projects.

"To these eager adventurers, the conversion of five tons of crude molten iron into cast steel, in a few minutes, was the realisation of the fabled philosopher's stone, that transmuted lead into gold." – Sir Henry Bessemer, 1905 [295].

During the 1880's, landowners were demanding taller buildings to be constructed in Chicago following its recovery from the great fire of 1871. The value of land in the city's central business district had risen greatly in recent years and necessitated more efficient use of its occupying area. In 1885, the Home Insurance Company Building was completed, considered by many to be the first skyscraper in terms of height and the use of an iron and steel supporting structure merely clad in, and not supported by, masonry. This structure consisted of cast iron columns, supporting either wrought iron or the new revolutionary rolled steel beams, with the columns encased in brick or clay tile for increased fire protection [292].

Reportedly, this design was met with scepticism, with construction being halted by both the Home Insurance Company as well as the City of Chicago so that they could verify that the building was indeed structurally sound [296]. With the success of the Home Insurance Building, the design was repeated in Chicago, with the merits of this design being slowly incorporated into successive high density urban structures, eventually leading to high-rise buildings becoming common within urban landscapes.

This chain of events is just one example of the behaviour of heavy industry, and its gradual evolution based upon what is available, desirable, and justifiable. As steel technology was independently developed, and the desire for comfortable, high density urban property increased, the pursuit for steel framed skyscraper buildings became justifiable. Materials that were both economically viable and met the performance requirements were available, meaning that the steel structures performance requirements were achievable.

The way in which urban centres were being developed had matured, with a balance being met between city expansion and infilling. Infilling required the more efficient use of the land space in certain city districts, which the development of skyscrapers was perfectly suited to [297]. This was driven by the increased desirability of living in an urban centre, with more financial prospects and a higher quality of

living than many rural areas (suburban living would have to wait until mass transport became more available). The risks involved in such a development were therefore worth taking.

To many in positions where innovation is desirable, such as those involved in research and development, the gradually paced adoption of innovative technologies and practises can be frustratingly slow. Even during the more relaxed regulatory environments of the 18th, 19th, and even 20th centuries, scepticism has always had an influential role in the behaviour of heavy industry. Iron workers in Sheffield were reportedly reluctant to accept the new Bessemer process at first, suspicious of its deviation from tried and trusted methods [295].

"Sheffield wrapped itself in absolute security and believed that it could afford to laugh at the absurd notion of making five tons of cast steel from pig-iron in twenty or thirty minutes, when by its own system fourteen or fifteen days and nights were required to obtain a 40-lb. or 50-lb. crucible of cast steel from pig-iron. So, the Yorkshire town was allowed to stand aside while the more enterprising ironmaster gave the invention a trial, as far as bar-iron making was concerned. At this period, the ironmaster would never have dreamed of changing his trade to that of a cast-steel manufacturer, had such a thing been proposed to him." – Sir Henry Bessemer, 1905 [295].

As mentioned previously, heavy industry requires a huge quantity of resources, personnel, and finance in order to operate. Quite unlike in other industries, all these assets are put at risk when a heavy industrial operation commences. Operators, personnel, and equipment are put physically at risk when carrying out a function. Users and consumers can also be exposed to physical risks when involved. Material resources can be spoilt, or the supply chain disrupted. Regulatory restrictions or legal proceedings could also disrupt operations, potentially as a direct result of another action within the industry. There also may simply not be the need or appetite for the product in question, or its marketing might not be effective. Potential risks need to be understood and mitigated in order to protect financial interests and continue operations, because new or developing technologies always present a risk with no guarantee of a return.

Availability, or accessibility, refers to whatever resources or technology can be used. Firstly, materials availability is especially important to large scale manufacturing processes that rely upon bulk to operate within a slim profit margin, such as the manufacture of cement. The availability of sufficient limestone or chalk is of paramount importance to economically viable PC production, as importation over any great distance is likely to write off any profitability [9]. The quality or grade of a material is also as important as its availability.

Historically, coal was the main driver of industry in the UK, and its proximity would have considerable impact upon a locations heavy industry. For example, the city of Sheffield was ideally suited for the production of iron, and as a result became a hub of metallurgical innovation and expertise [298]. The river Don has many fast-flowing tributaries as they come off the surrounding moorlands, powering watermills and their equipment such as bellows and hammers. Ironstone, a sedimentary iron oxide-containing sandstone, is prevalent within the region, as is wood from the neighbouring valleys [299]. The availability of bituminous coal, however, was crucial to the steel making success of the region [300]. Bituminous coal is of intermediate energy density compared to other grades at approximately 24 MJ/kg and a carbon content up to 86% [301-303]. It is the main ingredient of coke, wherein bituminous coal is heated in the absence of air to drive off volatiles and moisture, producing a hard and energy dense material yielding approximately 30 MJ/kg, suitable for stoking blast furnaces and producing iron and steel [302, 304].

The area became synonymous with metallurgy, with generations of workers becoming skilled craftsmen and operators. The availability of labour and expertise is another vitally important resource to heavy industry, which allowed for operations to not only continue, but improve and innovate. Later, but to some degree analogously, the Sellafield nuclear facility, formerly the Windscale and Calder sites, required a considerable amount of labour and expertise to transform the former ordinance factory into a pioneering nuclear facility. In 1947, the neighbouring village of Seascale became a dormitory community for those with ties to Sellafield, with the UK Atomic Energy Authority financing the construction of housing and facilities for the residents to develop and encourage the growth of the community [305].

Without the availability of these resources, these industries would not have been able to start or develop and therefore make up a significant part of whether an enterprise is available or justifiable. These variables will shape heavy industry and change its course, albeit often gradually. Business decisions such as beginning or moving operations are not taken lightly and come with considerable operational upset and financial investment. The most mobile of these resources are personnel, who may be willing to relocate if infrastructure and financial incentives are provided, such as in the case of Seascale.

In times of economic stagnation, such as the 1970's, the UK government heavily incentivised businesses to set up heavy industries in areas of high unemployment. Two examples of this initiative are the Rootes Group factory in Linwood, Scotland, building the Hillman Imp economy car, and the DeLorean factory in Dunmurry, Northern Ireland, building the DMC-12 sports car. The DeLorean Motor Company was founded by automotive industry veteran John DeLorean, producing its first cars in January 1981. The Dunmurry site was chosen as so to benefit from $117 million of UK taxpayer funding in 1978, equating to approximately £534 million in 2023 [306].

Whilst this incentive was a considerable financial boost to help establish production facilities, the vast majority of the workforce were not skilled in manufacturing or industrial management, and intensive training was required at all levels of the fledgling company. When completed cars were exported to their respective dealerships, primarily spread across the United States, the build quality of cars was such that quality assurance centres had to be established in order to rectify cars before sale. Poor reliability and prolific build issues quickly tainted the reputation of the DMC-12, which compounded the financial pressures the company was experiencing, eventually leading to bankruptcy in December 1982 [306, 307].

Figure 66: An epitaph written within one of the controversial gullwing style stainless steel doors by members of the Dunmurry workforce during the final days of DeLorean DMC-12 production [308].

The Rootes Linwood factory had similar issues, despite the financial incentives that facilitated production start-up. Unlike DeLorean, Rootes was an established manufacturer that was set up primarily in Coventry and the Midlands. Whilst Hillman Imp pressing, casting, and final assembly operations would take place at Linwood, engine block machining for example had to be undertaken in Coventry, necessitating a nearly 700-mile round trip of road transport in order to cast, machine, and install that engine block. This inherent inefficiency, that could only be resolved by yet more costly financial investment in the area, never allowed for the Linwood facility to meet its potential [309, 310].

At the other end of the process, it is important to review the ability of a market or consumer base to do business with. For example, a cement manufacturer will need to be placed in close proximity to both quarries and concrete merchants, as well as the infrastructural projects that will require it. Electrical power generation will ideally be placed nearby infrastructure, so as to minimise the grid infrastructure required and the efficiency losses through transport. In relation to city planning, large housing projects need to be constructed in either well populated or rapidly growing population centres. There is a delicate balance between city infill and expansion, with an excessive amount of either risking a drop in property demand, its value, and potentially a huge amount of vacant or even abandoned property [297].

Currently in China, there is a large amount of vacant housing. In 2017, reportedly around 65 million, or >10% of all homes were unoccupied [311]. In a mismatch between supply and demand, excessive urban expansion has led to large areas of unfinished or merely unoccupied developments. China's economic growth is tied significantly to real estate, with it being the single largest contributor to China's gross domestic product at 29% [312]. The sale or leasing of land to developers reportedly accounted for $4.3 trillion of income in China, highly incentivising the expansion of cities [313]. Residential properties are also typically sold or leased before construction is completed, with the liquidity allowing for the project to be completed. With rampant urbanisation predicted in line with previously reported rates, investment in housing led to rising prices and even more investment, with many purchasing multiple properties. This rapid growth has proved to be unsustainable, with many unwilling to move into newly built areas with minimal established infrastructure and employment opportunities [314]. Second or third homes bought as investments are vacant, with so called 'ghost cities' becoming infamous. In 2022, China's second biggest property developer reached a debt of over $300 billion, and unfinished or vacant tower blocks are reportedly being demolished [312, 313, 315].

Finally, even if all of the necessary resources and technology is available, and that the end product is desirable, change within heavy industry must be justified. Desirability and justifiability are directly linked and overlap in many circumstances; however, justifiability covers more as to what is practicable, as opposed to merely marketable or considered beneficial.

An example of this difference took place during the 1960's and 70's with the development of hovertrain technology. At the time, rail transport was in significant decline with the mass adoption of personal transport and more efficient and faster highways taking away both passengers and freight work. Much of the national and international rail network had been established in the 19th century, and as a result was inefficiently laid with tortuous routes compared to modern high-speed standards. Rail traffic was also suffering from speed restrictions due to antiquated signalling and issues such as hunting oscillation. This is where the conical wheel sets would not remain central and balanced between the parallel rails at speed, instead riding up one rail and then the opposite side, causing the wheel set to sway from side to side and potentially causing derailment on even straight track [316].

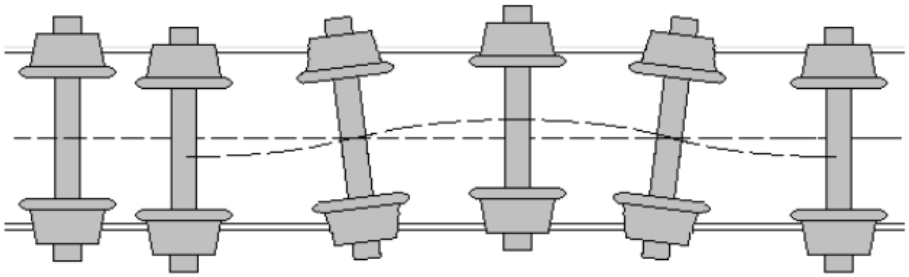

Figure 67: A diagram illustrating the movement of hunting oscillation and its detriment to railed transport, as depicted in Mazilu [316].

A solution was proposed by French engineer Jean Bertin, wherein the rails and wheels would be replaced by a concrete track and a cushion of air [317]. A vehicle would produce lateral and vertical thrust, both propelling and lifting the vessel, so that it may glide utilising the low drag aerodynamic ground effect. This is a highly efficient means of producing lift and forms the basis of all ground-effect machines or vehicles, such as hovercraft or the ill-fated ekranoplan [318]. The result was fast transport that was cheap to build, with the concrete beam or T-shaped track being far easier and more cost effective to build and maintain than a railway, with far less groundwork necessary. The Aérotrain was deemed such an innovation that the technology was adopted all over Europe and North America. In the UK, the technology was developed to produce the RTV31, replacing the gas turbine engine design employed by the early Aérotrain with a linear induction electric motor, significantly reducing operating noise and pollution [319]. The US High-Speed Ground Transport act of 1965 culminated in a similar linear induction motored design developed by ROHR Inc, that ran its near 6-mile Pueblo test track at 145 mph in 1974. The French Aérotrain I-80 would break the classes world land speed record later that year [320, 321].

Figure 68:The ROHR Inc tracked air cushion vehicle (TACV) in Pueblo, Colorado. Driven by a linear induction motor to 145 mph, with a seating capacity of 60 in airline style comfort [320].

Plans were made and contracts signed for major links between airports and metropolitan areas in each respective country, the most significant outcome being the construction of 18 km of track that would form a transport link between Paris and Orléans. By the end of the 1970's, however; funding was withdrawn internationally, and none of the plans ever came to fruition. Economic pressures experienced during the 1970's led governments to reassess their funding for innovative projects. In 1975, the French government announced its plans for the TGV 'train à grande vitesse' high speed train, which featured the latest in conventional-style rail transport technologies [321].

The British government had also recently brought its APT-E advanced passenger train experiment into service, the first iteration of the tilting train cornering technology used today [319]. The decision was made to invest into existing infrastructure and foundational technologies, as opposed to chase new, radical departures from what had already been established as conventional. Incremental improvements were made instead to the production of rails, wheel sets, and signalling, allowing for older infrastructure to be updated and new rail sections or lines to be integrated into it. More investment would also go into highways, with pressure mounting from continually increasing road traffic. Despite its promise and long-term benefits, it was not practical to construct an entirely new system to be put into place when the existing one was still practical and could still be improved upon. In 1972, it was estimated that the RTV31 project would not be ready for deployment until 1985 [319].

Figure 69: The remains of the abandoned Paris to Orléans Aérotrain link as can be seen currently [320].

To summarise from these historical examples given, it can be determined that in order to change the direction of heavy industry there must be a great deal of support in terms of the maturity of the technology, the accessibility of resources, an appetite for the product, and whether the change can practically be applied in a timely and straightforward manner without great disruption or detriment. These factors steer heavy industry to a more conservatively led development.

5.5. Disrupting Heavy Industry

In the preceding section, the more natural behaviour of heavy industry was discussed, where gradual and incremental development is favoured over more radical technologies, and those within the terms of what was achievable, justifiable, and desirable. This more conservative behaviour can, however, be disrupted by circumstance either suddenly or more gradually.

In this instance, a sudden change is categorised as an event that unfolds in a couple of days. The outcome might be positive, like the unexpected discovery of a resource such as an oil field. In such a short timescale however, and given that the event is unplanned, sudden disruption is more often than not in

the form of failure or catastrophe. Undoubtedly one of the most severe and far-reaching disasters of modern Britain is the Grenfell Tower fire of 2017.

Completed in 1974, Grenfell Tower is a residential tower block designed in the 1960's as part of the Lancaster West scheme. Its exterior is made up of pre-cast concrete spandrel panels, the tower being supported primarily by reinforced concrete columns and reaching 25 storeys or 67 m tall. Between 2012 and 2016 the tower block was refurbished, updating many heating and other pipework systems, but critically it involved upgrading the building insulation, windows, and exterior aesthetic [322]. The exterior of the building was clad in foam insulating panels and a rain screen, a composite comprised of 0.5 mm aluminium sheets sandwiching 3 mm of highly flammable polyethylene (Figure 70) [323].

Several factors contributed to the scale of the tragedy. The use of flammable material in the renovations, selected as part of a cost saving exercise that amounted to £293,000, allowed for the fire to spread rapidly and unpredictably [324]. The rain screen aesthetic panels, Reynobond PE 55, carried an acceptable fire resistance rating in riveted panel form, but proved to be highly flammable when used in cassette form and screening applications (Figure 70). This result was supressed internally by the manufacturer, and even after eventually being reclassified, the revised flammability was not communicated to customers by the sales team [325].

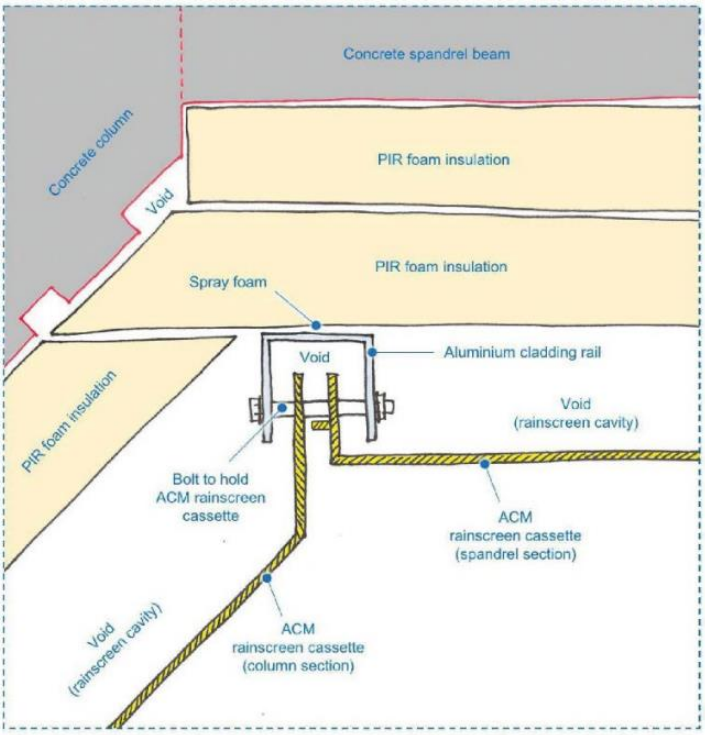

Figure 70: Diagram from the phase 1 Grenfell Tower fire report showing the insulation and cladding structure attached to the original concrete tower exterior (image top). This shows the composite cassettes hung upon the exterior of the building, with the void which accelerated the fire's spread [322].

The severity of the blaze was amplified by the lack of a sprinkler system and the 'stay put' fire procedure still in place, where it was advised that residents remain in their flats as the concrete structure was once deemed fire retardant enough to protect them, avoiding the possibility of a crush incident occurring on the stairwell [322, 324]. The consequences of the Grenfell Tower fire were, and still are, far reaching. Cladding has become extremely commonplace upon buildings greater than 2 storeys, in order to increase the aesthetic appeal of their steel and concrete based construction and meet thermal efficiency targets. The tragedy became a catalyst for safety reform within the industry. In 2018, the external wall system safety certificate (EWS1) was introduced in order to reassure lenders that residential buildings that employed cladding carried a low risk of fire so that valuers would allow for mortgages to be obtained [326].

EWS1 required all buildings over 6 storeys or 18m tall with cladding to be assessed by a fire safety officer, irrespective of any other fire safety certification [326-328]. The EWS1 form would then be

filled out, clarifying its compliance or outlining improvements that are required, which in England certifies that building for 5 years [329]. The rapid introduction of this measure helped to reaffirm the urban property market, but also led to further uncertainty as in 2019 the EWS1 criteria were revised to cover all buildings that employed cladding irrespective of height, only to be reversed again a year later [326]. For many people to sell their properties, a fire safety officer had to have carried out the EWS1 certification so that a potential buyer could obtain a mortgage; however, an extensive backlog quickly formed, with waiting times still estimated at between 6 – 12 months as of 2023 and reportedly as high as 48 months initially [330, 331]. There are also concerns that EWS1 may be putting fire safety officers and consultants at risk of liability claims, as they can only go so far as to assess whether the use of combustible materials still allows for a reasonable level of fire safety [332]. The polyethylene composite panels were eventually banned in revised building regulations published in December of 2022 [333]. This event therefore drastically changed the construction and property market within a short timeframe, with long lasting effects that have yet to be fully resolved.

Material availability is the linchpin of heavy industry, that can be disrupted gradually through the phasing out of a material or process, or via a sudden event that can cut off supply, such as political turmoil or a natural disaster. The declining availability of a consistent supply of pulverised fuel ash (PFA) and blast furnace slag (BFS) is one of the main driving forces that has led the UK nuclear industry to explore alternative cement systems. Coal is a fundamental component in both the manufacturing of steel using a blast furnace, and in coal fired power stations that have produced the supply of PFA for use in concrete and cementitious grouts for many decades. Coal has been gradually phased out in the UK since towards the end of the 20th century, which although a necessary movement away from the UK's reliance on coal for electricity, this has proven problematic in areas where a smaller quantity of high-quality coal is extremely beneficial [206].

Ffos-y-fran in South Wales is the biggest opencast coal mine left in the UK [334]. Originally set to cease mining operations in September 2022, many industries that used the Welsh metallurgical and steam coal began to explore alternative fuel sources [335]. With UK sources dwindling, a suitable alternative was found in a similar grade of Russian coal [336]. The importation of Russian coal abruptly

came to a stop with the Russian invasion of Ukraine in February 2022, although at this time Ffos-y-fran remained open [337]. In March of 2022, the coal washing plant which removes non-combustible impurities failed, which suddenly cut short the supply of Welsh coal [336]. With the impending closure of the site only 6 months away, there was debate as to whether repairing the wash plant was economically viable. As retained coal supplies dwindled, industries once again rushed to source a suitable alternative, with trials of Polish and Colombian coal currently being conducted [337].

Figure 71: Aerial view of Ffos-y-fran open cast coal mine, the largest left in the UK [334].

Opening in 1865, the Talyllyn railway on the Welsh coast served the former slate mining quarries. This narrow-gauge railway is a local attraction today, one of many heritage railways running steam locomotives for tourists. The Talyllyn railway consumes just 95 tons of coal per year, however; the quality of the coal is subject to stringent requirements [336]. The volatility of the coal must produce a long, sustained heat, so as not to burn up too quickly (a volatility of 24%), and the coal must also produce enough ash to lay a stable, heat retaining bed for the fire without smothering it (4% ash content) [336]. Poorer quality coal that produces more ash and clinkers may also require more firebox maintenance and repair work, and may also produce substantially more smoke, which has been noted in many imported coal alternatives [336]. The requirement for high quality material at low capacity for a relatively niche application is a similar situation that the UK Nuclear industry has found itself in with

regards to its cementitious material needs. As is the case with UK Nuclear, operators of steam driven machinery have looked to alternative sources.

Aside from other coals that can be imported or blended, with the negative attributes worked around as best as possible, the price of coal has also been a driving force in trailing alternative fuelling. Even with Ffos-y-fran coming online once again towards the end of 2022 with the coal washing plants repaired, albeit delayed again due to a landslide, the price of coal has increased from £150 – 200 per ton in 2021, to £300 – 600 per ton in 2022 [336, 338].

Figure 72: Oilseed meal briquettes [339].

Two alternative products being trialled by Talyllyn, as well as other locations like Stainmore and Apedale, are e-coal and rapeseed briquettes [336, 338, 340]. E-coal is a coal-based product from Sheffield of approximately 50% coal or coke and 50% biomass, with the biomass content consisting within the region of 30% crushed olive stones and 20% molasses (Figure 72) [341]. This product is sold as a low smoke fuel for home open fire heating, with a higher energy density than standard coal or kiln dried wood, it has been used successfully in steaming trials [340]. Rapeseed briquettes, or oil seed logs, are made entirely out of compacted meal from oilseed rape production and are a waste product from the biofuel industry [339]. The total heat released is directly comparable to that of Welsh steam coal, although the rate of that release is twice as high, and the fuel must not be allowed to become wet [338]. Both materials are therefore usable alternatives to conventional coal products, with both products having once exceeded the price of coal, but now being in more direct competition [336].

Disruption of heavy industry occurs more gradually with societal changes, which is often the driving force behind many other secondary changes or limitations, such as material availability, legal standards, or taxation. One significant societal change within the UK is its change of economy type from manufacturing to service based. A 2023 study by the House of Commons found that between July and September of 2022, service based industry accounted for 82% of all employment within the UK [342]. In 1948, 46% of employment was service based, with 42% involved in manufacturing (Figure 73) [343].

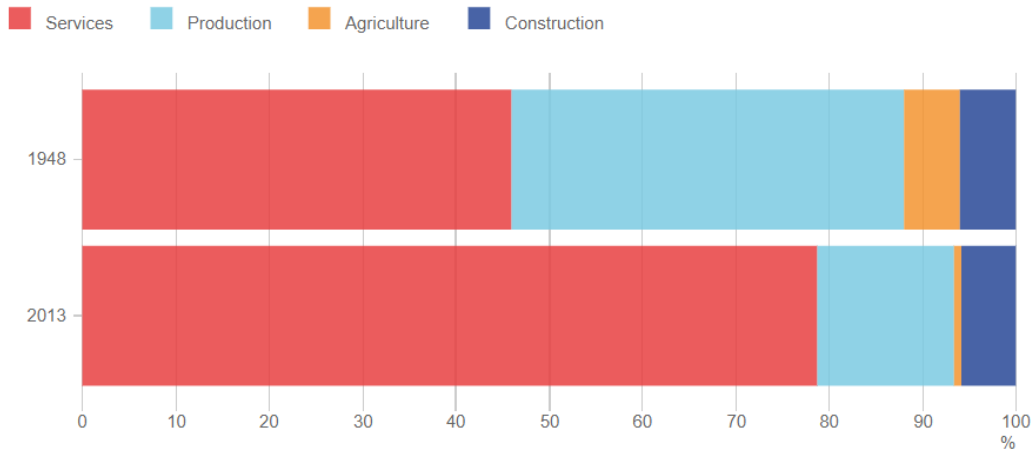

Figure 73: A comparison between the percentages of those employed in service, manufacturing, agricultural, and construction industries in the UK, separated by 65 years. Study and image by the Office of National Statistics [343].

A service-based industry delivers non-tangible value, such as education, healthcare, entertainment, consultancy, legal work, or retail [344]. Whilst this transition is seen as the natural progression of a more developed economy, with standards of living undoubtedly improving significantly since 1948, there are some drawbacks [345]. A service-based economy is a consumer of goods, and the infrastructural and material needs of that society will only increase as it becomes more developed. The manufacturing needs of that society therefore must be fulfilled by other, arguably less developed economies, with material being imported from international suppliers [346]. This has always been a fundamental element of the global economy, and national economies that isolate themselves from the global community become insular and rarely thrive [347]. Importing goods also gives a breadth of choice, from world leading producers of materials or technology, and access to a wealth of knowledge and experience [348].

An international supply chain, however, offers significantly less control, and might leave a nation with supply shortages or at the mercy of foreign policy and international relations [346, 348]. The risk of disruption to the supply chain is therefore much higher. Within the duration of this thesis research, the blockage of the Suez Canal and the disruption of fossil fuel supplies as a result of the conflict in Ukraine and aggression towards Europe are two particularly important examples [349, 350]. Once again bringing up the subject of coal, disruption in the coal supply chain has led to the re-exploration of opening an underground coal mine in the mid-Copeland coalfield of Cumbria, in order to secure a supply of metallurgical coal [351]. The UK is unwilling to completely surrender its remaining steel producing capabilities. This transition also leads to a change in a community's skillset. Workington in Cumbria produced steel for 130 years and was famously adept at the production of the rails which make up the track and point infrastructure of the world's railways [352]. With the dissolution of this industry at the beginning of the 21st century, this knowledge and skillset was lost, as the chain of skill sharing from one generation to the next was broken. As mentioned previously, the availability of expertise is a vitally important resource when developing heavy industry.

Whilst the change of economy is undoubtedly an important factor in the gradual disruption of heavy industry, perhaps proving to be the underlying cause of a more immediate disruption to industrial operations, arguably the most significant societal change within the past half century is the exponential concern surrounding climate change.

5.6. Climate Change

"Everything we've achieved in the last 10,000 years was enabled by the stability during this time. Our burning of fossil fuels, our destruction of nature, our approach to industry, construction and learning are releasing carbon into the atmosphere at an unprecedented pace and scale. We are already in trouble. The stability we all depend on is breaking." – Sir David Attenborough, speaking at 26th United Nations Climate Change Conference (COP26), Glasgow, 2021 [353].

What began as an apathetic concern has increased exponentially to become a constant anxiety, as the environmental repercussions of modern living became harder to ignore at the dawn of the 21st century [354]. In 2022, a United Nations (UN) report to the general assembly stated that *"human-induced climate change is the largest, most pervasive threat to the natural environment and societies the world has ever experienced, and the poorest countries are paying the heaviest price"* [355]. In December of 2015, the United Nations Framework Convention on Climate Change (UNFCCC) established the Paris agreement which dictates a 2˚C Scenario (2DS) [356, 357]. This agreement sets national targets, or Nationally Determined Contributions (NDC), in order to give a 50% chance of global average temperatures being increased to 2˚C above preindustrial levels in 2100 [357]. In the UK, the NDC requires that net carbon emissions are reduced to 68% of the level produced in 1990 by 2030, with net zero to be achieved by 2050 [358].

The 2018 Chatham House report compiled by Lehne & Preston [6] states that in order to remain within the Paris agreement, the global cements industry needs to reduce its emission level by 16% before 2030, with an estimated 8% of global CO_2 emissions currently being attributed to the production of Portland cement [6]. Aïtcin [9] describes this as a significant undertaking, achievable through a combination of fuel switching, increased operational thermal efficiency, a reduction of the clinker component of a cement, and more innovative technologies [9]. It is noted that the reductions that can arise at this time from fuel switching and increased thermal efficiency are marginal, as the production of PC is a mature and well-honed process with the only modest improvements available from older production facilities [9].

Clinker substitution is an effective means of lowering attributed CO_2 per tonne of cement produced [359, 360]. This is a technique currently employed to a varying degree dependent upon the cement specification in force (e.g. BS EN 197-1:2011 in the UK) [86]. Over 80% of supplementary cementitious materials (SCM) employed are either BFS, PFA, or limestone, with standard limestone generally only applicable up to 10% before having a negative impact on the strength of the product [361]. The implementation of BFS and PFA is already essentially at full capacity, but other materials

such as calcined clays as well more reactive limestones are being explored as viable alternatives [147, 361-363].

The International Energy Agency (IEA) in 2009 published their low-carbon trajectory for the cements industry, concluding that commitment to the best currently available techniques, alternative fuelling and clinker substitution was not sufficient for *"meaningful reduction of CO_2"*, and that there is a requirement for innovative new technologies such as carbon capture and storage (CCS) and new types of cements [364]. This position was clarified in 2018, as the IEA published their updated report outlining the clear benefits of CCS for the cement industry, given that CO_2 emissions are concentrated, allowing for recovery from both the raw material and the fuel [365, 366]. In order to meet the 2DS scenario, CCS solutions will begin to come online before 2030, and by 2050 will capture and store 25 – 29% of directly generated CO_2 emissions [365]. This has put a significant amount of pressure upon the development of CCS in a way that is effective, practicable, and financially viable. Currently, it is debatable as to whether CCS is on track to meet this requirement, with the IEA report for cement in September 2022 stating that the cements industry is not currently on track to meet its goals, and that CCS deployment needs to increase dramatically over the next decade [6, 19, 367-369]. This represents a huge disruption for the cements industry, in a timeframe that does not represent the usual progression of heavy industry.

With the perceived reliance of these policies upon CCS technology for the reduction of CO_2 emissions, more attention has been paid towards alterative binder technologies, with these receiving more emphasis in more recent reports [6, 365, 370, 371]. In addition to carbon taxes, Baylin-Stern & Berghout [372] estimate that CCS technologies could cost between \$60 – 120 per ton of CO_2 removed from the cement manufacturing process, which increases the financial viability of, and incentivises the production of, lower-CO_2 cements [372].

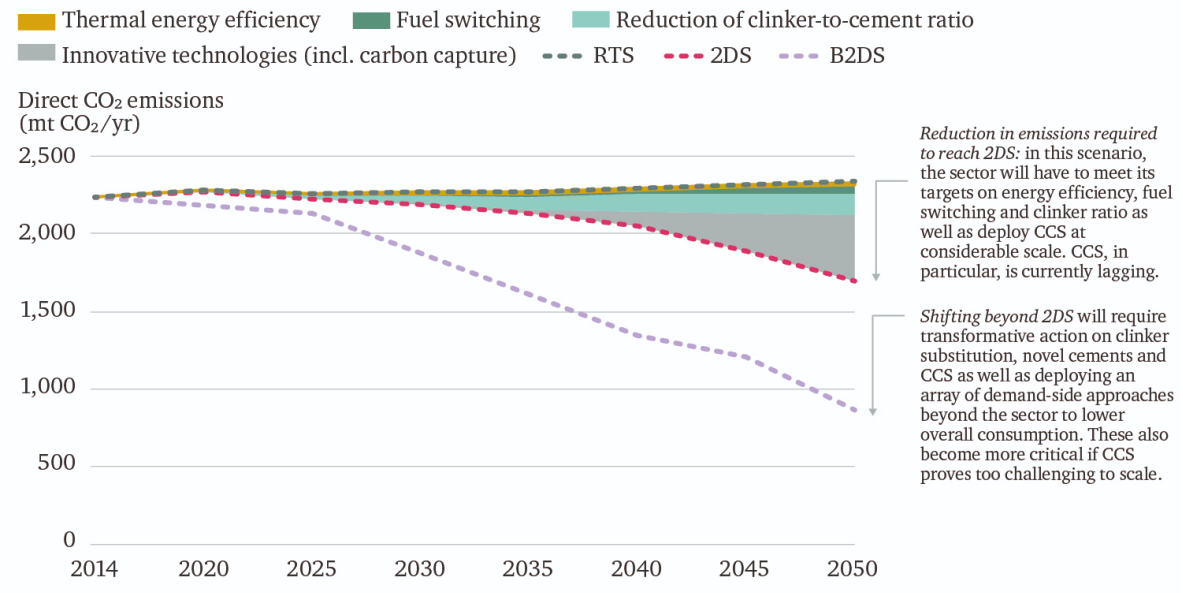

Figure 74: Figure from the 2018 Chatham House report compiled by Lehne & Preston [6], showing the required trajectory, split into individual technologies, required to achieve the 2DS scenario by 2050. Also shown are the beyond 2DS and reference technology scenarios [6].

Climate change is undoubtedly driving change and disruption of the cements industry, and as a result is also driving innovative approaches and cutting-edge research [373, 374]. Whilst a significant challenge for the global community, change does present the opportunity to improve the sustainability and operations of modern heavy industry. Scepticism of climate change is still an issue at all institutional levels, encouraged through motivated reasoning, political followership, and disinformation [375]. This most often comes in the form of resistance towards disruption and may be best exemplified though the lobbying for the retention of thermal coal power. For example, the Lignite Energy Council (LEC) is a lobbying group established to *"protect, maintain and enhance development of our region's abundant lignite resource"*, lignite being a low grade of coal used primarily for power generation due to its poor energy density [376-378]. The lignite mining industry has been a primary source of employment for the rural communities of North Dakota, with the local population fearing that the dissolution of this industrial practise could lead to an economic downturn and destabilise the reliability of the electricity grid.

The LEC, along with along with other similar organisations throughout the United States, Australia, and historically the United Kingdom, like 'Friends of Coal' and 'Count on Coal', fund (or have funded)

advertising campaigns and education seminars persuasive to the reasoning that coal use should be maintained to ensure the stability of communities [379-381]. The LEC in particular directly funds educational programs in schools, as well as other forms of school sponsorship and educational awards [380, 382]. One argument put forward by the LEC argument is that CCS would allow for the continued operation and advancement of coal processes, and therefore justifies continued investment in the industry [383].

Figure 75: Lignite Energy Council advertising their award as part of their sizable funding towards local high schools in the North Dakota area [379, 382].

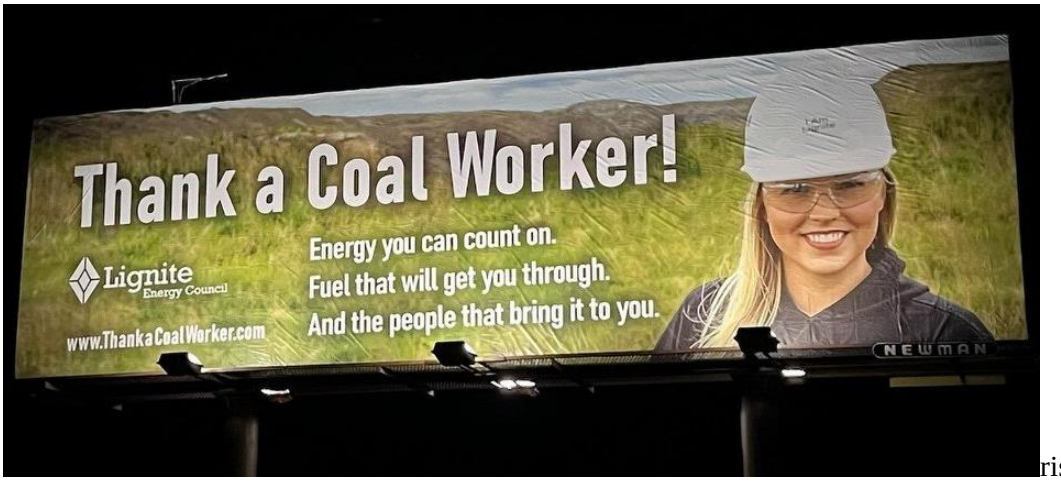

risk

Figure 76: Billboard erected by the Lignite Energy Council to promote their 'Thank a Coal Worker' campaign, where individuals can submit praise online via their website in regards to the coal industry [384].

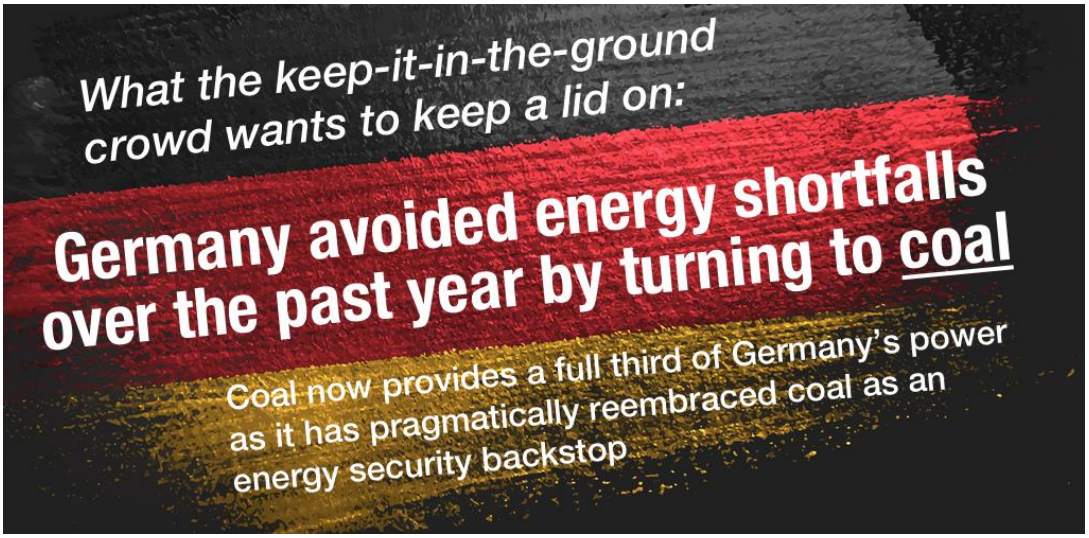

Figure 77: Propaganda from the lobbyist group 'Count on Coal', published in March 2023, in reference to Germany being forced to turn back to thermal coal power due to gas shortages as a result of the war in Ukraine [350, 377, 381].

In the context of climate change, it is vitally important to be aware of the resistance towards the disruption that advances in sustainable policy and practices cause to entrenched industries. Climate concern, however, is still accelerating, with increase pressure and activism towards industries and institutions that have the power to make meaningful changes. In December of 2022, a reported 200 climate change activists stormed the Lafarge-Holcim Marseille Cement Plant, sabotaging infrastructure and destroying product in protest of local air pollution concerns [385]. This extreme event is symptomatic of the ever-increasing public perception of climate change, and their concerns that not enough is being accomplished.

Figure 78: Climate activists sabotaging the Lafarge-Holcim Marseille Cement Plant in December of 2022 [385].

5.7. Innovation, the Chasm of Adoption, and the Technology Readiness Level assessment

Dewald & Achternbosch [386] raise the question of why more sustainable and innovative cements have failed to penetrate the cements market (prior to their publication in 2016) [386]. Three small scale alternative startups are accessed, among which as of 2023, the two more conventional applications are seemingly still being pursued over a decade after their inception [387, 388]. As evidenced by the European Technical assessments (such as ETA-13/0417) the more technologically inclusive standards being set in the UK (BS EN 197-5, BS 8500-2 clause 4.4.3, PAS 8820:2016 for AAM), and the sourcing of commercially available alternative binders in the aforementioned studies (chapters 3 and 4), innovative cement products are now available on the cements market [198, 199, 369, 389]. The mass market adoption is still near-insignificant in comparison to the market share of PC, which will inevitably represent the vast majority of cement for the foreseeable future, aided by SCMs, CCS, and other improvements in production efficiency [369, 370]. Further pragmatic adoption of alternative binder systems, such as those discussed in chapters 3 and 4, represents an obtainable reduction in CO_2 emissions and the potential improvement of capability for specialist applications [359, 365, 370].

Introducing innovation into a market, especially a conservative one, is difficult as discussed in the preceding sections of this chapter. The difficulty encountered by an innovative product accruing an increasing market share can be represented by the technology adoption curve, which involves the concept of ‘crossing the chasm’ [390]. First proposed by James & Warren Schirtzinger in 1989, the chasm concept represents the difficult transition into the more conservative marketplace, where a product must win over the pragmatic [391, 392]. The full model illustrates the general uptake of new technology to market and shows the uncertainty in establishing a product [393]. When a new product enters the marketplace, its first users are the early adopters or backers; these are those that are invested in technology early on [392]. In the case of an alternative binder product, this represents the scientific community, niche product development by cement firms, and its use in experimental or explorative applications.

As time progresses after the early adoption and the product begins to be rolled out to the open market, it is met by a chasm. The chasm is where promising ideas fail to achieve their market potential, typically through the inability to change their marketing strategy to appeal to a wider, less enthusiastic consumer base [392].

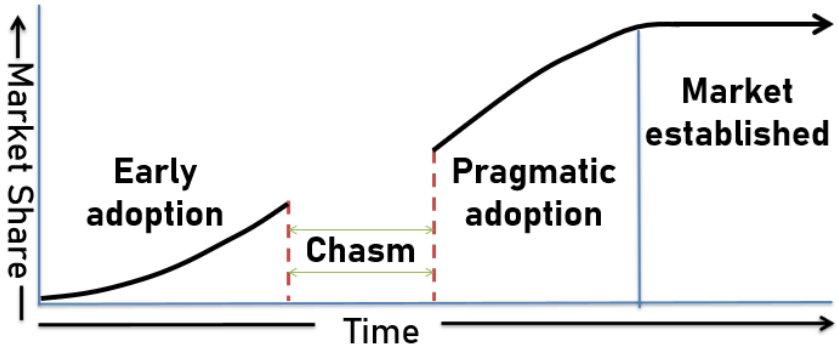

Figure 79: Representation of the first half of the technology adoption profile, showing the theoretical chasm between the early adopters and the pragmatic.

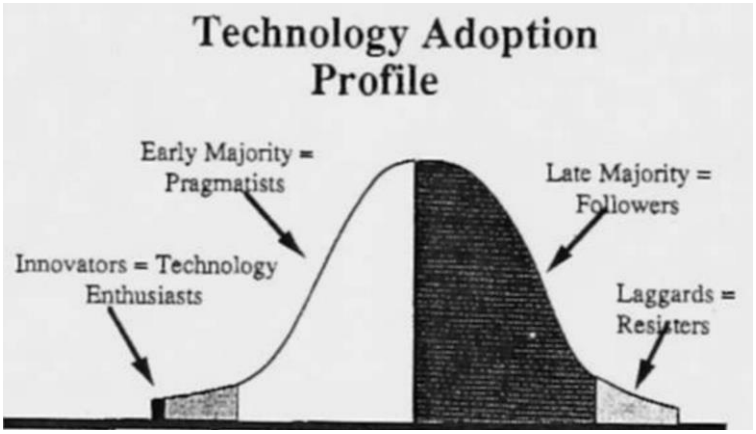

Figure 80: The original drawing of the technology adoption profile, shown in 1989 [392].

Crossing this chasm is made much easier when the new technology is sufficiently incentivised. An excellent example of this happening in the last decade or so is the adoption of the electric car, which has progressed significantly in the UK even through the 4-year duration of this PhD project [394].

Historically, the steam engine, the jet engine, and the internal combustion engine are all examples of radical new technologies that presented huge advantages and were set to change their industry forever, and yet it took years if not decades for them to finally be adopted and start to become the norm [395, 396]. Towards the end of the 19th century, it was decided that horse drawn transport was becoming a

problem in built up areas due to the vast quantities of manure being produced [395]. Horseless carriages were seen to be the answer, with three variants rising in a race to become the accepted means of transport: steam cars, cars with an ICE (Internal Combustion Engine), and electric cars [397]. After a couple of decades, the ICE became the norm, due in no small part to the convenience of being able to simply fill a fuel tank in a matter of minutes to extend their range, whilst steam cars required solid fuel and water, and a carefully maintained and well stoked fire [398].

Electric cars were held back by the crude battery technology available at the time, being laden with slow charging and extremely heavy lead-acid batteries to power inefficient electric motors [397, 399]. Whilst initially popular as taxi cabs, it has taken the electric car in excess of 100 years to become a viable alternative to their ICE driven counterparts [395, 397, 398]. Electric cars, or electric vehicles (EV), would remain an area of research throughout the 20th century, with prototypes and small batches being produced, such as with the Lucas electric vehicle program [400]. Battery technology would continue to progress, with the first lithium-ion batteries being developed throughout the 1970's and 1980's [401]. The EV was arguably eventually popularised and brought to the mass market through both the Toyota Prius hybrid technology, which gave the mass market its first taste on EV benefits in a real-world environment, and then the Tesla Roadster of 2008 with its unprecedented advertised single charge range of 245 miles [402-404]. Adoption steadily grew with government grant incentives, improved battery and charging technology, and increased investment in national charging infrastructure. In the UK, pure battery EV car sales accounted for 16.6% of new car sales in 2022, surpassing diesel to become the second most popular powertrain [394].

With increasing mainstream adoption, the perceived value of a mass market product such as an innovative cement will improve, adding value to a project and reassurance against uncertainty. This cannot happen without standardisation and approval, such as the aforementioned European technical assessments which aid to introduce and regulate innovative products [198, 199]. Proven safety and reliability records are crucial for pragmatic adoption, followed by expert and operator familiarity which will aid in the adoption by the later majority. In the work of Giesekam et al. [405], when reviewing the opinions of leaders in the construction industry, highlighted points included concerns about high costs,

ineffective allocation of responsibility (such as in the case of the Grenfell disaster, section 5.5), security of supply, and the poor availability of data [405]. It was surmised that actions that could be taken to better address these concerns include more proactive engagement of industry along the supply chain, availability of whole life costing (considering the approximate average building life of 50 years), as well as more accommodating contract and tenders for low carbon material implementation [405-407].

When contemplating the introduction of new technology, a technology readiness assessment, also known as the technology readiness level (TRL) or innovation readiness level (IRL), is useful for the quick comprehension as to how ready a technology is to be implemented or quantifying it for comparison against another potential technological route [408]. The TRL was first developed by the National Aeronautics and Space Administration (NASA) in 1974 as a management system to assess technological maturity for their projects [409]. Since then, the defined scale has been adopted by many multidisciplinary industries across the globe [369, 410]. The scale operates like a ladder, where in order to move up and achieve a TRL, all of the current and preceding achievements must have been met [409, 411]. For example, both Hills et al. [368] and the IEA have made TRL assessments for CCS [368, 412].

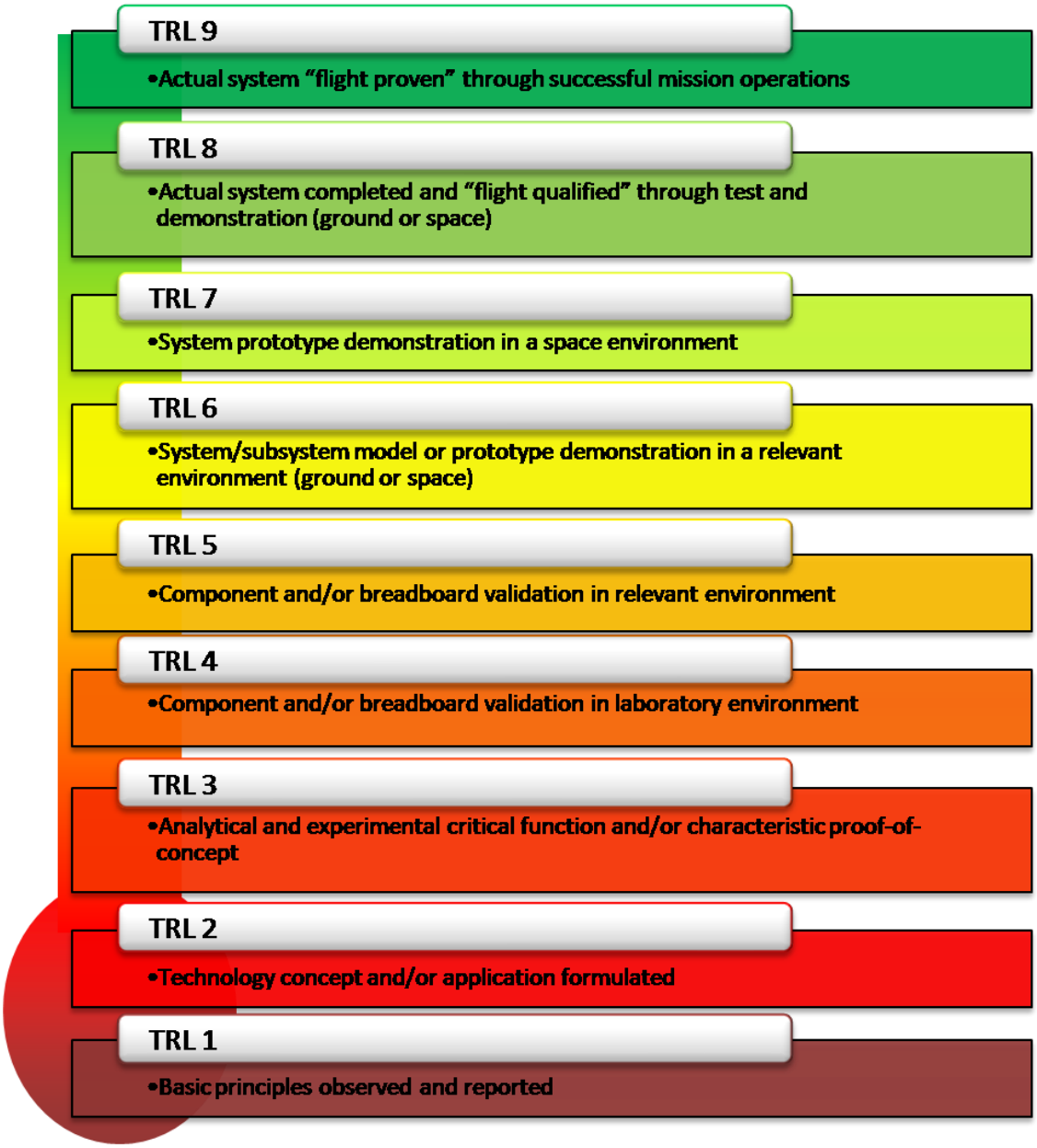

Figure 81: TRL assessment as adopted and used by NASA [409].

Table 13: TRL defined scale, based upon the descriptions by Hills et al. [368] which itself is based upon the NASA adopted scale [368, 409].

TRL	Description of Level Achievements
1	Basic principles observed and reported
2	Technology concept and/or application formulated
3	Analytical and experimental critical function and characteristic proof of concept
4	Component and system validation in a laboratory environment
5	Laboratory-scale similar-system validation in a relevant environment
6	Engineering and pilot-scale prototypical system demonstrated in a relevant environment
7	System prototype demonstrated in a plant environment
8	Actual system completed and qualified through test and demonstration in a plant environment
9	Actual system operated over the full range of expected conditions

Table 14: TRL evaluation conducted by Hills et al. [368] for a number of innovative carbon capture technologies [368].

CCS Technology	2015 TRL	2020 TRL (estimate)	Estimated Availability
Amine gas treating	5 - 6	6	2025
Calcium looping	5 - 6	7	2030
Full Oxy-fuelling	4	4	2035
Partial Oxy fuelling	6	6	2030
Direct Capture	4 - 5	7	2025

The IEA have adopted an 11 tier TRL to account for the greater levels of maturity that would help establish a novel technology such as CCS into conservative heavy industry [412]. The 2020 conclusions brought about from both studies yield very similar results, with a significant push still to go for full implementation within the next decade [368, 412].

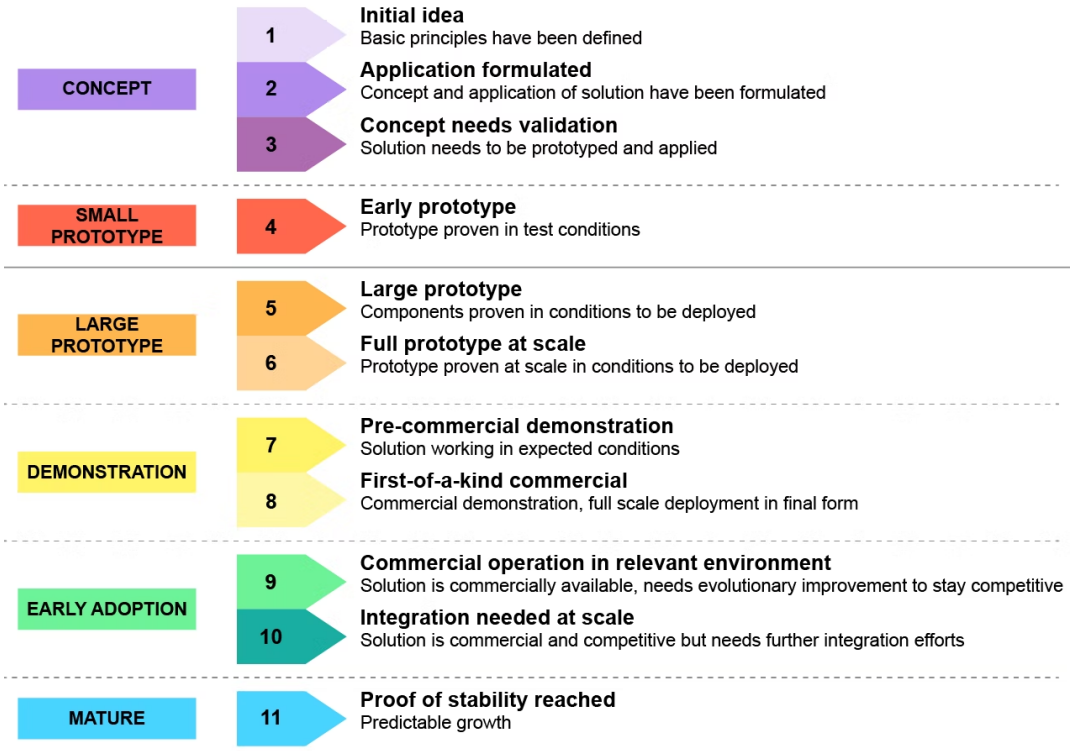

Figure 82: TRL scale adopted for use by the IEA, adapted to feature 11 different levels so as to account for greater levels of maturity demanded by conservative heavy industries [412].

Figure 83: Conclusions drawn by the IEA in 2020 for the progress and TRL of CCS technologies, utilising the 11 tier system defined in Figure 79 [412].

6. Future Directions

6.1. Introduction

Unlike many other areas of heavy industry throughout the UK and continental Europe, the cements industry has maintained its presence whilst largely consolidating to form a number of mega-corporations [29]. This is likely a combination of the uneconomical position for the import or export of PC across long distances, the excellent availability of raw materials locally, and as seen in Figure 73, the construction industry has remained a constant large-scale employer [9, 343]. With cement remaining a titan of industry within the UK and the EU, it has undoubtedly retained its expertise in the manufacturing of cement. When also bolstered by the cutting-edge research conducted by some of the top universities and institutions in the world, this puts the UK and the EU at the forefront of innovation with regards to adopting alternative binder cement technology.

In the following chapter, both CSA and metakaolin geopolymer systems are evaluated in terms their current technical maturity, industrial application and adoption, and their suitability as a future encapsulant for radioactive waste streams.

6.2. Calcium Sulfoaluminate

The CSA family of cements has enjoyed considerable interest during the past couple of decades, warranting European technical assessments (ETA) and notably large-scale implementation on the western coast of the United States [173, 198, 199]. Buzzi Unicem of Italy has submitted a number of European technical assessments, the first to be approved being ETA-13/0417 which granted it conformational CE marking upon a CSA product containing >45% ye'elimite content, which was again renewed in 2018 [389]. Similarly, historic French cement manufacturer Vicat achieved the approval of ETA-16/0850 for a similar >45% ye'elimite CSA cement in 2016 [199]. This is representative of the higher ye'elimite CSA cements being more mature than other types, having been developed first and used extensively in regions such as China as their third series cement [175]. The recognition of higher

ye'elimite CSA does, however, make it significantly easier for all other types of CSA to be adopted. In 2020, cement producer CTS from the USA secured ETA-19/0458 for a 58% belite CSA (BCSA) [198]. CTS has also succeeded in producing CSA products conforming to both ASTM C845 as an expansive additive for PC, and ASTM C1600 'Standard Specification for Rapid Hardening Hydraulic Cement' in the form of a BCSA [413, 414].

As stated by Harrison et al. [192] and Scrivener et al. [370], the main limiting factor for the mass adoption of CSA is the supply of alumina bearing raw material [192, 370]. Primarily this has been bauxite, which is a material in high demand for other applications including the production of aluminium metals [415, 416]. China is a region rich in alumina bearing material, and less so in limestone, which greatly encouraged the development and adoption of CSA in many applications [192]. In the context of global industry wide adoption, minimising the alumina content is a pathway which makes CSA a more viable option to many nations, potentially favouring the belitic branch of CSA cements [184]. BCSA has been shown to perform admirably in a range of operations where the characteristic properties of a CSA are advantageous and would not be considered inferior to higher ye'elimite content CSA cements in typical construction applications [185, 193, 417].

By lowing the alumina requirement in CSA, which for example according to Scrivener et al. [370] is approximately 16% Al_2O_3 in a belite ye'elimite ferrite system (BYF), the opportunity to employ low grades of alumina material, such as bauxite residues, red mud, and industrial waste materials increases, with options available to lower that amount further [176, 370, 418]. Currently, there is no clear and standardised distinction between BCSA and BYF, such as upon the ferrite (C_4AF) phase content. In the UK, during the mass adoption of HAC in the post WWII period, red mud and aluminium dross (slag type waste from the aluminium smelting process) were employed to achieve the required approximately 40% Al_2O_3 content during a period of bauxite shortage [284]. BCSA types therefore appear to be a promising avenue for the incorporation of alternative binders into the wider cements market, with a significant CO_2 saving and desirable characteristics for certain applications which may offset their higher price, which would help to encourage their adoption by conservative heavy industries [185, 187, 370, 419].

The UK nuclear industry wishes to consider employing CSA with a ye'elimite majority, to maximise the potential benefits for radioactive waste encapsulation [88]. Whilst the wider cements industry appears to be heading in the direction of more belitic CSA types, this is likely to remain to the benefit of other forms of CSA. As previously discussed, PC is certain to remain as the primary cementitious material in the 21st century, bolstered by SCMs, post-process CCS technologies when available, as well as alternative binders and additives [365]. CSA was originally developed as a PC additive, and with increasing familiarity with the CSA family of systems and the sustained dominance of PC, it would seem logical that higher ye'elimite CSA would remain in production to lower the attributed CO_2 of a PC based binder and incorporate advantageous CSA characteristic properties [182, 420]. In terms of the needs of the nuclear industry, a small but consistent supply of high-quality material is all that is required for encapsulation operations, which can likely be fulfilled by high ye'elimite CSA binders even if they are manufactured primarily as a PC addition.

There are, however, some further resistances to the wider adoption and availability of CSA. Firstly, as outlined in Table 9 (section 3.2.), the naming conventions of CSA binders has been inconsistent for many years, and yet still it can continue to be difficult to differentiate between, for example, CSA and BCSA in literature, as well as occasionally HAC [176]. The lack of a clear universal naming convention may confuse the more pragmatic or sceptical adopters of this technology. There is also a lack of general user guides, and easily accessible large scale experimental trials aimed at demonstrating the robustness of the material in an application (an area that this thesis aims to contribute to). Publications showcasing effective use are, inevitably, far more numerous and accessible for PC. The adoption of CSA, as well as all other alternative binder systems, could be undermined by CCS solutions if the industry decides to fully commit to CCS as the primary solution to achieve the reduced emission targets. There may be some resistance to adopting multiple means of addressing the problem, instead opting for a one-size-fits-all approach in an attempt to minimise disruption within the industry [421]. This is also a tactic used to delay change and keep a business as usual route, as demonstrated by thermal coal groups in the United States [383]. This rather drastic approach seems unlikely, as much of the international expertise

within the cement industry and associated research groups are well aware of the needs for a multifaceted approach to addressing such a serious issue as climate change [365, 373, 374].

The option of addressing some of the associated carbon emissions from cement manufacture by introducing CSA as an alternative binder option, does offer a number of advantages for the cements industry. The manufacturing of CSA is extremely similar to the process of manufacturing PC, allowing for infrastructure to be re-used and retrofitted with minimal investment [187, 191, 417, 422, 423]. Similarly, the handling and usage is also very similar to PC, or any other hydraulic binder, so that it can be implemented into a construction environment with a low training requirement and minimal changes to safety procedures [193].

The availability of CSA is steadily increasing, as is the national technical expertise and those familiar with the system, both peripherally and directly. Multiple European, American, and Asian suppliers are now offering CSA as part of their catalogue of cementitious materials [103]. Many of the characteristics of CSA are desirable for the nuclear industry, but the unique advantageous characteristics of CSA, namely the shrinkage compensation as well as its early strength, are admirable and unique selling points that can help justify its inclusion into the wider cements market [176]. The requirement to produce more sustainable building materials and reduce the cement industry's contribution to global greenhouse gas emissions also justify the position of introducing more sustainable alternative binder systems [373, 419].

The NDA estate uses a TRL scale similar to that adopted by NASA, using nine tiered levels in order to assess the maturity of a technology [409, 410]. Whilst the descriptions of these categories are specific to the implementation of technology into radioactive environments, to assess the TRL of these alternative binder systems the original system proposed by NASA shall be used, allowing for a degree of compatibility.

Table 15: TRL assessment for the CSA family of cements, as based upon the NASA criteria [409]

TRL	Justification
1	The CSA family of systems has achieved the proof-of-concept phase. The key hydration mechanisms are well understood, and the phase assemblage can be clearly defined and identified.
2	
3	
4	The CSA family of systems has also achieved the small-scale experimental phase. A large number of small-scale experiments have been undertaken, providing results that validate its progression into larger scale and real-world trials.
5	
6	
7	A number of real-world applications have now been completed successfully.
8	The material has received technical approval for both CSA and Belitic-CSA.
9	System is available commercially and is being applied commercially, although not widespread internationally as of yet.
TRL Verdict: 8 – 9 There is still some discussion in regard to the long-term performance of CSA, and whether it can be applied in structural applications, such as for pre-stressed beams similar to how HAC was employed in the mid-20th century. For that reason, the technology has not quite reached its full maturity as yet, but with interest having seemingly accelerated even during the timescale of this project, it would appear that this technology is likely to reach maturity.	

If accounting for the IEA 11 tier TRL, a level of between 8-9 is still appropriate as CSA has yet to achieve a secure commercial footing [412]. For this to be accomplished, the following need to be established on the international stage:

- A consistent nomenclature and definition of systems, such as what separates BYF from BCSA.
- Decisions need to be made as to whether CSA is going to be produced to conform to existing PC materials standards, such as BS EN 197-1, and compatible to experimental test standards such as ASTM G109 (Determining Effects of Chemical Admixtures on Corrosion of Embedded Steel Reinforcement in Concrete Exposed to Chloride Environments), or if standards have to

be modified and new standards created [86, 424]. The latter would allow for a better evaluation of the performance of CSA without tying it to the behaviour of PC, such as its much-improved chemical attack resistance, but requires significant legal work to establish.

- The commercial suppliers need to decide which systems are to be sold as a PC additive and which are to be sold as standalone systems.
- If a large-scale commercial product is finalised, such as a BCSA, how suitable are material supplies for a commercial expansion and how will it be priced against PC.

The mass adoption scale of a CSA is not paramount to its suitability of application in radioactive waste encapsulation, although this would likely benefit both its security of supply and its economic viability. A relatively low, but steady volume production, such as that seen currently with HAC, is appropriate for the powder quantities required for UK operations. This means that the UK nuclear industry has a choice between perusing the likely higher ye'elimite CSA additive for PC to compensate for shrinkage, or the potentially higher volume produced BCSA products if they are adopted by more international markets with a larger supply chain. CSA as an additive for what can be known as Type K cements seems likely to remain as a useful addition to the wide range of PC additives, a market that will increase as PC specifications are modified to comply with restriction upon associated carbon emissions. The result will be a material more expensive than PC, limited in terms of volume and price by the availability by the alumina bearing material that the manufacturer sources [182].

BCSA is potentially still subject to compositional change, as potential suppliers alter products to achieve the performance and economic viability desired. BCSA such as BYF and BCT (Table 9) could still be selected as the best option for mass market appeal, which in turn means that its price must remain attractive to large volume buyers. An increase in price compared to PC is justifiable if the product is a more niche, higher performance alternative to PC, but it must still remain competitive.

The choice between each system could be justified based upon their security of supply, merit of rheology, performance, and chemistry, as well as cost. A high ye'elimite content may increase the beneficial ettringite content, but a reduction may also be beneficial in lowering the heat of hydration.

Each system carries the benefits discussed previously in section 3.3, including that of reduced free water in the pore structure and a lower pH, which would both help reduce the corrosion rate of amphoteric metals, such as aluminium fuel cladding used in the Windscale Piles [74]. A type of CSA could prove to be a beneficial and viable alternative to PC, and if implemented effectively could allow for increased waste loading and therefore fewer waste packages.

6.3. Metakaolin Geopolymer

Geopolymers are a departure from traditional hydraulic binders. Whilst not as familiar to the cements industry as PC, or even CSA, geopolymer research and technology has made significant advances in the past couple of decades [136]. This departure from more conventional systems may allow for engineering problems to be addressed using a new perspective. The geopolymer system can allow for a degree of autonomy, allowing for unique regional materials such as industrial by-products or local aluminosilicate minerals to be utilised [14, 425, 426]. Whilst less of a concern for the UK and Europe, which host areas rich in limestone, this could be extremely beneficial in areas where this is not the case such as South Africa [9]. Metakaolin, the calcined form of kaolinite clay, is a material commonly used in the production of porcelain and to whiten paper [427]. Kaolin is widely available in the UK and Europe, with the UK mining 1.36 million dry tons of kaolinite clay (also known as China clay) as of 2008, down from a peak of 2.78 million dry tons in 1988, and with 88% of kaolin being exported in 2008 [139].

In 2012, an estimated 250,000 tons of metakaolin were reportedly produced, with more than half going in to the production of concrete primarily as a SCM [428, 429]. Metakaolin is typically expensive, estimated at around $300 per ton [139]. With a wide availability of precursors, the activating solution may have a greater impact upon the adoption of metakaolin geopolymers [430]. Turner & Collins [431] estimate that the production of sodium hydroxide leads to the release of 1.915 kg of CO_2 equivalent emissions per kg produced, and 1.514 kg of CO_2 equivalent emissions per kg for sodium silicate manufactured [431]. These are notable contributors to the overall emissions for a geopolymer, however

the true total emissions for a geopolymer system are entirely based upon the required alkali activator concentration, the precursor and any required precursor, allowing for considerable CO_2 reduction in comparison to PC [241, 432]. The alkali activating solutions made for laboratory experiments typically employ reagent grade materials, which are expensive but highly commercialised and obtainable.

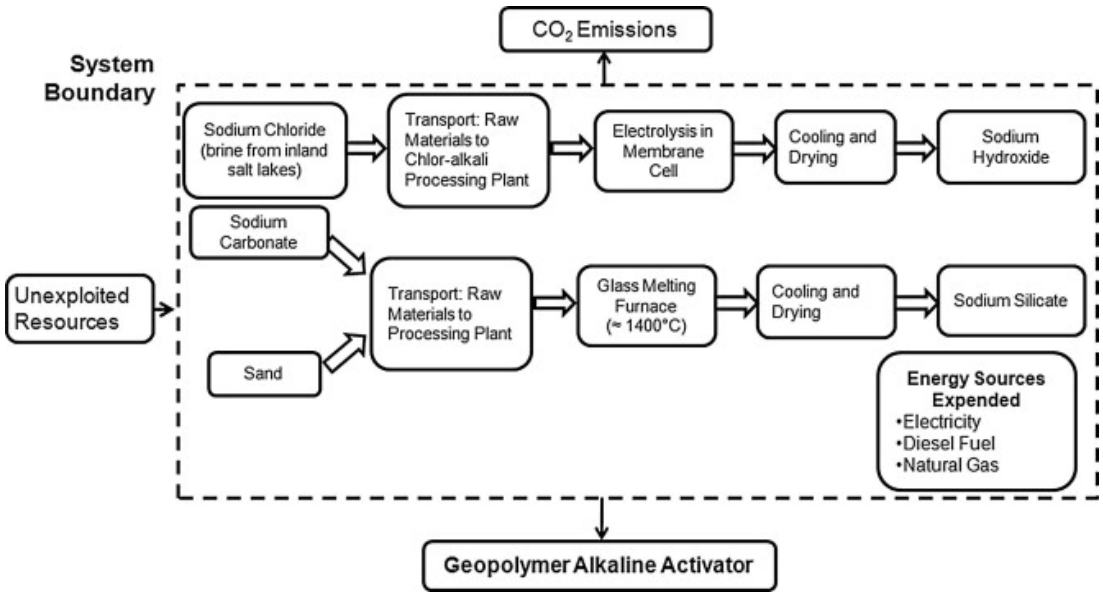

Figure 84: Illustration depicting the manufacturing processes for sodium hydroxide and sodium silicate, commonly used for the production of geopolymer alkali activator solutions, as depicted by Turner & Collins [431].

Material availability for the UK nuclear industry is therefore good. Geopolymer mixes also allow for complete control over the mix, as the alkali solution and precursor are sourced separately and the reactions occurring at the time of the mix, unlike PC where the material undergoes a clinkering process. The defining point will be the reactivity of the sourced metakaolin [146, 433, 434]. The on-site mixing does however present challenges in more typical construction environments, as the techniques for employing a geopolymer are significantly different to that of a typical hydraulic binder [134]. This is less of an issue in a controlled environment, such as in the production of pre-cast concrete elements or in nuclear waste immobilisation, but otherwise the activating solution presents a chemical hazard to its operators in a way unlike that in PC usage. The activating solution would require handling training, chemical storage facilities, and revised health and safety procedures to protect the workforce and the surrounding environment.

There is also a reduced awareness of alkali activated materials by more pragmatic or sceptical adopters, who would likely prefer more conventional solutions. This is not helped by confusion related to what is classed as an alkali activated material, or geopolymer, and the multitude of overlapping names that are highlighted in section 4.2 [14]. Understandably too, for a material that is the subject of so much active research, there is not nearly the wealth of knowledge and experience available when compared to most hydraulic binder systems. There is also a degree of hype behind elements of alkali activated material research. Geopolymers can be diversely produced to incorporate many potential excellent properties, however some publications can depict geopolymers as being able to simultaneously perform an extensive range of impressive properties, as opposed to being a material that can be designed to perform a select function much like a grade of steel is.It after all would be counterintuitive to publish research claiming that a newly developed cement is merely adequate or mediocre. Duxson et al. [136] gives a list of potential properties, including high compressive strength, low shrinkage, fast or slow setting, acid resistance, fire resistance, low thermal conductivity, but describes that although these properties may not be mutually exclusive, not all geopolymer formulations will benefit from high performance in every characteristic [136]. Whilst geopolymers are a more unconventional alternative binder system, the host of potential properties would be advantageous to the cements industry if it is willing to expand its range to accommodate more novel technologies.

The availability of the required materials for a geopolymer mix is good, and the UK and Europe are particularly well placed with abundant technological expertise, as well as research and development being conducted in the near vicinity [370]. If the industry does wish to take advantage of this diverse range of potential properties, then the geopolymer system will be desirable, especially if it can be used in an application that makes use of industrial by-products or overcomes a particularly challenging engineering problem, which in turn will justify its exploration and use [239, 241, 426]. Its potential to make use of waste products to produce a highly sustainable product is particularly compelling [241, 435]. The highly customisable performance will make introduction slower than other alternative binder systems, however if more of this class of materials begin to be adopted by the mass market, it will undoubtedly make it easier for the geopolymer system to be more widely adopted.

Table 16: TRL assessment for geopolymers, based upon the NASA criteria [409].

TRL	Justification
1	Key geopolymer formulations have achieved the proof-of-concept phase. The mechanisms behind their formation are increasingly better understood, and the phase assemblage can be clearly defined and identified.
2	
3	
4	Geopolymers have also proved capable at the small-scale experimental phase. A large number of small-scale experiments have now been undertaken, providing results that validate its progression into larger scale and real-world trials.
5	
6	
7	A number of real-world applications have now been completed successfully.
8	Recognition of AAM in standardisation is beginning to occur.
9	The materials required to produce geopolymers are commercially available.
TRL Verdict: 7 – 8 This diverse range of materials still requires some more time to mature, requiring a greater number of large-scale, real-world applications, and more experience when it comes to using geopolymers. All materials to produce geopolymers are available, and with the growing recognition and standardisation for AAM, geopolymers are likely to eventually be incorporated into that explored area. In terms of the requirements of the UK nuclear industry, the TRL is adequate for continued exploration, with the enhanced level of control and the availability of the required materials allowing for more direct control over its formulations.	

This level of between 7 – 8 is the same when accounting for the expanded TRL as used by the IEA [412]. Both the reactive metakaolin and the alkali activator are relative expensive materials when compared to the PC and BFS or PFA components currently employed by the UK nuclear industry. Unlike BFS and PFA however, metakaolin is not a waste material the production of which relies upon the separate operation of another heavy industrial process, offering a much greater security of supply. If another acceptable source of metakaolin is identified, such as a specification used for the production

of ceramics, the production of a metakaolin geopolymer for radioactive waste encapsulation purposes could be achieved separately from the cement and concrete industry. With the current interest in calcined clays as a supplementary cementitious material to lower associated carbon emissions, to source metakaolin from a large volume cementitious material supplier is likely to be the competitive and cost-effective route.

The unique phase composition and gelation chemistry may offer significant benefits for diverse radioactive waste streams, such as a highly modifiable system pH and the use of its closed porosity system to encapsulate oil-based wastes. If correctly baselined and understood, the control achievable over the formulation through the adjustment of the alkali activator of a geopolymer system might allow for the encapsulation of a greater variety of waste streams at higher waste loading than can currently be achieved. Whilst geopolymers and other AAM may take longer to become adopted into the cements industry, being far less well defined in both understanding and standardisation, the way in which geopolymer formulations work allows the nuclear industry a degree of autonomy not achievable with other cement systems.

7. Conclusion

In the preceding chapters, two extensive experimental procedures have been undertaken to evaluate two commercially available CSA and metakaolin geopolymer systems in the context of ILW encapsulation and implementation by the UK nuclear industry. Following this, a discussion was held on the conservative behaviour of heavy industries, such as those involved in construction and cement.

Although heavy industries are typically slow and somewhat resistant to change and the adoption of innovative technologies, throughout the duration of this project (2018 – 2023), there has been a noticeable acceleration in terms of climate change awareness, the willingness to adopt more unconventional solutions, and the quantity of exciting and forward-thinking publications in this area of research. To not take on the challenge of combating climate change with a multifaceted approach that also introduces a range of potential benefits, could prove to be a missed opportunity.

Even at their current low levels of adoption, both CSA and metakaolin geopolymers objectively appear to be in a position that supports the decision to explore these systems for radioactive waste encapsulation applications. Heightened industry interest and perception of these systems suggests that the availability of these systems will increase over the coming decades, offering an enhanced security of supply over materials produced by declining industries. Whilst Portland cement, in one form or another, will remain the dominant system throughout the 21st century, given the relatively small bulk volume requirement for cement for grout encapsulation purposes it is practicable to consider other systems that seem likely to remain commercially available. Chapters 2 and 3 have shown that both systems have produced acceptable wasteform products, which when combined with rheological and physical property data, will contribute significantly to setting a baseline expectation for what these systems can achieve and how they behave, strengthening their technological readiness for future consideration. As highlighted, a number of future considerations need to be made before these alternative binder systems can be adopted, however, the current industrial climate and the results of these experimental programs have shown that there may well be substantial benefits in the use of alternative binder systems, and an appetite to do so.

References

[1] Jacobs UK Ltd and AFRY Solutions UK Ltd, "2022 UK Radioactive Waste Detailed Data," in "2022 UK Radioactive Waste and Material Inventory," Nuclear Decomissioning Authority, 2022.

[2] G. V. Hutson, "Waste Treatment," in *The Nuclear Fuel Cycle from Ore to Wastes*, P. D. Wilson Ed. Oxford: Oxford University Press, 1996, ch. 9, pp. 161-183.

[3] Nuclear Decommissioning Authority, "Implementing Geological Disposal," 2014. [Online]. Available: https://assets.publishing.service.gov.uk/government/uploads/system/uploads/attachment/data/file/332890/GDF/White/Paper/FINAL.pdf

[4] Nuclear Decommissioning Authority, "LLWR Plan 2018-2023," 2018. [Online]. Available: https://www.gov.uk/government/publications/llwr-plan-2018-to-2023#:~:text=The%20LLWR%20Plan%20is%20a,costs%20and%20schedules%20for%20delivery.

[5] H. F. W. Taylor, "Portland Cement and its Major Constituent Phases," in *Cement chemistry*, 1997, ch. 1, pp. 1-28.

[6] J. Lehne and F. Preston, "Making Concrete Change - Innovation in Low-carbon cement and Concrete," in "Chatham House Report," Royal Institute of International Affairs, London, 9781784132729, 2018. [Online]. Available: www.chathamhouse.org

[7] A. Hasanbeigi, L. Price, and E. Lin, "Emerging energy-efficiency and CO_2 emission-reduction technologies for cement and concrete production: A technical review," *Renewable and Sustainable Energy Reviews*, vol. 16, no. 8, pp. 6220-6238, 2012, doi: 10.1016/j.rser.2012.07.019.

[8] C. Roskos, D. Cross, M. Berry, and J. Stephens, "Identification and Verification of Self-Cementing Fly Ash Binders for “Green” Concrete," presented at the World of Coal Ash Conference, Denver, CO, USA, 2011.

[9] P.-C. Aïtcin, *Binders for Durable and Sustainable Concrete*, 1st ed. London: CRC Press, 2007, p. 500.

[10] United States Census Bureau. "Population estimates and projections for 227 countries and areas." https://www.census.gov/data-tools/demo/idb/#/country?COUNTRY_YEAR=2022&COUNTRY_YR_ANIM=2022 (accessed 03/05, 2022).

[11] L. G. Mallinson and L. I. Davies, "A Historical Examination of Concrete," in "Nuclear Science and Technology," Commission of the European Communitie, 1987. [Online]. Available: https://op.europa.eu/en/publication-detail/-/publication/f0b7c189-37a4-4b45-9abe-cc13dfebb9ef

[12] A. P. Thurston, "Parker’s “Roman” Cement," *Transactions of the Newcomen Society*, vol. 19, no. 1, pp. 193-206, 2014, doi: 10.1179/tns.1938.013.

[13] D. Moore. "About Roman Cement." https://www.cementkilns.co.uk/roman.html (accessed 27/04, 2022).

[14] J. L. Provis and J. S. J. van Deventer, *Alkali Activated Materials - State of the Art Report*. Springer, 2014, p. 388.

[15] T. Easton. "Learning from Ancient Roman Concrete to Improve Modern Masonry." https://watershedmaterials.com/blog/2014/10/28/learning-from-ancient-roman-concrete-to-improve-modern-masonry (accessed 27/04, 2022).

[16] P. Duxson, J. L. Provis, G. C. Lukey, and J. S. J. van Deventer, "The role of inorganic polymer technology in the development of ‘green concrete’," *Cement and Concrete Research*, vol. 37, no. 12, pp. 1590-1597, 2007, doi: 10.1016/j.cemconres.2007.08.018.

[17] F. M. Lea and C. H. Desch, "The History of Calcareous Cements," in *The Chemistry of Cement and Concrete*, Second ed.: Edward Arnold Ltd, 1956, pp. 1-12.

[18] C. Stanley, *Highlights in the History of Concrete*, 1st ed. Cement and Concrete Association, 1979.

[19] International Energy Agency. "Cement." https://www.iea.org/reports/cement (accessed 17/03, 2023).
[20] United Nations, "World Urbanization Prospects: The 2018 Revision," 2018.
[21] Recons Group of Companies. "Cements Prices." http://www.reconsgroup.com/ (accessed 27/04, 2022).
[22] M. Garside. "Cement prices in the United States from 2010 to 2022." https://www.statista.com/statistics/219339/us-prices-of-cement/ (accessed.
[23] B&Q Ltd. "Blue Circle Multipurpose Cement, 25kg Bag." https://www.diy.com/departments/blue-circle-multipurpose-cement-25kg-bag/35715_BQ.prd (accessed 27/04, 2022).
[24] Mister Concrete. "Ready mix concrete prices." https://www.misterconcrete.co.uk/ready-mix-concrete-prices (accessed 27/04, 2022).
[25] Home Guides. "Your Guide To Concrete Prices." https://homeguides.co.uk/concrete/ (accessed 27/04, 2022).
[26] M. A. Helsel, C. F. Ferraris, and D. Bentz, "Comparative Study of Methods to Measure the Density of Cementitious Powders," National Institute of Standard and Technology, 2015. [Online]. Available: https://tsapps.nist.gov/publication/get_pdf.cfm?pub_id=917856#:~:text=The%20commonly%20assumed%20density%20of,is%20interground%20into%20the%20cement
[27] The European Cement Association. "Cement 101: Key Facts and Figures." https://cembureau.eu/cement-101/key-facts-figures/ (accessed 27/04, 2022).
[28] Pro Global Media Ltd, "Global Cement Top 100 Report 2017 - 2018," *Global Cement Magazine*, 2017. [Online]. Available: http://www.globalcement.com/magazine/articles/1054-global-cement-top-100-report-2017-2018.
[29] LafargeHolcim. "LafargeHolcim at a glance." https://www.lafargeholcim.com/lafargeholcim-at-a-glance (accessed 27/04, 2022).
[30] WHD Microanalysis Consultants Ltd. "Understanding Cement - Cement History." https://www.understanding-cement.com/history.html (accessed 27/04, 2022).
[31] D. Moore. "Cement Kilns: Hope." https://www.cementkilns.co.uk/cement_kiln_hope.html (accessed 27/04, 2022).
[32] Global Cement. "Adani Group to build two cement plants in Andhra Pradesh." Pro Global Media Ltd. https://www.globalcement.com/news/item/15424-adani-group-to-build-two-cement-plants-in-andhra-pradesh (accessed 08/03, 2023).
[33] A. Pahuja. "The Indian cement sector – technological status and prospects." National Council for Cement and Building Materials India. https://www.zkg.de/en/artikel/zkg_The_Indian_cement_sector_technological_status_and_prospects-2467959.html (accessed 08/03, 2023).
[34] Informa Plc. "Dual Process Cement Technology At J.K. Cement Works." https://www.concreteshowindia.com/blog/dual-process-cement-technology-at-j-k-cement-works/ (accessed 27/04, 2022).
[35] Institution of Civil Engineers. "Calder Hall nuclear power station." https://www.ice.org.uk/what-is-civil-engineering/what-do-civil-engineers-do/calder-hall-nuclear-power-station (accessed 27/04, 2022).
[36] J. Morrissey. "Obninsk Nuclear Power Plant." http://large.stanford.edu/courses/2015/ph241/morrissey2/ (accessed 27/04, 2022).
[37] World Nuclear Association. "Nuclear Power in the United Kingdom." http://www.world-nuclear.org/information-library/country-profiles/countries-t-z/united-kingdom.aspx (accessed 27/04, 2022).
[38] Nuclear Engineering International. (2013) The Magnox life extension story. *Nuclear Engineering International*. Available: https://www.neimagazine.com/features/featurethe-magnox-life-extension-story/#:~:text=HS%3A%20Absolutely%3B%20Magnox%20had%20a,that%20go%20well%20beyond%20life.
[39] P. Lobner. "Farewell Magnox: 1956 – 2015." https://lynceans.org/all-posts/farewell-magnox-1956-2015/ (accessed 10/06, 2022).

[40] World Nuclear Association. "Nuclear Development in the United Kingdom." http://www.world-nuclear.org/information-library/country-profiles/countries-t-z/appendices/nuclear-development-in-the-united-kingdom.aspx (accessed 27/04, 2022).
[41] S. Fetter. "How long will the world's uranium supplies last?" https://www.scientificamerican.com/article/how-long-will-global-uranium-deposits-last/ (accessed 27/04, 2022).
[42] World Nuclear Association. "Supply of Uranium." http://www.world-nuclear.org/information-library/nuclear-fuel-cycle/uranium-resources/supply-of-uranium.aspx (accessed 27/04, 2022).
[43] G. R. Plumb, "Review of developments in U.K. commercial reprocessing," *Progress in Nuclear Energy*, vol. 13, no. 1, pp. 3-18, 1984, doi: 10.1016/0149-1970(84)90003-9.
[44] S. E. Jensen and P. L. Olgaard, "Description of the Prototype Fast Reactor at Dounreay," 87-550-2265-0, 1995. [Online]. Available: https://inis.iaea.org/collection/NCLCollectionStore/_Public/28/026/28026107.pdf
[45] K. Hesketh, R. Gregg, G. Butler, and A. Worrall, "Key conclusions from UK strategic assessment studies of fast reactor fuel cycles," *Annals of Nuclear Energy*, vol. 110, pp. 330-337, 2017, doi: 10.1016/j.anucene.2017.06.053.
[46] A. N. Laboratory. "Closing the Nuclear Fuel Cycle." https://www.ne.anl.gov/nce/closing-nuclear-cycle/ (accessed 27/04, 2022).
[47] World Nuclear Association. "Fast Neutron Reactors." http://www.world-nuclear.org/information-library/current-and-future-generation/fast-neutron-reactors.aspx (accessed 27/04, 2022).
[48] Nuclear Decommissioning Authority. "What is Reprocessing?" https://nda.blog.gov.uk/2018/10/23/what-is-reprocessing/ (accessed 27/04, 2022).
[49] UK Radioactive Wase Inventory. "How is radioactive waste produced?" https://ukinventory.nda.gov.uk/about-radioactive-waste/how-is-radioactive-waste-produced/ (accessed 10/06, 2022).
[50] Nuclear Decommissioning Authority and E. I. S. Department of Business, "UK Radioactive Waste Inventory," 2019.
[51] la Repubblica. "Popular referendum 12-13 June 2011." https://www.repubblica.it/elezioni/2011/referendum/mondo.html#risultati (accessed 27/04, 2022).
[52] World Nuclear Association. "Nuclear Energy in Denmark." https://world-nuclear.org/information-library/country-profiles/countries-a-f/denmark.aspx (accessed.
[53] Nuclear Energy Agency, "Nuclear Legislation in OECD and NEA Countries - Ireland," 2009.
[54] The Economist. "A Nuclear Disaster That Brought Down an Empire." https://www.economist.com/europe/2016/04/26/a-nuclear-disaster-that-brought-down-an-empire (accessed 27/04, 2022).
[55] S. Taylor, *The Fall and Rise of Nuclear Power in Britain*, 1st ed. Cambridge: UIT Cambridge, 2016, p. 245.
[56] E. I. S. Department of Business. "Nuclear energy: What you need to know." https://www.gov.uk/government/news/nuclear-energy-what-you-need-to-know#:~:text=EDF%20are%20the%20lead%20investor,potential%20project%20in%20the%20UK. (accessed 10/06, 2022).
[57] Rolls-Royce Plc, "UK SMR: A National Endeavour," 2018. [Online]. Available: https://www.rolls-royce.com/~/media/Files/R/Rolls-Royce/documents/customers/nuclear/a-national-endeavour.pdf
[58] Sellafield Ltd. "New era at Sellafield as Thorp reprocessing ends." https://www.gov.uk/government/news/new-era-at-sellafield-as-thorp-reprocessing-ends (accessed 28/10, 2023).
[59] Sellafield Ltd. "Magnox Reprocessing plant achieves final milestone." https://www.gov.uk/government/news/magnox-reprocessing-plant-achieves-final-milestone (accessed 28/10, 2023).
[60] Nuclear Decommissioning Authority. "How do we manage radioactive waste?" https://ukinventory.nda.gov.uk/about-radioactive-waste/how-do-we-manage-radioactive-waste/ (accessed 20/01, 2022).

[61] Nuclear Decommissioning Authority. "What are the main waste categories?" https://ukinventory.nda.gov.uk/about-radioactive-waste/what-is-radioactivity/what-are-the-main-waste-categories/ (accessed 20/01, 2022).
[62] Radioactive Waste Management. "Why Underground?" https://www.gov.uk/guidance/why-underground (accessed 27/04, 2022).
[63] D. P. Prentice, B. Walkley, S. A. Bernal, M. Bankhead, M. Hayes, and J. L. Provis, "Thermodynamic modelling of BFS-PC cements under temperature conditions relevant to the geological disposal of nuclear wastes," *Cement and Concrete Research*, vol. 119, pp. 21-35, 2019, doi: 10.1016/j.cemconres.2019.02.005.
[64] Nuclear Waste Services, "Community Guidance: How we will work with communities in England," in "Geological Disposal Facility," 2022.
[65] Nuclear waste Services. "National Geological Screening for a GDF - Northern Ireland region." https://www.gov.uk/guidance/northern-ireland-sub-region-2 (accessed 23/01, 2023).
[66] Department of Business Energy & Industrial Strategy, "Implementing Geological Disposal – Working with communities," 2018.
[67] A. Jasi. "UK Relaunches Search for a GDF Site." https://www.thechemicalengineer.com/news/uk-relaunches-search-for-a-gdf-site/ (accessed 27/04, 2022).
[68] G. Cavanagh. "Seismic testing completed in Irish Sea as GDF process rolls-on." https://www.newsandstar.co.uk/news/20848107.seismic-testing-completed-irish-sea-gdf-process-rolls-on/ (accessed 23/01, 2023).
[69] Enviroment Agency. "Regulatory scrutiny and engagement for geological disposal: annual report 2021 to 2022." https://www.gov.uk/government/publications/geological-disposal-scrutiny-of-rwms-work-annual-reports/regulatory-scrutiny-and-engagement-for-geological-disposal-annual-report-2021-to-2022 (accessed 23/01, 2023).
[70] N. B. Milestone, "Reactions in cement encapsulated nuclear wastes: need for toolbox of different cement types," *Advances in Applied Ceramics*, vol. 105, no. 1, pp. 13-20, 2006, doi: 10.1179/174367606x81678.
[71] E. Duque-Redondo, K. Yamada, and H. Manzano, "Cs retention and diffusion in C-S-H at different Ca/Si ratio," *Cement and Concrete Research*, vol. 140, 2021, doi: 10.1016/j.cemconres.2020.106294.
[72] F. P. Glasser and L. Zhang, "High-performance cement matrices based on calcium sulfoaluminate–belite compositions," *Cement and Concrete Research*, vol. 31, pp. 1881-1886, 2001.
[73] V. Häußler *et al.*, "Uptake of actinides by calcium silicate hydrate (C-S-H) phases," *Applied Geochemistry*, vol. 98, pp. 426-434, 2018, doi: 10.1016/j.apgeochem.2018.08.021.
[74] M. I. Ojovan, "Immobilisation of Radioactive Waste in Cement," in *An Introduction to Radioactive Waste Immobilisation*, 2005, ch. 15, pp. 220-225.
[75] F. P. Glasser, "Cements in Radioactive Waste Disposal," University of Aberdeen, 2013.
[76] D. Geddes, S. Bernal, M. Hayes, and J. Provis, "Gamma Irradiation of geopolymers at early age," presented at the 15th International Congress on the Chemistry of Cement, 2019.
[77] B. Biwer, D. Ma, Y. Xi, and Y. Jing, "Review of Radiation-Induced Concrete Degradation and Potential Implications for Structures Exposed to High Long-Term Radiation Levels in Nuclear Power Plants," United States Nuclear Regulatory Comission,, NUREG/CR-7280, 2021.
[78] H. K. Hilsdorf, J. Kropp, and H. J. Koch, "The Effects of Nuclear Radiation on the Mechanical Properties of Concrete," 2016. [Online]. Available: http://large.stanford.edu/courses/2015/ph241/anzelmo1/docs/hilsdorf.pdf
[79] F. M. Lea and C. H. Desch, "Some Special Cements and Cement Properties," in *The Chemistry of Cement and Concrete*, F. M. Lea Ed., Second ed. London: Edward Arnold Ltd, 1956, ch. 17, pp. 461-482.
[80] S. Kearney, B. Walkley, C. Corkhill, and J. Provis, "Radiation damage effects in cementitious grouts used for nuclear waste disposal in the UK," presented at the 15th International Congress on the Chemistry of Cement, 2019.

[81] M. J. Angus, I. H. Godfrey, M. Hayes, and S. Foster, "Managing Change in the Supply of Cement Powders for Radioactive Waste Encapsulation – Twenty Years of Operational Experience," presented at the Waste Management Symposium, Pheonix, Arizona, 2010.
[82] R. A. Sanderson, "Optimising Blends of Blast Furnace Slag for the Immobilisation of Nuclear Waste," March, 2019.
[83] Nuclear Decommissioning Authority, "Waste Package Specifiaction and Guidance Documentation," 2008.
[84] S. Kearney, "Radiolysis and radiation damage effects in cements used in nuclear waste storage and disposal in the UK," Doctor of Philosophy, Materials Science and Engineering, The University of Sheffield, Sheffield, 2020.
[85] F. M. Lea and C. H. Desch, "Cements Made from Blastfurnace Slag," in *The Chemistry of Cement and Concrete*, vol. 2, Second ed., 1956, ch. 15, pp. 397-425.
[86] *BS EN 197-1:2011*, British Standards Institution, London, 2011.
[87] H. F. W. Taylor, "Composite Cements," in *Cement Chemistry*, 2 ed., 1997, ch. 9, pp. 261-294.
[88] Q. Zhou, N. B. Milestone, and M. Hayes, "An Alternative to Portland Cement for Waste Encapsulation -the Calcium Sulfoaluminate Cement System," *Journal of Hazardous Materials*, vol. 136, no. 1, pp. 120 - 129, 2006, doi: 10.1016/j.jhazmat.2005.11.038.
[89] M. Moranville-Regourd, "Cements Made From Blastfurnace Slag," in *Lea's Chemistry of Cement and Concrete*, P. C. Hewlett and M. Liska Eds., Fifth ed.: Butterworth-Heinemann, 1998, ch. 11, pp. 637-678.
[90] M. J. Angus, "The Specification of Cement Powders for Waste Encapsulation Processes at Sellafield site," NUWCEM, 2011.
[91] R. A. Sanderson, "Optimising Blends of Blast Furnace Slag for the Immobilisation of Nuclear Waste," Department of Materials Science and Engineering, The University of Sheffield, 2019.
[92] M. Ojovan and W. Lee, *An Introduction to Nuclear Waste Immobilisation*. Elsevier, 2014.
[93] E. Ofer-Rozovsky *et al.*, "Cesium immobilization in nitrate-bearing metakaolin-based geopolymers," *Journal of Nuclear Materials*, vol. 514, pp. 247-254, 2019, doi: 10.1016/j.jnucmat.2018.11.003.
[94] F. M. Lea and C. H. Desch, "The Raw Materials and Processes of Manufacture of Portland Cement," in *The Chemistry of Cement and Concrete*, Second ed.: Edward Arnold Ltd, 1956, ch. 3, pp. 22-31.
[95] H. F. W. Taylor, "The Chemistry of Portland Cement Manufacture," in *Cement chemistry*, 1997, ch. 3, pp. 55-87.
[96] E. Gartner, "Are there any practical alternatives to the manufacture of portland cement clinker?," *Journal of The Chinese Ceramic Society*, vol. 40, 2011.
[97] D. Zheng, M. Monasterio, W. Feng, W. Tang, H. Cui, and Z. Dong, "Hydration Characteristics of Tricalcium Aluminate in the Presence of Nano-Silica," *Nanomaterials (Basel)*, vol. 11, no. 1, Jan 14 2021, doi: 10.3390/nano11010199.
[98] J. W. Bullard *et al.*, "Mechanisms of cement hydration," *Cement and Concrete Research*, vol. 41, no. 12, pp. 1208-1223, 2011, doi: 10.1016/j.cemconres.2010.09.011.
[99] P. K. Mehta and P. J. M. Monteiro, "Hydraulic Cements," in *Concrete - Microstructure, Properties and Materials*, 2001, ch. 6, pp. 91-106.
[100] MIT Concrete Sustainability Hub, "Improving Concrete Sustainability Through Alite and Belite Reactivity," 2013.
[101] P. K. Mehta and P. J. M. Monteiro, "Durability," in *Concrete - Microstructure, Properties and Materials*, 2001, ch. 5, pp. 61-90.
[102] A. Ouzia and K. Scrivener, "Old textbooks are outdated about cement hydration mechanisms – The needle model, the main hydration peak and the later ages," presented at the 15th International Congress on the Chemistry of Cement, 2019.
[103] M. G. Maté, "Processing and characterisation of calcium sulphoaluminate (CSA) eco-cements with tailored performances," Departamento Química Inorgánica, Cristalografía, Mineralogía, Universidad de Málaga, 2014.
[104] I. Bolaños-Vásquez, R. Trauchessec, J. I. Tobón, and A. Lecomte, "Influence of the ye'elimite/anhydrite ratio on PC-CSA hybrid cements," *Materials Today Communications*, vol. 22, 2020, doi: 10.1016/j.mtcomm.2019.100778.

[105] F. Winnefeld and B. Lothenbach, "Hydration of calcium sulfoaluminate cements — Experimental findings and thermodynamic modelling," *Cement and Concrete Research,* vol. 40, no. 8, pp. 1239-1247, 2010, doi: 10.1016/j.cemconres.2009.08.014.
[106] L. G. Baquerizo, T. Matschei, and K. L. Scrivener, "Impact of water activity on the stability of ettringite," *Cement and Concrete Research,* vol. 79, pp. 31-44, 2016, doi: 10.1016/j.cemconres.2015.07.008.
[107] M. L. D. Gougar, B. E. Scheetz, and D. M. Roy, "Ettringite and C-S-H Portland Cement Phases for Waste Ion Immobilisation: A Review," *Waste Management,* vol. 16, no. 4, pp. 295 - 303, 1996.
[108] A. M. Cody, H. Lee, R. D. Cody, and P. G. Spry, "The effects of chemical environment on the nucleation, growth, and stability of ettringite [Ca3Al(OH)6]2(SO4)3·26H2O," *Cement and Concrete Research,* vol. 34, no. 5, pp. 869-881, 2004, doi: 10.1016/j.cemconres.2003.10.023.
[109] S. Nie and J. Skibsted, "Characterization of Monochromate and Hemichromate AFm Phases and Chromate-Containing Ettringite by 1H, 27Al, and 53Cr MAS NMR Spectroscopy," *Minerals,* vol. 12, no. 3, 2022, doi: 10.3390/min12030371.
[110] W. Lan and F. P. Glasser, "Hydration of calcium sulphoaluminate cements," *Advances in Cement Research,* vol. 8, no. 31, pp. 127-134, 1996, doi: 10.1680/adcr.1996.8.31.127.
[111] Q. Zhou and F. P. Glasser, "Thermal stability and decomposition mechanisms of ettringite at < 120°C," *Cement and Concrete Research,* vol. 31, pp. 1333–1339, 2001.
[112] Q. Zhou, E. E. Lachowski, and F. P. Glasser, "Metaettringite, a decomposition product of ettringite," *Cement and Concrete Research,* vol. 34, no. 4, pp. 703-710, 2004, doi: 10.1016/j.cemconres.2003.10.027.
[113] K. Ndiaye, M. Cyr, and S. Ginestet, "Durability and stability of an ettringite-based material for thermal energy storage at low temperature," *Cement and Concrete Research,* vol. 99, pp. 106-115, 2017, doi: 10.1016/j.cemconres.2017.05.001.
[114] S. Ghazizadeh, T. Hanein, J. L. Provis, and T. Matschei, "Estimation of standard molar entropy of cement hydrates and clinker minerals," *Cement and Concrete Research,* vol. 136, 2020, doi: 10.1016/j.cemconres.2020.106188.
[115] J. Kaufmann, F. Winnefeld, and B. Lothenbach, "Stability of ettringite in CSA cement at elevated temperatures," *Advances in Cement Research,* vol. 28, no. 4, pp. 251-261, 2016, doi: 10.1680/jadcr.15.00029.
[116] Y. Shimada and J. F. Young, "Thermal stability of ettringite in alkaline solutions at 80 °C," *Cement and Concrete Research,* vol. 34, no. 12, pp. 2261-2268, 2004, doi: 10.1016/j.cemconres.2004.04.008.
[117] D. Damidot and F. P. Glasser, "Thermodynamic investigation of the CaO Al2O3 CaSO4 H2O system at 50°C and 85°C," *Cement and Concrete Research,* vol. 22, no. 6, pp. 1179-1191, 1992, doi: 10.1016/0008-8846(92)90047.
[118] H. F. W. Taylor, C. Famy, and K. L. Scrivener, "Delayed ettringite formation," *Cement and Concrete Research,* vol. 31, no. 5, pp. 683-693, 2001, doi: 10.1016/s0008-8846(01)00466-5.
[119] J. Bizzozero, C. Gosselin, and K. L. Scrivener, "Expansion mechanisms in calcium aluminate and sulfoaluminate systems with calcium sulfate," *Cement and Concrete Research,* vol. 56, pp. 190-202, 2014, doi: 10.1016/j.cemconres.2013.11.011.
[120] A. Jiménez and M. Prieto, "Thermal Stability of Ettringite Exposed to Atmosphere: Implications for the Uptake of Harmful Ions by Cement," *Environmental Science & Technology,* vol. 49, no. 13, pp. 7957-7964, 2015, doi: 10.1021/acs.est.5b00536.
[121] Y. Lou, Z. Ye, S. Wang, S. Liu, and X. Cheng, "Influence of synthesis methods on ettringite dehydration," *Journal of Thermal Analysis and Calorimetry,* vol. 135, no. 4, pp. 2031-2038, 2018, doi: 10.1007/s10973-018-7391-8.
[122] P. W. Brown and J. V. Bothe, "The stability of ettringite," *Advances in Cements Research,* vol. 5, no. 18, pp. 47 - 63, 1993.
[123] L. U. D. Tambara, M. Cheriaf, J. C. Rocha, A. Palomo, and A. Fernández-Jiménez, "Effect of alkalis content on calcium sulfoaluminate (CSA) cement hydration," *Cement and Concrete Research,* vol. 128, 2020, doi: 10.1016/j.cemconres.2019.105953.

[124] I. Santacruz *et al.*, "Structure of stratlingite and effect of hydration methodology on microstructure," *Advances in Cement Research*, vol. 28, no. 1, pp. 13-22, 2016, doi: 10.1680/adcr.14.00104.
[125] E. Bescher and J. Kim, "Belitic Calcium Sulfoaluminate Cement: History, Chemistry, Performance, and Use in the United States," presented at the 1st International conference on innovation in low-carbon cement & concrete technology, 2019.
[126] J. Aupoil, J.-B. Champenois, J.-B. d'Espinose de Lacaillerie, and A. Poulesquen, "Interplay between silicate and hydroxide ions during geopolymerization," *Cement and Concrete Research*, vol. 115, pp. 426-432, 2019, doi: 10.1016/j.cemconres.2018.09.012.
[127] A. Cadix and S. James, "Chapter 5 - Cementing additives," in *Fluid Chemistry, Drilling and Completion*: Gulf Professional Publishing, 2022, pp. 187-254.
[128] A. Buchwald, C. Kaps, and M. Hohmann, "Alkali-activated binders and pozzolan cement binders – compete binder reaction or two sides of the same story?," in *11th International Conference on the Chemistry of Cement*, Durban, South Africa, 2003, pp. 1238-1246.
[129] N. Ranjbar, C. Kuenzel, J. Spangenberg, and M. Mehrali, "Hardening evolution of geopolymers from setting to equilibrium: A review," *Cement and Concrete Composites*, vol. 114, 2020, doi: 10.1016/j.cemconcomp.2020.103729.
[130] The Hudson Institute of Mineralogy. "Tobermorite." The Hudson Institute of Mineralogy. https://www.mindat.org/min-3985.html (accessed 10/10, 2022).
[131] J. L. Provis and S. A. Bernal, "Geopolymers and Related Alkali-Activated Materials," *Annual Review of Materials Research*, vol. 44, no. 1, pp. 299-327, 2014, doi: 10.1146/annurev-matsci-070813-113515.
[132] R. J. Myers, S. A. Bernal, and J. L. Provis, "A thermodynamic model for C-(N-)A-S-H gel: CNASH_ss. Derivation and validation," *Cement and Concrete Research*, vol. 66, pp. 27-47, 2014, doi: 10.1016/j.cemconres.2014.07.005.
[133] R. J. Myers, S. A. Bernal, R. San Nicolas, and J. L. Provis, "Generalized structural description of calcium-sodium aluminosilicate hydrate gels: the cross-linked substituted tobermorite model," *Langmuir*, vol. 29, no. 17, pp. 5294-306, Apr 30 2013, doi: 10.1021/la4000473.
[134] J. L. Provis, A. Palomo, and C. Shi, "Advances in understanding alkali-activated materials," *Cement and Concrete Research*, vol. 78, pp. 110-125, 2015, doi: 10.1016/j.cemconres.2015.04.013.
[135] B. Walkley, S. J. Page, G. J. Rees, J. V. Hanna, and J. L. Provis, "Nanostructural development of biphasic C-(N)-A-S-H/N-A-S-H gels in synthetic alkali-activated materials revealed by multinuclear MQMAS solid state NMR," presented at the 15th International Congress on the Chemistry of Cement, 2019.
[136] P. Duxson, A. Fernández-Jiménez, J. L. Provis, G. C. Lukey, A. Palomo, and J. S. J. van Deventer, "Geopolymer technology: the current state of the art," *Journal of Materials Science*, vol. 42, no. 9, pp. 2917-2933, 2006, doi: 10.1007/s10853-006-0637-z.
[137] A. Fernández-Jiménez and A. Palomo, "Mid-infrared spectroscopic studies of alkali-activated fly ash structure," *Microporous and Mesoporous Materials*, vol. 86, no. 1-3, pp. 207-214, 2005, doi: 10.1016/j.micromeso.2005.05.057.
[138] J. L. Provis, G. C. Lukey, and J. S. J. van Deventer, "Do Geopolymers Actually Contain Nanocrystalline Zeolites? A Reexamination of Existing Result," *Chemistry of Materials*, vol. 17, no. 12, pp. 3075-3085, 2005.
[139] F. Hart. (2017) A hard sell? Metakaolin in highperformance concrete. *Industrial Minerals*.
[140] D. Geddes, "A study of the suitability of metakaolin–based geopolymers for the immobilisation of problematic intermediate level waste," Doctor of Philosophy, Materials Science and Engineering, The University of Sheffield, Sheffield, 2020.
[141] IMCD Deutschland, "MetaMax - Typical Physical and Chemical Data," IMCD Deutschland GmbH & Co. KG, 2015.
[142] Argeco Development, "Argicem® - fiche technique produit," 2016.
[143] C. Kuenzel *et al.*, "Encapsulation of aluminium in geopolymers produced from metakaolin," *Journal of Nuclear Materials*, vol. 447, no. 1-3, pp. 208-214, 2014, doi: 10.1016/j.jnucmat.2014.01.015.

[144] M. Lizcano, H. S. Kim, S. Basu, and M. Radovic, "Mechanical properties of sodium and potassium activated metakaolin-based geopolymers," *Journal of Materials Science*, journal article vol. 47, no. 6, pp. 2607-2616, 2012, doi: 10.1007/s10853-011-6085-4.
[145] M. A. Longhi, E. D. Rodríguez, B. Walkley, Z. Zhang, and A. P. Kirchheim, "Metakaolin-based geopolymers: Relation between formulation, physicochemical properties and efflorescence formation," *Composites Part B: Engineering*, vol. 182, 2020, doi: 10.1016/j.compositesb.2019.107671.
[146] C. P. Ralph Davidovits, Joseph Davidovits, "Standardized Method in Testing Commercial Metakaolins for Geopolymer Formulations," in "Technical Paper #26-MK-testing," Geopolymer Institute Library, 2019.
[147] M. Antoni, "Investigation of Cement Substitution by Blends of Calcined Clays and Limestone," Docteur Ès Sciences, Ecole Polytechnique Fédérale de Lausanne, 2013.
[148] S. Nelson *et al.*, "Hydrate assemblage stability of calcium sulfoaluminate-belite cements with varying sulfate content," *Construction and Building Materials*, vol. 383, 2023, doi: 10.1016/j.conbuildmat.2023.131358.
[149] F. Winnefeld, A. Schöler, and B. Lothenbach, "Sample preparation," in *A Practical Guide to Microstructural Analysis of Cementitious Materials*, K. Scrivener, R. Snellings, and B. Lothenbach Eds., 1 ed. London: CRC Press, 2016, ch. 1, pp. 1-36.
[150] A. Altomare *et al.*, "The Rietveld Refinement in the EXPO Software: A Powerful Tool at the End of the Elaborate Crystal Structure Solution Pathway," *Crystals*, no. Rietveld Refinement in the Characterization of Crystalline Materials, pp. 12-29, 2018.
[151] Y. Jeong, C. W. Hargis, S.-C. Chun, and J. Moon, "The effect of water and gypsum content on strätlingite formation in calcium sulfoaluminate-belite cement pastes," *Construction and Building Materials*, vol. 166, pp. 712-722, 2018, doi: 10.1016/j.conbuildmat.2018.01.153.
[152] Ian. C. Madsen and N. V. Scarlett, "Quantitative Phase Analysis," in *Powder Diffraction Theory and Practise*, Robert. E. Dinnebier and S. J. L. Billinge Eds., 1st ed. Cambridge UK: Royal Society of Chemistry, 2008, ch. 11, pp. 298-332.
[153] F. Goetz-Neunhoeffer and J. Neubauer, "Refined ettringite (Ca6Al2(SO4)3(OH)12·26H2O) structure for quantitative X-ray diffraction analysis," *Powder Diffraction*, vol. 21, no. 1, pp. 4-11, 2006, doi: 10.1154/1.2146207.
[154] H. Saalfeld and M. Wedde, "Refinement of the crystal structure of gibbsite, A1(OH)3," *Zeitschrift für Kristallographie - Crystalline Materials*, vol. 139, no. 1-6, pp. 129-135, 1974, doi: doi:10.1524/zkri.1974.139.16.129.
[155] R. Allmann, "Refinement of the hybrid layer structure [Ca2Al(OH)6]+*[1/2SO4*3H2O]," *Journal of Mineralogy and Geochemistry*, pp. 136-144, 1977.
[156] Y. Dai and J. Post, "Crystal structure of hillebrandite: A natural analogue of calcium silicate hydrate (CSH) phases in Portland cement," *American Mineralogist*, vol. 80, 1995.
[157] N. J. Calos, C. H. L. Kennard, A. K. Whittaker, and R. L. Davis, "Structure of calcium aluminate sulfate Ca4 Al6 O16 S," *Journal of Solid State Chemistry*, vol. 119, pp. 1-7, 1995.
[158] A. Kirfel and G. Will, "Charge density in anhydrite, CaSO4, from X-ray and neutron diffraction measurements," *Acta Crystallographica Section B*, vol. 36, no. 12, pp. 2881-2890, 1980, doi: doi:10.1107/S0567740880010461.
[159] T. Fukami, S. Tahara, K. Nakasone, and C. Yasuda, "Synthesis, Crystal Structure, and Thermal Properties of CaSO4·2H2O Single Crystals," *International Journal of Chemistry*, vol. 7, no. 2, 2015, doi: 10.5539/ijc.v7n2p12.
[160] W. G. Mumme, R. J. Hill, G. Bushnellwye, and E. R. Segnit, "Rietveld crystal structure refinements, crystal chemistry and calculated powder diffraction data for the polymorphs of dicalcium silicate and related phases," (in English), *Neues Jahrbuch für Mineralogie - Abhandlungen*, vol. 169, no. 1, pp. 35-68, APR 1995.
[161] H. Petch, "The hydrogen positions in portlandite, Ca(OH)2, as indicated by the electron distribution," *Acta Crystallographica*, vol. 14, no. 9, pp. 950-957, 1961, doi: 10.1107/S0365110X61002771.
[162] M. Bellotto, M. C. Dalconi, S. Contessi, E. Garbin, and G. Artioli, "Formulation , performance , hydration and rheological behavior of ‘ just add water ' slag -based binders," presented at the 1st International conference on innovation in low-carbon cement & concrete technology, 2019.

[163] D. K. Smith and H. R. Leider, "Low-temperature thermal expansion of LiH, MgO and CaO," *Journal of Applied Crystallography,* vol. 1, no. 4, pp. 246-249, 1968, doi: 10.1107/S0021889868005418.
[164] C. Bezou, A. Nonat, J. C. Mutin, A. N. Christensen, and M. S. Lehmann, "Investigation of the crystal structure of gamma-Ca S O4, Ca S O4 . 0.5(H2 O), and Ca S O4 . 0.6(H2 O) by powder diffraction methods," *Journal of Solid State Chemistry,* vol. 117, pp. 165-176, 1995.
[165] S. Sasaki, C. T. Prewitt, J. D. Bass, and W. A. Schulze, "Orthorhombic perovskite CaTiO3 and CdTiO3: structure and space group," *Acta Crystallographica Section C,* vol. 43, no. 9, pp. 1668-1674, 1987, doi: 10.1107/S0108270187090620.
[166] X. Bao *et al.*, "A new Ca3MgSi2O8 compound and some of its thermodynamic properties," *Journal of Solid State Chemistry,* vol. 255, pp. 145-149, 2017/11/01/ 2017, doi: https://doi.org/10.1016/j.jssc.2017.08.005.
[167] I. Pajares, Á. G. De la Torre, S. Martínez-Ramírez, F. Puertas, M.-T. Blanco-Varela, and M. A. G. Aranda, "Quantitative analysis of mineralized white Portland clinkers: The structure of Fluorellestadite," *Powder Diffraction,* vol. 17, no. 4, pp. 281-286, 2002, doi: 10.1154/1.1505045.
[168] S. Sasaki, K. Fujino, Tak, Eacute, and Y. Uchi, "X-Ray Determination of Electron-Density Distributions in Oxides, MgO, MnO, CoO, and NiO, and Atomic Scattering Factors of their Constituent Atoms," *Proceedings of the Japan Academy, Series B,* vol. 55, no. 2, pp. 43-48, 1979, doi: 10.2183/pjab.55.43.
[169] P. B. Moore and T. Araki, "The crystal structure of bredigite and the genealogy of some alkaline earth orthosilicates," *American Mineralogist,* vol. 61, pp. 74-87, 1976.
[170] R. Rinaldi, M. Sacerdoti, and E. Passaglia, "Strätlingite: crystal structure, chemistry, and a reexamination of its polytpye vertumnite," *European Journal of Mineralogy,* vol. 2, no. 6, pp. 841-850, 1990, doi: 10.1127/ejm/2/6/0841.
[171] D. A. Kulik, F. Winnefeld, A. Kulik, G. D. Miron, and B. Lothenbach, "CemGEMS – an easy-to-use web application for thermodynamic modeling of cementitious materials," *RILEM Technical Letters,* vol. 6, pp. 36-52, 2021, doi: 10.21809/rilemtechlett.2021.140.
[172] H. Ma, "Mercury intrusion porosimetry in concrete technology: tips in measurement, pore structure parameter acquisition and application," *Journal of Porous Materials,* vol. 21, no. 2, pp. 207-215, 2013, doi: 10.1007/s10934-013-9765-4.
[173] E. Bescher, K. Vallens, and J. Kim, "Belitic Calcium Sulfoaluminate Cement: History, Chemistry, Performance, and Use in the United States," presented at the 15th International Congress on the Chemistry of Cement, 2019.
[174] B. Ost, "Very High Early Strength Cement," United States Patent 3860433 Patent Appl. 257,629, 1975.
[175] L. Zhang, M. Su, and Y. Wang, "Development of the use of sulfo- and ferroaluminate cements in China," *Advances in Cement Research,* vol. 11, no. 1, pp. 15-21, 1999.
[176] M. A. G. Aranda and A. G. De la Torre, "Sulfoaluminate cement," in *Eco-Efficient Concrete*, 2013, pp. 488-522.
[177] L. Pelletier-Chaignat, F. Winnefeld, B. Lothenbach, and C. J. Müller, "Beneficial use of limestone filler with calcium sulphoaluminate cement," *Construction and Building Materials,* vol. 26, no. 1, pp. 619-627, 2012, doi: 10.1016/j.conbuildmat.2011.06.065.
[178] V. Isteri *et al.*, "Production and properties of ferrite-rich CSAB cement from metallurgical industry residues," *Sci Total Environ,* vol. 712, p. 136208, Apr 10 2020, doi: 10.1016/j.scitotenv.2019.136208.
[179] J. Šipušić, N. Ukrainczyk, and M. Đopar, "Iron-Aluminum Solid Solution in Klein's Compound," presented at the 3rd International Symposium on Environmental Management Towards Sustainable Technologies, Croatia, 2011.
[180] M. C. Martín-Sedeño *et al.*, "Aluminum-rich belite sulfoaluminate cements: Clinkering and early age hydration," *Cement and Concrete Research,* vol. 40, no. 3, pp. 359-369, 2010, doi: 10.1016/j.cemconres.2009.11.003.
[181] X. Fu, C. Yang, Z. Liu, W. Tao, W. Hou, and X. Wu, "Studies on effects of activators on properties and mechanism of hydration of sulphoaluminate cement," *Cement and Concrete Research,* vol. 33, pp. 317-324, 2003.

[182] I. Odler, "Cements Containing Calcium Sulfoaluminate," in *Special Inorganic Cements*. London: Taylor & Francis Group, 2000, ch. 4, pp. 63-81.
[183] I. Janotka, U. Krajèi, and S. C. Mojumdar, "Performance Of Sulphoaluminate-Belite Cement With High C4A3S Content," *Ceramics − Silikáty,* vol. 51, no. 2, pp. 74-81, 2007.
[184] E. Gartner, "What are BYF cements, and how do they differ from CSA cements?," *The Future of Cement, 200 years after Louis Vicat*, no. June, pp. 6--8, 2017. [Online]. Available: http://www.ecobinder-project.eu.
[185] W. Dienemann, D. Schmitt, F. Bullerjahn, and M. B. Haha, "Belite-Calciumsulfoaluminate-Ternesite (BCT) - A new low-carbon clinker Technology," *Cement International*, vol. 11, 2013.
[186] V. Afroughsabet, L. Biolzi, and S. Cattaneo, "Evaluation of Engineering Properties of Calcium Sulfoaluminate Cement-based Concretes Reinforced with Different Types of Fibers," *Materials (Basel)*, vol. 12, no. 13, Jul 4 2019, doi: 10.3390/ma12132151.
[187] T. Hanein, J.-L. Galvez-Martos, and M. N. Bannerman, "Carbon footprint of calcium sulfoaluminate clinker production," *Journal of Cleaner Production*, vol. 172, pp. 2278-2287, 2018, doi: 10.1016/j.jclepro.2017.11.183.
[188] S. Galluccio, T. Beirau, and H. Pöllmann, "Maximization of the reuse of industrial residues for the production of eco-friendly CSA-belite clinker," *Construction and Building Materials*, vol. 208, pp. 250-257, 2019, doi: 10.1016/j.conbuildmat.2019.02.148.
[189] M. García-Maté, I. Santacruz, Á. G. De la Torre, L. León-Reina, and M. A. G. Aranda, "Rheological and hydration characterization of calcium sulfoaluminate cement pastes," *Cement and Concrete Composites*, vol. 34, no. 5, pp. 684-691, 2012, doi: 10.1016/j.cemconcomp.2012.01.008.
[190] T. Hanein, F. P. Glasser, and M. Bannerman, "Thermodynamics of Portland Cement Clinkering," presented at the 14th International Congress on the -Chemistry of Cement, China, 2015.
[191] T. Hanein *et al.*, "Production of belite calcium sulfoaluminate cement using sulfur as a fuel and as a source of clinker sulfur trioxide: pilot kiln trial," *Advances in Cement Research*, vol. 28, no. 10, pp. 643-653, 2016, doi: 10.1680/jadcr.16.00018.
[192] T. Harrison, M. R. Jones, and D. Lawrence, "The Production of Low Energy Cements," in *Lea's Chemistry of Cement and Concrete*, 5 ed., 2019, pp. 341-362.
[193] E. P. Bescher, "Calcium Sulfoaluminate-Belite Concrete: Structure, Properties, Practice," ed. UCLA, 2018.
[194] M. Ben Haha, F. Winnefeld, and A. Pisch, "Advances in understanding ye'elimite-rich cements," *Cement and Concrete Research*, vol. 123, 2019, doi: 10.1016/j.cemconres.2019.105778.
[195] Caltra, "The advantages of C.S.A. cement," 2016.
[196] I. Santacruz, J. D. Zea-garcia, D. Londono-zuluaga, A. Cuesta, M. A. G. Aranda, and A. G. D. Torre, "Water-to-cement ratio influence on low-carbon cements performances," presented at the 1st International conference on innovation in low-carbon cement & concrete technology, 2019.
[197] F. Canonico, "5 years of experience of an European technical approved CSA cement," presented at the International Workshop on Calcium Sulfoaluminate Cements, 2018.
[198] *Belitic Calcium Sulphoaluminate Cement*, European Organisation for Technical Assessment, Germany, 2020.
[199] *Calcium Sulphoaluminate based Cement*, European Organisation for Technical Assessment, France, 2016.
[200] C. Cau Dit Coumes, S. Courtois, S. Peysson, J. Ambroise, and J. Pera, "Calcium sulfoaluminate cement blended with OPC: A potential binder to encapsulate low-level radioactive slurries of complex chemistry," *Cement and Concrete Research*, vol. 39, no. 9, pp. 740-747, 2009, doi: 10.1016/j.cemconres.2009.05.016.
[201] M. Hayes and I. H. Godfrey, "Development of the Use of Alternative Cements for the Treatment of Intermediate Level Waste," presented at the Waste Management Symposium, Arizona, 2007.
[202] S. A. Saslow *et al.*, "Immobilizing Pertechnetate in Ettringite via Sulfate Substitution," *Environmental Science and Technology*, vol. 54, no. 21, 2020.

[203] C. C. D. Coumes, O. Farcy, P. Antonucci, J.-B. Champenois, D. Lambertin, and A. Mesbah, "Design of self-dessicating binders using calcium sulfoaluminate cement: influence of the cement composition and sulfate source," *HAL Open Science*, 2019.
[204] J. Dachtar, "Calcium Sulfoaluminate Cement as Binder for Structural Concrete," Doctor of Philosophy, Department of Civil and Structural Engineering, The University of Sheffield, Sheffield, 2004.
[205] C. W. Hargis, A. P. Kirchheim, P. J. M. Monteiro, and E. M. Gartner, "Early age hydration of calcium sulfoaluminate (synthetic ye'elimite,) in the presence of gypsum and varying amounts of calcium hydroxide," *Cement and Concrete Research*, vol. 48, pp. 105-115, 2013, doi: 10.1016/j.cemconres.2013.03.001.
[206] E. I. S. Department of Business, "Implimenting the end of unabated coal by 2025," 2018. [Online]. Available: https://assets.publishing.service.gov.uk/government/uploads/system/uploads/attachment_data/file/672137/Government_Response_to_unabated_coal_consultation_and_statement_of_policy.pdf
[207] A. Atteridge and C. Strambo, "Decline of the United Kingdom's steel industry," in "Lessons from industrial transitions," Stockholm Environment Institute, 2021.
[208] Y. V. Seryotkin, E. V. Sokol, S. N. Kokh, and M. N. Murashko, "Natural Cr3+-rich ettringite: occurrence, properties, and crystal structure," *Physics and Chemistry of Minerals*, vol. 45, no. 3, pp. 279-292, 2017, doi: 10.1007/s00269-017-0917-y.
[209] Y. Shen, J. Qian, J. Chai, and Y. Fan, "Calcium sulphoaluminate cements made with phosphogypsum: Production issues and material properties," *Cement and Concrete Composites*, vol. 48, pp. 67-74, 2014, doi: 10.1016/j.cemconcomp.2014.01.009.
[210] S. Ioannou, K. Paine, L. Reig, and K. Quillin, "Performance characteristics of concrete based on a ternary calcium sulfoaluminate–anhydrite–fly ash cement," *Cement and Concrete Composites*, vol. 55, pp. 196-204, 2015, doi: 10.1016/j.cemconcomp.2014.08.009.
[211] F. Winnefeld, L. H. J. Martin, C. J. Müller, and B. Lothenbach, "Using gypsum to control hydration kinetics of CSA cements," *Construction and Building Materials*, vol. 155, pp. 154-163, 2017, doi: 10.1016/j.conbuildmat.2017.07.217.
[212] S. Berger, C. C. D. Coumes, P. Le Bescop, and D. Damidot, "Influence of a thermal cycle at early age on the hydration of calcium sulphoaluminate cements with variable gypsum contents," *Cement and Concrete Research*, vol. 41, no. 2, pp. 149-160, 2011, doi: 10.1016/j.cemconres.2010.10.001.
[213] A. Cuesta, A. Ayuela, and M. A. G. Aranda, "Belite cements and their activation," *Cement and Concrete Research*, vol. 140, 2021, doi: 10.1016/j.cemconres.2020.106319.
[214] M. Borštnar, N. Daneu, and S. Dolenec, "Phase development and hydration kinetics of belite-calcium sulfoaluminate cements at different curing temperatures," *Ceramics International*, vol. 46, no. 18, pp. 29421-29428, 2020, doi: 10.1016/j.ceramint.2020.05.029.
[215] M. Liu, S. Luo, L. Yang, and J. Ren, "Influence of water removal techniques on the composition and microstructure of hardened calcium sulfoaluminate cement pastes," *Materials and Structures*, vol. 53, no. 4, 2020, doi: 10.1617/s11527-020-01527-3.
[216] A. G. De la Torre, D. Londono-Zuluaga, and J. M. Pineda, "Behavior of Belite cement blended with Calcium sulfoaluminate cement: an Ecocement," presented at the 15th International Congress on the Chemistry of Cement, 2019.
[217] M. Mrak, F. Winnefeld, B. Lothenbach, and S. Dolenec, "The influence of calcium sulfate content on the hydration of belite-calcium sulfoaluminate cements with different clinker phase compositions," *Materials and Structures*, vol. 54, no. 6, 2021, doi: 10.1617/s11527-021-01811-w.
[218] C. Murie *et al.*, "Normalization of mass spectrometry data (NOMAD)," *Adv Biol Regul*, vol. 67, pp. 128-133, Jan 2018, doi: 10.1016/j.jbior.2017.11.005.
[219] N. C. Collier, "Transition and Decomposition Temperatures of Cement Phases - a Collection of Thermal Analysis Data," *Ceramics - Silikaty*, pp. 338-343, 2016, doi: 10.13168/cs.2016.0050.

[220] O. Linderoth and P. Johansson, "A comparative study of thermogravimetric analysis conducted on two different instruments," presented at the 15th International Congress on the Chemistry of Cement, 2019.
[221] J. Seo, S. Park, S. Kim, H. N. Yoon, and H. K. Lee, "Local Al network and material characterization of belite-calcium sulfoaluminate (CSA) cements," *Materials and Structures*, vol. 55, no. 1, 2021, doi: 10.1617/s11527-021-01842-3.
[222] G. Ke, J. Zhang, Y. Liu, and S. Xie, "Pore characteristics of calcium sulfoaluminate cement paste with impact of supplementary cementitious materials and water to binder ratio," *Powder Technology*, vol. 387, pp. 146-155, 2021, doi: 10.1016/j.powtec.2021.04.027.
[223] Z. Lafhaj, M. Goueygou, A. Djerbi, and M. Kaczmarek, "Correlation between porosity, permeability and ultrasonic parameters of mortar with variable water/cement ratio and water content," *Cement and Concrete Research*, vol. 36, no. 4, pp. 625-633, 2006, doi: 10.1016/j.cemconres.2005.11.009.
[224] J. Busby, A. Kingdon, and J. Williams, "The measured shallow temperature field in Britain," in "British Geological Survey," 2011. [Online]. Available: https://dx.doi.org/10.1144/1470-9236/10
[225] J. Davidovits, "Why a new theory on how the pyramids were built?," in *Why the pharaohs built the Pyramids with fake stones*: Geopolymer Institute, 2009, ch. 1, pp. 1-8.
[226] D. Roy, "Alkali-Activated Cements Opportunities and Challenges," *Cement and Concrete Research*, vol. 29, no. 2, pp. 249--254, 1998.
[227] J. Whiting, "Manufacture of cement," United States, 1895.
[228] H. Kühl, "Slag cement and process of making the same," United States, 1908.
[229] A. O. Purdon, "The action of alkalis on blast-furnace slag," *Journal. of the Society of Chemical Industry*, vol. 59, pp. 191-202, 1940.
[230] J. L. Provis and S. A. Bernal, "Milestones in the analysis of alkali-activated binders," *Journal of Sustainable Cement-Based Materials*, vol. 4, no. 2, pp. 74-84, 2014, doi: 10.1080/21650373.2014.958599.
[231] R. M. Rosse, "The Working of Communist China's Five Year Plan," *Pacific Affairs*, vol. 27, no. 1, pp. 16-26, 1954.
[232] V. Glukhovsky, *Gruntosilikaty*. Kiev, 1959.
[233] P. Krivenko, "Why Alkaline Activation – 60 Years of the Theory and Practice of Alkali-Activated Materials," *Journal of Ceramic Science and Technology*, vol. 8, no. 3, pp. 323-334, 2017, doi: 10.4416/JCST2017-00042.
[234] A. Palomo, P. Krivenko, I. Garcia-Lodeiro, E. Kavalerova, O. Maltseva, and A. Fernández-Jiménez, "A review on alkaline activation: new analytical perspectives," *Materiales de Construcción*, vol. 64, no. 315, 2014, doi: 10.3989/mc.2014.00314.
[235] J. Davidovits, "Synthesis of new high-temperature geo-polymers for reinforced plastics/composites," presented at the 4th Annual Pacific Technical Conference and Technical Displays on Plastics Technology, California, 1979.
[236] J. Davidovits, "Why Alkali-Activated Materials (AAM) are NOT Geopolymers ?," 2018.
[237] A. Palomo, O. Maltseva, I. Garcia-Lodeiro, and A. Fernandez-Jimenez, "Portland Versus Alkaline Cement: Continuity or Clean Break: "A Key Decision for Global Sustainability"," *Front Chem*, vol. 9, p. 705475, 2021, doi: 10.3389/fchem.2021.705475.
[238] B. Walkley, S. J. Page, G. J. Rees, J. L. Provis, and J. V. Hanna, "Nanostructure of CaO-(Na2O)-Al2O3-SiO2-H2O Gels Revealed by Multinuclear Solid-State Magic Angle Spinning and Multiple Quantum Magic Angle Spinning Nuclear Magnetic Resonance Spectroscopy," *The Journal of Physical Chemistry C*, vol. 124, no. 2, pp. 1681-1694, 2019, doi: 10.1021/acs.jpcc.9b10133.
[239] N. A. Lloyd and B. V. Ranga, "Geopolymer concrete : A review of development and opportunities," presented at the 35th conference on our world in concrete & structures, Singapore, 2010.
[240] B. Planel, S. Lanier, C. Davy, and D. Lambertin, "Refining the pore structure of geopolymer cements for improving radioactive waste conditioning," presented at the 15th International Congress on the Chemistry of Cement, 2019.

[241] A. Fernández-Jiménez, N. Cristelo, T. Miranda, and Á. Palomo, "Sustainable alkali activated materials: Precursor and activator derived from industrial wastes," *Journal of Cleaner Production*, vol. 162, pp. 1200-1209, 2017, doi: 10.1016/j.jclepro.2017.06.151.
[242] A. Telesca, A. Mobili, F. Tittarelli, and M. Marroccoli, "Calcium Sulfoaluminate Cement and Fly Ash-Based Geopolymer as Sustainable Binders for Mortars," *Chemical Engineering Transactions*, vol. 74, 2019, doi: 10.3303/CET1974209.
[243] B. Walkley, X. Ke, O. H. Hussein, S. A. Bernal, and J. L. Provis, "Incorporation of strontium and calcium in geopolymer gels," *J Hazard Mater*, vol. 382, p. 121015, Jan 15 2020, doi: 10.1016/j.jhazmat.2019.121015.
[244] C. Kuenzel *et al.*, "Encapsulation of Cs/Sr contaminated clinoptilolite in geopolymers produced from metakaolin," *Journal of Nuclear Materials*, vol. 466, pp. 94-99, 2015, doi: 10.1016/j.jnucmat.2015.07.034.
[245] W. E. Lee, M. Gilbert, S. T. Murphy, R. W. Grimes, and D. J. Green, "Opportunities for Advanced Ceramics and Composites in the Nuclear Sector," *Journal of the American Ceramic Society*, vol. 96, no. 7, pp. 2005-2030, 2013, doi: 10.1111/jace.12406.
[246] C. M. Jantzen, W. E. Lee, and M. I. Ojovan, "Radioactive Waste Conditioning, Immobilisation, and Encapsulation Processes and Technologies: Overview and Advances," in *Radioactive Waste Management and Contaminated Site Clean-up: Processes, Technologies and International Experience*, 1 ed. United States: Woodhead Publishing, 2012, ch. 7, pp. 273-381.
[247] T. Vehmas, E. Myllykylä, M. Nieminen, J. Laatikainen-Luntama, M. Leivo, and M. Olin, "Geopolymerisation of gasified ion-exchange resins, mechanical properties and short-term leaching studies," presented at the Theramin 2020 conference: thermal treatment of radioactive waste, Manchester, 2020.
[248] I. Luhar *et al.*, "Solidification/Stabilization Technology for Radioactive Wastes Using Cement: An Appraisal," *Materials (Basel)*, vol. 16, no. 3, Jan 19 2023, doi: 10.3390/ma16030954.
[249] The Materials Project. "Materials Data on K2CO3." https://materialsproject.org/materials/mp-3963 (accessed 13/12, 2022).
[250] M. A. Longhi, Z. Zhang, E. D. Rodríguez, A. P. Kirchheim, and H. Wang, "Efflorescence of Alkali-Activated Cements (Geopolymers) and the Impacts on Material Structures: A Critical Analysis," *Frontiers in Materials*, vol. 6, 2019, doi: 10.3389/fmats.2019.00089.
[251] M. A. Longhi *et al.*, "Metakaolin-based geopolymers: Efflorescence and its effect on microstructure and mechanical properties," *Ceramics International*, vol. 48, no. 2, pp. 2212-2229, 2022, doi: 10.1016/j.ceramint.2021.09.313.
[252] M. Hartman, K. Svoboda, B. Čech, M. Pohořelý, and M. Šyc, "Decomposition of Potassium Hydrogen Carbonate: Thermochemistry, Kinetics, and Textural Changes in Solids," *Industrial & Engineering Chemistry Research*, vol. 58, no. 8, pp. 2868-2881, 2019, doi: 10.1021/acs.iecr.8b06151.
[253] S. A. Bernal, J. L. Provis, V. Rose, and R. Mejía de Gutierrez, "Evolution of binder structure in sodium silicate-activated slag-metakaolin blends," *Cement and Concrete Composites*, vol. 33, no. 1, pp. 46-54, 2011, doi: 10.1016/j.cemconcomp.2010.09.004.
[254] Q. Wan *et al.*, "Geopolymerization reaction, microstructure and simulation of metakaolin-based geopolymers at extended Si/Al ratios," *Cement and Concrete Composites*, vol. 79, pp. 45-52, 2017, doi: 10.1016/j.cemconcomp.2017.01.014.
[255] C. Martin, I. Martin, V. Rives, B. Grzybowska, and I. Gressel, "A FTIR spectroscopy study of isopropanol reactivity on alkali-metal-doped MoO3/TiO2 catalysts," *Spectrochimica Acta Part A: Molecular and Biomolecular Spectroscopy*, vol. 52, no. 7, pp. 733-740, 1996/07/15/ 1996, doi: https://doi.org/10.1016/0584-8539(96)01665-0.
[256] M. Król, J. Minkiewicz, and W. Mozgawa, "IR spectroscopy studies of zeolites in geopolymeric materials derived from kaolinite," *Journal of Molecular Structure*, vol. 1126, pp. 200-206, 2016/12/15/ 2016, doi: https://doi.org/10.1016/j.molstruc.2016.02.027.
[257] C. A. Rees, J. L. Provis, G. C. Lukey, and J. S. J. van Deventer, "The mechanism of geopolymer gel formation investigated through seeded nucleation," *Colloids and Surfaces A: Physicochemical and Engineering Aspects*, vol. 318, no. 1, pp. 97-105, 2008/04/01/ 2008, doi: https://doi.org/10.1016/j.colsurfa.2007.12.019.

[258] V. C. Farmer, *The Infrared Spectra of Minerals*. Mineralogical Society of Great Britain and Ireland, 1974.
[259] N. Y. Mostafa, S. A. S. El-Hemaly, E. I. Al-Wakeel, S. A. El-Korashy, and P. W. Brown, "Characterization and evaluation of the pozzolanic activity of Egyptian industrial by-products: I: Silica fume and dealuminated kaolin," *Cement and Concrete Research*, vol. 31, no. 3, pp. 467-474, 2001/03/01/ 2001, doi: https://doi.org/10.1016/S0008-8846(00)00485-3.
[260] C. A. Rees, J. L. Provis, G. C. Lukey, and J. S. J. van Deventer, "In Situ ATR-FTIR Study of the Early Stages of Fly Ash Geopolymer Gel Formation," *Langmuir*, vol. 23, no. 17, pp. 9076-9082, 2007/08/01 2007, doi: 10.1021/la701185g.
[261] J. L. Provis, S. L. Yong, and J. S. J. van Deventer, "Characterising the Reaction of Metakaolin in an Alkaline Environment by XPS, and Time and Spatially-Resolved FTIR Spectroscopy," in *Calcined Clays for Sustainable Concrete*, Dordrecht, K. Scrivener and A. Favier, Eds., 2015// 2015: Springer Netherlands, pp. 299-304.
[262] Department of Geology at University of Tartu. "Quartz." Institute of Chemistry University of Tartu, Estonia. https://spectra.chem.ut.ee/paint/fillers/quartz/ (accessed 03/02, 2023).
[263] E. Najafi Kani, A. Allahverdi, and J. L. Provis, "Efflorescence control in geopolymer binders based on natural pozzolan," *Cement and Concrete Composites*, vol. 34, no. 1, pp. 25-33, 2012, doi: 10.1016/j.cemconcomp.2011.07.007.
[264] M. Rowles and B. O'Connor, "Chemical optimisation of the compressive strength of aluminosilicate geopolymers synthesised by sodium silicate activation of metakaolinite," *Journal of Materials Chemistry*, vol. 13, no. 5, pp. 1161-1165, 2003, doi: 10.1039/b212629j.
[265] A. Autef *et al.*, "Influence of metakaolin purities on potassium geopolymer formulation: The existence of several networks," *Journal of Colloid and Interface Science*, vol. 408, pp. 43-53, 2013, doi: http://dx.doi.org/10.1016/j.jcis.2013.07.024.
[266] T. Skorina, "Ion exchange in amorphous alkali-activated aluminosilicates: Potassium based geopolymers," *Applied Clay Science*, vol. 87, pp. 205-211, 2014, doi: 10.1016/j.clay.2013.11.003.
[267] M. Ben Haha, G. Le Saout, F. Winnefeld, and B. Lothenbach, "Influence of activator type on hydration kinetics, hydrate assemblage and microstructural development of alkali activated blast-furnace slags," *Cement and Concrete Research*, vol. 41, no. 3, pp. 301-310, 2011, doi: 10.1016/j.cemconres.2010.11.016.
[268] S. A. Bernal, J. L. Provis, and J. S. J. v. Deventer, "Impact of Water Content on the Performance of Alkali-Activated Slag Concretes," presented at the Sixth International Conference on Durability of Concrete Structures, Leeds, 18-20/07, 2018, ICC06.
[269] S. Maus, M. Schneebeli, and A. Wiegmann, "An X-ray micro-tomographic study of the pore space, permeability and percolation threshold of young sea ice," *The Cryosphere Discussions*, 2020, doi: 10.5194/tc-2020-288.
[270] E. A. R. Trout, "The History of Calcareous Cements," in *Lea's Chemistry of Cement and Concrete*, P. C. Hewlett and M. Liska Eds., 5 ed. Oxford: Butterworth-Heinemann, 2019, ch. 1, pp. 1-30.
[271] A. C. Davis, *A Hundred, Years of Portland Cement 1824-1924*, 1st ed. London: Concrete Publications Ltd, 1925, p. 282.
[272] A. Butler-Warke and M. R. Warke, "Foundation stone of empire: The role of Portland stone in 'heritage', commemoration, and identity," *Transactions of the Institute of British Geographers*, vol. 46, no. 4, pp. 958-972, 2021, doi: 10.1111/tran.12462.
[273] R. Courland, "The Development of Modern Concrete," in *Concrete Planet*, 1 ed.: Prometheus Books, 2011, pp. 143-210.
[274] R. Courland, "The Development of Modern Concrete," in *Concrete Planet: The Strange and Fascinating Story of the Worlds Most Common Man-Made Material*, 1st ed.: Prometheus, 2011, ch. 5, pp. 145-210.
[275] University of Bristol. "Brunel cement find is world first." https://www.bristol.ac.uk/news/2008/212017945245.html (accessed 16/11, 2022).
[276] L. Shaw-Taylor and X. You, "The development of the railway network in Britain 1825-1911," in "Transport, urbanization and economic development in England and Wales c.1670-1911," The Cambridge Group for the History of Population and Social Structure, 2018.

[277] M. M. Chrimes, "The Development of Concrete Bridges in the British Isles prior to 1940," *Proceedings of the Institution of Civil Engineers - Structures and Building*, vol. 116, no. 3, pp. 404-431, 1996.
[278] D. C. M. Urquhart, "The early concrete bridges of Scotland: a heritage at risk?," *Journal of Architectural Conservation*, vol. 26, no. 3, pp. 201-214, 2020, doi: 10.1080/13556207.2020.1780052.
[279] R. Brueckner and P. Lambert, "Unexpected effects of historic concrete innovations," *International Journal of Heritage Architecture: Studies, Repairs and Maintence*, vol. 1, no. 4, pp. 549-563, 2017, doi: 10.2495/ha-v1-n4-549-563.
[280] L. W. king, "The Law Code of Hammurabi," 1915.
[281] S. Houghton, "Hydration and Durability of Calcium Aluminate Cements," Doctor of Philosophy, Department of Materials Science and Engineering, University of London, London, 1995.
[282] A. Neville, "History of high-alumina cement," *Proceedings of the Institution of Civil Engineers - Engineering History and Heritage*, 2009, doi: 10.1680/ehh.2009.162.
[283] K. L. Scrivener, J.-L. Cabiron, and R. Letourneux, "High-performance concretes from calcium aluminate cements," *Cement and Concrete Research*, vol. 29, no. 8, pp. 1215-1223, 1999, doi: 10.1016/s0008-8846(99)00103-9.
[284] J. H. Ideker, K. L. Scrivener, H. Fryda, and B. Touzo, "Calcium Aluminate Cements," in *Lea's Chemistry of Cement and Concrete*, P. C. Hewlett and M. Liska Eds., 5 ed. Oxford: Butterworth-Heinemann, 2019, ch. 12, pp. 537-584.
[285] R. J. Currie and N. J. Crammond, "Assessment of existing high alumina cement construction in the UK," *Proceedings of the Institution of Civil Engineers - Structures and Buildings*, vol. 104, no. 1, pp. 83-92, 1994.
[286] I. Garcia-Lodeiro, K. Irisawa, Y. Meguro, and H. Kinoshita, "Development of phosphate modified CAC cementitious systems with reduced water content for the immobilization of radioactive wastes," presented at the 15th International Congress on the Chemistry of Cement, 2019.
[287] Oxford University Press. "Meaning of heavy industry in English." https://www.lexico.com/definition/heavy_industry (accessed 23/06, 2022).
[288] Corporate Finance Institute. "What is Heavy Industry?" https://corporatefinanceinstitute.com/resources/knowledge/economics/heavy-industry/ (accessed 27/06, 2022).
[289] Strabo, *The Geography of Strabo*. London: G. Bell & Sons, 1903, p. 7.
[290] O. Fabián, "The legend of Benjamin Huntsman and the early days of modern steel," *MRS Bulletin*, vol. 43, no. 8, p. 637, 2018, doi: 10.1557/mrs.2018.195.
[291] E. J. T. Collins, "At the cutting edge: edge tool production in southern and south-west England, 1740 to 1960," *The Agricultural History Review*, vol. 64, no. 2, pp. 196-225, 2016.
[292] J. Zukowsky, "The Iron Skeleton Frame: Interactions Between Europa and the United States," in *Chicago architecture, 1872-1922 : birth of a metropolis*, 2nd ed., 1987, ch. 2, pp. 39-56.
[293] M. Angel, Yescas-Gonzalez, and H. K. D. H. Bhadeshia. "Cast Irons." https://www.phase-trans.msm.cam.ac.uk/2001/adi/cast.iron.html (accessed.
[294] H. Bessemer, "The Genesis of the Bessemer Process," in *Sir Henry Bessemer, F.R.S. An Autobiography*. London, 1905, ch. 11, pp. 138-151.
[295] H. Bessemer, "The Bessemer Process," in *Sir Henry Bessemer, F.R.S. An Autobiography*. London, 1905, ch. 12, pp. 152-177.
[296] C. Marshall. "The world's first skyscraper: a history of cities in 50 buildings, day 9." The Guardian. https://www.theguardian.com/cities/2015/apr/02/worlds-first-skyscraper-chicago-home-insurance-building-history (accessed 07/12, 2022).
[297] Somik. Lall, Mathilde. Lebrand, Hogeun. Park, Daniel. Sturm, and Anthony. Venables, "Pancakes to Pyramids: City Form to Promote Sustainable Growth," International Bank for Reconstruction and Development, 2021.
[298] D. Hey, "The South Yorkshire Steel Industry and the Industrial Revolution," *Northern History*, vol. 42, no. 1, pp. 91-96, 2013, doi: 10.1179/174587005x38435.

[299] R. Jones. "How Sheffield became Steel City: what local history can teach us about innovation." http://www.softmachines.org/wordpress/?p=2057 (accessed 10/01, 2023).
[300] G. D. B. Gray, "The South Yorkshire Coalfield," *Geographical Association*, vol. 47, no. 3, pp. 113-131, 1947.
[301] University of Calgary. "Bituminous coal." https://energyeducation.ca/encyclopedia/Bituminous_coal#cite_note-2 (accessed.
[302] International Energy Agency. "Coal Definition." https://iea.blob.core.windows.net/assets/imports/events/45/Coal.pdf (accessed 10/01, 2023).
[303] S. P. Schweinfurth, "Coal—A Complex Natural Resource," in "U.S. Geological Survey Circular," US Department of the Interior, 2002, vol. 1143.
[304] A. Tikkanen. "Coke." Encyclopedia Britannica. https://www.britannica.com/technology/coke (accessed 10/01, 2023).
[305] Seascale Parish Council. "Seascale History and Information." https://www.seascaleparish.com/history-and-information/#:~:text=In%201947%20the%20nuclear%20building,the%20brainiest%20place%20in%20Britain. (accessed 10/01, 2023).
[306] K. Adams. "The cars: DeLorean DMC-12 development story." https://www.aronline.co.uk/cars/de-lorean/dmc-12/the-cars-delorean-dmc-12/ (accessed 09/01, 2023).
[307] C. Parnham and A. Withers, *DeLorean - Celebrating the Impossible*, 1st ed. DMCL, 2014.
[308] B. Hundreds. "The Hundreds X Delorean Motor Company pt. V." https://thehundreds.com/blogs/bobby-hundreds/the-hundreds-x-delorean-motor-company-pt-v (accessed.
[309] Franka. "Linwood in Renfrewshire, Scotland." https://www.imps4ever.info/linwood/linwood.html (accessed 09/01, 2023).
[310] K. Adams. "The cars: Hillman Imp development story." https://www.aronline.co.uk/cars/hillman/imp/apex-development-story/ (accessed 09/01, 2023).
[311] L. Batarags. "China has at least 65 million empty homes — enough to house the population of France. It offers a glimpse into the country's massive housing-market problem." Insider Inc. https://www.businessinsider.com/china-empty-homes-real-estate-evergrande-housing-market-problem-2021-10?r=US&IR=T (accessed 10/01, 2023).
[312] L. Batarags. "The Evergrande crisis: 4 questions that explain why China's property market, which is twice as big as America's and where 20% of homes are empty, matters." Insider Inc. https://www.businessinsider.com/china-housing-market-explainer-cost-debt-wealth-evergrande-impact-2021-9?r=US&IR=T (accessed 10/01, 2023).
[313] A. M. Roantree, C. Jim, and R. Woo. "Factbox: China's indebted property market and the Evergrande crisis." Reuters. https://www.reuters.com/world/china/chinas-indebted-property-market-evergrande-crisis-2021-10-22/ (accessed 10/01, 2023).
[314] Eduardo. Baptista and Xiaoyu. Yin. "In China, home buyers occupy their 'rotting', unfinished properties." Reuters. https://www.reuters.com/markets/asia/china-home-buyers-occupy-their-rotting-unfinished-properties-2022-09-26/ (accessed 10/01, 2023).
[315] T. Rees. "China tears down tower blocks in effort to boost stalling economy." The Telegraph. https://www.telegraph.co.uk/business/2022/08/23/china-tears-tower-blocks-effort-boost-stalling-economy/ (accessed 10/01, 2023).
[316] T. Mazilu, "An analysis of bogie hunting instability," *UPB Scientific Bulletin, Series D: Mechanical Engineering*, vol. 71, 01/01 2009.
[317] J.-B. Bonaventure. "Jean Bertin's Aérotrain." https://www.midnight-trains.com/post/jean-bertins-aerotrain (accessed 22/03, 2023).
[318] K. V. Rozhdestvensky, "Wing-in-ground effect vehicles," *Progress in Aerospace Sciences*, vol. 42, no. 3, pp. 211-283, 2006, doi: 10.1016/j.paerosci.2006.10.001.
[319] K. Wenham-Ross. "A Train to Nowhere." https://foreignpolicy.com/2020/04/03/hovertrain-technology-transportation-britain-artifact/ (accessed 13/01, 2023).
[320] Pueblo Railway Foundation. "The Rohr." https://pueblorailway.org/roster/rocket-cars/the-rohr/ (accessed 13/01, 2023).

[321] H. Parkinson. "Back to the future: How the Aérotrain almost revolutionised France's public transport system." https://www.completefrance.com/travel/guide-to-the-aerotrain-in-loiret-france-8715220/ (accessed 13/01, 2023).
[322] Grenfell Tower Inquiry, "Grenfell Tower Inquiry: Phase 1 Report," 2019.
[323] Grenfell Tower Inquiry, "Module 2 - Cladding Products Factsheet," 2021.
[324] The Open University. "The Fires that Foretold Grenfell." https://connect.open.ac.uk/society-psychology-and-criminology/the-fires-that-foretold-grenfell (accessed 21/01, 2023).
[325] P. Apps. "How the products used in Grenfell Tower's cladding system were tested and sold." Inside Housing. https://www.insidehousing.co.uk/insight/insight/how-the-products-used-in-grenfell-towers-cladding-system-were-tested-and-sold-70011 (accessed 21/01, 2023).
[326] Home Owners Alliance. "What is an EWS1 Form." https://hoa.org.uk/advice/guides-for-homeowners/i-am-selling/what-is-an-ews1-form/ (accessed 07/03, 2023).
[327] Hackney Council. "How to request an external wall system (EWS) form." https://hackney.gov.uk/request-ews-form (accessed 07/03, 2023).
[328] House of Commons. "The Cladding External Wall System (EWS)." https://commonslibrary.parliament.uk/the-external-wall-fire-review-process-ews/ (accessed 07/03, 2023).
[329] Royal Institution of Chartered Surveyors. "Cladding External Wall System (EWS) FAQs." https://www.rics.org/news-insights/current-topics-campaigns/fire-safety/cladding-external-wall-system-ews-faqs (accessed 07/03, 2023).
[330] A. Khosravi. "What is the ews1 form? How much does it cost, how long does it take, and why do i need it?" Oliver Fisher Solicitors,. https://oliverfisher.co.uk/what-is-the-ews1-form-how-much-does-it-cost-how-long-does-it-take-and-why-do-i-need-it/#:~:text=To%20complete%20an%20EWS1%20form,are%20less%20than%20300%20nationwide. (accessed 07/03, 2023).
[331] A2Dominion. "Frequently asked questions about EWS1 certificates, remortgaging and selling." https://my.a2dominion.co.uk/help/article/KA-01898/en-gb (accessed 07/03, 2023).
[332] S. Sood. "Sign the EWS1 form at your peril." https://www.building.co.uk/comment/sign-the-ews1-form-at-your-peril/5108132.article (accessed 07/03, 2023).
[333] R. Hull. "Grenfell Tower: finally, the worst type of cladding is to be banned, five years on." The Conversation Trust Ltd. https://theconversation.com/grenfell-tower-finally-the-worst-type-of-cladding-is-to-be-banned-five-years-on-185040#:~:text=The%20inquiry%20into%20the%20disaster,are%20lightweight%2C%20stiff%20and%20cheap. (accessed 08/03, 2023).
[334] R. O'Neill. "Living in the noise, dust and pollution of the UK's largest open coal mine at Ffos-y-Fran, Merthyr Tydfil." Wales Online. https://www.walesonline.co.uk/news/wales-news/ffos-y-fran-coal-mine-25300397 (accessed 07/03, 2023).
[335] A. Lewis. "Plans put forward for Merthyr coal mine to keep operating for a further nine months to help steel industry and with the security of energy supply." Wales Online. https://www.walesonline.co.uk/news/local-news/plans-put-forward-merthyr-coal-25060902 (accessed 08/03, 2023).
[336] C. Price, "We Need To Talk About Coal - Talyllyn Railway," S. Williams, Ed., ed. YouTube: Talyllyn Railway, 2022.
[337] N. Cornish. "Coal and Alternative Fuels Update." The National Traction Engine Trust. https://ntet.co.uk/2022/04/16/coal-and-alternative-fuels-update/ (accessed 08/03, 2023).
[338] C. White. "Net Zero Steam becomes a reality at Stainmore Railway Company." RailAdvent. https://www.railadvent.co.uk/2022/10/net-zero-steam-becomes-a-reality-at-stainmore-railway-company.html (accessed 08/03, 2023).
[339] Suffolk Green Fuel Oilseed Logs. "Oilseed Logs - From Field to Fire." https://www.sgfoilseedlogs.co.uk/ (accessed 08/03, 2023).
[340] Focus Transport. "E-coal on Trial at The Apedale Valley Railway." https://www.focustransport.org/2022/04/e-coal-on-trial-at-apedale-valley.html (accessed 08/03, 2023).
[341] CPL Industries Ltd, "CPL Industries Limited Product Safety Data Sheet E-Coal," 2017.

[342] House of Commons, "A5: Services," in "Economic Indicators," House of Commons Library, 2023.
[343] Office of National Statistics. "Five facts about... The UK service sector." https://www.ons.gov.uk/economy/economicoutputandproductivity/output/articles/fivefactsabouttheukservicesector/2016-09-29 (accessed 08/03, 2023).
[344] Corporate Finance Institute. "What is the Service Sector?" https://corporatefinanceinstitute.com/resources/economics/service-sector/ (accessed 08/03, 2023).
[345] S. Horrell, "Living standards in britain 1900–2000: Women's century?," *National Institute Economic Review,* vol. 172, pp. 62-77, 2000.
[346] Organisation for Economic Co-Operation and Development, "The Service Economy," in "Business And Industry Policy Forum Series," 2000.
[347] Trade and Development Board, "The role of the services economy and trade in structural transformation and inclusive development," in "United Nations Conference on Trade and Development," United Nations, 2017.
[348] D. T. L. Shek, P. P. Y. Chung, and H. Leung, "Manufacturing economy vs. service economy: implications for service leadership," *International Journal on Disability and Human Development*, vol. 14, no. 3, 2015, doi: 10.1515/ijdhd-2015-0402.
[349] M.-A. Russon. "The cost of the Suez Canal blockage." https://www.bbc.co.uk/news/business-56559073 (accessed 18/03, 2023).
[350] International Energy Agency. "Russia's War on Ukraine." https://www.iea.org/topics/russias-war-on-ukraine (accessed 18/03, 2023).
[351] R. Sachin and M. Muvija. "Britain approves first new coal mine in decades despite climate targets." https://www.reuters.com/world/uk/britain-approves-first-new-coal-mine-decades-2022-12-07/ (accessed 18/03, 2023).
[352] Times & Star. "Heartbreak and tears as rail-making bids farewell to Workington." https://www.timesandstar.co.uk/news/17057236.heartbreak-and-tears-as-rail-making-bids-farewell-to-workington/ (accessed 18/03, 2023).
[353] D. Vetter. "David Attenborough's Powerful Speech To COP26 Leaders: 'The World Is Looking To You'." https://www.forbes.com/sites/davidrvetter/2021/11/01/david-attenboroughs-powerful-speech-to-cop26-leaders-the-world-is-looking-to-you/?sh=346fc9bd6f1b (accessed 15/03, 2023).
[354] Intergovernmental Panel on Climate Change, *Climate Change 2007 - The Physical Science Basis*. Cambridge: Cambridge Univerdity Press, 2007.
[355] United Nations. "Climate change the greatest threat the world has ever faced, UN expert warns." https://www.ohchr.org/en/press-releases/2022/10/climate-change-greatest-threat-world-has-ever-faced-un-expert-warns (accessed 15/03, 2023).
[356] United Nations, "Adoption of the Paris Agreement," in "Paris Agreement," 2015. [Online]. Available: https://unfccc.int/sites/default/files/english_paris_agreement.pdf
[357] E. Commission, "The Road from Paris: assessing the implications of the Paris Agreement and accompanying the proposal for a Council decision on the signing, on behalf of the European Union, of the Paris agreement adopted under the United Nations Framework Convention on Climate Change," in "Communication from the Commision to the European Parliment and the Council," Brussels, 2016. [Online]. Available: https://eur-lex.europa.eu/legal-content/EN/TXT/?uri=COM:2016:110:FIN
[358] E. Secretary of State for Business, and Industrial Strategy,, "United Kingdom of Great Britain and Northern Ireland's Nationally Determined Contribution," UK Parliment, 2022.
[359] G. Habert, "Assessing the environmental impact of conventional and 'green' cement production," in *Eco-efficient Construction and Building Materials*, 2014, pp. 199-238.
[360] I. H. Shah, S. A. Miller, D. Jiang, and R. J. Myers, "Cement substitution with secondary materials can reduce annual global CO_2 emissions by up to 1.3 gigatons," *Nat Commun,* vol. 13, no. 1, p. 5758, Sep 30 2022, doi: 10.1038/s41467-022-33289-7.
[361] K. Scrivener, F. Martirena, S. Bishnoi, and S. Maity, "Calcined clay limestone cements (LC3)," *Cement and Concrete Research,* vol. 114, pp. 49-56, 2018, doi: 10.1016/j.cemconres.2017.08.017.

[362] H. Du, S. D. Pang, and A. Dixit, "High Performance Concrete with Calcined Clay and Limestone as Cement Substitute," presented at the 15th International Congress on the Chemistry of Cement, 2019.
[363] G. L. P. Falla, "Reactive Limestone as a Strategy Towards Low-Clinker Factor Cements," Doctor of Philosophy, Civil Engineering, University of California, Los Angeles, 2016.
[364] European Comission, "2013 Technology Map of the European Strategic Energy Technology Plan," in "JRC Science and Policy Reports," European Union, Luxembourg, 2013.
[365] International Energy Agency, "Technology Roadmap - Low-Carbon Transition in the Cement Industry," 2018.
[366] M. Simoni, "Towards more sustainable cement production: a no-combustion approach for the decarbonisation of CaCO3," Doctor of Philosophy, Materials Science and Engineering, The University of Sheffield, Sheffield, 2022.
[367] E. Martin-Roberts, V. Scott, S. Flude, G. Johnson, R. S. Haszeldine, and S. Gilfillan, "Carbon capture and storage at the end of a lost decade," *One Earth*, vol. 4, no. 11, pp. 1569-1584, 2021, doi: 10.1016/j.oneear.2021.10.002.
[368] T. Hills, D. Leeson, N. Florin, and P. Fennell, "Carbon Capture in the Cement Industry: Technologies, Progress, and Retrofitting," *Environ Sci Technol*, vol. 50, no. 1, pp. 368-77, Jan 5 2016, doi: 10.1021/acs.est.5b03508.
[369] Low Carbon Concrete Group, "Low Carbon Concrete Routemap," Institution of Civil Engineers, 2022.
[370] K. L. Scrivener, V. M. John, and E. M. Gartner, "Eco-efficient cements: Potential economically viable solutions for a low-CO_2 cement-based materials industry," *Cement and Concrete Research*, vol. 114, pp. 2-26, 2018, doi: 10.1016/j.cemconres.2018.03.015.
[371] T. Watari, Z. Cao, S. Hata, and K. Nansai, "Efficient use of cement and concrete to reduce reliance on supply-side technologies for net-zero emissions," *Nature Communications*, vol. 13, no. 1, 2022, doi: 10.1038/s41467-022-31806-2.
[372] A. Baylin-Stern and N. Berghout. "Is carbon capture too expensive?" Internation Energy Agency. https://www.iea.org/commentaries/is-carbon-capture-too-expensive (accessed 17/03, 2023).
[373] Global Cement and Concrete Association, "Future Concrete - The GCCA 2050 Cement and Concrete Industry Roadmap for Net Zero Concrete," London, 2021.
[374] Mineral Products Association, "UK Concrete and Cement Industry Roadmap to Beyond Net Zero," London, 2020.
[375] M. J. Hornsey and S. Lewandowsky, "A toolkit for understanding and addressing climate scepticism," *Nature Human Behaviour*, vol. 6, no. 11, pp. 1454-1464, 2022, doi: 10.1038/s41562-022-01463-y.
[376] Lignite Energy Council. "Lignite Energy Council - About Us." https://lignite.com/about-us/ (accessed 19/03, 2023).
[377] J. Bateman. "The end of the world's capital of brown coal." BBC. https://www.bbc.com/future/article/20210419-the-end-of-the-worlds-capital-of-brown-coal (accessed 19/03, 2023).
[378] Minnesota Campaign Finance and Public Disclosure Board. "Lobbying organizations - Lignite Energy Council." https://cfb.mn.gov/reports-and-data/viewers/lobbying/lobbying-organizations/3892/2023.1/ (accessed 19/03, 2023).
[379] Lignite Energy Council. "Lignite Energy Foundation." https://www.lecfoundation.org/about (accessed 19/03, 2023).
[380] Ordinary things, "ApoCOALypse Now!," 1st ed. United Kingdom: YouTube, 2022, p. 33:55.
[381] Count on Coal. "Coal to the Rescue in Europe." https://www.countoncoal.org/2023/03/coal-to-the-rescue-in-europe/ (accessed 19/03, 2023).
[382] Bismarck Larks. "Teachers of the Year Announced." https://northwoodsleague.com/bismarck-larks/larks-and-lignite-name-teachers-of-the-year/ (accessed 19/03, 2023).
[383] Lignite Energy Council. "Informing the public about carbon capture, utilization and storage in 2020." https://lignite.com/members/member-update/informing-the-public-about-carbon-capture-utilization-and-storage-in-2020/ (accessed.

[384] Lignite Energy Council. "Thank a Coal Worker." https://lignite.com/thank-a-coal-worker/ (accessed.
[385] OurWarsToday. "200 French Environmental Activists Sabotage Lafarge-Holcim Marseille Cement Plant." https://theatlasnews.co/conflict/2022/12/12/200-french-environmental-activists-sabotage-lafarge-holcim-marseille-cement-plant/ (accessed 19/03, 2023).
[386] U. Dewald and M. Achternbosch, "Why more sustainable cements failed so far? Disruptive innovations and their barriers in a basic industry," *Environmental Innovation and Societal Transitions,* vol. 19, pp. 15-30, 2016, doi: 10.1016/j.eist.2015.10.001.
[387] Celitement GmbH. "Publications about Celitement." https://celitement.de/en/publications/ (accessed 19/03, 2023).
[388] Semco Productions. "Partnership revisits Calera-refined carbon dioxide mineralization." https://concreteproducts.com/index.php/2020/01/20/partnership-revisits-calera-refined-carbon-dioxide-mineralization/ (accessed 19/03, 2023).
[389] *Calcium Sulphoaluminate based Cement*, European Organisation for Technical Assessment, France, 2018.
[390] P. Software. "In a nutshell: the technology adoption lifecycle and crossing the chasm." https://www.parkersoftware.com/blog/in-a-nutshell-the-technology-adoption-lifecycle-and-crossing-the-chasm/ (accessed 20/03, 2023).
[391] High Tech Strategies. "Crossing the Chasm Summary." https://www.hightechstrategies.com/crossing-the-chasm-summary/ (accessed 18/03, 2023).
[392] W. Schirtzinger and L. James, "NeuroCom - Technology Adoption Lifecycle," Regis McKenna Inc,, 1989.
[393] K. McGourty. "Crossing the Chasm: Safe crossing or a death fall?" https://inpdcenter.com/blog/crossing-the-chasm-safe-crossing-or-a-death-fall/ (accessed 20/03, 2023).
[394] S. George. "EVs accounted for one-third of all UK car sales last month, Society of Motor Manufacturers and Traders confirms." Edie. https://www.edie.net/evs-accounted-for-one-third-of-all-uk-car-sales-last-month-smmt-confirms/ (accessed 18/03, 2023).
[395] A. Nikiforuk. "The Big Shift Last Time: From Horse Dung to Car Smog." https://thetyee.ca/News/2013/03/06/Horse-Dung-Big-Shift/ (accessed 25/01, 2021).
[396] R. Martin. "The Race for the Ultra-Efficient Jet Engine of the Future." https://www.technologyreview.com/s/601008/the-race-for-the-ultra-efficient-jet-engine-of-the-future/ (accessed 20/03, 2023).
[397] I. N. Laboratory, "History of Electric Cars," 2016. [Online]. Available: https://avt.inl.gov/sites/default/files/pdf/fsev/HistoryOfElectricCars.pdf
[398] F. Ken, W. Purdy, G. Orville, and C. Cromer. "History Of The Automobile." https://www.britannica.com/technology/automobile/Early-electric-automobiles (accessed 20/03, 2023).
[399] L. S. Martins, L. F. Guimaraes, A. B. Botelho Junior, J. A. S. Tenorio, and D. C. R. Espinosa, "Electric car battery: An overview on global demand, recycling and future approaches towards sustainability," *J Environ Manage,* vol. 295, p. 113091, Oct 1 2021, doi: 10.1016/j.jenvman.2021.113091.
[400] G. Harding, B. Phillips, and J. HAMMOND, "The Lucas Electric Car," 0148-7191, 1983.
[401] United Kingdom Research Institute. "A brief history of climate change discoveries." (accessed 18/03, 2023).
[402] C. Diaz. "1 in 7 cars sold globally now is electric." Quartz Things team. https://www.weforum.org/agenda/2023/03/ev-car-sales-energy-environment-gas/#:~:text=Global%20sales%20of%20electric%20cars,International%20Energy%20Agency%20(IEA). (accessed 19/03, 2023).
[403] C. Thompson, K. Lee, and T. Levin. "Tesla just celebrated its 12th year as a public company. Here are the most important moments in its history." Insider Inc. https://www.businessinsider.com/most-important-moments-tesla-history-2017-2?r=US&IR=T (accessed 19/03, 2023).
[404] J. Clifford. "History of the Toyota Prius." Toyota. https://mag.toyota.co.uk/history-toyota-prius/ (accessed 19/03, 2023).

[405] J. Giesekam, J. R. Barrett, and P. Taylor, "Construction sector views on low carbon building materials," *Building Research & Information*, vol. 44, no. 4, pp. 423-444, 2015, doi: 10.1080/09613218.2016.1086872.
[406] K. Jones. "Overcoming Conservatism in Construction." https://usefulprojects.co.uk/overcoming-conservatism-in-construction/ (accessed 27/04, 2022).
[407] C. F. Dunant, T. Shah, M. P. Drewniok, M. Craglia, and J. M. Cullen, "A new method to estimate the lifetime of long-life product categories," *Journal of Industrial Ecology*, vol. 25, no. 2, pp. 321-332, 2020, doi: 10.1111/jiec.13093.
[408] L. Tao, "Developing the Concept – Innovation Readiness Levels (IRL)," Centre for Technology Management, University of Cambridge, 2006.
[409] I. Tzinis. "Technology Readiness Level." NASA. https://www.nasa.gov/directorates/heo/scan/engineering/technology/technology_readiness_level (accessed 19/03, 2023).
[410] Nuclear Decommissioning Authority, "Guide to Technology Readiness Levels for the NDA Estate and its Supply Chain," 2014, vol. 2.
[411] T. Altunok and T. Cakmak, "A technology readiness levels (TRLs) calculator software for systems engineering and technology management tool," *Advances in Engineering Software*, vol. 41, no. 5, pp. 769-778, 2010, doi: 10.1016/j.advengsoft.2009.12.018.
[412] International Energy Agency, "Energy Technology Perspectives 2020 - Special Report on Carbon Capture Utilisation and Storage," 2020.
[413] M. Ross. "Rapid-Setting Non-Portland Cement Concrete Applications." https://docs.lib.purdue.edu/cgi/viewcontent.cgi?article=4336&context=roadschool (accessed 1/12, 2023).
[414] ASTM International. "Standard Specification for Rapid Hardening Hydraulic Cement." https://www.astm.org/c1600_c1600m-19.html (accessed.
[415] A. Federation, "UK Aluminium Industry Fact Sheet 17: Primary Aluminium Production," 2019.
[416] International Aluminium Institute, "Opportunities for use of bauxite residue in special cements," United Kingdom, 2016.
[417] C. D. Popescu, M. Muntean, and J. H. Sharp, "Industrial trial production of low energy belite cement," *Cement and Concrete Composites*, vol. 25, no. 7, pp. 689-693, 2003, doi: 10.1016/s0958-9465(02)00097-5.
[418] A. Telesca, M. Marroccoli, and T. Matschei, "Enhancement of the environmentally friendly features of belite- calcium sulfoaluminate cements through the use of industrial by- products," presented at the 1st International conference on innovation in low-carbon cement & concrete technology, 2019.
[419] E. Gartner, "Industrially interesting approaches to "low-CO_2" cements," *Cement and Concrete Research*, vol. 34, no. 9, pp. 1489-1498, 2004, doi: 10.1016/j.cemconres.2004.01.021.
[420] M. Taiichiro, N. Yuta, H. Takayuki, and S. Etsuo, "Hydration products in moderate-heat Portland cement expansive additive - CaO•2Al2O3 system and utilization of carbonation reaction," presented at the 15th International Congress on the Chemistry of Cement, 2019.
[421] D. Y. C. Leung, G. Caramanna, and M. M. Maroto-Valer, "An overview of current status of carbon dioxide capture and storage technologies," *Renewable and Sustainable Energy Reviews*, vol. 39, pp. 426-443, 2014, doi: 10.1016/j.rser.2014.07.093.
[422] C. Ren *et al.*, "Comparative life cycle assessment of sulfoaluminate clinker production derived from industrial solid wastes and conventional raw materials," *Journal of Cleaner Production*, vol. 167, pp. 1314-1324, 2017, doi: 10.1016/j.jclepro.2017.05.184.
[423] J. H. Sharp, C. D. Lawrence, and R. Yang, "Calcium sulfoaluminate cements—low-energy cements, special cements or what?," *Advances in Cement Research*, vol. 11, no. 1, 1999.
[424] ASTM International. "Standard Test Methods for Determining Effects of Chemical Admixtures on Corrosion of Embedded Steel Reinforcement in Concrete Exposed to Chloride Environments." https://www.astm.org/g0109-21.html (accessed 1/12, 2023).
[425] H. Uvegi, B. Traynor, P. Chaunsali, and E. Olivetti, "Determining viability of industrial byproducts in alkali activated systems," presented at the 15th International Congress on the Chemistry of Cement, 2019.

[426] S. A. Bernal, E. D. Rodríguez, R. Mejía de Gutiérrez, M. Gordillo, and J. L. Provis, "Mechanical and thermal characterisation of geopolymers based on silicate-activated metakaolin/slag blends," *Journal of Materials Science*, vol. 46, no. 16, pp. 5477-5486, 2011, doi: 10.1007/s10853-011-5490-z.
[427] British Geological Survey, "Mineral Planning Factsheet: Kaolin," 2009.
[428] B. H. Zaribaf, "Metakaolin-Portland Limestone Cements: Evaluating the Effects of Chemical Admixtures on Early And Late Age Behavior," School of Civil and Environmental Engineering, Georgia Institute of Technology, 2017.
[429] M. d. Spot and M. Wojtarowicz, "EcoSmart™ Metakaolin Study," Action Plan 2000 on Climate Change – Minerals and Metals, 2003.
[430] A. Kadhim, M. Sadique, W. Atherton, and P. Kot, "Development of alkali activated cementitious binder synthesised from metakaolin , volcanic tuff and lime waste," presented at the 1st International conference on innovation in low-carbon cement & concrete technology, 2019.
[431] L. K. Turner and F. G. Collins, "Carbon dioxide equivalent (CO_2-e) emissions: A comparison between geopolymer and OPC cement concrete," *Construction and Building Materials*, vol. 43, pp. 125-130, 2013, doi: 10.1016/j.conbuildmat.2013.01.023.
[432] M. Weil, K. Dombrowski, and A. Buchwald, "Life-cycle analysis of geopolymers," in *Geopolymers : Structures, Processing, Properties and Industrial Applications*: Elsevier Science & Technology, 2009, ch. 10, pp. 194-210.
[433] R. San Nicolas, M. Cyr, and G. Escadeillas, "Characteristics and applications of flash metakaolins," *Applied Clay Science*, vol. 83-84, pp. 253-262, 2013, doi: 10.1016/j.clay.2013.08.036.
[434] F. Avet, X. Li, and K. Scrivener, "Methods to determine the reaction degree of metakaolin in cementitious blends," presented at the 15th International Congress on the Chemistry of Cement, 2019.
[435] G. Habert, J. B. d'Espinose de Lacaillerie, and N. Roussel, "An environmental evaluation of geopolymer based concrete production: reviewing current research trends," *Journal of Cleaner Production*, vol. 19, no. 11, pp. 1229-1238, 2011, doi: 10.1016/j.jclepro.2011.03.012.